Copyright Warning & Restrictions

The copyright law of the United States (Title 17, United States Code) governs the making of photocopies or other reproductions of copyrighted material.

Under certain conditions specified in the law, libraries and archives are authorized to furnish a photocopy or other reproduction. One of these specified conditions is that the photocopy or reproduction is not to be "used for any purpose other than private study, scholarship, or research." If a, user makes a request for, or later uses, a photocopy or reproduction for purposes in excess of "fair use" that user may be liable for copyright infringement,

This institution reserves the right to refuse to accept a copying order if, in its judgment, fulfillment of the order would involve violation of copyright law.

Please Note: The author retains the copyright while the New Jersey Institute of Technology reserves the right to distribute this thesis or dissertation

Printing note: If you do not wish to print this page, then select "Pages from: first page # to: last page #" on the print dialog screen

DESIGN OF LINEAR CONTROL SYSTEMS WITH DISTRIBUTED PARAMETER ELEMENTS BY PARAMETER PLANE TECHNIQUES

BY

MURRAY WEINBERG

A DISSERTATION

PRESENTED IN PARTIAL FULFILLMENT OF

THE REQUIREMENTS FOR THE DEGREE

OF

DOCTOR OF ENGINEERING SCIENCE

ELECTRICAL ENGINEERING

AT

NEWARK COLLEGE OF ENGINEERING

Newark, New Jersey

1968

DESIGN OF LINEAR CONTROL SYSTEMS WITH DISTRIBUTED PARAMETER ELEMENTS BY PARAMETER PLANE TECHNIQUES

BY: Murray Weinberg

ADVISER: Dr. L. Eisenberg

ABSTRACT

This dissertation extends the application of parameter plane techniques to a number of areas. Specifically, the parameter plane technique can now be used to determine absolute stability, relative stability, and the location of roots of the closed-loop characteristic equation of systems containing both lumped and distributed parameter elements. The advantages of utilizing this technique are that results can be obtained as two system parameters are varied simultaneously and higher order systems can be treated as easily as low order ones.

Investigation of the mapping of real roots resulted in the derivation of a theorem which relates the number of real roots of the characteristic equation when parameters specify a given point in the parameter plane with the number of tangents which can be drawn from the operating point to certain segments of the zeta equals $\pm$ 1 contours.

The parameter plane is also used to treat systems containing a hypothetical element whose transfer function is a member of the set of functions $\exp(-(sT)^{p/q})$ where p and q are integers and p is less than q . The technique developed here involves two different mappings. The first mapping transforms the s-plane equation into a complex w-plane in which the equation is single valued and then parameter plane mapping techniques are applied. In addition, the parameter plane technique is also extended to systems containing elements with transfer functions of the form $\exp(-(s^{p}T))$.

The predictor configuration described in the literature and used to compensate transport lag in the plant of a feedback system is investigated for systems with plants containing distributed parameter elements . The difficulty with this configuration of exactly synthesizing the distributed element in the auliliary predictor loop is overcome through use of one of a set of rational polynomials for the distributed parameter element. A system with distributed lag is analyzed applying the newly extended parameter plane method in order to determine which polynomial approximation is optimum for the system under consideration. Also, the method is used to show how parameters associated with the polynomial can be chosen to make the system stable with wide gain variations and also achieve a minimum of damping of the transient response compared with the

uncompensated system.

Several methods are derived for estimating the transient response of feedback systems with distributed parameter elements. The concept of the response consisting of the sum of rational and irrational terms is introduced and attention is focused initially on the rational portion of the response. A geometric interpretation is presented for the time to first peak, T_p, and the amount of first overshoot, M, for the case of distributed lag in terms of roots and zeros of the closed loop transfer function transformed into a new complex plane. This interpretation assumes that one pair of roots are dominant. In addition, a set of curves are presented which show the relationship between T_p, M, and settling time T_s and the s-plane location of the dominant root for systems with distributed lag.

APPROVAL OF DISSERTATION

DESIGN OF LINEAR CONTROL SYSTEMS WITH DISTRIBUTED PARAMETER ELEMENTS BY PARAMETER PLANE TECHNIQUES

BY

MURRAY WEINBERG

FOR

DEPARTMENT OF ELECTRICAL ENGINEERING

NEWARK COLLEGE OF ENGINEERING

BY

FACULTY COMMITTEE

APPROVED: _____ CHAIRMAN

_____

_____

_____

_____

NEWARK, NEW JERSEY

1968

ACKNOWLEDGMENT

The author wishes to express his appreciation to Dr. L. Eisenberg for his guidance and encouragement during the course of this research. Also, the financial assistance provided by ITT Defense Communications, Nutley , New Jersey is gratefully acknowledged since it helped to make this period of research a pleasurable one.

TABLE OF CONTENTS

TABLE OF CONTENTS (Cont.)

TABLE OF CONTENTS (Cont.)

TABLE OF CONTENTS (Continued)

LIST OF FIGURES

LIST OF FIGURES

LIST OF FIGURES

LIST OF TABLES

CHAPTER 1

INTRODUCTION

1-1. Purpose and Definitions

The primary purpose of this dissertation is to present to the engineer the means to design feedback systems containing both lumped and distributed parameter elements by means of parameter plane techniques. The use of these techniques, in conjunction with a digital computer, will enable the designer to investigate the stability and transient response of these systems when two parameters are varied simultaneously.

The specific goals of this dissertation are:

1. To extend the parameter plane technique[1] to feedback systems containing distributed parameter elements with transfer functions of the form

$$F_D(s) = \exp\left(- d \sqrt{(Ls + R)(Cs + G)} \right) \qquad (1.1.1)$$

2. To investigate applications of the parameter plane technique[1] by which systems containing elements with transfer functions of the form

$$F_D(s) = \exp\left(-(sT)^{p/q}\right) \qquad (1.1.2)$$

can be analyzed for stability.

1 The parameters α and β chosen for the parameter plane are assummed to be associated with the lumped parameter elements in the system. Examples are gain and time constant.

The effect of both absolute and relative stability is considered when two free system parameters (such as gain and controller time constant) are varied.

3. To investigate the use of polynomial approximants which will maximize the allowable gain for a specified plant containing a distributed lag element. Specifically the class of polynomial approximants derived by Pierre [80] will be in a network configuration proposed by Smith [105] for transport lag and extended here to distributed lag.
4. To investigate techniques by which the transient response of systems with distributed lag can be approximated. The basis of this approximation is the extension of the dominant root philosophy developed by Mulligan [71] for lumped parameter systems.

In general, terms appearing in this dissertation will be defined as they are introduced. However, in the case of terms involving stability, the definition of terms are as follows:

- System stability - defined as $\lim_{t \to \infty} h(t) = 0$ where h(t) is the impulse response.
- Absolute stability - A linear system in which the transfer function is analytic in the closed right half of the principal sheet of the s-plane (including the imaginary axis). Also "stability".

- Relative stability - A linear system in which the transfer function is analytic in a closed region to the right of a pair of conjugate radial lines on the principal sheet of the s-plane.

1.2. Potential Value of this Dissertation

Systems containing distributed parameter elements occur in many fields of science. Problems of distributed parameter feedback control arise as a consequence of efforts to control processes containing these elements. Some areas in which distributed parameter elements arise include:

1. Electrical Transmission Lines. When a signal is transmitted over a line, it is distorted, attenuated and delayed as a consequence of the parameters of the line.
2. Pneumatic and Hydraulic Lines. These lines are used when large forces are transmitted over short distances, as in movement of aircraft control surfaces, or when small forces are transmitted over long distances, as in temperature control of large buildings [57, 74, 90, 91] .
3. Temperature Dependent Processes. Thermostatic devices [16, 17] and heat sensitive chemical processes [3, 123, 113] are subject to the laws of heat flow.
4. Control of Nuclear Reactors. The neutron diffusion processes within a reactor are distributed in nature [95, 42].

5 Applied Electronics. Distributed parameter problems include time delay equations characterizing electron energy distribution in a gas tube [28], and irrational and transcendental base transport factors in the performance equations of transistors [5, 67]. In addition, the microminiaturization of electronic circuits has led to the development of new RC distributed parameter components [20, 43, 48].

6 Biomedical Research. Man has been characterized as a distributed parameter system and various sense organs respond distributively, see [112]. In addition, when a human being forms an integral part of a system [33, 46] his distributive characteristics [8] effects overall system performance.

7 Aircraft and Missile Control. Problems include the effect of time delay on the control of vertical and lateral motions [2] and , in missile control , the effects of combustion instability caused by time delay [26].

8 Economic Systems. Mans economic and organizational societies are characterized by distributed time delay elements [121].

The above mentioned applications illustrate the value and usefulness of formulation of problems in terms of distributed parameters. In addition to this, a new parameter plane technique [98, 99, 29, 30] has recently been developed in which linear feedback systems can be analyzed in terms of two free system parameters. This technique is superior to the root locus method developed by Evans [34] in which system performance can be investigated when only one system parameter (usually gain) is varied. One of the purposes of this dissertation is to extend the parameter plane technique to systems with distributed parameter elements. This is accomplished in Chapter 4.

A class of distributed parameter elements with transfer function

$$F_D(s) = \exp\left(-(sT)^{p/q}\right) \qquad (1.1.3)$$

is defined in Chapter 5. Gain and phase (ie. complex) functions for this class of element are also developed and the parameter plane technique is applied to feedback systems containing this type of element. The parameter plane technique is applied to a transformed complex plane in which the characteristic equation of the system is rendered single valued.

Smith [103] suggests that his linear predictor controller developed for systems with transport lag can be generalized but did not provide either analytic justification or illustrative examples. In Chapter 6,

Smith's predictor controller is extended to feedback systems with distributed parameter elements. In addition, a rational polynomial approximation of the distributed parameter element is used in the local feedback loop and the parameter plane technique is applied.

A special type of feedback system, in which the distributed parameter element is a distributed lag, is also analyzed in Chapter 6, and the parameter plane technique is used to determine a polynomial approximant which renders the system absolutely stable with gain variation. Application of this type of system would be in atomic reactor control where safety is a prime consideration.

The transient response of feedback systems with distributed parameter elements, in general, involves both evaluation of an irrational integral and evaluation of residues at roots of the system characteristics equation falling within the contour of integration. When dealing with systems containing distributed lag, several approximate methods of determining the transient response are set forth and compared in Chapter 7. Through use of these methods a designer can rapidly determine the system parameters to use in order to achieve a desired response.

1-3. Organization of the Dissertation

The dissertation proper consists of 8 chapters, with recommendations in Chapter 9 for continued work in this field.

- Chapter 2 consists of a review of the literature associated with control systems that contain distributed parameter elements. This literature is concerned with all techniques except parameter plane, which will be treated separately.
- Chapter 3 is a review of the history of parameter plane techniques starting from the work of Vishnegradski, and includes the contributions made by Niemark, Mitrovic, Siljak, Thaler, and Eisenberg.
- Chapter 4 consists of an extension of the parameter plane[1] technique to feedback systems containing distributed parameter elements with transfer functions of the form

$$F_D(s) = \exp\left(- d\sqrt{(Ls + R)\,(Cs + G)}\right) \qquad (1.1.4)$$

- Chapter 5 consists of the development of techniques which will enable the application of parameter plane[1] techniques to feedback systems containing distributed parameters elements with transfer functions of the form

$$F_D(s) = \exp\left(- (sT)^{p/q}\right)$$

- Chapter 6 consists of an extension of the Smith predictor technique to systems with distributed lag. In particular, a specific system containing a distributed lag element in its plant is analyzed.
- Chapter 7 contains the derivation of the unit step response of a feedback system with both lumped and distributed parameter elements. In addition, approximations to the transient response are also derived based upon extension of the dominant root technique.
- Chapter 8 presents a summary of the more important results of this dissertation.
- Chapter 9 contains recommendations for continued work which could lead to future dissertations.

CHAPTER 2

REVIEW OF CONTROL SYSTEMS WITH LINEAR-TIME INVARIANT DISTRIBUTED PARAMETER ELEMENTS[1]

2.1 Introduction

A distributed parameter element is defined as an element characterized by a differential equation in two or more independent variables (usually, time and one or more space variables). A distributed parameter system is defined as one having one or more distributed parameter elements. In general, therefore, distributed parameter systems are characterized by partial differential equations in several variables as opposed to lumped parameter systems, which are characterized by ordinary differential equations involving a single independent variable.

In a control system with one or more distributed parameter elements, interest is usually focused upon the relationships between various quantities such as output response, error, etc. For example, in a control system containing a uniform transmission line, interest may be on the time relationship between the input and the output of the line. In this case, the actual distributed nature of the problem is disguised in that time is the only independent variable present, the space variable appearing as a constant.

[1] Often many non-linear distributed parameter systems may be linearized for small signal operation about an equilibrium.

If a transmission line is distortionless, its output is a scaled replica of its input, delayed in time. Such response behavior is characterized as "transport lag." Equivalent terms used in the literature are "time delay", "dead time" [15, 23, 64, 65] "time lag" [1, 22, 53, 61] "transport delay" [56, 100] "distance velocity lag" [75] and "retarded variable" [83, 96] .

Transport lag is but one special case of the distributed parameter element. Another well known form of the distributed parameter element is termed "distributed lag." Assuming zero initial conditions, the transfer function of a distributed lag element is characterized by an exponential raised to the half power of s. The distinction between transfer functions for systems containing "transport lag" and those for "distributed lag" is that the singularities of the former are poles and/or an essential singularity at infinity while those of the latter are branch points.

Since most of the literature on distributed parameter elements in control systems is concerned with the analysis and synthesis of systems with transport lag, this literature review will be divided into two parts:

1.) Work concerning the analysis of control systems with transport lag is done in Section 2.2

2.) Work concerning the analysis and/or synthesis of control systems with distributed parameter elements, other than transport lag is done in Section 2.3.

2.2 Transport Lag

Control systems with transport lag can be characterized by difference differential equations. Methods of solving these equations are directly applicable to the determination of the transient response of these systems. Since difference differential equations have been used to characterize various problems for approximately 200 years, a large body of literature has been produced concerned with classical methods of solution of these equations. Several books [9, 82] devoted to the theory of difference differential equations contain a description of these methods.

The use of operation and transform methods in the analysis of systems with transport lag is of the same importance and value as in the analysis of lumped parameter control systems. In 1934, Neufeld [73] formalized use of Heaviside's operational calculus for the solution of mixed difference differential equations. In 1940,

Heins [45] presented a method of solution of these equations by Laplace transform techniques.

In the s-plane one commonly used technique for determining the transient response of a linear single loop system with transport lag is to expand the denominator of the associated Bromwich integral, utilizing the binomial expansion and then to perform a term by term inversion on the resulting series of integrals. Thus, considering a typical Bromwich integral of a single loop feedback system with transport lag, expansion of the exponential term in the denominator yields

$$\frac{1}{2\pi j}\int_{Br} \frac{e^{st}\,A(s)}{1+B(s)e^{-sT}}\,ds = \frac{1}{2\pi j}\int_{Br} e^{st}\,A(s)[\,1-B(s)e^{-sT}+\ldots]\,ds \qquad (2.2.1)$$

where $|B(s)e^{-sT}| < 1$. This procedure, which was used by Pipes [83] and by Elgerd [32], is cumbersome if many terms of the series must be inverted to obtain the time response accurately. Also the use of this technique to determine the transient response of systems with more complex transfer functions, becomes increasingly difficult.

The transient response of a linear system with transport lag can be obtained by inverting the Laplace transform of the response C(s). In lumped parameter system analysis, well-known expansion

theorems, such as Heaviside's, can be used to simplify inversion since the required values of the finite number of roots of the associated characteristic equation can easily be found through use of one of many techniques. But systems with transport lag give rise to characteristic equations having an infinite number of roots. Thus a closed-form expression, when it exists, is more laborious to find. These roots are considered poles since they are present on every sheet of the s-plane (i.e. they are roots when θ is increased by 2π). This is in contrast with roots of characteristic equations which are multivalued functions of s as well as transcendental, since in this case roots exist only on specific sheets (e.g. every other sheet for systems with distributed lag).

In a stable system interest often can be centered on the dominant roots and various special techniques for finding these roots have been developed [37, 23, 37, 71] . Once these roots are known, the corresponding response terms are easily found. Eisenberg [31] extended Chu's method [24] to feedback systems with transport lag. The resultant geometric interpretation, used in connection with parameter plane techniques (also extended to systems with transport lag by Eisenberg [29] formed a foundation for a synthesis procedure.

Knowledge of the location of the roots of the characteristic equation of a system with transport lag is, as for lumped parameter systems, the important consideration with respect to determination of stability. If one or more roots are in the right half-plane of the s-plane or one or more multiple roots are on the imaginary axis, the system is unstable; if all roots are in the left half-plane, the system is stable; if all are in the left half-plane except possible for single roots on the imaginary axis, the system is limitedly stable. Correspondingly, the nature of the stability as characterized by root location can be determined by Satche's modification of Nyquist's criterion [92]. A method developed by Eisenberg [29], detailed in Section 3.4, utilizes parameter plane techniques to determine the stability of feedback systems with transport lag. This technique permits stability analysis when two system parameters are varied simultaneously and is exact because the exponential term is used in the analysis thus taking into consideration all the roots of $F(s) = 0$. Many other techniques are advanced in numerous papers devoted to the topic of the stability of systems with transport lag [among which are 9, 10, 41, 87, 96, 97, 118].

Most of the standard frequency response techniques developed for lumped parameter control systems have been extended to this type of system. Application of some of these techniques is not much

more complicated than those used for control systems characterized by rational fraction transfer functions. Thus, Nyquist diagrams, Bode plots, dual stability plots such as Satche diagrams, and other associated frequency response techniques are easily applied. Analytic methods of obtaining transient response from frequency response, such as the work of Solodovnikov [109] are directly applicable.

Smith [103] introduces certain s-plane transformations that provide useful aids in the analysis of time delay systems. Also the root-locus technique, as first applied to single-loop system by Chu [23] is useable by appropriately combining the phase-angle loci stemming from e^{-sT} with those of the lumped parameter elements.

In 1951, Oldenbourg [76] noted that a given continuous time delayed problem can be approximately solved as if it were a step-control problem. Thus, the solution avoided transcendental equations. Boxer and Thaler [13] and Schroeder [94] then developed this idea by use of z-form and z-transform sampled data theory. Transient response is thereby obtained from the resulting approximations by use of well-known techniques in sampled data theory which were originally developed for use with lumped parameter systems. Pierre [81] also utilized sample data techniques to obtain the transient response of feedback systems with transport lag. This method

consists of first converting a continuous system to a sampled-data system by mathematically placing sampling and sample-and-hold circuits at various points in the system (usually before and after transport lag elements). A sampling rate 1/T is chosen consistent with Nyquist's sampling theorem, and by z-transform techniques the desired response is obtained as an infinite series of the form

$$C(z) = \sum_{n=0}^{\infty} a_n z^{-n} \qquad (2.2.2)$$

The coefficients a_n are therefore the values of the transient response at the sampling instant nT.

Another method of analysis appliicable to systems with transport lag depends on use of suitable rational approximations for e^{-sT}. A rather simple approach involves substituting a truncated Maclaurin series expansion for e^{-sT} in the characteristic equation: thus obtaining the characteristic equation of an approximating lumped parameter system. There is, however, no simple criterion which enables determination of the domain of validity of the results obtained by use of this so generated approximating system. In fact Pinney [82] states:

> "this method is invalid (in the large) and should never be used, for however small their coefficients may be, higher derivative terms must not be neglected in solving a differential equation."

This is illustrated for example by use of an alternate replacement for e^{-sT} based on the definition

$$e^{-sT} = \lim_{n \to \infty} 1/[\,1 + s\,(T/n)\,]^{n} \qquad (2.2.3)$$

and thus replacement of e^{-sT} by

$$e^{-sT} = 1/[\,1 + s(T/n)\,]^{n} \qquad (2.2.4)$$

For small values of n, however, the approximation of (2.2.4) is crude and use of it yields poor results in general.

A more accurate characterization of e^{-sT} is based on use of Padé approximations [61, 63, 111, 118, 125] . Other rational approximations of e^{-sT} have also been given by [4, 108] . These approximations are especially useful in analog simulation of a system.

Smith [101, 105] proposed a method of controlling systems with transport lag. His scheme requires inclusion of a model of the plant and of the time delay in the compensator of the system. If the model accurately describes the system, loop gain can be set at a value which yields specified steady state error and adequate system performance. Schliessmann [93] obtains a similar controller through use of a somewhat more direct analytic technique. It is of interest to note that he shows, by illustrative example, that a slight difference between the time delay of the plant and that of the model

may lead in some cases to system instability. This same result was also found by Eisenberg [31]. Buckley [15] compares feed-forward controllers, conventional controllers and Smith type (deadtime) controllers. His study also contains data taken on an experimental dye mixing process with time delay. Application of the above methods has also been of use in the control of a chemical reactor [64, 65].

Oldenbourg [76] determined the optimal location of the roots of the characteristic equation of a system controlled by a "step-by-step" controller which is designed by use of the criterion of minimization of the integral of a nonoscillatory error. A limitation on use of the approach is that if the error is to remain nonoscillatory, the length of the control interval should, in general, be greater than, or equal to, the time delay of the system. Specific analysis based on using a control interval greater than the time delay has been applied successfully in practice .

Kalman and Bertram [50] point out that the "state variable" approach can be extended to systems with time delay if the control signal at any instant is computed in accordance with the anticipated state of the plant T seconds later, T being equal to the time delay constant. This approach requires some method of predicting the state of the plant T seconds in advance: for example, by use of an analog or a digital model of the plant.

Kramer [53] utilizes dynamic programming techniques to obtain "optimum" control functions for control systems with transport lag. This work comprises continuation of the work initiated by Bellman and Kalaba on the solution of control problems by use of dynamic programming. The basis for this approach is Bellman's "Principle of Optimality", namely, "regardless of the choice of the initial control function, the succeeding functions must be chosen optimally with respect to the state resulting from the application of the initial function".

Other means of utilizing time delay elements for system control are given by Smith [104], So and Thaler [107] and Reswick [89]. Smith and So and Thaler utilized "posicast" control, i.e., the control of a system having lightly damped poles by a series time delay element. Reswick describes a controller of which the only adjustable parameter is a pure time delay. In that process dynamics are often time varying. He suggests the time delay of the controller be so instrumented that variation to compensate for changes in process dynamics is automatically effected.

2.3 Methods of Analysis and Synthesis for Systems with Distributed Parameter Elements Other than Transport Lag

Distributed parameter control systems are characterized by partial differential equations for which solutions can be obtained by classical methods [36] . Partial differential equations can also be solved by finite difference techniques, (see Kunz [55] , Forsythe and Rosenbloom [35]). These methods of solution are applied to open loop distributed parameter systems.

In feedback control system analysis and synthesis, the integral transform solution of distributed parameter control problems often provides a useable approach. For such, the Laplace, Mellin, Hankel, Fourier, sine, cosine and yet other transforms are available (as detailed in theory by, for example, Tranter [116] and Sneddon[106]). The most frequently employed of these is the Laplace transform. Laplace transformation of a linear differential equation with constant coefficients yields an algebraic polynomial equation. Therefore, systems described by linear differential equations can be represented and manipulated by blocks containing polynomial functions in block diagrams. In contrast to lumped parameter systems, the resulting

algebraic equations obtained for distributed parameter systems are not, in general, polynomial equations. Therefore, inversion of the associated Laplace transforms and the nature of the corresponding block diagram structure so obtained are more complicated.

Instead of dealing with non-rational characteristic equations, several approximating techniques utilizing lumped parameter elements are applicable:

1) The distributed parameter process could be approximated by a cascaded series (or other arrangement) of lumped parameter processes, reducing the system to one which can be described by ordinary differential equations.

2) In the process of solving the partial differential equations characterizing the distributed parameter processes, simplifying approximations could be introduced by use of the integral series method .

3) The distributed parameter elements in the transfer function of the system could be rationally approximated.

These approaches find considerable use in electric analog computer study although circuitry required may be extensive for even relatively simple distributed parameter problems. For example, Pierre [80] derived a series of rational polynomial approximants

to the transfer functions $\exp(-(sT))^{1/2}$ and the more general form $\exp\left[-\sqrt{(s+a)\cdot(s+b)}\right]$. Through use of these approximants, distributed parameter elements may be approximated by lumped parameter circuits.

Carlson [18] derived analog circuits for simulating $s^{1/2}$ and $1/s^{1/2}$. In study of various systems, he found that use of $K/s^{1/2}$ in the forward path of a simple control loop yields a fast initial rise to a step function input. After this initial rise, however, the output of the system might approach the steady state condition at a slower rate than in a conventional system using K/s. He thus concluded that, alternatively, a weighted transfer function which would afford the advantages stemming both from $K/s^{1/2}$ and K/s might better be used.

The nature of the stability of lumped parameter systems, and systems with transport lag can be determined by well known techniques. For distributed parameter control systems in general, however, there is no known all encompassing criterion for determination of stability other than that based on direct use of the transient time response of the system.

Papoulis [77] presents certain theorems concerning the stability of single loop control systems. For example, if the open loop step response is known and is of prescribed monotonic character, the closed loop system is stable over a known range of loop gain (the system may also be stable for gains that lie outside of this range).

Kadymov [49]considers the stability of systems that are characterized by equations of the form $(1-e^{-kV})/W(s) = 0$, where $V=(s^2c+sb+a)^{1/2}$. In this case, Nyquist and related criteria apply.

The root locus method is utilized for distributed parameter systems by Chu [23]and by Radant [86] . Chu presents a root locus procedure for systems involving $e^{-(sT)^{1/2}}$ that is analogous to his procedure for systems with transport lag but fails to take into account the double valued nature of the transfer function. Radant considers root locus plots for systems containing factors of the form $(s+a)^{1/2}$. The latter's procedure leads to two loci, only one of which, the principal locus, satisfies the original equation. Much of the advantage resulting from the use of root locus methods in lumped parameter analysis is lost when it is applied to distributed parameter systems because the rules permitting a quick sketch of loci do not apply in the extension although Ghausi and Kelly [40] have recently improved this situation.

Ball and Rekoff [7] consider the extension of root locus techniques to systems with distributed lag and propose the transformation $w^2 = s$. The w-plane thus provides a domain in which the transfer function is single valued and in which there are no branch points.

Bode plots and associated frequency response techniques are useful in the analysis of distributed parameter systems. This approach is used in the analysis and design of thin film RC distributed circuits, which are attaining considerable use in the field of microelectronics [20, 38 , 40, 44, 59].

The literature concerning the optimization of control systems distributed parameter elements other than those characterized by pure time delay is limited. Smith [103]suggests that the controller he advocates for systems with transport lag can be generalized to control distributed parameter systems of quite arbitrary types, but analytic justification and specific illustrative examples are not given.

Doetsch [27] notes that in applying Laplace transform techniques to systems with distributed lag, the Bromwich integral can be evaluated by considering a closed path of integration in a region of the s-plane which is simply connected and single valued. Pierre [79] points out that only singularities (i.e. roots of the characteristic

equation) on the principal sheet of the two sheeted Riemann surface representation of the s-plane need be considered in determining the transient response. Pierre also extends the sampled data approach for determining transient response to systems with distributed parameter elements.

CHAPTER 3

DEVELOPMENT OF THE PARAMETER PLANE TECHNIQUE

3.1 Introduction

The parameter plane technique originated in Eastern Europe and until recently little information about it has been reported in English language technical literature. This technique considers the closed-loop structure of a control system and, in particular, is an analysis of the roots of the characteristic equation of the closed-loop system when one or more (usually two) of the system parameters are varied. By contrast, the root locus technique developed by Evans [34]is a method in which only one system parameter can be varied and where the open-loop system is the basis for analysis and synthesis.

The work of Vishnegradski [120], Neimark [72] , Mitrovic [69] , Siljak [99], and Eisenberg [29] in parameter plane is pertinent to this dissertation and will be outlined in this chapter. In addition, work performed by Thaler[115], Hollister [47] , Moore [70] , Bitel[12] , as well as other work by Eisenberg [30] and Siljak [100] also provides insight into this technique. Presently, there are three main centers of research in parameter plane techniques within the United States. These are at the University

of Santa Clara (Siljak), the U.S. Naval Postgraduate School (Thaler), and The University of Pennsylvania (Eisenberg).

The contributions of Vishnegradski and Neimark have been summarized in the book by Meerov [68], and in a dissertation by Eisenberg [30]. Paragraphs from Meerov's book and Eisenberg's dissertation will be quoted in this chapter with only some minor editing for the purpose of achieving a consistent mathematical symbology. The work done by Mitrovic was described most adequately in a chapter of a book by Thaler [114]. A summary of this chapter also will be presented here. Similarly, Siljak's work was described in detail by Eisenberg and will be quoted herein.

3.2 Vishnegradski's Work[1]

I. A. Vishnegradski [120]considered the general third order characteristic equation of the form $Z^3 + \alpha Z^2 + \beta Z + 1 = 0$, and, in the co-ordinate system of the parameters α and β, plotted curves which divide the plane into stable and unstable regions. The parameters α and β are functions of the coefficients of the equation and are known as the Vishnegradski parameters and the curves mentioned above are called the Vishnegradski curves. In general, a

[1] Abstracted from Meerov [68], pp. 127-129

cubic equation can be reduced to a form in which it depends on the parameters α and β. Consider a third order equation

$$F(s) = a_0 s^3 + a_1 s^2 + a_2 s + a_3 = 0. \qquad (3.2.1)$$

Dividing by a_3 and introducing the notation,

$$b_0 = \frac{a_0}{a_3}, \quad b_1 = \frac{a_1}{a_3}, \quad b_2 = \frac{a_2}{a_3} \qquad (3.2.2)$$

gives,

$$F(s) = b_0 s^3 + b_1 s^2 + b_2 s + 1 = 0 \qquad (3.2.3)$$

Carrying out the following substitution of variables,

$$s = \frac{Z}{\sqrt[3]{b_0}} \qquad (3.2.4)$$

gives,

$$F(Z) = Z^3 + \frac{b_1}{\sqrt[3]{b_0^2}} Z^2 + \frac{b_2}{\sqrt[3]{b_0}} Z + 1 = 0. \qquad (3.2.5)$$

Defining

$$\frac{b_1}{\sqrt[3]{b_0^2}} = \alpha, \quad \frac{b_2}{\sqrt[3]{b_0}} = \beta \qquad (3.2.6)$$

and substituting (3.2.6) into (3.2.5) gives the Vishnegradski form

$$F(Z) = Z^3 + \alpha Z^2 + \beta Z + 1. \qquad (3.2.7)$$

If $\alpha > 0$ and $\beta > 0$, the Routh-Hurwitz criterion gives the stability conditions for equation (3.2.7) to be

$$\alpha \beta - 1 > 0 \qquad (3.2.8)$$

The equation of the stability boundary is obtained if, instead of the inequality sign in (3.2.8), the equality sign is introduced, whence

$$\alpha \beta = 1. \qquad (3.2.9)$$

This is the equation of a hyperbola, which divides the α β plane into the stable and unstable regions, and was the starting point for the parameter plane concept. The Vishnegradski curve is shown in Figure 3.2.1, where the regions of stability and instability are easily determined from the inequality of equation (3.2.8).

3.3 Neimark's Work

The concept of D-partition boundaries[2] was formulated by Neimark [72]. It is the basis for modern parameter plane techniques. Consider the general characteristic equation.

$$F(s) = s^n + a_{n-1}s^{n-1} + \ldots + a_1 s + a_0 = 0. \qquad (3.3.1)$$

[2]The symbol D represents the usual operational notation of differential equations, i.e., d/dt or s.

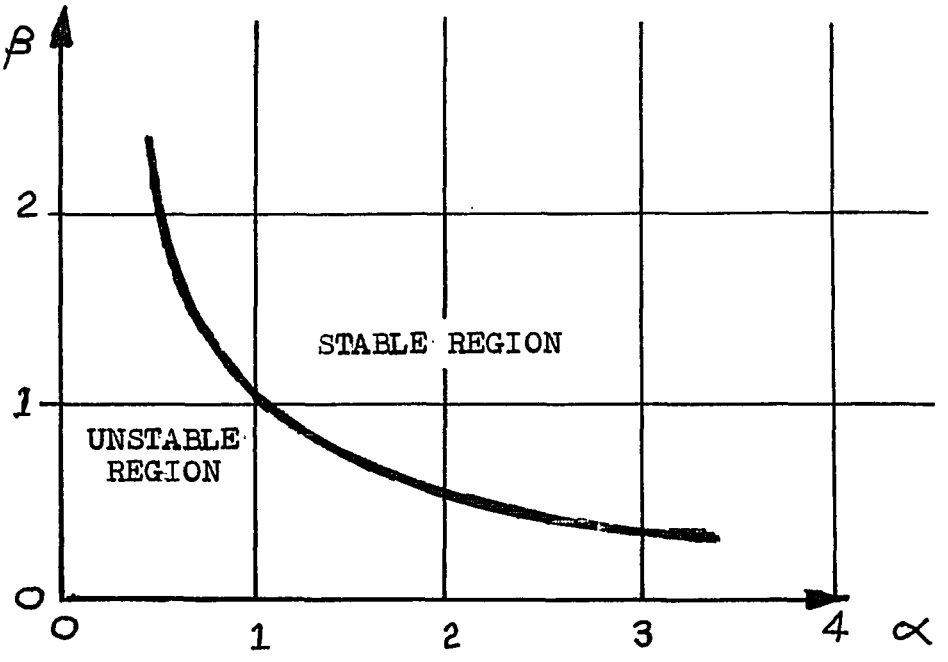

FIGURE 3.2.1 THE VISHNEGRADSKI CURVE

The values of the coefficient a_0, a_1, a_2, . . . , a_{n-1} may be interpreted geometrically as a point in an (n)-dimensional space. To each point of this space there correspond definite values of the coefficients and consequently definite values of the roots s_1, s_2, s_3, . . . , s_n of the characteristic equation. Thus, if a region, R, exists in this space such that all the roots of (3.3.1) lie to the left of the imaginary axis in the s-plane, then the hypersurface bounding R is called "boundary of the region of stability". When there are only two independent coefficients, this region is bounded by a plane; when there are three, by a three-dimensional surface, etc.

Since the coefficients, a_k, are functions of the system parameters, such as gains and time constants, stability regions can be plotted in terms of these system parameters. Consider a characteristic equation in which all the coefficients except two (for example, a_0 and a_1) are known. Suppose that for some definite values of a_0 and a_1 the characteristic equation has k roots lying to the left and n-k roots lying to the right of the imaginary axis in the s-plane (see Figure 3.3.1a). It follows that there is a curve on the a_0-a_1 plane that bounds a region in which each point defines a polynomial also having k roots lying to the left and n-k roots to the right of the imaginary axis (see Figure 3.3.1b). Neimark denoted this region

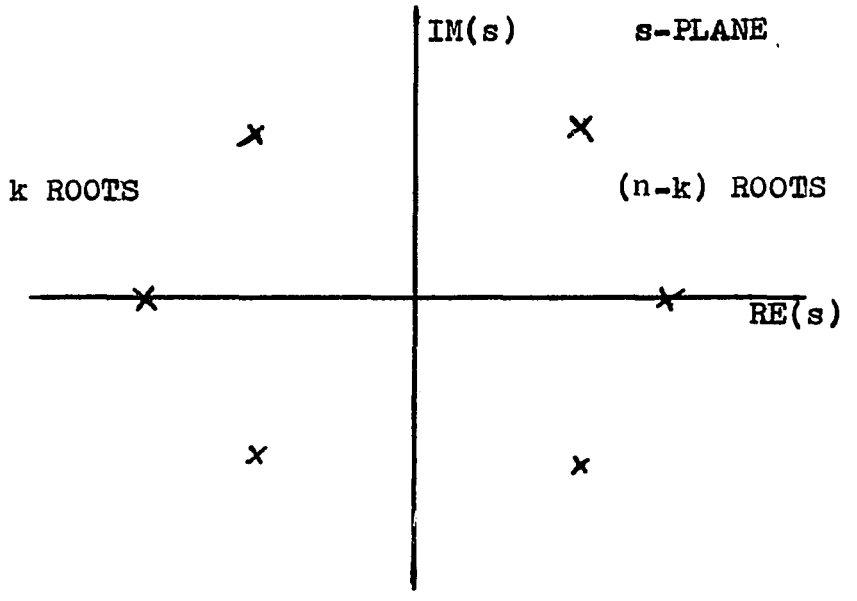

a- s-PLANE ROOT LOCATIONS

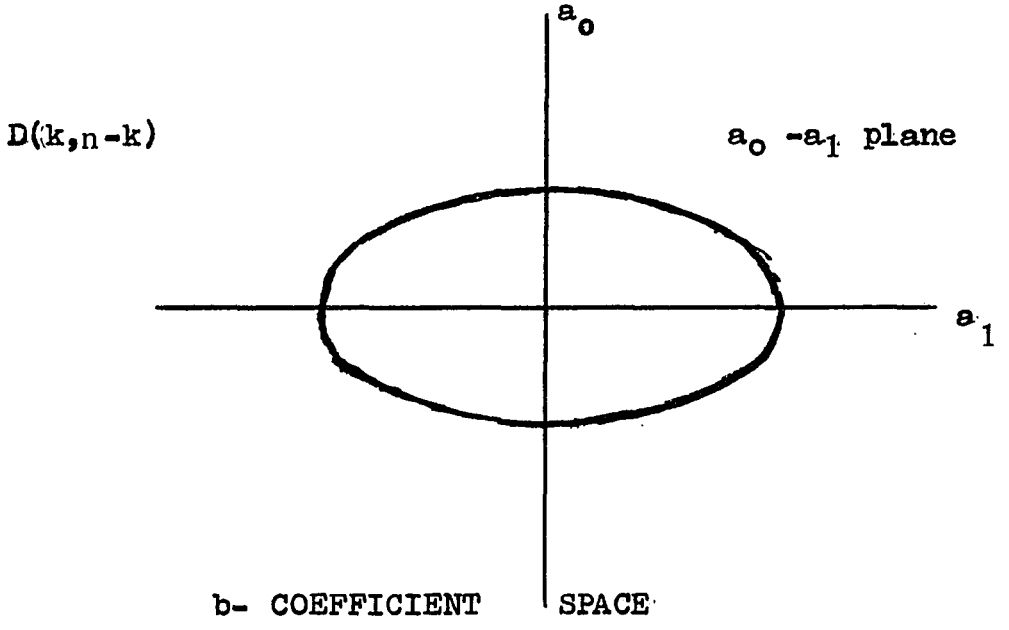

b- COEFFICIENT SPACE

FIGURE 3.3.1 s-PLANE ROOT LOCATIONS AND THE COEFFICIENT SPACE

by D (k, n-k) where, for example, if (3.3.1) is of third order (n=3), then in general the regions D(0, 3), D(1, 2), D(2, 1) and D(3, 0) can be found in the a_0-a_1 plane. The region D(3, 0) is the region of stability in the a_0-a_1 plane. The partition of the a_0-a_1 plane of (3.3.1) into regions corresponding to the same number of roots lying to the left of the imaginary axis is called the D-partition.

Thus the imaginary axis of the s-plane is the reflection of the boundary of the D-partition, and the crossing of the latter in the a_0-a_1 plane is represented by the roots in the s-plane crossing the imaginary axis. This suggests the method for determining the D-partition boundary: its equation is found in parametric form by replacing s by $j\omega$ in the given polynomial (where ω is the variable). From this equation the boundary may be constructed by varying ω from $-\infty$ to $+\infty$.

3.3.1 The construction of stability regions in the plane of one parameter--Neimark's technique.[3] Define α to be a complex parameter whose value is varied in order to investigate stability and assume that the characteristic equation can be reduced to the form

$$Q(s) + \alpha R(s) = 0 \text{ or } \alpha = -\frac{Q(s)}{R(s)} . \qquad (3.3.2)$$

[3] Abstracted from Meerov [68], pp. 123-125

Thus, for example, in the case of the equation

$$s^2 + s + \alpha = 0 \qquad (3.3.3)$$

it follows that

$$Q(s) = s^2 + s, \quad R(s) = 1. \qquad (3.3.4)$$

Only real values of α have any practical value. However, for now assume that α is complex and transform the imaginary axis in the s-plane into the α -plane. To do this set $s=j\omega$ in (3.3.2) giving

$$\alpha(j\omega) = -\frac{Q(j\omega)}{R(j\omega)} \qquad (3.3.5)$$

Separating real and imaginary parts gives

$$\alpha(j\omega) = u(\omega) + jv(\omega) \qquad (3.3.6)$$

By giving ω values from $-\infty$ to $+\infty$ a curve is constructed which is the transformation of the imaginary axis of the s-plane on the α -plane, i.e., the boundary of the D-partition in the α -plane.

If ω varies from $-\infty$ to $+\infty$ in the s-plane (Figure 3.3.2a) then the region of stability will always be on the left (the shaded side of Figure 3.3.2a). Since the mapping is conformal, the region to the left in the s-plane maps into the region in the α -plane that is to the left of the D-partition when ω varies from $-\infty$ to $+\infty$. Thus, proceeding along the boundary curve of the D-partition from the point corresponding to $\omega = -\infty$ to the point corresponding to $\omega = +\infty$,

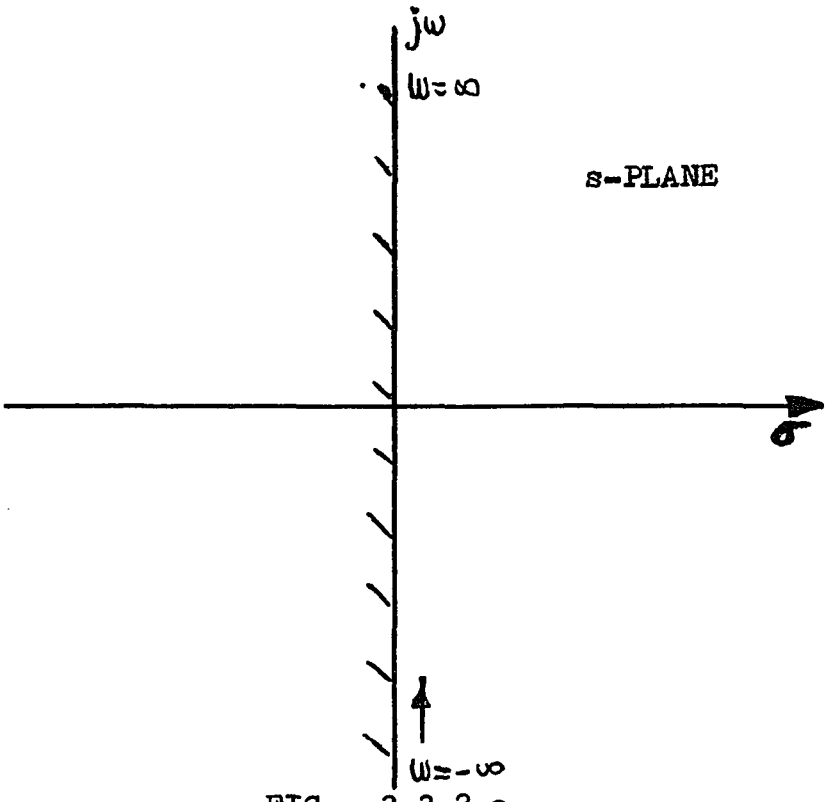

FIG. 3.3.2 a

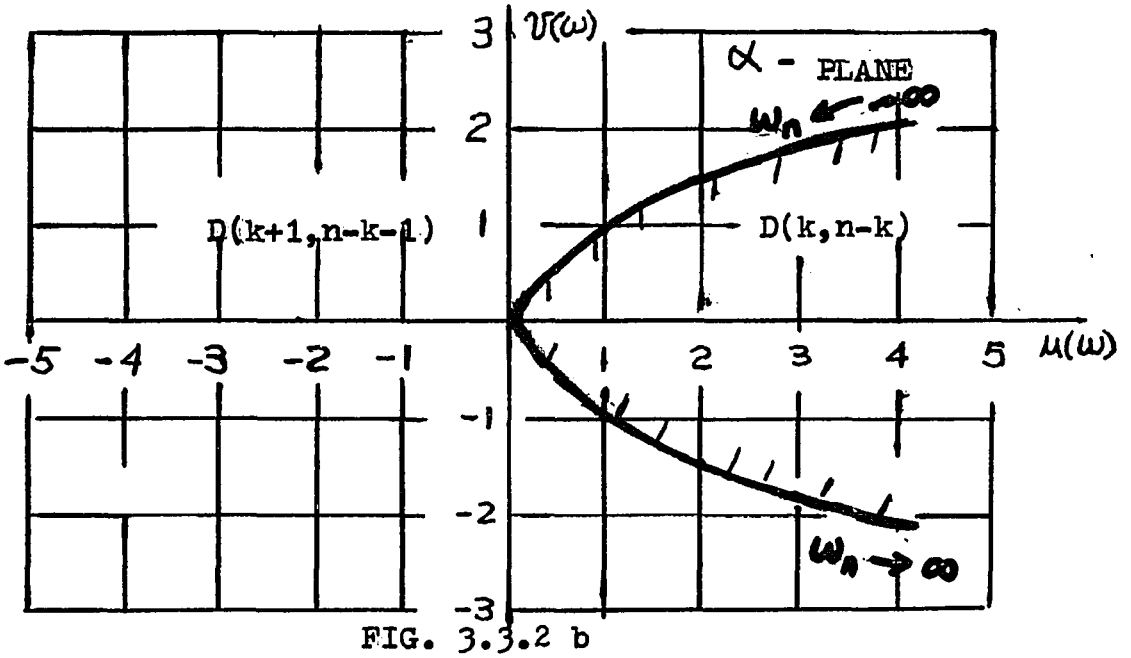

FIG. 3.3.2 b

FIGURE 3.3.2 D- PARTITION BOUNDARIES

the curve is shaded on the left (Figure 3.3.2b). If α takes on a series of values such that the boundary of the D-partition in the α -plane is crossed from the shaded to the unshaded side, then in the s-plane one root has crossed the imaginary axis, passing from the left-hand plane to the right-hand plane.

Thus, it is sufficient to know the distribution of the roots relative to the imaginary axis for any one arbitrary value of α (α is usually set to zero for this determination) in order to determine the distribution for any other value of α .

3.3.2 The construction of stability regions in the plane of two parameters--Neimark's Technique. Neimark extended his technique discussed in the previous section to account for the variation of two system parameters [72]. Since this is basically an extension of Vishnegradski's method, the resulting curves are called the generalized Vishnegradski diagrams. A Vishnegradski diagram is a plane of any two real parameters of a system in which the lines separating the region of stability are plotted. The Vishnegradski diagram may thus be obtained by constructing the D-partition of the plane of two parameters.

Suppose that the coefficients of the characteristic equation (3.3.1) of the system depend on two parameters, α and β , and further assume that the parameters enter into the equation linearly, so that this

equation can be reduced to the form

$$\alpha\, Q(s) + \beta\, P(s) + R(s) = 0. \qquad (3.3.7)$$

Substituting $s = j\omega$ into (3.3.7) gives

$$\alpha\, Q(j\omega) + \beta\, P(j\omega) + R(j\omega) = 0 \qquad (3.3.8)$$

Now denoting

$$\begin{aligned} Q(j\omega) &= Q_1(\omega) + jQ_2(\omega) \\ P(j\omega) &= P_1(\omega) + jP_2(\omega) \\ R(j\omega) &= R_1(\omega) + jR_2(\omega) \end{aligned} \qquad (3.3.9)$$

equation (3.3.8) can be written in the following form

$$\alpha\, Q_1(\omega) + \beta P_1(\omega) + R_1(\omega) + j[\alpha\, Q_2(\omega) + \beta\, P_2(\omega) + R_2(\omega)] = 0 \qquad (3.3.10)$$

This yields two equations for the determination of α and β which satisfy equation (3.3.8), namely,

$$\begin{aligned} \alpha\, Q_1(\omega) + \beta P_1(\omega) + R_1(\omega) &= 0 \\ \alpha\, Q_2(\omega) + \beta\, P_2(\omega) + R_2(\omega) &= 0 \end{aligned} \qquad (3.3.11)$$

Solving equations (3.3.11) for α and β, gives,

$$\alpha = \frac{\begin{vmatrix} -R_1(\omega) & P_1(\omega) \\ -R_2(\omega) & P_2(\omega) \end{vmatrix}}{\begin{vmatrix} Q_1(\omega) & P_1(\omega) \\ Q_2(\omega) & P_2(\omega) \end{vmatrix}}, \qquad \beta = \frac{\begin{vmatrix} Q_1(\omega) & -R_1(\omega) \\ Q_2(\omega) & -R_2(\omega) \end{vmatrix}}{\begin{vmatrix} Q_1(\omega) & P_1(\omega) \\ Q_2(\omega) & P_2(\omega) \end{vmatrix}} \tag{3.3.12}$$

Equations (3.3.11) are valid only for those values of ω at which equations (3.3.11) remain linearly independent and compatible. See Meerov [68] for a complete discussion of this point. The shading rule now involves the following procedure. For all ω values, at which:

$$\Delta = \begin{vmatrix} Q_1(\omega) & P_1(\omega) \\ Q_2(\omega) & P_2(\omega) \end{vmatrix} > 0 \tag{3.3.13}$$

the left-hand side of the boundary is shaded; when $\Delta < 0$ the right-hand side of the boundary is shaded [68] . Hence, if α or β takes on a series of values such that the boundary of the D-partition in the α - β plane is crossed from a shaded side to an unshaded side, then in the s-plane one[4] root has crossed the imaginary axis from the

[4] In most practical systems the α -β plot for negative values of ω will lie directly over the plot for positive values of ω . However, the sign of Δ will usually be such that the shading of the plot will always be on the same side. The result is a doubly shaded plot indicating that two roots leave the left-hand s-plane when the D-partition is crossed from a shaded side to an unshaded side. This is the case when, for example, a pair of complex conjugate roots crosses the imaginary axis in the s-plane.

left-hand plane to the right-hand plane.

Having obtained regions in the $\alpha - \beta$ plane with an equal number of roots to the left of the imaginary axis, it is then necessary to establish whether a region of stability does or does not exist. This is accomplished by choosing an arbitrary point in a region and verifying the stability of the original equation in which the co-ordinates of the chosen points have been substituted for α and β. This stability verification can be performed by using any one of the standard stability tests.

3.4 Mitrovic's Method

Mitrovic [69] utilized the general concept of the parameter plane and the basic theorem of Cauchy. His contribution was to depart from the $j\omega$ axis and move out into the entire s-plane. The method is explained as follows.[5] Consider the equation

$$F(s) = a_n s^n + a_{n-1} s^{n-1} + \ldots + a_2 s^2 + a_1 s + a_0 = 0 \qquad (3.4.1)$$

which may be considered the characteristic equation of a closed-loop system. Assume that all the roots are in the left-hand half of the s-plane so that equation (3.4.1) may be factored to give

[5] This section follows Thaler's interpretation of Mitrovic's work as presented in Chapter 10 of Reference 114 .

$$F(s) = a_n(s + r_1)(s + r_2)(s + r_3) \ldots (s + r_n) = 0 \qquad (3.4.2)$$

Figure 3.4.1 shows a few of these roots plotted on the s-plane and indicates the vectors which represent the factors of equation (3.4.2). Note that in equation (3.4.2) the angle associated with F(s) is the sum of the angles of all the factors and is therefore the algebraic sum of all the angles associated with the vectors in Figure 3.4.1.

It is apparent that if the point s is allowed to move along any selected path, the angles of all the vectors will change as s moves. If any path is selected which is a closed path enclosing all the roots, then each of the vectors makes a complete revolution as s traverses this path. Assume counterclockwise movement of s along such a closed path; then the vectors rotate counterclockwise and the angle of F(s) goes through a total positive angle of $n(2\pi)$, where n is the number of roots encircled. To check absolute stability the selected contour of the s-plane must encircle the entire left-hand plane. Since the order of the equation is known to be n, the number of roots is also known to be n and the F(s) curve on the F(s) plane must encircle the origin n times if all the roots are enclosed by the contour. If there are fewer than n encirclements, some roots lie outside the contour, which means they are in the right-hand half-plane, and the system is therefore absolutely unstable.

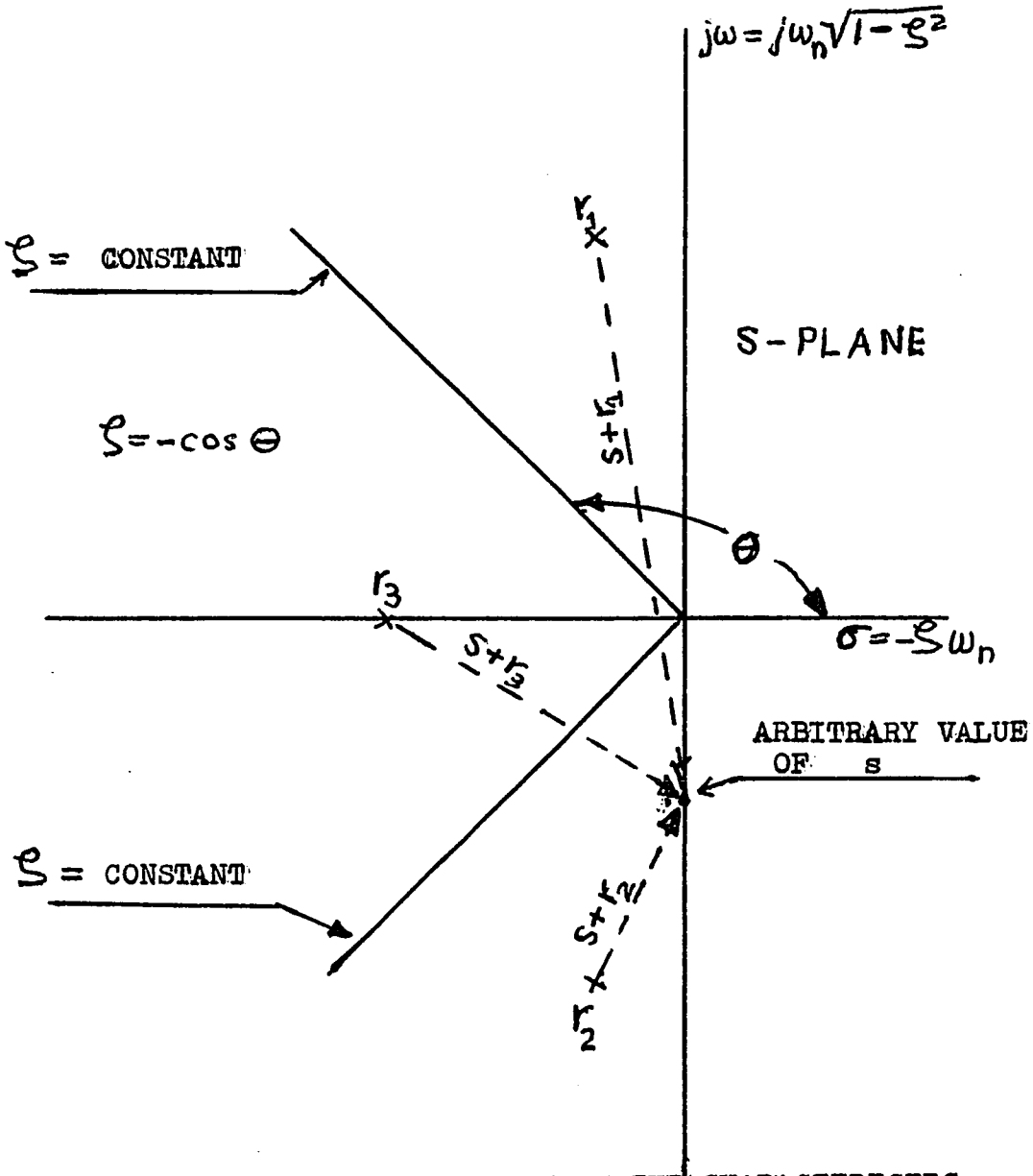

FIGURE 3.4.1 REPRESENTATION OF THE CHARACTERISTIC EQUATION ON THE s-PLANE

In a like manner the contour on the s-plane may follow a locus of constant $\zeta \neq 0$ (radial lines on Figure 3. 4. 1) and close with a circular arc of very large radius (often infinity). Note that when the contour is the imaginary axis the value of ζ is zero. A constant $\zeta \neq 0$ contour does not enclose the entire left half of the s-plane, but may enclose all the roots, in which case the number of encirclements by the F(s) curve is once again the number n. In addition, if all the roots are thus enclosed, it guarantees that no roots have a value of ζ less than the value specified by the mapping contour. If the selected contour on the s-plane passes through a root, then for that particular value of s, F(s) = 0. This means that the polar plot on the F(s) plane must pass through the origin for such values. It should be noted that the contour on the s-plane for $\zeta = 1.0$ is the negative real axis and must pass through all the negative real roots of F(s).

The concept of mapping constant ζ lines is the basic contribution of Mitrovic's method and the algebraic manipulations arising out of this method are as follows. Let the contours selected for mapping be radial straight lines in the left-hand s-plane for any and all values of $0 \leq \zeta \leq 1$. Since the radial distance from the origin to any point on such a radial line is ω_n, then the values of s which are to be substituted in F(s) in the process of mapping are given by

$$s = \omega_n \cos\theta + j\,\omega_n \sin\theta = -\zeta\omega_n + j\,\omega_n\sqrt{1-\zeta^2} \tag{3.4.3}$$

where θ is the angle of the line ζ = constant (see Figure 3.4.1) and the values of s are in the second quadrant. Substituting equation (3.4.3) in equation (3.4.1), F(s) can be written in the following form.

$$F(s) = a_n\,\omega_n^{\,n}(-\zeta + j\sqrt{1-\zeta^2})^n + a_{n-1}\omega_n^{\,n-1}(-\zeta + j\sqrt{1-\zeta^2})^{n-1}$$
$$+ \ldots + a_2\,\omega_n^{\,2}(-\zeta + j\sqrt{1-\zeta^2})^2 + a_1\omega_n(-\zeta + j\sqrt{1-\zeta^2}) + a_0 = 0 \tag{3.4.4}$$

Mitrovic designates that coefficients a_1 and a_0 be considered variables where by definition a_1 is the α and a_0 is the β of Section 3.3.2.

If, for example, the characteristic equation is of sixth-order, equation (3.4.4) can be written as two simultaneous equations since the summation of the reals and imaginaries must go to zero independently. Solving these two equations for α and β gives

$$\alpha = a_2\,\omega_n(2\zeta) + a_3\omega_n^{\,2}(1 - 4\zeta^2) + a_4\,\omega_n^{\,3}(-4\zeta + 8\zeta^3)$$
$$+ a_5\,\omega_n^{\,4}(-1 + 12\zeta^2 - 16\zeta^4) + a_6\omega_n^{\,5}(6\zeta - 32\zeta^3 + 32\zeta^5) \tag{3.4.5}$$

$$\beta = a_2\omega_n^2 + a_3\omega_n^3(-2\zeta) + a_4\omega_n^4(-1 + 4\zeta^2) + a_5\omega_n^5(4\zeta - 8\zeta^3) + a_6\omega_n^6(1 - 12\zeta^2 + 16\zeta^4) \tag{3.4.6}$$

The functions which appear in the coefficients do not depend on the order of the equation; i.e., for a fourth-order equation merely discard all the terms above the a_4 terms, etc. This means that these coefficients may be computed and tabulated for selected values of ζ; then the tables are used when applying this method. Furthermore, a general formula may be obtained for each coefficient so that the coefficients of high-order terms are readily obtained as needed. To obtain the formula for the coefficients, it is first desirable to rearrange (3.4.6) by factoring out $-\omega_n^2$:

$$\beta = -\omega_n^2\left[a_2(-1) + a_3\omega_n(2\zeta) + a_4\omega_n^2(1 - 4\zeta^2) + a_5\omega_n^3(-4\zeta + 8\zeta^3) + a_6\omega_n^4(-1 + 12\zeta^2 - 16\zeta^4)\right] \tag{3.4.7}$$

Comparison of equation (3.4.7) with (3.4.5) shows that identical functions appear in both. Thus it is convenient to define

$$\phi_0(\zeta) = 0, \phi_1(\zeta) = -1, \phi_2(\zeta) = 2\zeta$$
$$\phi_3(\zeta) = 1 - 4\zeta^2, \phi_4(\zeta) = -4\zeta + 8\zeta^3$$
$$\phi_5(\zeta) = -1 + 12\zeta^2 - 16\zeta^4 \tag{3.4.8}$$

From equations (3. 4. 8) it is readily seen that each successive $\phi(\zeta)$ may be obtained from the two preceding $\phi(\zeta)$'s, according to the general formula

$$\phi_k(\zeta) = -[\,2\zeta\phi_{k-1}(\zeta) + \phi_{k-2}(\zeta)\,] \quad \text{for } k \geq 2 \tag{3.4.9}$$

The equations for α and β for application to any order equation are then:

$$\alpha = a_2\omega_n\phi_2(\zeta) + a_3\omega_n^2\phi_3(\zeta) + a_4\omega_n^3\phi_4(\zeta) + \ldots + a_n\omega_n^{n-1}\phi_n(\zeta) \tag{3.4.10}$$

$$\beta = -\omega_n^2[\,a_2\phi_1(\zeta) + a_3\omega_n\phi_2(\zeta) + a_4\omega_n^2\phi_3(\zeta) + \ldots + a_n\omega_n^{n-2}\phi_{n-1}(\zeta)\,] \tag{3.4.11}$$

Equations (3. 4. 10) and (3. 4. 11) are the fundamental tools in Mitrovic's method. The characteristic equation to be analyzed is used only to read off the values of its coefficients, which are then substituted into equations (3. 4. 10) and (3. 4. 11). The value of ζ is selected as desired; $\phi_k(\zeta)$ values are read from a previously tabulated table of $\phi_k(\zeta)$ functions and substituted into the equations. Thus all values in the equations are defined numerically except α, β and ω_n, so it is a simple matter to insert a sequence of values of ω_n and plot

a curve of α versus β . The points of the α - β curve define regions of absolute and relative stability in the s-plane. Figure 3.2.1 shows a typical region of absolute stability for a given characteristic equation.

3.5 Siljak's Methods

In 1964, D. D. Siljak[6] extended Mitrovic's method so that the variable parameters α and β could appear as coefficients of any two terms of the system characteristic equation [98]. Thus, the limitation that only the coefficients a_0 and a_1 of the characteristic equation be variable was removed. This work was then generalized once again by Siljak [99] in 1964 by developing a method whereby the two variable parameters α and β could appear linearly in all the coefficients of the characteristic equation, i. e., for example in the form,

$$F(s) = (\alpha b_0 + \beta c_0 + d_0) + (\alpha b_1 + \beta c_1 + d_1)s + \ldots + (\alpha b_n + \beta c_n + d_n)s^n = 0 \qquad (3.5.1)$$

The first generalization is described in [98] . Of greater interest is Siljaks second generalization. Consider the characteristic equation

$$F(s) = \sum_{k=0}^{n} a_k s^k = 0 \qquad (3.5.2)$$

[6] This section was abstracted from Eisenberg[30] pp. 22,23,26 and 28. It References [98 , 99].

Let s^k in the above equation be expressed as

$$s^k = \omega_n^k [\ T_k(-\zeta) + j\sqrt{1-\zeta^2}\ U_k(-\zeta)\ ] \qquad (3.5.3)$$

where

$$T_k(-\zeta) = (-1)^k T_k(\zeta) \text{ and } U_k(-\zeta) = (-1)^{k+1} U_k(\zeta) \qquad (3.5.4)$$

The $T_k(\zeta)$ and $U_k(\zeta)$ are Chebyshev functions of the first and the second kind, respectively. The argument ζ of these functions is $0 \leq |\zeta| \leq 1$, but for stable systems $0 \leq \zeta \leq 1$. The functions $T_k(\zeta)$ and $U_k(\zeta)$ may be obtained by applying the recurrence formulae

$$\begin{aligned} T_{k+1}(\zeta) - 2\zeta T_k(\zeta) + T_{k-1}(\zeta) &= 0 \\ U_{k+1}(\zeta) - 2\zeta U_k(\zeta) + U_{k-1}(\zeta) &= 0 \end{aligned} \qquad (3.5.5)$$

with $T_0(\zeta) = 1$, $T_1(\zeta) = \zeta$, $U_0(\zeta) = 0$, and $U_1(\zeta) = 1$. Since the functions $T_k(\zeta)$ and $U_k(\zeta)$ play an important role in future developments, their numerical values for pertinent values of ζ are given in Table 3.5.1. Substituting (3.5.3) into (3.5.2), and then applying the condition that the summation of the reals and the summation of the imaginaries must go to zero independently, gives

$$\begin{aligned} \sum_{k=0}^{n} a_k \omega_n^k\ T_k(-\zeta) &= 0 \\ \sum_{k=0}^{n} a_k \omega_n^k\ U_k(-\zeta) &= 0 \end{aligned} \qquad (3.5.6)$$

ζ	T_0	T_1	T_2	T_3	T_4	T_5	T_6	T_7	T_8	T_9	T_{10}
0.00		0.00	−1.000	0.0000	1.00000	0.000000	−1.0000000	0.00000000	1.000000000	0.0000000000	−1.0000000000
0.05		0.05	−0.995	−0.1495	0.98005	0.347505	−0.9452995	−0.44203495	0.901096005	0.5321445505	−0.84788154995
0.10		0.10	−0.980	−0.2960	0.92080	0.480100	[illegible]	[illegible]	[illegible]	0.7842626560	−0.53889274880
0.15		0.15	−0.955	−0.4365	0.82405	0.683715	−0.6189355	−0.86939565	0.358116805	0.9768306915	−0.06506754755
0.20		0.20	−0.920	−0.5680	0.69280	0.845120	−0.3547520	−0.98702080	−0.040056320	0.9709982720	0.42845562880
0.25		0.25	−0.875	−0.6875	0.53125	0.953125	−0.0546875	−0.98046875	−0.435546875	0.7626953125	0.81689453125
0.30		0.30	−0.820	−0.7920	0.34480	0.998880	0.2545280	−0.84616320	−0.762225920	0.3888276480	0.99552250880
0.35		0.35	−0.755	−0.8785	0.14005	0.976535	0.5435245	−0.59606785	−0.960771995	−0.0764725465	0.90724121245
0.40		0.40	−0.680	−0.9440	−0.07520	0.883840	0.7822720	−0.25802240	−0.988689920	−0.5329295360	0.46234629120
0.45		0.45	−0.595	−0.9855	−0.29195	0.722745	0.9424205	0.12543345	−0.829530395	−0.8720108055	0.04472067005
0.50	1	0.50	−0.500	−1.0000	−0.50000	0.500000	1.0000000	0.50000000	−0.500000000	−1.0000000000	−0.50000000000
0.55		0.55	−0.395	−0.9845	−0.68795	0.227755	0.9384805	0.80157355	−0.053449595	−0.8633681045	−0.93625531995
0.60		0.60	−0.280	−0.9360	−0.84320	−0.075840	0.7521920	0.97847040	0.421972480	−0.4721034240	−0.98849658880
0.65		0.65	−0.155	−0.8515	−0.95195	−0.386035	0.4501045	0.97117085	0.812407605	0.0849590365	−0.70196085755
0.70		0.70	−0.020	−0.7280	−0.99920	−0.670880	0.0599680	0.75483520	0.996801280	0.6406865920	−0.09984005120
0.75		0.75	0.125	−0.5625	−0.96875	−0.890625	−0.3671875	0.33984375	0.876953125	0.9755859375	0.58642578125
0.80		0.80	0.280	−0.3520	−0.84320	−0.997120	−0.7521920	−0.20638720	0.421972480	0.8815431680	0.98849658880
0.85		0.85	0.445	−0.0935	−0.60395	−0.933215	−0.9825155	−0.73706135	−0.270488795	0.2772303985	0.74178047245
0.90		0.90	0.620	0.2160	−0.23120	−0.632160	−0.9066880	−0.99987840	−0.893093120	−0.6076892160	−0.20074746880
0.95		0.95	0.805	0.5795	0.29605	−0.017005	−0.3283595	−0.60687805	−0.824708795	−0.9600686605	−0.99942165995
1.00		1.00	1.000	1.0000	1.00000	1.000000	1.0000000	1.00000000	1.000000000	1.0000000000	1.00000000000

ζ	U_{-1}	U_0	U_1	U_2	U_3	U_4	U_5	U_6	U_7	U_8	U_9	U_{10}
0.00				0.0	−1.00	0.000	1.0000	0.00000	−1.000000	0.0000000	1.00000000	0.000000000
0.05				0.1	−0.99	−0.199	0.9701	0.29601	−0.940499	−0.3900599	0.90149301	0.480209201
0.10				0.2	−0.96	−0.392	0.8816	0.56832	−0.767936	−0.7219072	0.62355456	0.846618112
0.15				0.3	−0.91	−0.573	0.7381	0.79443	−0.490771	[illegible]	0.21640261	1.009300083
0.20				0.4	−0.84	−0.720	[illegible]	0.95424	−0.163904	−1.0198016	−0.24401664	0.922194944
0.25				0.5	−0.75	−0.875	0.3125	1.03125	0.203125	−0.9296875	−0.66796875	0.595703125
0.30				0.6	−0.64	−0.984	0.0496	1.01376	0.558656	−0.6785664	−0.96579584	0.099088896
0.35				0.7	−0.51	−1.057	−0.2299	0.89607	0.857149	−0.2960657	−1.06439499	−0.449010793
0.40				0.8	−0.36	−1.088	−0.5104	0.67968	1.054144	0.1636352	−0.92323584	−0.902223872
0.45				0.9	−0.19	−1.071	−0.7739	0.37449	1.110941	0.6253569	−0.54811979	−1.118664711
0.50	−1	0	1	1.0	0.00	−1.000	−1.0000	0.00000	1.000000	1.0000000	0.00000000	−1.000000000
0.55				1.1	0.21	−0.869	−1.1659	−0.41349	0.711061	1.1956571	0.60416181	−0.531079109
0.60				1.2	0.44	−0.672	−1.2464	−0.82368	0.257984	1.1332608	1.10192896	0.189053952
0.65				1.3	0.69	−0.403	−1.2139	−1.17507	−0.313691	0.7672717	1.31114421	0.937215773
0.70				1.4	0.96	−0.056	−1.0384	−1.39776	−0.918464	0.1119104	1.07513856	1.393282584
0.75				1.5	1.25	0.375	−0.6875	−1.40625	−1.421875	−0.7265625	0.33203125	1.224609375
0.80				1.6	1.56	0.896	−0.1264	−1.09824	−1.630784	−1.5110144	−0.78683904	0.252071936
0.85				1.7	1.89	1.513	0.6821	−0.35343	−1.282931	−1.8275527	−1.82390859	−1.273091903
0.90				1.8	2.24	2.232	1.7776	0.96768	−0.035776	−1.0320768	−1.82196224	−2.247455232
0.95				1.9	2.61	3.059	3.2021	3.02499	2.545381	1.9112339	0.89596341	−0.108903421
1.00				2.0	3.00	4.000	5.0000	6.00000	7.000000	8.0000000	9.00000000	10.000000000

TABLE 3.5.1 VALUES OF $T_k(\zeta)$ AND $U_k(\zeta)$ FOR PERTINENT VALUES OF ζ

REPRINTED FROM REFERENCE [99]

Now, consider the coefficients a_k to be linear functions of variable system parameters α and β as follows

$$a_k = \alpha b_k + \beta c_k + d_k \tag{3.5.7}$$

Then equations (3.5.6) may be rewritten as

$$\begin{aligned} &\alpha B_1(\zeta, \omega_n) + \beta C_1(\zeta, \omega_n) + D_1(\zeta, \omega_n) = 0 \\ &\alpha B_2(\zeta, \omega_n) + \beta C_2(\zeta, \omega_n) + D_2(\zeta, \omega_n) = 0 \end{aligned} \tag{3.5.8}$$

where (omitting the arguments ζ, ω_n)

$$\begin{aligned} B_1 &= \sum_{k=0}^{n} (-1)^k b_k \omega_n^k U_{k-1}(\zeta) \quad , \qquad B_2 = \sum_{k=0}^{n} (-1)^k b_k \omega_n^k U_k(\zeta) \\ C_1 &= \sum_{k=0}^{n} (-1)^k c_k \omega_n^k U_{k-1}(\zeta) \quad , \qquad C_2 = \sum_{k=0}^{n} (-1)^k c_k \omega_n^k U_k(\zeta) \\ D_1 &= \sum_{k=0}^{n} (-1)^k d_k \omega_n^k U_{k-1}(\zeta) \quad , \qquad D_2 = \sum_{k=0}^{n} (-1)^k d_k \omega_n^k U_k(\zeta) \end{aligned} \tag{3.5.9}$$

Equations (3.5.8) are simultaneous equation in two unknowns, α and β, which may be solved thus:

$$\alpha = \frac{C_1 D_2 - C_2 D_1}{B_1 C_2 - B_2 C_1} \qquad \beta = \frac{B_2 D_1 - B_1 D_2}{B_1 C_2 - B_2 C_1} \tag{3.5.10}$$

The application of the second generalized method is identical to the original Mitrovic's method. The second generalization, however, is the most useful since the variable parameters, α and β, can appear

in the coefficients of the characteristic equation in the least restrictive manner. Refer to equation (3.5.7).

3.6. Eisenberg's Work

Parameter plane techniques have been extended to feedback systems with transport lag [29, 30]. A brief summary of this work is presented below.

Consider the feedback system with transport lag of Figure 3.6.1. The characteristic equation of the closed loop system is given by

$$F(s) = N(s)\exp(sT) + D(s) = \sum_{k=0}^{n} a_k(s)\, s^k = 0 \qquad (3.6.1)$$

where

$$s = -\zeta\omega_n + j\,\omega_n\sqrt{1-\zeta^2} = \sigma + j\,\omega$$

and where σ, ω, ζ, ω_n are defined and related in Figure 3.6.2. The coefficients of (3.6.1) can be expressed by

$$a_k(s) = \alpha b_k + \alpha c_k e^{sT} + \beta d_k + \beta e_k e^{sT} + f_k + g_k e^{sT} \qquad (3.6.2)$$

where α and β are system parameters to be varied (i.e., a system gain, time constant), b_k, c_k, d_k, e_k, f_k, and g_k are known system constants

gain, time constant), b_k, c_k, d_k, e_k, f_k, and g_k are known system constants

that system parameters α and β can be expressed by (3.5.10), where

$$B_1 = \sum_{k=0}^{n} \omega_n^k \left(Z_{k0} b_k + e^{-\phi} c_k Z_{k1} \right) \qquad (3.6.3)$$

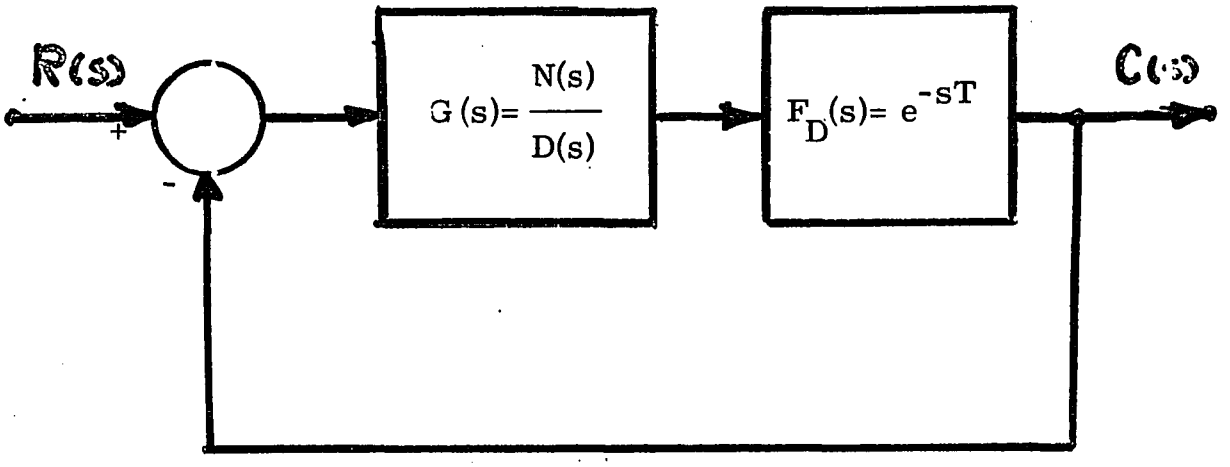

FIGURE 3.6.1 SYSTEM WITH TRANSPORT LAG - BLOCK DIAGRAM

$$
\begin{aligned}
C_1 &= \sum_{k=0}^{n}{}'' \omega_n^k \left(Z_{k0}\, d_k + e^{-\phi} e_k\, Z_{k1} \right) \\
D_1 &= \sum_{k=0}^{n}{}'' \omega_n^k \left(Z_{k0}\, f_k + e^{-\phi} g_k\, Z_{k1} \right) \\
B_2 &= \sum_{k=0}^{n}{}'' \omega_n^k \left(Z_{k2}\, b_k + e^{-\phi} c_k\, Z_{k3} \right) \\
C_2 &= \sum_{k=0}^{n}{}'' \omega_n^k \left(Z_{k2}\, d_k + e^{-\phi} e_k\, Z_{k3} \right) \\
D_2 &= \sum_{k=0}^{n}{}'' \omega_n^k \left(Z_{k2}\, f_k + e^{-\phi} g_k\, Z_{k3} \right)
\end{aligned}
\qquad (3.6.3)
$$

where

$$Z_{k0} = (-1)^k\, T_k(\xi)$$

$$Z_{k1} = (-1)^k\, T_k(\xi) \cos\theta - (-1)^{k+1} \sqrt{1-\xi^2}\, U_k(\xi) \sin\theta$$

$$Z_{k2} = (-1)^{k+1}\, U_k(\xi) \sqrt{1-\xi^2}$$

$$Z_{k3} = (-1)^{k+1}\, U_k(\xi) \sqrt{1-\xi^2} \cos\theta + (-1)^k\, T_k(\xi) \sin\theta$$

and where

$$
\begin{aligned}
\phi &= \zeta \omega_n T \\
\theta &= \omega_n T \sqrt{1-\zeta^2}
\end{aligned}
\qquad (3.6.4)
$$

and $T_k(\xi)$, $U_k(\xi)$ are Chebyshev functions of the first and second kind respectively subject to the relationships of equations (3.5.3), (3.5.4) and (3.5.5).

The absolute and relative stability of feedback systems with transport lag can be determined as a function of the two system parameters α and β through use of (3.5.10) in conjunction with (3.6.3) and (3.6.4). This method utilizes the expression for the transport lag exponential exp(-sT) and therefore considers the effect upon stability of all of the roots of the characteristic equation. The shading rules, for the $\alpha - \beta$ curves, and techniques for the determination of real roots of $F(s) = 0$ were also developed by Eisenberg for this type of system.

CHAPTER 4

STABILITY AND SINGULARITIES OF LINEAR FEEDBACK SYSTEMS WITH DISTRIBUTED PARAMETER ELEMENTS VIA THE PARAMETER PLANE

4.1 Introduction

Linear control systems containing distributed parameter elements are difficult to analyze due to the presence of a transcendental function in the system characteristic equation producing an infinite number of roots. This chapter treats systems containing distributed parameter elements in the form of terminated electrical transmission lines. These systems are assumed to be initially at rest and have the following transfer function.[1]

$$F_D(s) = \exp\left\{-d\left[(Ls + R)(Cs + G)\right]^{1/2}\right\} \qquad (4.1.1)$$

where the parameters L, C, R and G are the inductance, capacitance, resistance, and conductance per unit length; and where d is the length of the line and s is a complex variable. This transfer function is a double valued function of the complex variable s for all cases except transport lag (R = G = 0) and distortionless transmission (RC = LG) thereby making interpretation of singularities on the s-plane difficult.

---

[1] Systems with non-zero initial conditions are discussed in Appendix I.

Most of the investigations into feedback systems with distributed parameter elements have been restricted to transport and distributed lag networks. For example, Y. Chu [23] presented a phase-angle loci method that can be applied to systems with one free parameter (usually the system gain) as in the normal root locus method. However, Chu only treated the cases of transport and distributed lag and one must construct separate phase-angle loci for each of these cases. In addition, the complexity of Chu's method increases rapidly with the order of the system, since the root-locus is determined by first determining the phase-angle loci for all angles, not merely for the angle=180 degrees.

A method is presented for analyzing systems with distributed parameter elements in terms of two free system variables (such as a gain and a time constant). Furthermore, high-order systems can be handled as easily as low-order systems. The basic approach is the parameter plane representation of the closed-loop transfer function as introduced by Mitrovic [69], generalized by Siljak [99] and extended to systems with transport and distributed lag by Eisenberg [29]. The complexities introduced by the double-valued nature of the transfer function of the distributed parameter element are alleviated by use of results obtained by Pierre and Higgins [79]. A two sheeted Riemann surface is introduced upon which the system equations can be represented as single-valued functions. Other results of [79] are

used which focuses attention on one of the two sheets of this Riemann surface to determine system stability.[2]

If the closed loop transfer function, H(s), does not contain any singularities in the closed right half plane and is also absolutely integrable along the $j\omega$ axis of the s-plane, then h(t) is bounded. This can be shown by expressing h(t) as an inverse Fourier transform and taking its absolute value. Thus

$$|h(t)| = \frac{1}{2\pi} \left| \int_{-\infty}^{\infty} H(j\omega) \exp(j\omega t)\, d\omega \right| \leq \frac{1}{2\pi} \int_{-\infty}^{\infty} |H(j\omega)|\, d\omega \leq A \tag{4.1.2}$$

For the class of systems under consideration[3]

$$H(s) = \frac{N(s) \exp(-\gamma(s)\, d) / D(s)}{1 + N(s) \exp(-\gamma(s)\, d) / D(s)} \tag{4.1.3}$$

where N(s) and D(s) are polynomials of degree n and m respectively, $n \leq m$, and $\gamma(s)$ is given by (4.1.1). The absolute value of (4.1.3) on the $j\omega$ axis is

$$H(j\omega) = \frac{N(j\omega) \exp(-\mathrm{Re}[\gamma(j\omega)]\, d) / D(j\omega)}{1 + N(j\omega) \exp(-[\gamma(j\omega)]\, d) / D(j\omega)} \tag{4.1.4}$$

where $\mathrm{Re}[\gamma(j\omega)] > 0; |\omega| < \infty$. Since there are no singularities of H(s) on the $j\omega$ axis, the denominator of (4.1.4) is never zero and

$$H(j\omega) \leq A \exp(-\mathrm{Re}[\gamma(j\omega)]\, d); |\omega| < \infty \tag{4.1.5}$$

---

[2] System stability is defined in Section 1.1.

[3] This class of system is defined by Figure 4.2.1 and equation 4.1.1.

Equation (4.1.5) is absolutely integrable along the $j\omega$ axis and thus h(t) is asymptotically stable. The final value theorem applied to (4.1.3) yields $\lim_{t \to \infty} h(t) = 0$

4.2 Derivation of Parameter Plane Equations

Consider the time invariant linear feedback control system containing a distributed parameter network in the forward path as shown in Figure 4.2.1. The distributed parameter network is assumed to be an electrical transmission line terminated in its characteristic impedance (although the assumption of either its mechanical, thermal or fluid equivalent is equally valid). The transfer function of a terminated distributed parameter network is of the form

$$F_D(s) = e^{-\gamma(s)d} \tag{4.2.1}$$

where

$$\gamma(s) = + \left[(Ls + R)(Cs + G)\right]^{1/2} \tag{4.2.1a}$$

and where d is the length of the network, L, C, R and G are the inductance, capacitance, resistance and conductance per unit length and s is the complex variable

$$s = \sigma + j\omega = -\zeta\omega_n + j\omega_n\sqrt{1-\zeta^2} \tag{4.2.2}$$

where ζ is the dimensionless damping ratio and ω_n is the undamped natural frequency (see Figure 4.2.2). Substituting (4.2.2) into

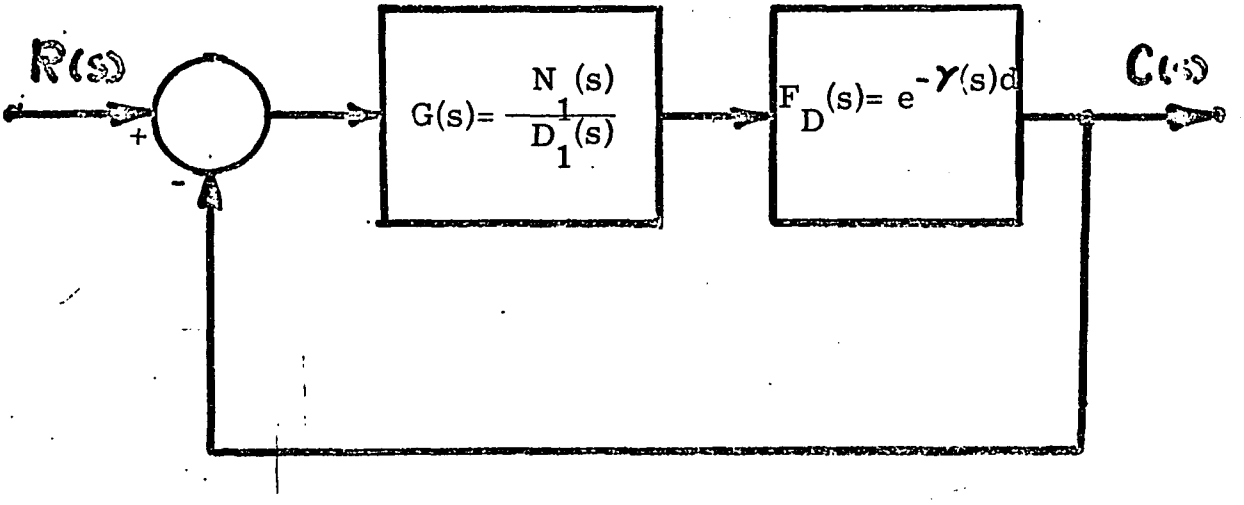

FIGURE 4.2.1 BLOCK DIAGRAM OF A SYSTEM WITH DISTRIBUTED PARAMETER ELEMENT

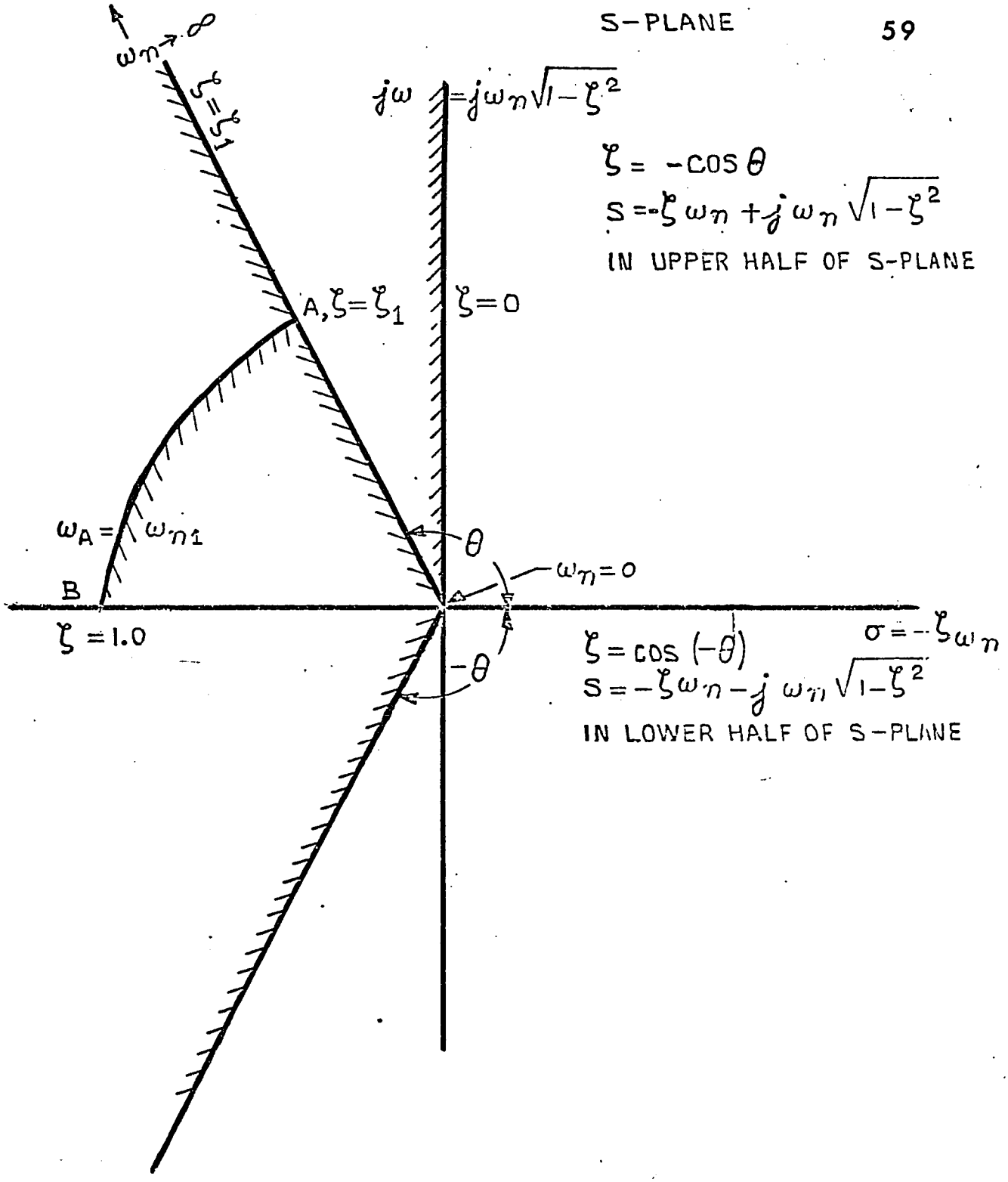

FIGURE 4.2.2 s-PLANE CONTOURS

(4.2.1) yields a general form for the transfer function

$$F_D(s) = e^{-\gamma(s)d} = e^{\psi(\omega_n, \zeta)} e^{-j\delta(\omega_n, \zeta)} \qquad (4.2.3)$$

where $e^{\psi(\omega_n, \zeta)}$ is the amplitude function and $e^{-j\delta(\omega_n, \zeta)}$ is the phase function. The system transfer function is given by

$$\frac{C}{R}(s) = \frac{N_1(s)}{D_1(s)e^{\gamma(s)d} + N_1(s)}$$

Substituting (4.2.3) into $\frac{C}{R}(s)$, noting $e^{+j\delta} = \cos\delta + j\sin\delta$ gives

$$\frac{C}{R}(s) = \frac{N_1(s)}{D_1(s)e^{-\psi}(\cos\delta + j\sin\delta) + N_1(s)} = \frac{N_1(s)}{F(s)} \qquad (4.2.4)$$

The stability of the system is determined by the location of the roots of the characteristic equation $F(s) = 0$. Setting $F(s) = 0$ yields[5]

$$F(s) = D_1(s)e^{-\psi}(\cos\delta + j\sin\delta) + N_1(s) = \sum_{k=0}^{n} a_k(s)s^k = 0 \qquad (4.2.5)$$

Since the $a_k(s)$ terms will be a function of $e^{\gamma(s)d}$ and will also contain the system parameters, the $a_k(s)$ terms are defined to include all possible linear[4] combinations of parameters. That is

$$a_k(s) = \alpha b_k + \alpha c_k e^{\gamma d} + \beta d_k + \beta e_k e^{\gamma d} + f_k + g_k e^{\gamma d} \qquad (4.2.6)$$

where α and β are the parameter plane variables which are to be related to two of the system parameters. This definition of $a_k(s)$ is a fairly standard one (see, for example, references [29] and [99]).

4 Other possibilities include non-linear combinations in which α and β appear as a product.

5 The symbol n in the summation represents the maximum degree of either $N_1(s)$ or $D_1(s)$ and is therefore finite.

If the complex variable is as defined in equation (4.2.2) then

$$s^k = \omega_n^k \left[T_k(-\zeta) + j\sqrt{1-\zeta^2}\, U_k(-\zeta) \right] \tag{4.2.7}$$

where $T(-\zeta)$ and $U(-\zeta)$ are Chebychev functions of the first and second kind, respectively [98], [99]. These functions can be evaluated through use of the following identities and recursion formulas

$$T_k(-\zeta) = (-1)^k\, T_k(\zeta), \quad U_k(-\zeta) = (-1)^{k+1}\, U_k(\zeta) \tag{4.2.8}$$

$$\begin{aligned} &T_{k+1}(\zeta) - 2\zeta\, T_k(\zeta) + T_{k-1}(\zeta) = 0 \\ &U_{k+1}(\zeta) - 2\zeta\, U_k(\zeta) + U_{k-1}(\zeta) = 0 \end{aligned} \tag{4.2.9}$$

where

$$T_0(\zeta) = 1, \; T_1(\zeta) = \zeta, \; U_0(\zeta) = 0, \; U_1(\zeta) = 1 \tag{4.2.10}$$

Substituting equations (4.2.6) and (4.2.7) into (4.2.5) and noting equation (4.2.8) yields

$$F(\omega_n, \zeta) = (\alpha B_1 + \beta C_1 + D_1) + j(\alpha B_2 + \beta C_2 + D_2) = 0 \tag{4.2.11}$$

where

$$\begin{aligned} B_1 &= \sum_{k=0}^{n} \omega_n^k \left(Z_{k0}\, b_k + e^{-\psi} c_k\, Z_{k1} \right) \\ C_1 &= \sum_{k=0}^{n} \omega_n^k \left(Z_{k0}\, d_k + e^{-\psi} e_k\, Z_{k1} \right) \\ D_1 &= \sum_{k=0}^{n} \omega_n^k \left(Z_{k0}\, f_k + e^{-\psi} g_k\, Z_{k1} \right) \\ B_2 &= \sum_{k=0}^{n} \omega_n^k \left(Z_{k2}\, b_k + e^{-\psi} c_k\, Z_{k3} \right) \end{aligned} \tag{4.2.12}$$

$$C_2 = \sum_{k=0}^{n} \omega_n^k \left(Z_{k2}\, d_k + e^{-\psi} e_k\, Z_{k3} \right)$$

$$D_2 = \sum_{k=0}^{n} \omega_n^k \left(Z_{k2}\, f_k + e^{-\psi} g_k\, Z_{k3} \right)$$

where

$$Z_{k0} = (-1)^k T_k(\zeta)$$

$$Z_{k1} = (-1)^k T_k(\zeta) \cos\delta - (-1)^{k+1} \sqrt{1-\zeta^2}\, U_k(\zeta) \sin\delta$$

$$Z_{k2} = (-1)^{k+1} U_k(\zeta) \sqrt{1-\zeta^2}$$

$$Z_{k3} = (-1)^{k+1} U_k(\zeta) \sqrt{1-\zeta^2} \cos\delta + (-1)^k T_k(\zeta) \sin\delta$$

Equations (4.2.12) are of the same form as equations derived by Eisenberg[29] for the case of transport lag. However, the variables ψ and δ in this case are generalized expressions for a distributed parameter element. Expressions for ψ and δ as a function of s-plane variables ω_n and ζ will be derived in the next section.

Since F(s) = 0, both the real and imaginary parts of (4.2.11) must be equal to zero. That is

$$\alpha B_1 + \beta C_1 + D_1 = 0, \qquad \alpha B_2 + \beta C_2 + D_2 = 0$$

giving

$$\alpha = \frac{C_1 D_2 - C_2 D_1}{\Delta} \qquad \beta = \frac{D_1 B_2 - D_2 B_1}{\Delta} \tag{4.2.13}$$

$$\Delta = B_1 C_2 - C_1 B_2$$

4.3 Derivation of Equations for ψ and δ

Given the transfer function $F_D(s)$ of equation (4.2.1) it is necessary to find expressions for variables $-\psi$ and δ as a function of both the complex plane parameters (ζ, ω_n) and the distributed parameter element variables d, L, C, R, and G. It will also be necessary to specify the appropriate signs of the functions $-\psi$ and δ in regions of the s-plane since (4.2.1) is a double-valued function of s. To accomplish this consider the function

$$\gamma\, d = d\, \sqrt{(Ls + R)(Cs + G)} \tag{4.3.1}$$

Substituting (4.2.2) into (4.3.1) and separating real and imaginary terms gives

$$\gamma\, d = d\, \sqrt{Re + jIm} \tag{4.3.2}$$

where

$$\begin{aligned} Re &= (\sigma L + R)(\sigma C + G) - \omega^2 LC \\ Im &= (\sigma L + R)\ \omega C + (\sigma C + G)\ \omega L \end{aligned} \tag{4.3.3}$$

Next, consider the function (Re + jIm). This function has an argument v given by

$$v = \tan^{-1} (Im/Re) \tag{4.3.4}$$

Equation (4.3.2) can be expressed in polar form as

$$\begin{aligned} \gamma\, d &= |A|\, e^{jv/2} = d\, (Re^2 + Im^2)^{1/4}\ e^{jv/2} \\ &= |A|\ \cos v/2 + j\ |A|\ \sin v/2 \end{aligned} \tag{4.3.5}$$

where the angles v and v/2 are shown in Figure 4.3.1. Note that the angle v consists of the sum of two angles v_1 and v_2 which are associated with the functions (Ls + R) and (Cs + G). Thus

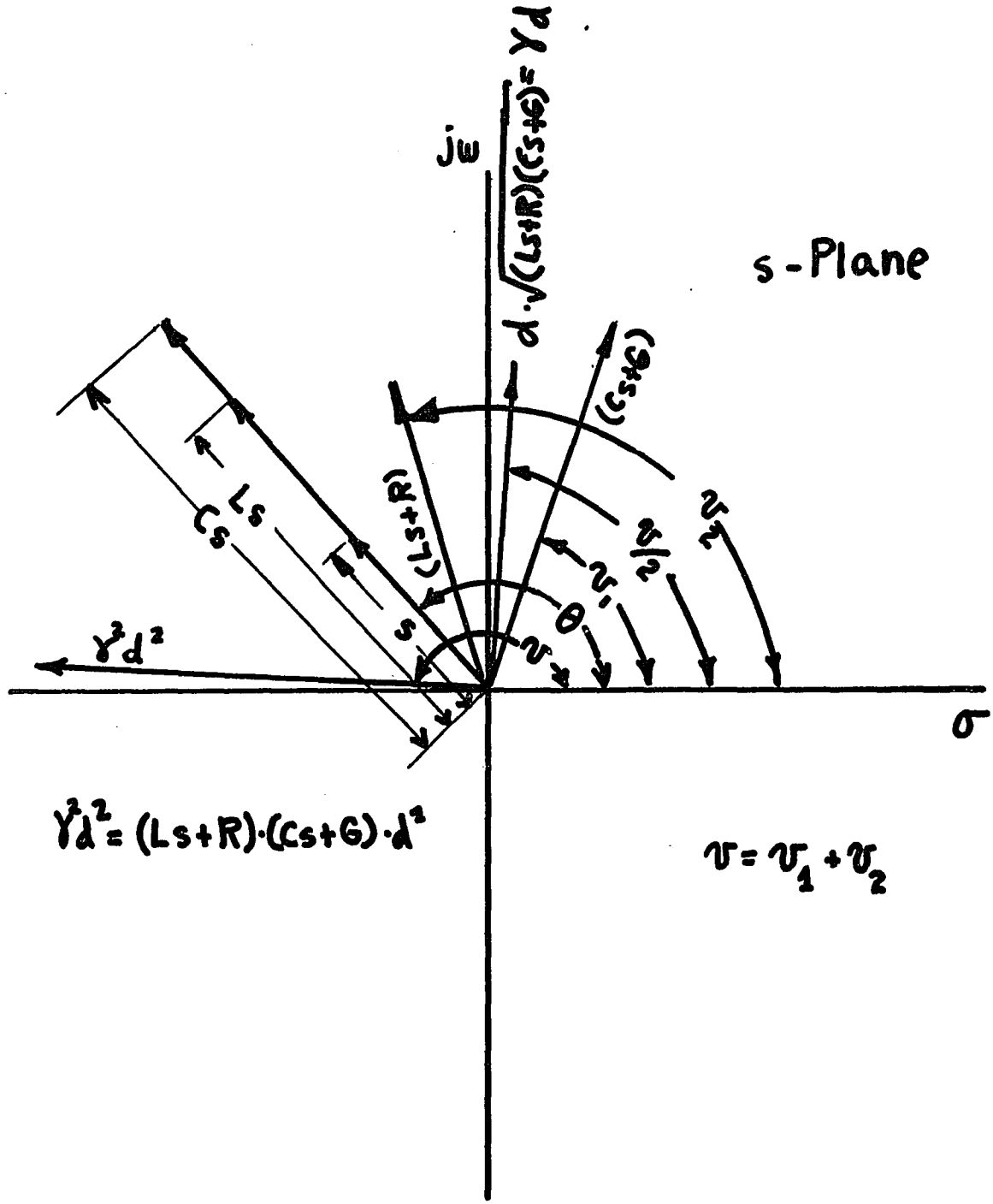

FIGURE 4.3.1 REPRESENTATION OF $\gamma(s)\,d$

$$|A| = d\,(Re^2 + Im^2)^{1/4} \tag{4.3.6}$$

and

$$v/_2 = 1/2 \tan^{-1}\left(\frac{Im}{Re}\right) \tag{4.3.7}$$

Using the rectangular coordinate form of (4.3.5), the transfer function (4.2.1) can be written as

$$e^{-\gamma d} = e^{-|A| \cos v/2} e^{-j|A| \sin v/2} = e^{\psi - j\delta} \tag{4.3.8}$$

where

$$\psi = -d\,(Re^2 + Im^2)^{1/4} \cos v/2 = -|A| \cos v/2 \tag{4.3.9}$$

and

$$\delta = d(Re^2 + Im^2)^{1/4} \sin v/2 = |A| \sin v/2 \tag{4.3.10}$$

Note that the angle v must travel through 4π radians for the angle of the function γd (i.e., v/2) to travel through 2π radians. Therefore γd is a double valued function of the angle v. Applying the half angle formulas to (4.3.8)

$$\cos (v/2) = \pm \sqrt{\frac{1 \mp \cos v}{2}} \tag{4.3.11}$$

$$\sin (v/2) = \pm \sqrt{\frac{1 - \cos v}{2}}$$

and noting that by virtue of (4.3.4)

$$\cos v = \frac{Re}{(Re^2 + Im^2)^{1/2}}$$

equation (4.3.8) can be rewritten as

$$e^{-\gamma_1 d} = e^{-d/\sqrt{2}\left(\pm\left[\left(Re^2+Im^2\right)^{1/2}+Re\right]^{1/2}+j\left[\left(Re^2+Im^2\right)^{1/2}-Re\right]^{1/2}\right)} \tag{4.3.12}$$

Each of the two terms in the exponent of (4.3.12) can take on two values, depending on its sign, resulting in a function with four different values. The value of this function in various portions of the s-plane will now be found. However, before doing this, recall that the function can be represented as a single valued function of the complex variable s over a two-sheeted Riemann surface. The principal sheet of this surface is defined as covering arguments of the variable s in the range $-\pi \leqq \theta \leqq \pi$ and the secondary sheet is defined as covering arguments in the range $\pi \leqq \theta \leqq 3\pi$. The procedure will be to correlate the signs of each of the two terms (4.3.12) with angles v and v/2 and also with regions of the s-plane. Equations (4.3.11) can be used to correlate the signs of $|A|\cos v/2$ and $|A|\sin v/2$ with the phase angle v.

Next a relationship must be established between the complex s-plane phase angle Θ and angle v/2 since the study of s-plane regions is essential to the determination of stability. This relationship can be established with the aid of Figure 4.3.2a. This figure shows the two branch points a and b and the branch cut associated with the distributed parameter element. These branch points are found by noting in equation (4.3.1) that $\gamma = 0$ when

$$s = s_1 = -\frac{R}{L}$$

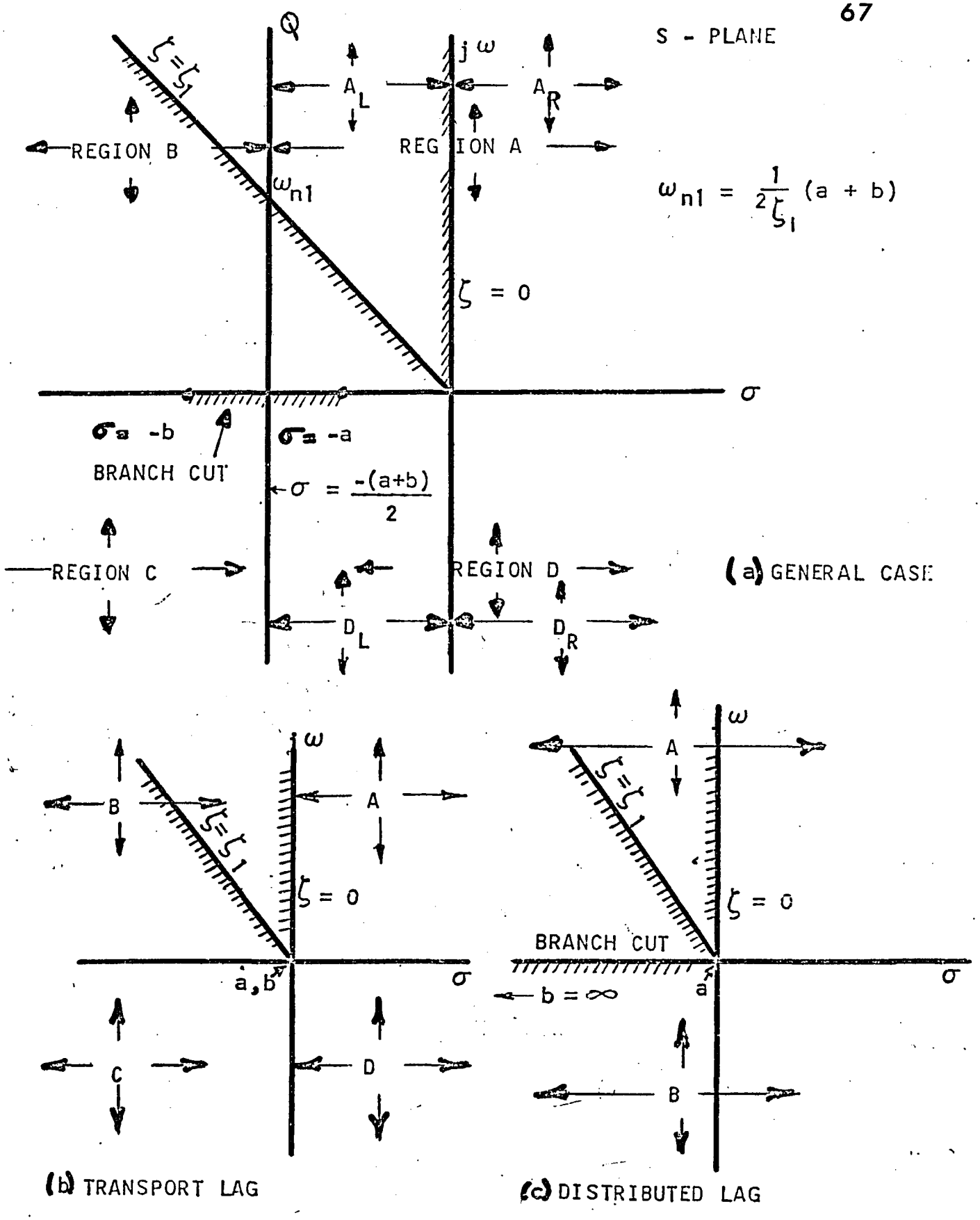

FIGURE 4.3.2PARTITIONING OF THE S-PLANE FOR VARIOUS CASES.

or

$$s = s_2 = -\frac{G}{C}$$

These two points are illustrated in Figure 4.3.2a as points at $\sigma = -a$ and $\sigma = -b$ representing the greater (less negative) and lesser (more negative) of these two values respectively. Boundary line Q bisects the branch cut and is expressed by the equation

$$\sigma = -1/2\left(\frac{R}{L} + \frac{G}{C}\right) = -\left(\frac{a+b}{2}\right) \qquad (4.3.13)$$

Line Q and the real axis divide each sheet of the s-plane into four regions. All points in region A of the principal sheet for example produce values of v between 0 and π radians. By virtue of (4.3.11), the signs of sin v/2 and cos v/2 are positive, therefore the signs associated with $-\psi$ and δ are also positive. The range of the angles v, v/2, and Θ as well as the signs associated with $-\psi$ and δ in each of the four regions of each of the two sheets of the Riemann surface are summarized in Table 4.3.1.

In practical applications involving double valued functions of s only the principal sheet of the Riemann surface need be considered. This is because it has been shown in [79] that the roots of the characteristic equation of a system containing double valued functions can exist in the right half portion of the second sheet of the Riemann surface and the system will be stable. However, instability will result if these roots exist in the right half portion of the principal sheet. Therefore, unless specified to the contrary, all

s-plane Sheet #	Region	v	v/2	$\|A\|\cos v/2=-\psi$	$\|A\|\sin v/2=\delta$	θ
1	A	0 to π	0 to $\pi/2$	+	+	0 to π
1	B	π to 2π	$\pi/2$ to π	-	+	$\pi/2$ to π
1	D	$-\pi$ to 0	$-\pi/2$ to 0	+	-	0 to $-\pi$
1	C	-2π to $-\pi$	$-\pi$ to $-\pi/2$	-	-	$-\pi/2$ to π
2	A	2π to 3π	π to $3\pi/2$	-	-	2π to 3π
2	B	3π to 4π	$3\pi/2$ to 2π	+	-	$\frac{5\pi}{2}$ to 3π
2	D	π to 2π	$\pi/2$ to π	-	+	π to 2π
2	C	0 to π	0 to $\pi/2$	+	+	π to $\frac{3\pi}{2}$

Table 4. 3. 1. Relationship between the signs of $|A|$ cos v/2 and $|A|$ sin v/2 and the regions of the two sheeted Riemann equivalent of the s-plane.

further references to the s-plane will refer to its principal sheet. The data presented in Table 4.3.1 for the principal sheet leads to the following conclusions:

1. The $\zeta = 0$ contour is either entirely within Region A or forms its boundary with Region B for $\omega_n > 0$. As a consequence

$$-\psi = +|A| \cos \frac{v}{2}, \quad \delta = +|A| \sin \frac{v}{2}$$

2. The $\zeta = \zeta_1$ contour for $0 \leqq \zeta \leqq 1$ starts in Region A at $\omega_n = 0$ and crosses into Region B at

$$\omega_n = \omega_{n_1} = \frac{1}{2\zeta_1} \left(\frac{R}{L} + \frac{G}{C}\right) = \frac{a+b}{2\zeta_1} \tag{4.3.14}$$

Further, this $\zeta = \zeta_1$ contour remains in Region B for values of ω_n from $\omega = \omega_{n_1}$ to $\omega_n = \infty$, so that in general

$$-\psi = +|A| \cos \frac{v}{2}, \quad \delta = +|A| \sin \frac{v}{2} \text{ for } 0 \leqq \omega_n \leqq \omega_{n_1}$$

and

$$-\psi = -|A| \cos \frac{v}{2}, \quad \delta = +|A| \sin \frac{v}{2} \text{ for } \omega_{n_1} \leqq \omega_n \leqq \infty$$

The partitioning of the s-plane for the special cases of transport and distributed lag are shown inFigures 4.3.2b and 4.3.2c respectively. Notice that for distributed lag, the $\zeta = 0$ and $\zeta = \zeta_1$ radials are entirely within region A when $\omega_n > 0$. However, for transport lag, when $\omega_n > 0$, the $\zeta = \zeta_1$ radial is entirely within region B and the $\zeta = 0$ radial is on the boundary between regions A and B.

Now that the signs of $|A|\cos v/2$ and $|A|\sin v/2$ have been established, the expressions for $-\psi$ and δ in terms of s-plane variables can be derived. Recall that for region A

$$-\psi = |A| \cos\frac{v}{2} = +d\sqrt{\frac{(Re^2 + Im^2)^{1/2} + Re}{2}} \qquad (4.3.15)$$

$$\delta = |A| \sin\frac{v}{2} = +d\sqrt{\frac{(Re^2 + Im^2)^{1/2} - Re}{2}}$$

inserting (4.3.3) into (4.3.15) gives

$$-\psi = d/\sqrt{2}\sqrt{F^{1/2} + M} \qquad (4.3.16)$$

$$\delta = d/\sqrt{2}\sqrt{F^{1/2} - M}$$

where

$$F = \left[(\sigma L + R)^2 + \omega^2 L^2\right]\left[(\sigma C + G)^2 + \omega^2 C^2\right] \qquad (4.3.16a)$$

$$M = (\sigma L + R)(\sigma C + G) - \omega^2 LC$$

An alternate form of (4.3.16) is obtained by substituting (4.2.2) into (4.3.16a) yielding

$$-\psi = d/\sqrt{2}\sqrt{H^{1/2} + J} \qquad (4.3.17)$$

$$\delta = d/\sqrt{2}\sqrt{H^{1/2} - J}$$

where

$$H = (\omega_n^2 L^2 - 2\zeta\omega_n RL + R^2)(\omega_n^2 C^2 - 2\zeta\omega_n GC - G^2)$$

$$J = \omega_n^2 LC(2\zeta^2 - 1) + RG - \zeta\omega_n(RC + LG) \qquad (4.3.17a)$$

Expressions for $-\psi$ and δ for other regions on the primary sheet and regions on the secondary sheet can be obtained by using the polarities for $-\psi$ and δ specified in Table 4.3.1. This Table indicates that $-\psi$ and δ on the secondary sheet are both opposite in sign to the values of $-\psi$ and δ given by (4.3.17) for the principal sheet of the s-plane. Upon utilizing the new values of $-\psi$ and δ for the second sheet, equations (4.2.12) become

$$
\begin{aligned}
B_{1s} &= \sum_{k=0}^{n} \omega_n^k \left[(-1)^k T_k b_k + e^{\psi} c_k Z_{k1} \right] \\
C_{1s} &= \sum_{k=0}^{n} \omega_n^k \left[(-1)^k T_k d_k + e^{\psi} e_k Z_{k1} \right] \\
D_{1s} &= \sum_{k=0}^{n} \omega_n^k \left[(-1)^k T_k f_k + e^{\psi} g_k Z_{k1} \right] \\
B_{2s} &= \sum_{k=0}^{n} \omega_n^k \left[Z_{k2} b_k + e^{\psi} c_k Z_{k3} \right] \\
C_{2s} &= \sum_{k=0}^{n} \omega_n^k \left[Z_{k2} d_k + e^{\psi} e_k Z_{k3} \right] \\
D_{2s} &= \sum_{k=0}^{n} \omega_n^k \left[Z_{k2} f_k + e^{\psi} g_k Z_{k3} \right]
\end{aligned}
\qquad (4.3.18)
$$

where

$$
\begin{aligned}
Z_{k1} &= (-1)^k T_k \cos\delta + (-1)^{k+1} U_k \sqrt{1-\varsigma^2} \sin\delta \\
Z_{k2} &= (-1)^{k+1} U_k \sqrt{1-\varsigma^2} \\
Z_{k3} &= (-1)^{k+1} U_k \sqrt{1-\varsigma^2} \cos\delta - (-1)^k T_k \sin\delta
\end{aligned}
$$

and T_k and U_k represent Chebychev functions as defined in [98].

By applying these new expressions for the parameter plane coefficients B_{1s}, C_{1s}, D_{1s}, B_{2s}, C_{2s}, and D_{2s} of equations (4.3.18) to (4.2.13), a new set of α - β equations are obtained. These equations represent mapping of contours from the secondary sheet of the s-plane onto the α - β plane.

4.4 Discussion of Method

The α - β curves specified by (4.2.13) are mappings of curves from the complex s-plane to the algebraic α - β plane. For example the α - β curve corresponding to the radial line $\zeta = \zeta_1$, shown in Figure 4.2.2, is found by setting $\zeta_1 = -\cos^{-1}\Theta_1$ (in the upper half of the s-plane) and varying ω_n from zero to infinity. The contour is first evaluated between $\omega_n = 0$ and $\omega_n = \omega_{n_1}$ where ω_{n_1} is computed by (4.3.14). The signs of the expressions for $-\psi$ and δ in region A of sheet 1 are determined by referring to Table 4.3.1. The expressions obtained from (4.3.17) are then used in (4.2.12) which in turn are used to form (4.2.13), the expressions for α and β in this region. The contour between $\omega_n = \omega_{n_1}$ and $\omega_n = \infty$ is evaluated in a manner similar to that described above except the signs of the expressions for $-\psi$ and δ in region B, sheet 1 are used.

In addition to obtaining α - β curves, care must be taken to determine which regions of the s-plane map into corresponding regions of the α - β plane. This determination is made by noting the sign

of Δ in (4.2.13) and the side of the shading of the curve in the s-plane. If a contour in the s-plane is shaded as shown in Figure 4.2.2 and $\Delta > 0$, then the curve in the α-β plane is shaded on the left facing the direction of increasing ω_n. If $\Delta < 0$ then the curve is shaded on the right in the direction of increasing ω_n. It is also important to note that when the contour either symmetrically encloses the entire left-hand s-plane or a region therein, it is not necessary to compute values of α and β for $\omega_n < 0$. This is because α-β curves generated for $\omega_n > 0$ will retrace the curves for $\omega_n > 0$. (see Appendix II). Therefore these α - β curves will be doubly shaded indicating that a point crossing one of these curves corresponds to a pair of complex conjugate roots crossing the appropriate boundary in the s-plane.

4.5 Parameter Plane Contours When Zeta Equals Plus Or Minus One

When the value of zeta approaches either plus or minus one, this represents the mapping of s-plane contours which respectively consist of the negative or positive portions of the real axis. In systems which contain distributed parameter elements each of these axes must be examined in order to determine whether the function, Δ , of (4.2.13) is a non-zero quantity. If this function is zero, then the equations for the parameter plane coefficients (4.2.12) must be examined to determine whether the singularity can be removed.

4.5.1 Zeta equals one ($\zeta = +1$). Care must be taken in applying equations (4.2.12) when $\zeta = +1$ because this contour involves the branch cut in almost all cases.[4] Examining the general case of a distributed parameter transmission line in which L, R, C and G are not equal to zero, and RC $\neq$ LG; defining

$r_1 = \frac{R}{L}, \quad r_2 = \frac{G}{C}$

a = the smaller of the two roots r_1 and r_2

b = the larger of the two roots r_1 and r_2

$T = (LC)^{1/2} d$

the exponent of the transfer function of (4.2.1) becomes

$$\gamma(s)d = (LC)^{1/2} d \left[(s+r_1)(s+r_2)\right]^{1/2} = T \left[(s+r_1)(s+r_2)\right]^{1/2} \qquad (4.5.1)$$

The branch cut is as shown in Figure 4.5.1. This figure shows the $\zeta = +1$ contour (i.e., the negative real axis) consisting of three line segments.

segment 1 $\quad -a < \omega_n < 0$

segment 2 $\quad \omega_n < -b$

segment 3 $\quad -b \leqq \omega_n \leqq -a$

---

4 The exceptions are the cases of transport lag (R = G = 0) and distortionless transmission (RC = LG). In these cases the branch cut degenerates into a point located at the origin of the s-plane or a point at $s = -\frac{L}{R}$ respectively.

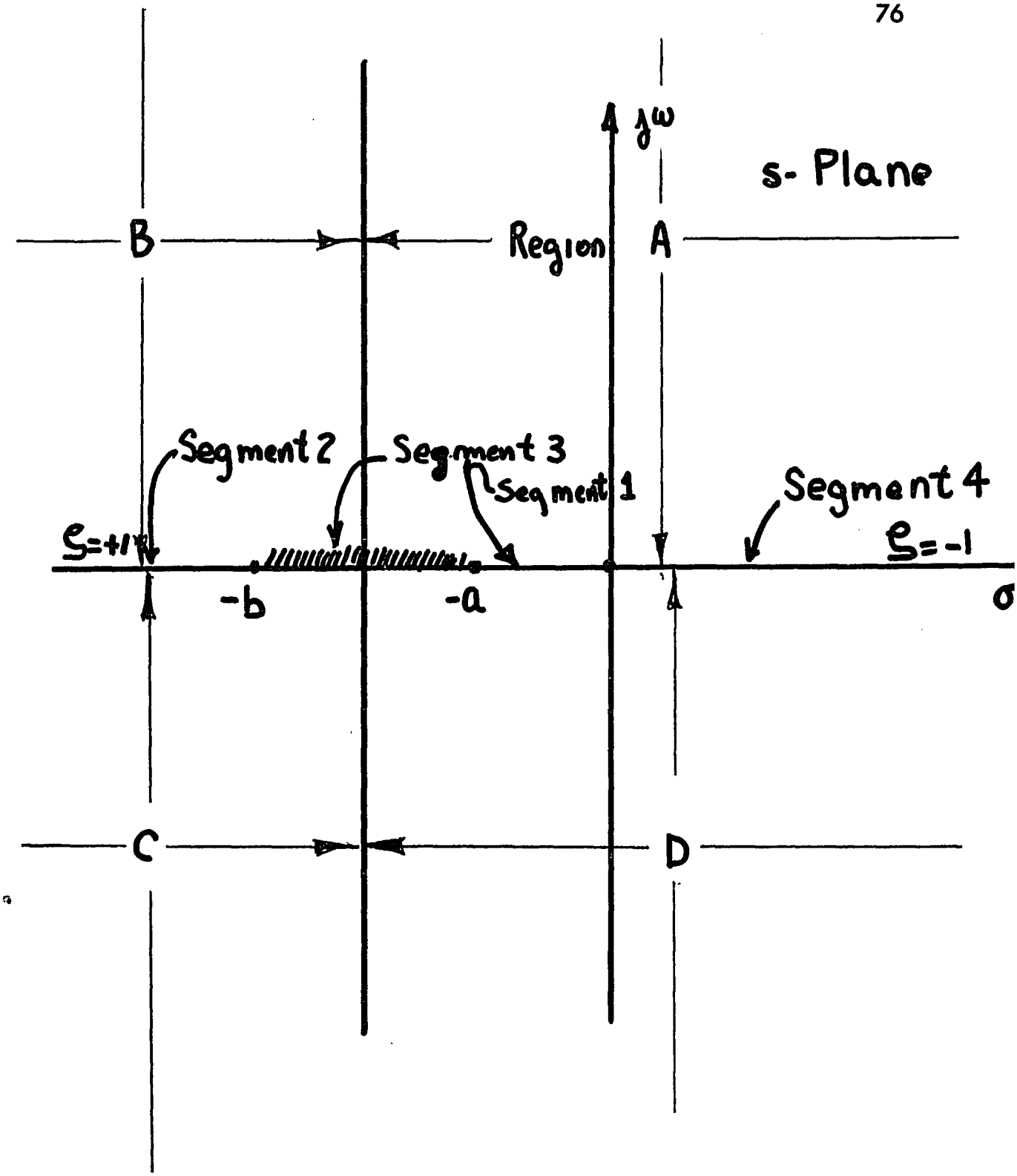

FIGURE 4.5.1 DEFINITION OF SEGMENTS OF THE REAL AXIS OF THE s - PLANE

The various special forms of a terminated distributed parameter network can be categorized by the size of these three line segments. Some examples are tabulated below

Type of Network	$\gamma(s)$	Length of Segment 1	2	3
Transport Lag	$(LCs^2)^{1/2}$	0	0 to $-\infty$	0
Distortionless Line	$(s+a)$	0 to $-a$	$-a$ to $-\infty$	0
Distributed Lag	$(RCs)^{1/2}$	0	0	0 to $-\infty$
Distributed Lag	$(LGs)^{1/2}$	0	0	0 to $-\infty$
G = 0 Line	$sC(sL+R)^{1/2}$	0	$-b$ to $-\infty$	0 to $-b$
L = 0 Line	$R(sC+G)^{1/2}$	0 to $-a$	0	$-a$ to $-\infty$

Applying equations (4.3.17) to each of these three line segments and noting that for a path along the negative real axis, $\zeta = +1$ and $s = -\omega_n$ yields the following:

Segment 1 $\qquad -a < s \leqq 0$

$$-\psi_1 = d\sqrt{(R-\omega_n L)(G-\omega_n C)}, \quad \delta_1 = 0 \qquad (4.5.2)$$

Segment 2 $\qquad -\infty \leqq s < -b$

$$-\psi_2 = -d\sqrt{(R-\omega_n L)(G-\omega_n C)}, \quad \delta_2 = 0 \qquad (4.5.3)$$

Segment 3 $\qquad -b \leqq s \leqq -a$

$$-\psi_3 = 0, \quad \delta_3 = d\sqrt{(R-\omega_n L)(G-\omega_n C)} \qquad (4.5.4)$$

$-\psi_1$ is the negative of $-\psi_2$ because segment 1 forms a portion of the boundary between Regions A and D of Figure 4.5.1, while segment 2 forms a portion of the boundary between Region B and C. Table 4.3.1 indicates that the polarity of $-\psi$ in Regions A and D is opposite to the polarity of $-\psi$ in Regions B and C.

The form of the parameter plane equations along each of these segments will be examined utilizing the values of $-\psi$ and δ given above. Applying the relationships of (4.5.2) to (4.2.12) and noting that $\zeta = +1$ yields for segment 1

$$B_{1,1} = \sum_{k=0}^{n} (-\omega_n)^k (b_k + \exp(-\psi_1)c_k)$$

$$C_{1,1} = \sum_{k=0}^{n} (-\omega_n)^k (d_k + \exp(-\psi_1)e_k) \qquad (4.5.5)$$

$$D_{1,1} = \sum_{k=0}^{n} (-\omega_n)^k (f_k + \exp(-\psi_1)g_k)$$

$$B_{2,1} = C_{2,1} = D_{2,1} = 0$$

Defining new variables

$$\overline{B}_{2,1} = \frac{B_{2,1}}{(1-\zeta^2)^{1/2}}, \quad \overline{C}_{2,1} = \frac{C_{2,1}}{(1-\zeta^2)^{1/2}}, \quad \overline{D}_{2,1} = \frac{D_{2,1}}{(1-\zeta^2)^{1/2}} \qquad (4.5.6)$$

Substitution of (4.2.12) into (4.5.6) and noting that $\zeta = +1$, $U_k(1) \leq K$, $T_k(1) = 1$ yields

$$\overline{B}_{2,1} = \sum_{k=0}^{n} (-\omega_n)^k \left[-kb_k + \exp(-\psi_1) c_k \left(-k + \frac{\sin\delta}{(1-\zeta^2)^{1/2}}\right)\right]$$

$$\overline{C}_{2,1} = \sum_{k=0}^{n} (-\omega_n)^k \left[-kd_k + \exp(-\psi_1) e_k \left(-k + \frac{\sin\delta}{(1-\zeta^2)^{1/2}}\right)\right] \quad (4.5.7)$$

$$\overline{D}_{2,1} = \sum_{k=0}^{n} (-\omega_n)^k \left[-kf_k + \exp(-\psi_1) g_k \left(-k + \frac{\sin\delta}{(1-\zeta^2)^{1/2}}\right)\right]$$

Defining $F_1(\zeta=1) = \underset{\zeta \to +1}{\text{Limit}} \dfrac{\sin\delta}{(1-\zeta^2)^{1/2}}$ (4.5.8)

and using the expression for δ given by (4.3.17) yields after some manipulation (see Appendix III)

$$F_1(\zeta=1) = F_1(1) = \frac{d}{2} \frac{\omega_n [RC + LG - 2\omega_n LC]}{[(\omega_n L - R)(\omega_n C - G)]^{1/2}} \quad (4.5.9)$$

Thus the singularity has been removed for segment 1 and (4.5.7) becomes

$$\overline{B}_{2,1} = \sum_{k=0}^{n} (-\omega_n)^k \left[-kb_k + \exp(-\psi_1) c_k (-k + F_1(1))\right]$$

$$\overline{C}_{2,1} = \sum_{k=0}^{n} (-\omega_n)^k \left[-kd_k + \exp(-\psi_1) e_k (-k + F_1(1))\right] \quad (4.5.10)$$

$$\overline{D}_{2,1} = \sum_{k=0}^{n} (-\omega_n)^k \left[-kf_k + \exp(-\psi_1) g_k (-k + F_1(1))\right]$$

and the parameter plane contour mapping segment 1 is computed using (4.5.10) and (4.5.5) in the following equations

$$\alpha_1 = \frac{C_{1,1}\overline{D}_{2,1} - D_{1,1}\overline{C}_{2,1}}{\Delta_1} \qquad \beta_1 = \frac{D_{1,1}\overline{B}_{2,1} - \overline{D}_{2,1}B_{1,1}}{\Delta_1} \tag{4.5.11}$$

$$\Delta_1 = B_{1,1}\overline{C}_{2,1} - \overline{B}_{2,1}C_{1,1}$$

Equations (4.5.10) and (4.5.5) can also be used to determine the parameter plane coefficients for the $\zeta = 1$ contour along line segment 2. This is accomplished by replacing the expression for $-\psi_1$ given by (4.5.2) with the expression for $-\psi_2$ given by (4.5.3) and replacing the expression for $F_1(1)$ given by (4.5.9) with the expression for $F_2(1)$ given by (III.9) in Appendix III. Note that $-\psi_2 = \psi_1$ and $F_2(1) = -F_1(1)$ so that ths substitution is not unwieldy. Examining line segment 3, which extends along the branch cut, substitution of $\zeta = +1$ and (4.5.4) into (4.2.12) yields

$$B_{1,3} = \sum_{k=0}^{n} (-\omega_n)^k (b_k + c_k \cos\delta)$$

$$C_{1,3} = \sum_{k=0}^{n} (-\omega_n)^k (d_k + e_k \cos\delta)$$

$$D_{1,3} = \sum_{k=0}^{n} (-\omega_n)^k (f_k + g_k \cos\delta) \tag{4.5.12}$$

$$B_{2,3} = \sum_{k=0}^{n} (-\omega_n)^k c_k \sin\delta$$

$$C_{2,3} = \sum_{k=0}^{n} (-\omega_n)^k e_k \sin\delta$$

$$D_{2,3} = \sum_{k=0}^{n} (-\omega_n)^k g_k \sin\delta$$

where δ is defined by (4.5.4). The expressions for α_3, β_3 and the determinant Δ_3 are given by

$$\alpha_3 = \frac{C_{1,3} D_{2,3} - C_{2,3} D_{1,3}}{\Delta_3}, \quad \beta_3 = \frac{D_{1,3} B_{2,3} - D_{2,3} B_{1,3}}{\Delta_3}$$

$$\Delta_3 = B_{1,3} C_{2,3} - B_{2,3} C_{1,3} = \sin\delta \; J_3(\omega_n) \qquad (4.5.13)$$

Considering the expression for Δ_3 in equation (4.5.13) indicates that an $\alpha - \beta$ contour will exist and each point in the s-plane will map into a point in the $\alpha - \beta$ plane when both $\sin\delta$ and $J_3(\omega_n)$ are non-zero quantities.

However, this one to one correspondence does not exist when either $\sin\delta = 0$ or $J_3 = 0$. Consider the case when $\sin\delta = 0$. Thus

$$\delta = \pm m\pi \quad , \quad m = 0, 1, 2, \ldots\ldots$$

Substituting into (4.5.4) gives

$$(\omega_n L - R)(G - \omega_n C) = \frac{m^2 \pi^2}{d^2} \qquad (4.5.14)$$

Equation (4.5.14) can be used to determine values of $\omega_n = \omega_n^*$ along segment 3 at which $\sin\delta = 0$. At these values of ω_n^*, $\cos\delta = (-1)^m$ and (4.5.12) can be rewritten as

---

[3] The function $J_3(\omega_n)$ is defined as

$$J_3(\omega_n) = B_{1,3} \sum_{K=0}^{n} (-\omega_n)^k e_k - C_{1,3} \sum_{K=0}^{n} (-\omega_n)^k c_k$$

$$B^*_{1,3} = \sum_{k=0}^{n} (-\omega_n^*)^k (b_k + (-1)^m c_k)$$

$$C^*_{1,3} = \sum_{k=0}^{n} (-\omega_n^*)^k (d_k + (-1)^m e_k) \qquad (4.5.15)$$

$$D^*_{1,3} = \sum_{k=0}^{n} (-\omega_n^*)^k (f_k + (-1)^m g_k)$$

$$B^*_{2,3} = C^*_{2,3} = D^*_{2,3} = 0$$

The singularity cannot be removed here since δ is defined by (4.5.4). Equations (4.5.15) state that at a point on the branch cut where $\sin \delta = 0$, equation (4.2.11) degenerates into an equation with real terms only. That is:

$$F(\omega_n, \zeta) = \alpha_3 B^*_{1,3} + \beta_3 C^*_{1,3} + D^*_{1,3} = 0 \qquad (4.5.16)$$

This equation therefore maps each of these special points into a straight line in the $\alpha - \beta$ plane. It should be noted that (4.5.16) also applies to the branch points at s = -a and s = -b. In these cases the appropriate value of the branch point is substituted into (4.5.15) and the value of m is set equal to unity.

4.5.2 Zeta equals minus one ($\zeta = -1$). It is easy to show that (4.5.5) and (4.5.10) can be used to determine the $\zeta = -1$ contour if

$$-\psi_1 = d\left[(\omega_n L + R)(\omega_n C + G) \right]^{1/2} \qquad (4.5.17)$$

$$F_4(-1) = \frac{d}{2} \frac{\omega_n (2\omega_n LC + RG + LC)}{\left[(R + \omega_n L)(G + \omega_n C) \right]^{1/2}}$$

Note that these equations are simply (4.5.2) and (4.5.9) with the polarity of ω_n reversed.

4.5.3 Summary. The real axis is composed of four different line segments, segments 1, 2, and 3 along the negative real axis and segment 4 along the positive real axis.

For segment 1 the parameter plane equations α and β are determined by (4.5.11), (4.5.10), and (4.5.15) in which $F_1(1)$ is defined by (4.5.9) and where $-\psi_1$ is defined by (4.5.2). For segment 2, the parameter plane equations are also determined by (4.5.11), (4.5.10), and (4.5.15). However, the function $F_2(1)$ must be used in place of $F_1(1)$ in (4.5.10) and the function $-\psi_2$ must be used in place of $-\psi_1$ in (4.5.10) and (4.5.15). This substitution is simple since $F_2(1) = -F_1(1)$ and $-\psi_2 = -(-\psi_1)$.

For segment 3 (*i.e.*, the branch cut and branch points), the $\alpha - \beta$ curve corresponding to points in which the determinant is not equal to zero ($\Delta_3 \neq 0$) is given by (4.5.13) where the coefficients are defined by (4.5.12) and $-\psi_3$ is defined by (4.5.4). The special points on segment 3, which produce a determinant of value equal to zero map into straight lines in

the α - β plane in accordance with (4.5.16) where the coefficients are defined by (4.5.15). The branch points s = -a and s = -b are included as special points.

The mapping of points along segment 4, (i.e., points along the positive real axis) is accomplished by application of (4.5.5) and (4.5.10) in which variables - ψ_1 and $F_4(-1)$ are defined by (4.5.17).

4.6 Example of Absolute and Relative Stability of a Feedback System with Distributed Parameter Elements

An example is now considered in order to demonstrate the use of the equations developed in sections 4.2 and 4.3 as well as to form a basis for the further development of the theory.

Consider the feedback system of Figure 4.2.1 where

1) $G_1(s)$ consists of a proportional-integral controller with transfer function K(s+W)/s and a plant with transfer function 1/s
2) The distributed parameter element is a distributed lag. That is, $e^{-\gamma(s)d} = e^{-d\sqrt{RCs}} = e^{-\sqrt{sT}}$

This example was also presented by Chu [23] so that comparisons can be made. The s-plane representation of the distributed parameter element is shown in Figure 4.3.2c. This figure indicates that region A extends over the entire upper-half of the s-plane. This can be verified by evaluating (4.3.13) which shows that $\sigma = -\infty$ when for G = L = 0. Next, Table 4.3.1 indicates that the signs are positive and

$-\psi$ and δ are in sheet 1, region A. Therefore equations (4.3.17) give

$$-\psi = \sqrt{\frac{\omega_n T(1-\zeta)}{2}} \qquad \delta = \sqrt{\frac{\omega_n T(1+\zeta)}{2}} \tag{4.6.1}$$

For a stability investigation of this system, form the characteristic equation (4.2.5)

$$F(s) = s^2 \exp(\sqrt{sT}) + Ks + KW = 0$$

Defining the adjustable parameters as $\alpha = K$, $\beta = KW$, F(s) becomes

$$F(s) = s^2 \exp(\sqrt{sT}) + \alpha s + \beta = 0 \tag{4.6.2}$$

Utilizing (4.6.2), (4.2.2), (4.2.6) and (4.2.13) gives

$$\alpha = \omega_n e^{-\psi}\left[2\zeta\cos\delta + \frac{(1-2\zeta^2)}{\sqrt{1-\zeta^2}}\sin\delta\right]$$

$$\beta = \omega_n^2 e^{-\psi}\left[\cos\delta - \frac{\zeta}{\sqrt{1-\zeta^2}}\sin\delta\right] \tag{4.6.3}$$

$$\Delta = -\omega_n\sqrt{1-\zeta^2}$$

The variables α and β are plotted where ζ is fixed and ω_n is the running parameter. The region of the s-plane to be mapped in order to determine absolute stability is shown in Figure 4.6.1a. For absolute stability, the $\alpha-\beta$ plane contour is obtained by setting $\zeta = 0$ and varying ω_n from zero to infinity. Because values for $\omega_n < 0$ map into the same values for $\omega_n > 0$, the contour obtained for positive values of ω_n represents the entire range of $-\infty \leq \omega_n \leq \infty$ (see Appendix II). Then, from (4.6.1), (4.6.3) and setting $\zeta = 0$ gives

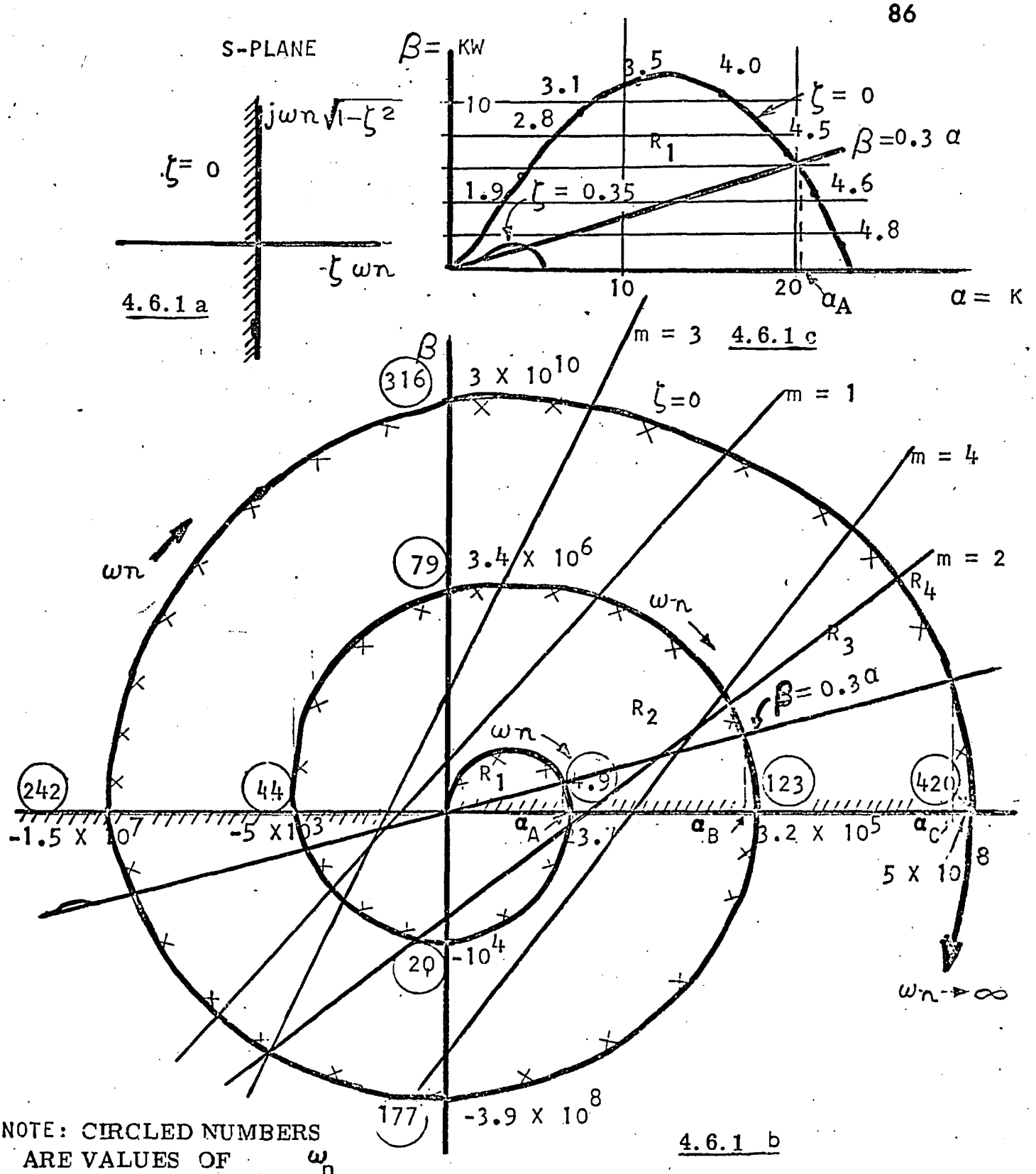

NOTE: CIRCLED NUMBERS ARE VALUES OF ω_n AT AXIS CROSSINGS.

FIGURE 4.6.1 ZETA =0 CONTOUR FOR DISTRIBUTED LAG PROBLEM

$$\alpha = \omega_n \exp(\sqrt{\omega_n T/2}) \sin(\sqrt{\omega_n T/2})$$
$$\beta = \omega_n^2 \exp(\sqrt{\omega_n T/2}) \cos(\sqrt{\omega_n T/2}) \qquad (4.6.4)$$

A graph of (4.6.4) is shown in Figure 4.6.1b where T is set equal to unity as in reference [23]. Notice that this curve spirals outward from the origin as ω_n increases. This is to be expected since both α and β in (4.6.4) contain exp $(+\sqrt{\omega_n T/2})$ terms which cause an increase in the α - β locus with increasing ω_n. The α - β curve for $\zeta = 0$ is a mapping of the $j\omega$ axis and the left half plane has been mapped within the indicated doubly shaded region. The shading is on the right of this curve in the direction of increasing ω_n since $\Delta = -\omega_n$ and $\omega_n > 0$. The singly shaded line $\beta = 0$ represents the mapping of the origin of the s- plane and is found by evaluating $F(s) = 0$ at $s = 0$. This singly shaded line is a real root boundary and will be discussed further in a subsequent section. Thus the α - β plane is divided into an infinite number of regions $R_1, R_2, R_3 \ldots\ldots R_\infty$ where $R_1 \supset R_2 \supset R_3 \ldots\ldots \supset R_\infty$. Only values of α and β chosen from region R_1 will produce a stable system. This is because crossing from a shaded to an unshaded region in the s- plane has the same meaning in the α - β plane and vice versa. Thus moving an operating point from region R_1 to R_2 implies that a pair of complex roots have migrated from the left-half into the

right-half of the principal sheet. Therefore only R_1 can contain all the roots since it is completely closed and contains no subregions. Now if W is set equal to 0.3, then $\beta = KW = 0.3K = 0.3\alpha$ which is the equation of a straight line as shown in Figure 4.6.1b. This line intersects the $\zeta = 0$ curve at $\alpha = \alpha_A, \alpha_B, \alpha_C, \ldots, \alpha_Z, \ldots \alpha_\infty$. It follows that these vlaues of α are the gains at which pairs of complex roots cross the imaginary axis. There will be an infinite number of such points since the characteristic equation is transcendental, giving rise to an infinite number of roots. The line $\beta = 0.3\alpha$ intersects the portion of the $\zeta = 0$ curve along the boundary of region R_1 at a gain of 20.3 and a value of $\omega_n = 4.52$ rad/sec (see Figure 4.6.1c). This is the maximum allowable gain for absolute stability. If W is varied, a new line $\beta = W\alpha$ results and its intersection with the boundary of region R_1 gives new values of critical gain K and undamped natural frequency ω_n of the dominant mode.

To investigate the relative stability of the system, a value of $\zeta = \zeta_1$ is substituted into equations (4.5.1) and 4.6.3) and a new $\alpha - \beta$ contour is formed. The general form of this contour is shown in Figure 4.6.2b for $\zeta = 0.35$. This curve which corresponds to the s-plane contour shown in Figure 4.6.2b also spirals out from the origin. This is because both α and β contain exponential terms of the form $\exp(\sqrt{0.325\ \omega_n})$ which increase the magnitude of both α and β with increasing ω_n. In addition, the first traversal of this curve

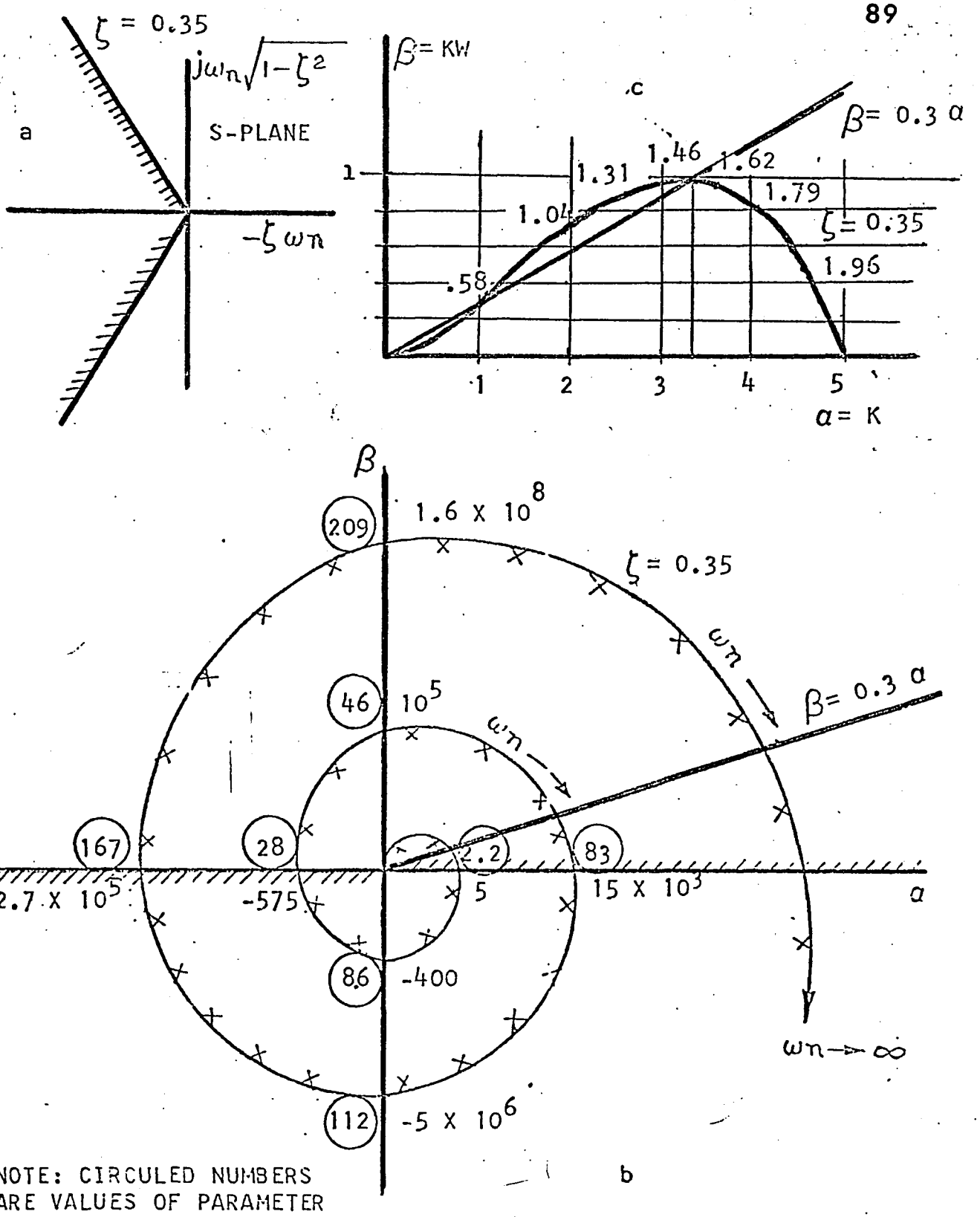

NOTE: CIRCULED NUMBERS ARE VALUES OF PARAMETER ω_n AT AXIS CROSSINGS

FIGURE 4.6.2 ZETA = 0.35 CONTOUR FOR DISTRIBUTED LAG PROBLEM

is completely within the R_1 boundary of the $\zeta=0$ curve (see Figure 4.6.1) 4.6.1c). The detailed plot of the first traversal of the $\zeta=0.35$ curve is shown in Figure 4.6.2c. One intersection of ths curve and the $\beta=0.3\alpha$ line occurs at a point M($\alpha_1=3.3$, $\beta_1=0.99$),[5] which corresponds to a gain of 3.3 and an $\omega_n=1.54$. This in turn indicates that a pair of complex conjugate roots exist at

$$s_{1,2} = -\zeta_1 \omega_{n1} \pm j \omega_{n1}\sqrt{1-\zeta_1^2} = -0.539 \pm j1.44 \qquad (4.6.5)$$

This complex root pair is in agreement with the results of [23].

The $\zeta=0.35$ curve spirals outward continously from the origin . This means that all other complex roots on the principal sheet of the s-plane must lie below the radials $\zeta=0.35$. This can be verified by noting that as the system gain is reduced from infinity, the operating point moves toward the origin of the $\alpha-\beta$ plane along the $\beta=0.3\alpha$ line and pairs of roots thus move from the unshaded to the shaded side of the radial contour of Figure 4.6.2a. When the gain is reduced to 3.3 all complex root pairs except one, the fundamental complex conjugate roots (which lie on the radial) have moved below this radial. The curves for all values of ζ in this example must also spiral out from the origin. This is because they correspond to operation in region A of Figure 4.3.2c where the polarity of the exponent $-\psi$ is positive. Once a working point, say M(3.3, 0.99), has been set, the intersection of $\alpha-\beta$ contours corresponding to other values of ζ and the working point will yield the locations of the higher order complex root pairs.

5 A second intersection occurs at a lower value of gain. This indicates that there are two intersections of the $\zeta=0.35$ radial and the first branch of the root locus curve in the s-plane. See[23].

It is of interest to compare this result of mapping the principal sheet of the s-plane with the results obtained if the distributed lag is replaced by transport lag. In this latter case there only one sheet to be mapped and Eisenberg[29] showed that the $\alpha - \beta$ contours for all values of $\zeta > 0$ eventually spiral inward toward the origin as ω_n approaches infinity. A contour that spirals inward toward the origin means that complex roots at successively higher values of ω_n must lie above the radial being mapped.

As observed by Ball [6] and Pierre [79], complex root pairs can be located on the secondary sheets of the Riemann surface equivalent of the s-plane. These roots can be located by first substituting the values of $-\psi$ and δ in region A of the second sheet

$$-\psi = -\sqrt{\frac{\omega_n T(1-\zeta)}{2}}, \qquad \delta = \sqrt{\frac{\omega_n T(1+\zeta)}{2}} \qquad (4.6.6)$$

then setting T = 1 and plotting the α β curves for various values of ω_n. The result of plotting values of ζ between 0.996 and 0.999 are shown in Figure 4.6.3 where it can be seen that the curve for $\zeta = 0.998$ is close to the operating point M(3.30, 0.99) at $\omega_n = 0.326$. This indicates that a pair of complex conjugate roots are located on the second sheet very close to the negative real axis at

$$s_{2A,\bar{A}} = -0.32 \pm j\ 0.02 \qquad (4.6.7)$$

The remaining roots on the secondary sheet can be found by plotting $\alpha - \beta$ contours corresponding to other values of ζ with ω_n as the

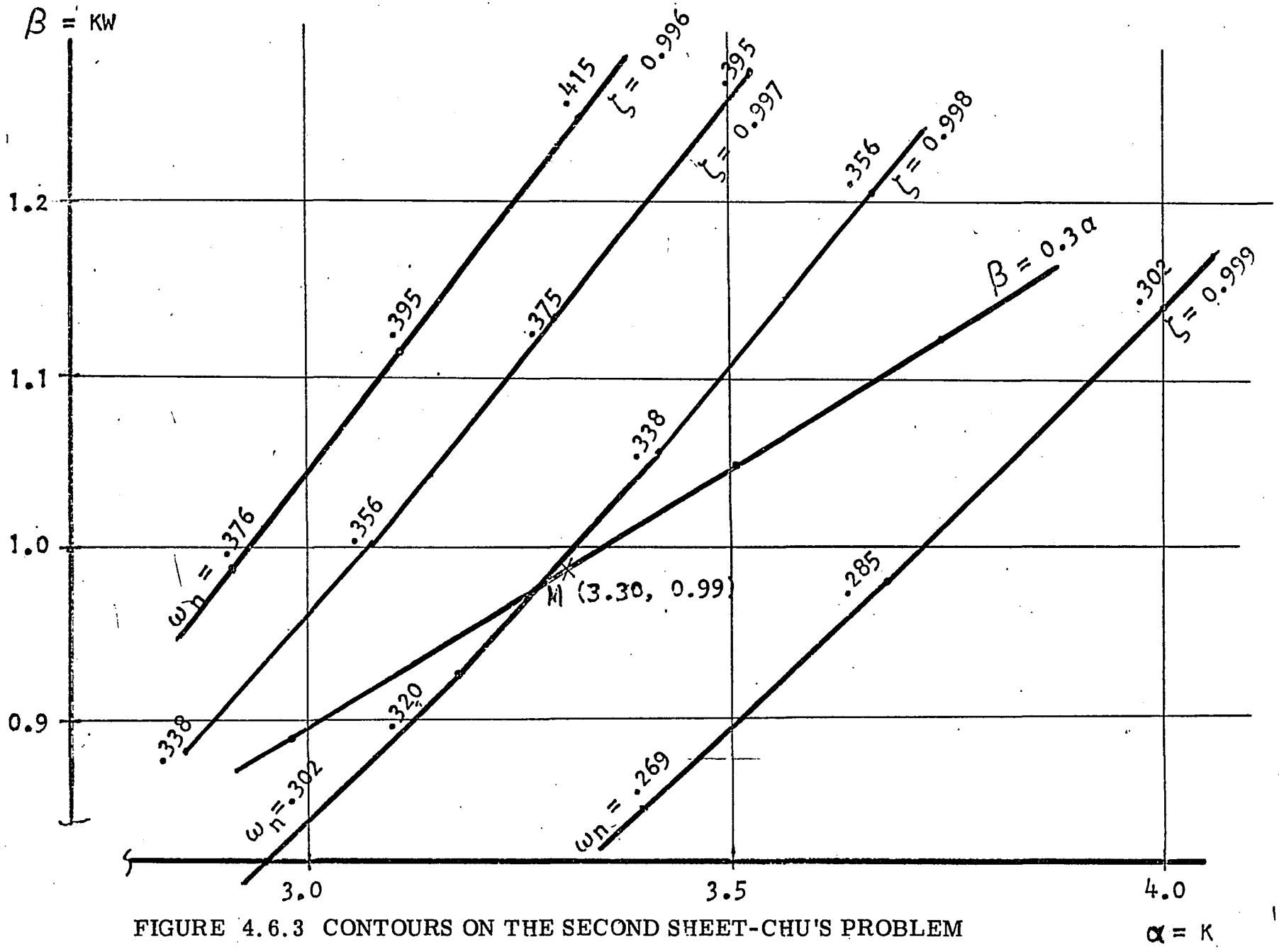

FIGURE 4.6.3 CONTOURS ON THE SECOND SHEET-CHU'S PROBLEM

running parameter. Figure 4.6.4 shows that the α - β contour for $\zeta = 0.68$, $\omega_n = 35.6$ is coincident with the point $\alpha = 3.30$, $\beta = 0.99$ indicating that a pair of complex conjugate roots are located on the second sheet at

$$s_{2B,\bar{B}} = -24.25 \pm j\ 26.1 \qquad (4.6.8)$$

4.7 Real Roots

The question of determining the real roots of the characteristic equation (4.2.5) will now be considered. The technique to be utilized is the one developed in sections 4.2 and 4.3 since this technique is applicable to any point in the s-plane.

In this case, only the real axis of the s-plane need to be considered substituting $s = \sigma + j0$ (where σ can take on positive or negative values) into the characteristic equation (4.2.5) gives

$$F(\sigma) = \sum_{k=0}^{n} a_k(\sigma)\ \sigma^k = 0 \qquad (4.7.1)$$

Then substituting (4.2.6) into (4.7.1) yields

$$\alpha \sum_{k=0}^{n} \sigma^k (b_k + c_k e^{\gamma d}) + \beta \sum_{k=0}^{n} \sigma^k (d_k + e_k e^{\gamma d}) + \sum_{k=0}^{n} \sigma^k (f_k + g_k e^{\gamma d}) = 0 \qquad (4.7.2)$$

where

$$\exp(\gamma d) = \exp\left(\sqrt{(\sigma L+R)(\sigma C+G)}\ .d\right) \qquad (4.7.2\text{-a})$$

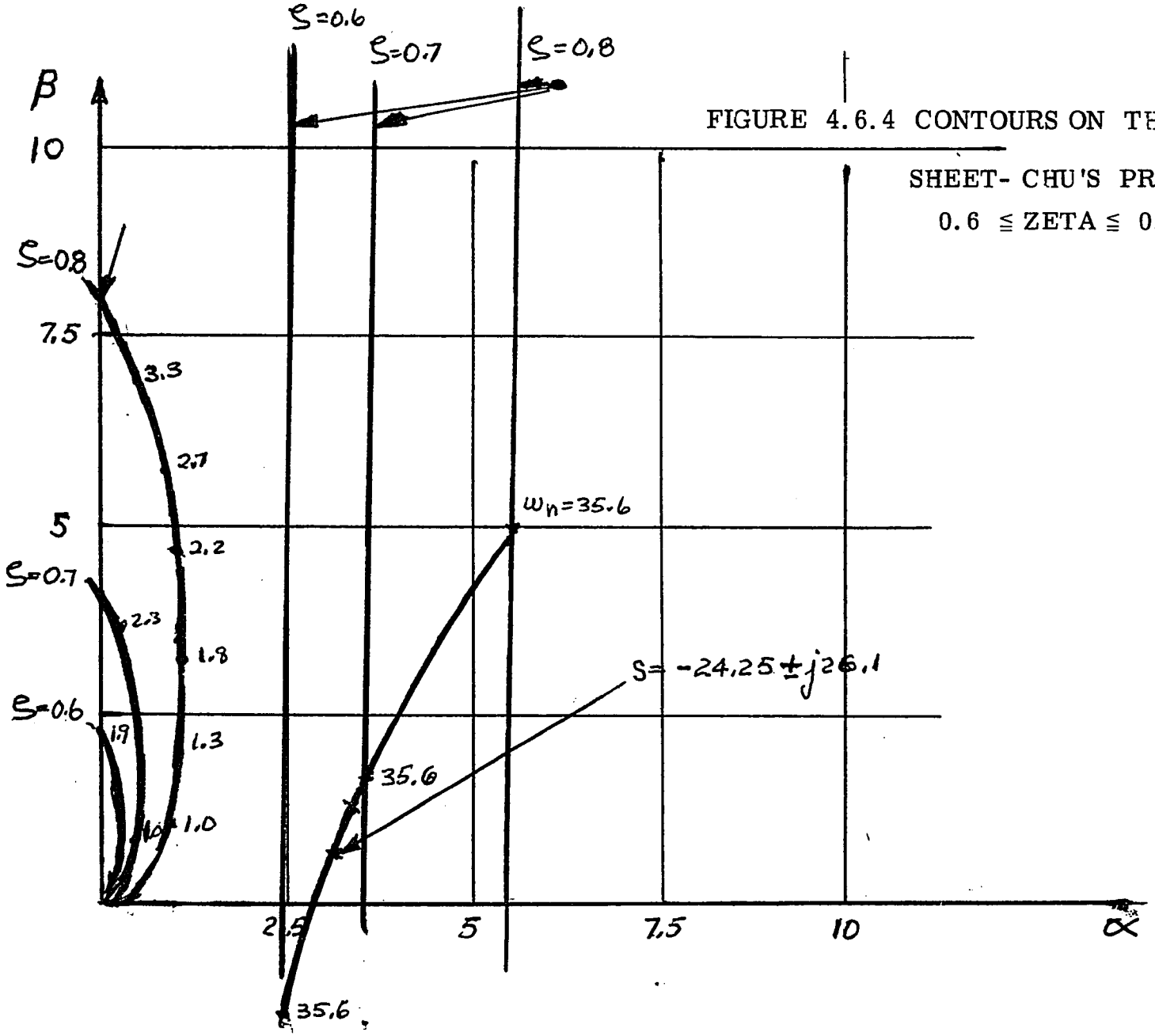

FIGURE 4.6.4 CONTOURS ON THE SECOND SHEET- CHU'S PROBLEM
0.6 ≦ ZETA ≦ 0.8

For values of σ which result in real values of γ equation (4.7.2) contains only real terms and therefore a given value of represents a straight line in the α - β plane. For example, γ will be positive and real for all positive values of σ. The function γ will also be positive and real for values of σ between zero and -a, negative and real for values of σ between -b and minus infinity, and imaginary for values of σ between the branch points (i.e., $-b \leqq \sigma \leqq -a$). Refocusing attention upon values of σ which produce real values of γ every value of σ that satisfies (4.7.2) is a real root of (4.2.5). These real roots may be determined by graphing (4.7.2) for different values of σ producing straight lines which intersect the working point $M(\alpha_1, \beta_1)$. The values of σ that produce these intersections are the real roots of (4.2.5). Since (4.7.2) is the equation of a straight line when γ is real, the graphing is not tedious and interpolation between curves is possible.

If a value of σ is selected which makes γ imaginary, then the characteristic equation is complex and can be separated into its real and imaginary parts. That is $F(\sigma)$ becomes

$$\alpha \sum_{k=0}^{n} \sigma^k(b_k+c_k\cos y) + \beta \sum_{k=0}^{n} \sigma^k(d_k+e_k\cos y) + \sum_{k=0}^{n} \sigma^k(f_k+g_k\cos y) = 0 \qquad (4.7.3)$$

and

$$\sin y \left[\alpha \sum_{k=0}^{n} \sigma^k c_k + \beta \sum_{k=0}^{n} \sigma^k e_k + \sum_{k=0}^{n} \sigma^k g_k \right] = 0 \qquad (4.7.4)$$

where

$$y = |\gamma^2|^{1/2} d$$

As mentioned previously, values of σ which make γ imaginary occur for negative values of σ which lie between the branch points $r_1 = -R/L$ and $r_2 = -G/C$. One solution of (4.7.4) is when $\sin(|\gamma^2|^{1/2} d) = 0$ or when

$$|\gamma^2| d^2 = m^2 \pi^2 \qquad m = (0, \pm 1, \pm 2, \ldots)$$

Thus

$$|\gamma^2| = |(R - \sigma L)(G - \sigma C)| = \frac{m^2 \pi^2}{d^2} \qquad (4.7.5)$$

Solving (4.7.5) for σ as m takes on successive integer values yields the absolute values of the real roots $\sigma_{R_1}, \sigma_{R_2} \ldots \sigma_{R_m}$. These roots, when they are substituted into equation (4.7.3) (and noting that at these values of σ, $\cos y = (-1)^m$) yield the following family of straight lines for integer values of m

$$\alpha \sum_{k=0}^{n} (-\sigma_R)^k (b_k + (-1)^m c_k) + \beta \sum_{k=0}^{n} (-\sigma_R)^k (d_k + (-1)^m e_k) \qquad (4.7.6)$$

$$+ \sum_{k=0}^{n} (-\sigma_R)^k (f_k + (-1)^m g_k) = 0, \quad m = 0, 1, 2 \ldots$$

The second general solution to (4.7.3) and (4.7.4) can occur when sin y $\neq$ 0 and these equations are independent. Under these conditions, each point $-\sigma_i$ on segment 3 of the negative real axis of the s-plane maps into a point (α_i, β_i). Therefore only a working point located at (α_i, β_i) will produce real roots for values of σ between the branch points (with the exception of points where sin y = 0). If (4.7.3) and (4.7.4) are not independent, the mapping is indeterminate.

The system under consideration in section 4.6 will now be examined for real roots. Since L = G = 0, $r_1 = -\infty$, $r_2 = 0$, $\gamma = \sqrt{RC\sigma}$ and equations (4.7.3) and (4.7.4) are applicable over the entire negative real axis. That is

$$\sigma^2 \cos(d\sqrt{RC|\sigma|}) + \alpha\sigma + \beta = 0$$

$$\sin(d\sqrt{RC|\sigma|}) \cdot \sigma^2 = 0 \qquad (4.7.7)$$

Considering values of σ which make sin y = 0 gives from (4.7.5)

$$|\sigma_R| = \frac{m^2\pi^2}{RCd^2} = \frac{m^2\pi^2}{T}, \quad m = 0, \pm1, \pm2 \ldots \qquad (4.7.8)$$

Therefore values of $\sigma = -\sigma_R$ for various integer values of m produce a family of straight lines through use of (4.7.6). These lines are

$$\beta = \frac{m^2\pi^2}{T}\alpha + \frac{(-1)^{m+1}m^4\pi^4}{T^2}, \quad m = 0, \pm1, \pm2, \ldots \qquad (4.7.9)$$

The characteristics of several lines from this family are summarized for T = 1 in Table 4.7.1. None of the lines in this family enter R_1, which is the region of stability of Figure 4.6.1b. Therefore this system when stable cannot have any negative real roots. This result is contrary to the one presented in [23]. The angle-loci method [20] produced the following roots for operation at $\zeta = 0.35$, T = 1, W = 0.3, and K = 3.1

$$s_{1A,\bar{A}} = 0.53 \pm j\ 1.41,$$

$$\sigma_1 = -0.33, \quad \sigma_2 = -3.20$$

As mentioned previously, the conjugate pair s_{1A} and s_{1A} are in close agreement with the root pair obtained from the $\zeta = 0.35$ contour in Figure 4.6.2c (see equation (4.6.5)). However, the negative real root σ_2 is obviously an error because substitution of this root into the open loop transfer function

$$G(-\sigma) = \frac{K(-\sigma + 0.3)e^{-\sqrt{(-\sigma)}}}{(-\sigma)^2} = 1e^{\pm j(2n+1)\pi}$$

does not satisfy the above root loci conditions. The negative real root $\sigma_1 = -0.33$ is in all probability the pair of complex conjugate roots on the second sheet of the Riemann surface very close to the negative real axis at

$$s_{2A,\bar{A}} = -0.32 \pm j\ 0.02$$

which were obtained in Section 4.6.

m	σ	EQUATION OF LINE	Gain at $\beta = 0$
0	0	$\beta = 0$	—
1	$-\pi^2$	$\beta = \pi^2\alpha + \pi^4$	$-\pi^2$
2	$-4\pi^2$	$\beta = 4\pi^2\alpha - 16\pi^4$	$+4\pi^2$
3	$-9\pi^2$	$\beta = 9\pi^2\alpha + 81\pi^4$	$-9\pi^2$
4	$-16\pi^2$	$\beta = 16\pi^2\alpha - 256\pi^4$	$+16\pi^2$

Table 4.7.1. Equations of lines in α - β plane representing negative real roots along the branch cut.

4.8 Alternate Procedure for Determining Real Roots

An alternate procedure can often be employed as an aid in determining real roots. This procedure can not only be used in determining how many real roots exist but also the approximate values of these roots. Consider the negative real axis of the s-plane for a feedback system containing a distributed parameter network with a transfer function given by (4.2.1). This half line can be divided into three segments as shown in Figure 4.5.1. Referring to this figure it was shown in section 4.7 that

- Segment 1 consists of values of σ such that the value of $\gamma(s)$ evaluated at $s = -\sigma$ is positive, due to both the $(R-\sigma L)$ and $(G-\sigma C)$ terms of (4.3.1) being real and positive.
- Segment 2 consists of values of σ such that $\gamma(s)$ is negative due to both the $(R-\sigma L)$ and $(G-\sigma C)$ terms of (4.3.1) being real and negative (i.e., vector with an argument of π)
- Segment 3 which is the branch cut of the function of equation (4.2.1) consists of values of σ such that one of the terms (either $(R-\sigma L)$ or $(G-\sigma C)$) is real and negative and the other is real and positive.
- Segment 4 (the positive real axis of the s-plane) consists of positive values of sigma.

The proof given in Appendix IV is applicable to systems in which the distributed parameter transfer function is of the form of (4.2.1). Thus the number of negative real roots of F(s) = 0 is equal to the number of straight lines drawn through a working point M(α_1, β_1) in the α - β plane that are tangent to the ζ = + 1 curves for segments 1 and 2. Furthermore, the values of these roots are equal to the negative of the frequencies ω_{n1}, ω_{n2} . . . noted on the ζ + 1 curves corresponding to these segments. Positive real roots, if any, can be found by determining the number of tangent lines than can be drawn from the working point M(α_1, β_1) to the ζ = -1 contour in the α - β plane. If any of these tangent lines exist, the system is unstable at that working point.

4.9 A Second Example

4.9.1 Stability and root locations. Given the feedback system of Figure 4.9.1 it would be instructive to investigate both its stability and the location of roots of its characteristic equation. The distributed parameter element in this case can be characterized by the following constants d = L = C = G = 1; R = 2 or the transfer function is

$$F_D(s) = \exp\left(- \sqrt{(s+1)\,(s+2)} \right) \qquad (4.9.1)$$

The open loop transfer function of the system of Figure 4.9.1 is

$$G(s) = \frac{K(s+W)\exp\left(-\sqrt{(s+1)\,(s+2)} \right)}{s^2} \qquad (4.9.2)$$

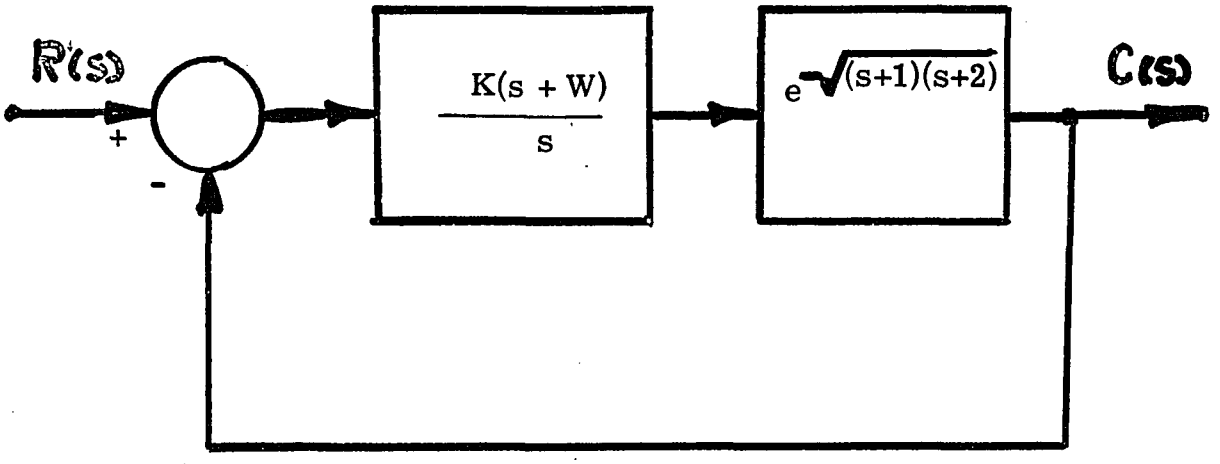

FIGURE 4.9.1 SYSTEM DIAGRAM -SECOND EXAMPLE

and the closed loop transfer function is given by

$$\frac{C}{R}(s) = \frac{K(s+W)}{s^2 \exp(-\sqrt{(s+1)(s+2)}) + Ks + KW} \qquad (4.9.3)$$

Consider the characteristic equation in which $\alpha = K$ and $\beta = KW$. That is

$$F(s) = s^2 \exp(\sqrt{(s+1)(s+2)}) + \alpha s + \beta = 0 \qquad (4.9.4)$$

Before proceeding with the mapping in the parameter plane, the relationships for the functions $-\psi$ and δ must be established. The s-plane diagram for the distributed parameter element is shown in Figure 4.9.2. The boundary line between the various regions is determined by equation 4.3.13 to be the line $\sigma = -3/2$ and the values for $-\psi$ and δ in region A of the principal sheet are given by (4.2.17) as

$$-\psi_A = \frac{1}{\sqrt{2}} \sqrt{H_a^{1/2} + J_a}$$

$$\delta_A = \frac{1}{\sqrt{2}} \sqrt{H_a^{1/2} - J_a} \qquad (4.9.5)$$

where

$$H_a = (\omega_n^2 - 4\zeta\omega_n + 4)(\omega_n^2 - 2\zeta\omega_n + 1)$$

$$J_a = (2\zeta^2 - 1)\omega_n^2 - 3\zeta\omega_n + 2$$

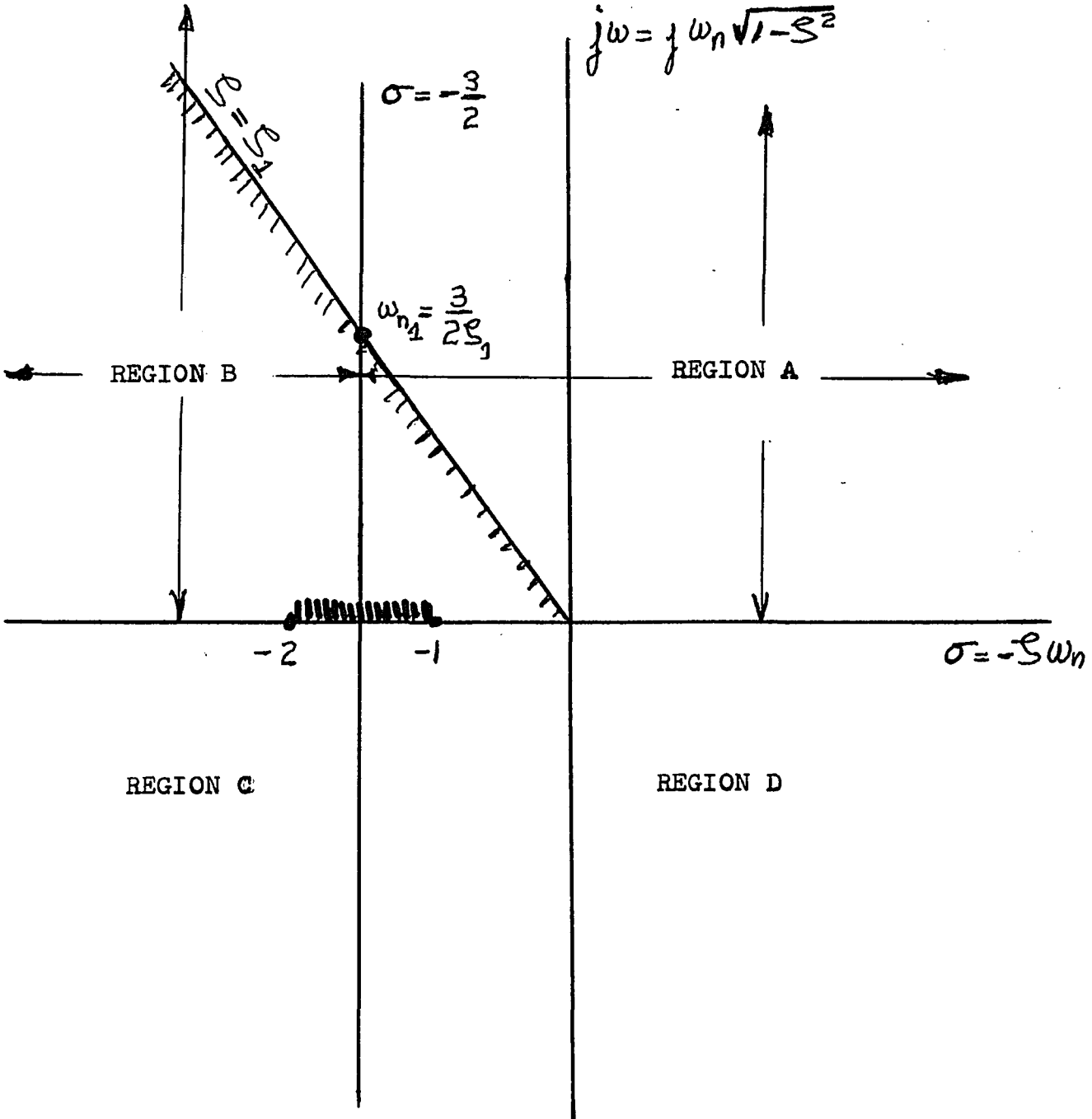

FIGURE 4.9.2 s-PLANE DIAGRAM - SECOND EXAMPLE

The value of ω_{n_1} given by (4.3.14) at which a radial line $\zeta = \zeta_1$ crosses from region A to region B is

$$\omega_{n_1} = - \frac{3}{2 \zeta_1} \qquad (4.9.6)$$

In region B, the polarity of the function for $-\psi$ changes while the polarity of the function δ remains the same. Thus in region B

$$-\psi_B = \psi_A$$

$$\delta_B = \delta_A$$

With the exception of a different function for $\gamma(s)$, the characteristic equation (4.9.4) is of the same form as the characteristic equation in the problem for distributed lag discussed in Chapter 4 Section 6. Therefore the equations for α, β and Δ are identical to (4.6.3) and are repeated below

$$\alpha = \omega_n e^{-\psi} \left[2 \zeta \cos \delta + \frac{(1-2\zeta^2) \sin \delta}{(1-\zeta^2)^{1/2}} \right]$$

$$\beta = \omega_n^2 e^{-\psi} \left(\cos \delta - \frac{\zeta \sin \delta}{(1-\zeta^2)^{1/2}} \right) \qquad (4.9.8)$$

$$\Delta = - \omega_n (1-\zeta^2)^{1/2}$$

where $-\psi$ and δ are defined by (4.9.5) for region A of the principal sheet of the s-plane.

In order to investigate absolute stability, ζ is set equal to zero and ω_n is varied from zero to infinity. From Figure 4.9.2 it can be seen that only Region A need by considered when $\zeta = 0$. The parameter plane equations for $\zeta = 0$ are

$$\alpha = \omega_n e^{-\psi} \sin \delta$$

$$\beta = \omega_n^2 e^{-\psi} \cos \delta \qquad (4.9.9)$$

$$\Delta = -\omega_n$$

where

$$-\psi = \sqrt{\frac{[(\omega_n^2 + 1)(\omega_n^2 + 4)]^{1/2} - \omega_n^2 + 2}{2}} \qquad (4.9.10)$$

$$\delta = \sqrt{\frac{[(\omega_n^2 + 1)(\omega_n^2 + 4)]^{1/2} + \omega_n^2 - 2}{2}}$$

This $\zeta = 0$ contour is plotted in Figure 4.9.3. Note that as ω_n is increased the contour spirals outward from the origin. The $\zeta = 0.3$ contour is plotted in Figure 4.9.4. Note in this case that as ω_n increases, the contour first spirals outward from the origin and then inward toward the origin as the s-plane path moves into region B. This transition from region A to region B occurs at $\omega_n = 10.0$. This means that as ω_n increases toward infinity the roots of F(s) = 0 must eventually lie above the $\zeta = 0.3$ radial. The first traversal of the $\zeta = 0$ contour is also shown in Figure 4.9.4.

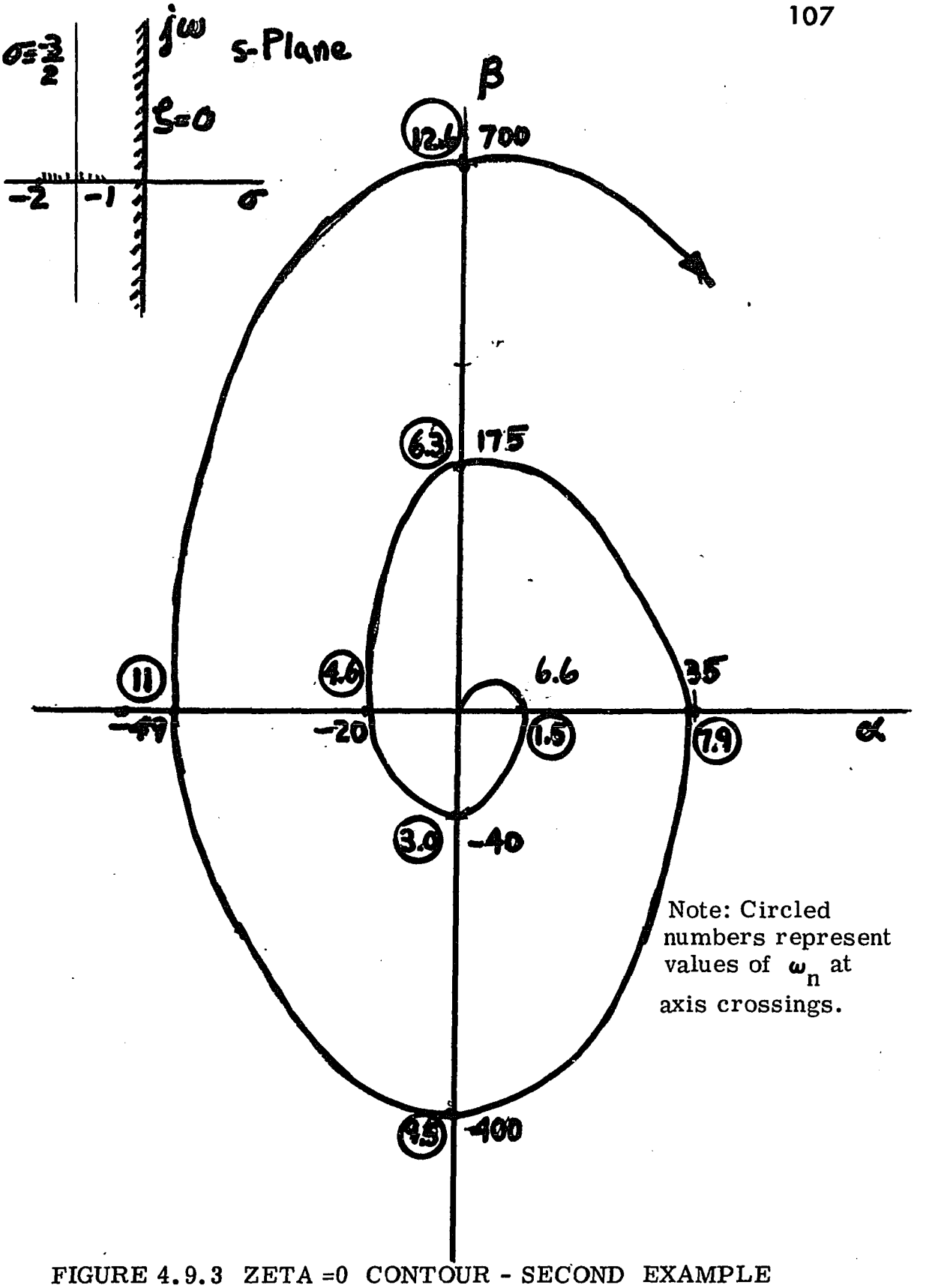

FIGURE 4.9.3 ZETA =0 CONTOUR - SECOND EXAMPLE

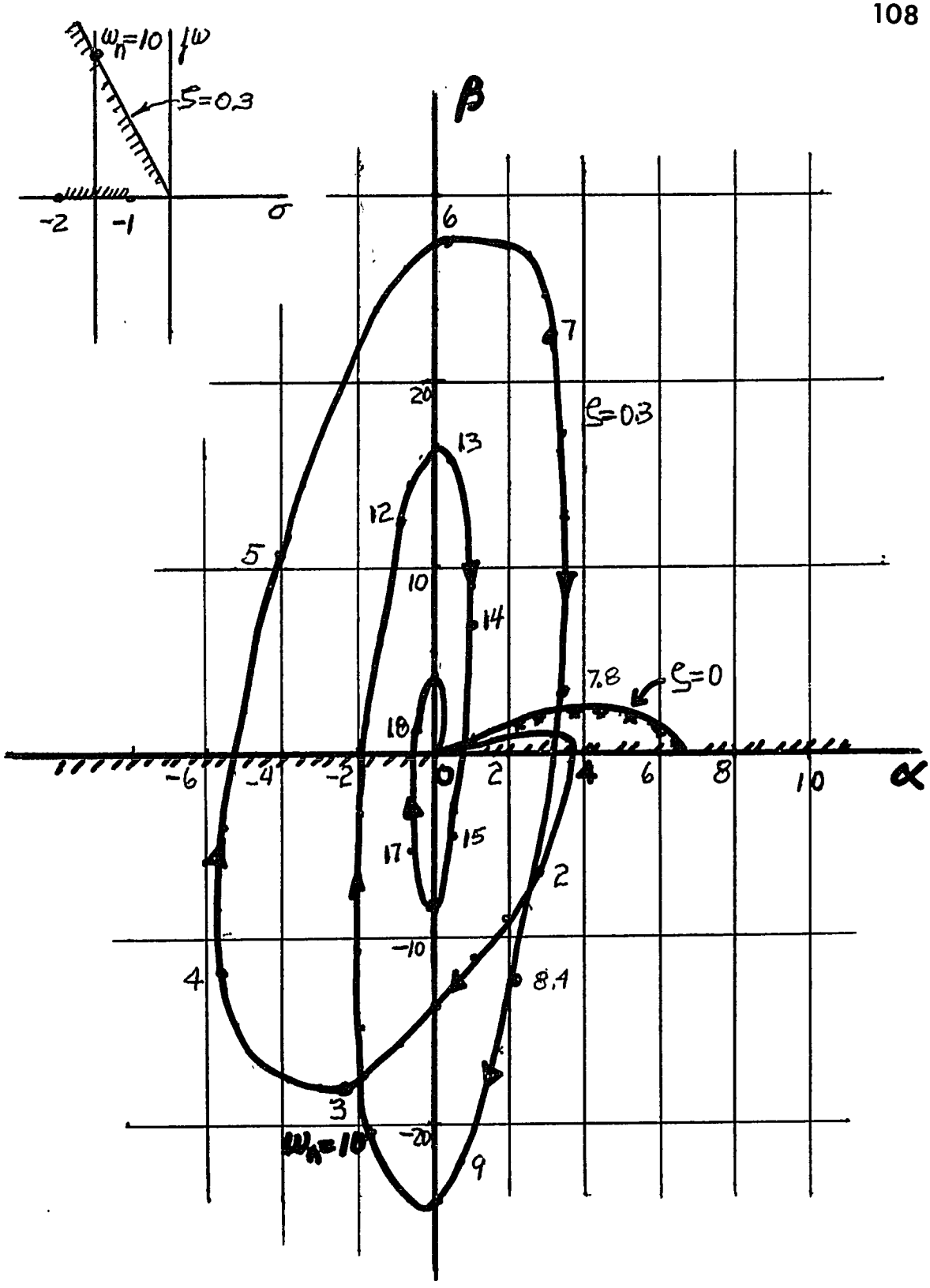

FIGURE 4.9.4 ZETA= 0.3 CONTOUR- SECOND EXAMPLE

The first traversal of the $\alpha = \beta$ contours corresponding to various values of ζ between zero and 0.9 are shown in Figure 4.9.5. Also shown in this figure is the line $\beta = 0.3\,\alpha$ corresponding to a value of W equal to 0.3. The intersection of this line and the $\zeta = 0$ contour indicates that when W = 0.3 the maximum gain for stable operation is 5.40 and the frequency of oscillation at this gain is 1.30 radians/sec. When W is set equal to zero, the maximum allowable system gain for stability is 6.55.

4.9.2 $\zeta = \pm 1$ Contours. The $\zeta = \pm 1$ contour must be considered for each of three line segments shown in Figure 4.9.2. On segment 1, which covers values of ω_n between zero and one, $F_1(\zeta = 1)$ of (4.5.9) is given by

$$F_1(\zeta = 1) = F_1(1) = \frac{\omega_n(3-2\,\omega_n)}{2\,[(\omega_n-2)(\omega_n-1)]^{1/2}}$$

In addition, the functions $-\psi$ and δ are given by (4.5.2) as

$$-\psi_1 = [(2-\omega_n)(1-\omega_n)]^{1/2}, \quad \delta_1 = 0$$

and the parameter plane equations α and β are obtained by application of (4.5.11) utilizing (4.5.10), and (4.5.5). That is

$$\alpha = \omega_n e^{-\psi}\,(2-F_1(1))$$

$$\beta = \omega_n^2 e^{-\psi}\,(1-F_1(1))$$

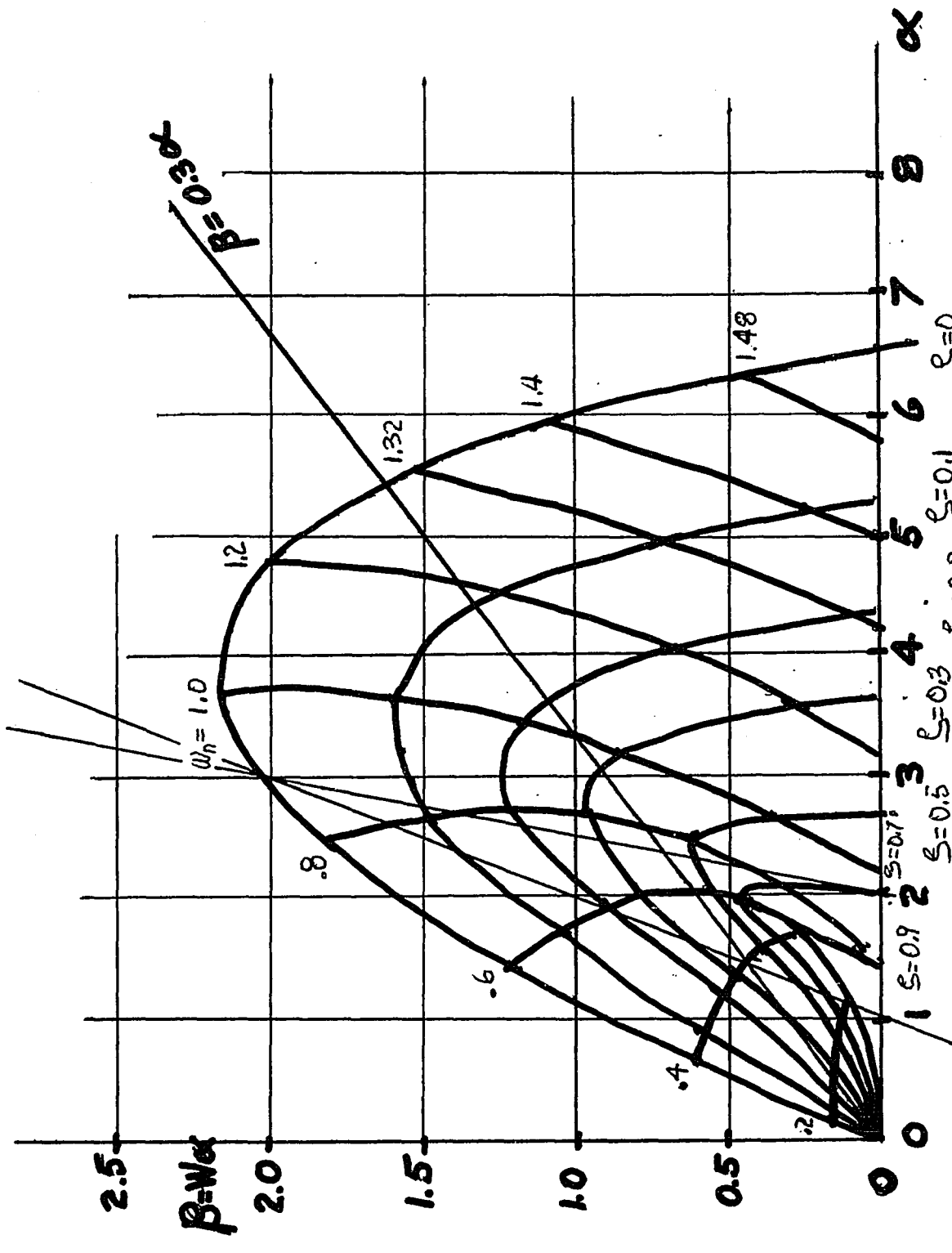

FIGURE 4.9.5 FIRST TRAVERSAL OF CONTOURS BETWEEN $\zeta=0$ AND $\zeta=0.9$

This contour is plotted in Figure 4.9.6 for values of ω_n between zero and one.

Similarly along line segment 2, which covers values of ω_n between 2 and infinity, the following equations are obtained

$$F_2(\zeta=1) = F_2(1) = \frac{\omega_n(2\ \omega_n-3)}{2\sqrt{(\ \omega_n-2)\ (\ \omega_n-1)}} = -F_1(1)$$

$$-\psi_2 = -\sqrt{(\ \omega_n-2)\ (\ \omega_n-1)}$$

$$\delta_2 = 0$$

$$\alpha = \omega_n e^{-\psi_2}\ (2-F_2(1)\ )$$

$$\beta = \omega_n^2 e^{-\psi_2}\ (1-F_2(1)\ )$$

This contour is also plotted in Figure 4.9.6 for values of ω_n greater than two.

To examine the ζ =1 curve along segment 3 (i.e. values of ω_n between 1 and 2), first values of ω_n for which sin δ = 0 must be found and then the remainder of the segment (if determinate) is mapped. Values of ω_n along segment3 of the negative real axis which make sin δ = 0 can be found by solving (4.5.14) for values of the integer m. Since R/L is greater than G/C and d = 1, equation (4.5.14) becomes

$$(2-\ \omega_n)\ (\ \omega_n-1) = \pm m^2\pi^2$$

for values of ω_n along segment 3. When m = 0

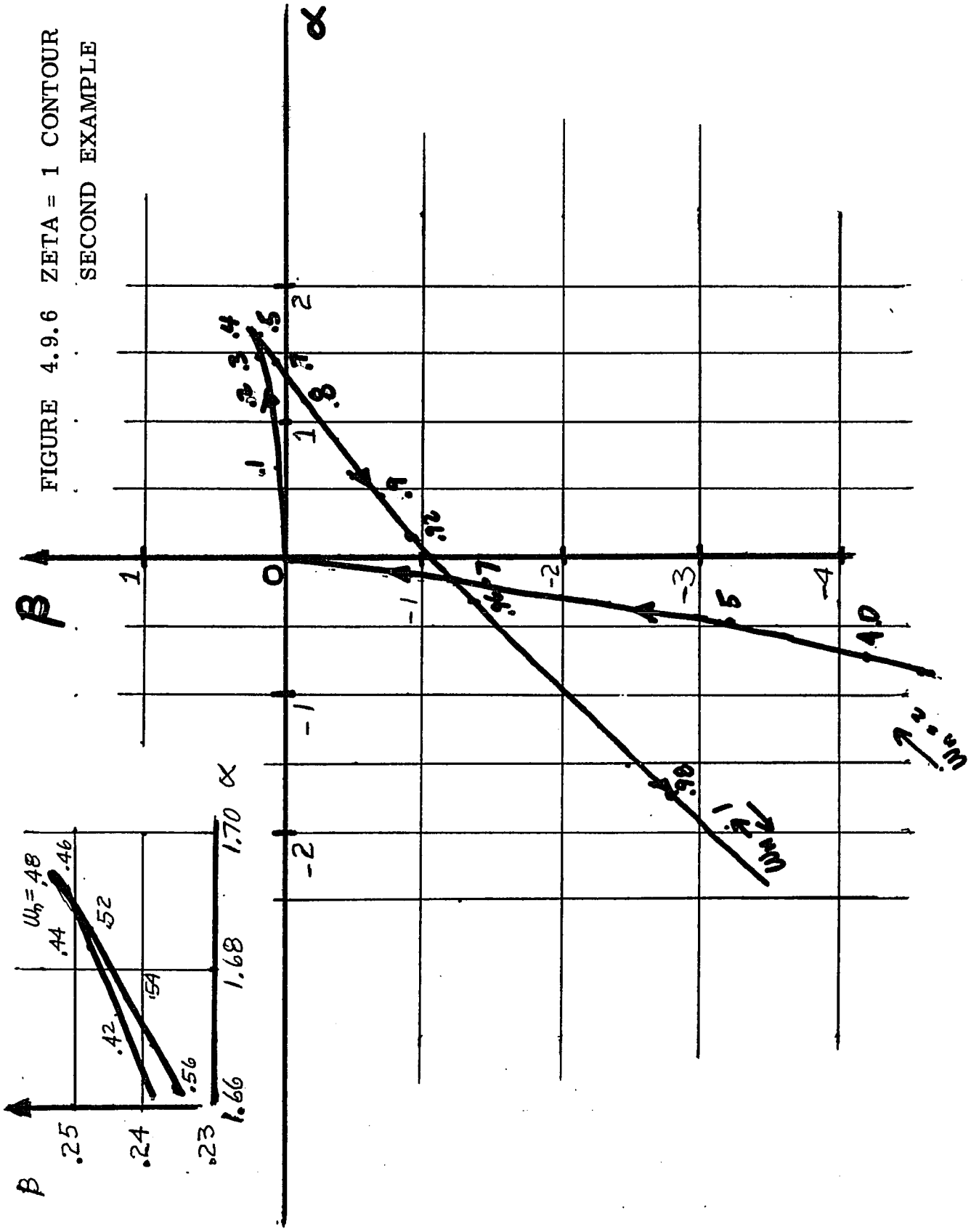

FIGURE 4.9.6 ZETA = 1 CONTOUR
SECOND EXAMPLE

$$\omega_n^2 - 3\ \omega_n + 2 = 0$$

Thus $\omega_n = 2$ and $\omega_n = 1$. For values of m other than zero the values of ω_n fall outside of segment 3 and therefore do not apply. Applying equation (4.5.6) and (4.5.15) to the two roots found when m = 0 produces two straight lines

$$\beta = \alpha - 1$$

$$\beta = 2\alpha - 4$$

Operating points chosen along one of these lines will yield a real root at the indicated value of sigma. For the remainder of segment 3, equation (4.5.13) is applied and results in

$$\Delta_3 = \text{Sin}\ \delta \left[(-\omega_n) \cdot 0 - (1) \cdot 0\right] = 0$$

and the $\zeta = 1$ curve is therefore indeterminate between the branch points.

4.10 Constant Sigma Contours

Contours which consist of constant sigma lines (instead of constant dimensionless damping lines) will now be discussed. A typical constant sigma line is shown in Figure 4.3.2a. Also shown in the figure are the branch points and branch cut associated with the distributed parameter element as well as line Q, the branch cut bisector. In the upper half of the principal sheet of the s-plane, the constant sigma line can be either region A, region B or coincident with line Q, the boundary between the two regions. When in either regions A

or B, the polarity of the function $-\psi$ should conform with the polarity specified in Table 4.3.1. When the constant settling time line is on the boundary, the value of $-\psi$ is zero.

The mapping of constant sigma lines can be accomplished by either deriving the $\alpha - \beta$ equations in terms of σ and ω or by modifying the parameter plane coefficients of equations (4.2.12). In this case, the s-plane path consists of a contour of constant $\sigma = -\zeta \omega_n$ and it therefore becomes necessary to eliminate either ζ or ω_n in order to effect the mapping. Again, it should be noted that when symmetrically enclosing the left half, of the s-plane or a region therein, it is only necessary to compute values of α and β for $\omega_n > 0$ (see Appendix II). A constant sigma line can be mapped by either

1. Setting σ equal to a constant and varying ω_n from the absolute value of σ to infinity or
2. Setting σ equal to a constant and varying ζ from +1 to zero.

The generalized $\alpha - \beta$ equations for systems containing a distributed parameter element will be derived for both cases.

4.10.1 Case 1 - Parameter plane equations which are functions of σ and ω_n. The equations for the parameter plane coefficients, (4.2.12) and the distributed parameter functions (4.3.17) must be rearranged so that the variable ζ never appears alone, but only in the product $\sigma = -\zeta \omega_n$. This is accomplished by multiplying the numerator and

denominator of all terms containing unconverted ζ terms by ω_n thereby permitting the ζ term to be converted into a σ term. Thus for region A, sheet 1 (4.3.17) becomes

$$-\psi = \frac{d}{\sqrt{2}} \sqrt{H_1^{1/2} + J_1}$$

$$\delta = \frac{d}{\sqrt{2}} \sqrt{H_1^{1/2} - J_1} \qquad (4.10.1)$$

where

$$H_1 = (\omega_n^2 L^2 + 2\sigma RL + R^2) \cdot (\omega_n^2 C^2 + 2\sigma GC + G^2)$$

$$J_1 = LC(2\sigma^2 - 1) + RG + \sigma(RC + LG) \qquad (4.10.2)$$

Values of $-\psi$ and δ for region B, sheet 1 are obtained by reversing the polarity of the expression for $-\psi$ above and using the above value of δ directly.

Furthermore the following expression can be expressed as

$$(1 - \zeta^2)^{1/2} = \frac{(\omega_n^2 - \sigma^2)^{1/2}}{\omega_n} \qquad (4.10.3)$$

Since the Chebychev polynominals are also functions of ζ they can be rewritten as

$$P_k(\sigma, \omega_n^2) = (-1)^k \omega_n^k T_k(\zeta)$$

$$Q_k(\sigma, \omega_n^2) = (-1)^{k+1} \omega_n^{k-1} U_k(\zeta) \qquad (4.10.4)$$

The P_k and Q_k functions can be obtained from the following recursion formulas

$$P_k\ (\sigma, \omega_n^2) - 2\sigma P_k(\sigma, \omega_n^2) + \omega_n^2 P_{k-1}(\sigma, \omega_n^2) = 0$$

$$Q_k\ (\sigma, \omega_n^2) - 2\sigma Q_k(\sigma, \omega_n^2) + \omega_n^2 Q_{k-1}(\sigma, \omega_n^2) = 0 \qquad (4.10.5)$$

where

$$P_0 = 1, \qquad P_1 = \sigma, \qquad P_2 = 2\sigma^2 - \omega_n^2$$

$$Q_0 = 0, \qquad Q_1 = 1, \qquad Q_2 = 2\sigma$$

Thus, under the condition that $\omega_n \geq |\sigma|$, equations (4.2.12) can be rewritten as

$$B_1 = \sum_{k=0}^{n} Z_{0s} b_k + e^{-\psi} c_k Z_{1s}$$

$$C_1 = \sum_{k=0}^{n} Z_{0s} d_k + e^{-\psi} e_k Z_{1s}$$

$$D_1 = \sum_{k=0}^{n} Z_{0s} f_k + e^{-\psi} g_k Z_{1s} \qquad (4.10.6)$$

$$B_2 = \sum_{k=0}^{n} Z_{2s} b_k + e^{-\psi} c_k Z_{3s}$$

$$C_2 = \sum_{k=0}^{n} Z_{2s} d_k + e^{-\psi} e_k Z_{3s}$$

$$D_2 = \sum_{k=0}^{n} Z_{2s} f_k + e^{-\psi} g_k \quad Z_{3s}$$

where

$$Z_{0s} = P_k, \quad Z_{2s} = Q_k(\omega_n^2 - \sigma^2)^{1/2}$$

$$Z_{1s} = P_k \operatorname{Cos} \delta - (\omega_n^2 - \sigma^2)^{1/2} Q_k \operatorname{Sin} \delta$$

$$Z_{3s} = Q_k (\omega_n^2 - \sigma^2)^{1/2} \operatorname{Cos} \delta + P_k \operatorname{Sin} \delta$$

where $-\psi$ and δ are defined by (4.10.1) for region A of sheet 1. For mapping constant sigma contours in other regions in sheet 1, the polarity of the variables $-\psi$ and δ are determined by Table 4.3.1. Through use of (4.10.6) σ can be set equal to a constant and ω_n varied from the absolute value of σ to infinity with the parameter plane coefficients, α, and β being computed for each value of ω_n.

4.10.2 Case 2 - Parameter plane equations which are functions of σ and ζ. By eliminating the variable ω_n from (4.3.17) through use of the relationship $\sigma = -\zeta \omega_n$ the following is obtained for region A of sheet 1 of the s-plane

$$-\psi = \frac{d}{\sqrt{2}} \sqrt{H_2^{1/2} + J_2}$$

$$\delta = \frac{d}{\sqrt{2}} \sqrt{H_2^{1/2} - J_2} \qquad (4.10.7)$$

where

$$H_2 = \left(\frac{\sigma^2 L^2}{\zeta^2} + 2\sigma RL + R^2\right)\left(\frac{\sigma^2 C^2}{\zeta^2} + 2\sigma GC + G^2\right)$$

$$J_2 = \frac{\sigma^2 LC}{\zeta^2}\left(2\zeta^2 - 1\right) + RG + \sigma(RC + LG) \qquad (4.10.8)$$

Expressions for $-\psi$ and δ in other regions of the s-plane can be determined through use of Table 4.3.1 and (4.10.7). The parameter plane coefficients of (4.2.12) upon elimination of the variable ω_n become

$$B_1 = \sum_{k=0}^{n} Z_{0d}\, b_k + e^{-\psi} c_k Z_{1d}$$

$$C_1 = \sum_{k=0}^{n} Z_{0d}\, d_k + e^{-\psi} e_k Z_{1d}$$

$$D_1 = \sum_{k=0}^{n} Z_{0d}\, f_k + e^{-\psi} g_k Z_{1d}$$

$$B_2 = \sum_{k=0}^{n} Z_{2d}\, b_k + e^{-\psi} c_k Z_{3d} \qquad (4.10.9)$$

$$C_2 = \sum_{k=0}^{n} Z_{2d}\, d_k + e^{-\psi} e_k Z_{3d}$$

$$D_2 = \sum_{k=0}^{n} Z_{2d}\, f_k + e^{-\psi} g_k Z_{3d}$$

where

$$Z_{0d} = \frac{\sigma^k}{\zeta^k} T_k \quad , \quad Z_{2d} = \frac{\sigma^k}{\zeta^k} U_k (1 - \zeta^2)^{1/2}$$

$$Z_{1d} = \frac{\sigma^k}{\zeta^k} (T_k \text{ Cos } \delta + (1 - \zeta^2)^{1/2} U_k \text{ Sin } \delta)$$

$$Z_{3d} = \frac{\sigma^k}{\zeta^k} (-U_k (1 - \zeta^2)^{1/2} \text{ Cos } \delta + T_k \text{ Sin } \delta)$$

Mathematically, it makes little difference whether constant sigma lines (i.e. $\sigma = -\sigma_1$) are mapped with either ω_n or as the running parameter. In most applications, however, ω_n is chosen as the running parameter because of its range (i.e. $|\sigma| \leqq \omega_n \leqq \infty$ as opposed to $1 \geqq \zeta \geqq 0$) and its physical interpretation.

CHAPTER 5

ANALYSIS OF FEEDBACK SYSTEMS CONTAINING DISTRIBUTED PARAMETER ELEMENTS WITH TRANSFER FUNCTIONS OF THE FORM $\exp[-(sT)^{p/q}]$

5.1 INTRODUCTION

A class of transfer functions which contain both transport and distributed lag as special cases will now be investigated. This class of transfer functions is expressed by

$$F_D(s) = [-(sT)^{p/q}] \qquad (5.1.1)$$

where

T is a constant

s is the complex variable

p and q are integers with $p \leqq q$

When the integers p and q are equal, (5.1.1) is the familiar expression for transport lag. When $2p = q$, (5.1.1) becomes the transfer function for distributed lag. When an element with transfer function describable by (5.1.1) is present in a feedback system, the absolute and relative stability as well as roots of the characteristic equation can be determined by applying the methods of Chapter 4. However these methods would have to be applied to each case individually.

A new method of analysis of feedback systems containing distributed parameter elements is presented in this chapter. This method makes use of a complex variable transformation which, in essence, maps a q-sheeted Riemann surface onto a single sheet. Parameter plane techniques are then applied in the transformed domain in order to determine stability and roots of the characteristic equation. The root values can be converted back to their original "s" plane values by an inverse complex variable transformation.

5.2 Transformation of Singularities in The s-Plane into the w -Plane

It is known[6]that a simple pole in the s-plane transformed into a complex conjugate pair of poles on the imaginary axis of the w -plane under the transformation $s = w^2$. In addition, under this transformation, a complex conjugate pair of s-plane poles transformed into a quartet of real-complex conjugate poles in w (see Figure 5.2.1). In generalizing this concept consider a simple pole at s = -a. That is

$$F(s) = \frac{1}{s + a} \qquad (5.2.1)$$

Under the transformation $w^q = s$, (5.2.1) becomes

$$F(w) = \frac{1}{(w^q + a)} \qquad (5.2.2)$$

The transformed function now possesses poles at points determined by the roots of the denominator of (5.2.2)

$$w^q = a \exp(j(\pi + 2\pi n)), \qquad n = (0, 1, \ldots, q-1)$$

or

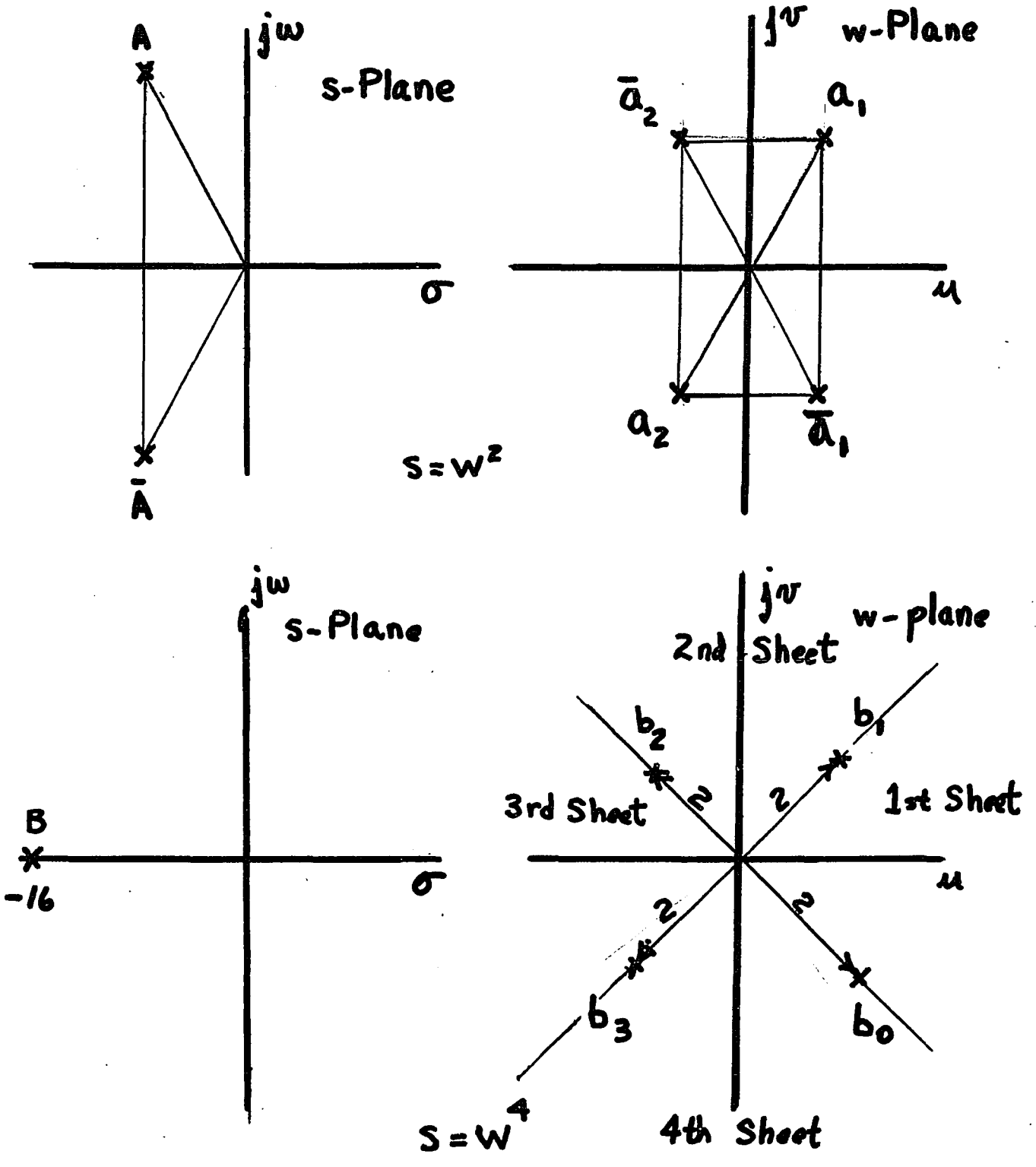

FIGURE 5.2.1 s-PLANE AND w-PLANE DIAGRAMS FOR $w^2 = s$ AND $w^4 = s$ TRANSFORMATIONS

$$w = a^{1/q} \exp\left(j \frac{\pi (1+2n)}{q}\right) \qquad (5.2.3)$$

Similarly, it can be shown that poles appearing in complex conjugate pairs at $s = r \exp(\pm j \theta)$ in the s-plane transform, under the transformation $w^q = s$, into poles at

$$w = r^{1/q} \exp\left(j \frac{\pm \theta + 2 \pi n}{q}\right), \qquad n = (0, 1, 2, \ldots, q-1) \qquad (5.2.4)$$

The result is that a simple pole in the s-plane transforms into q simple poles in the w -plane under a $w^q = s$ transformation. Each of these q poles in w appears in a sector of w which represents the image of one of the sheets of the "q" sheeted Riemann surface in "s". An example of this transformation of poles is illustrated in Figure 5.2.1. This figure depicts a simple pole at $s = -16$ mapped into w under a $w^4 = s$ transformation. In addition, the figure shows the sector of the w -plane occupied by each of the four sheets comprizing the Riemann surface.

Other properties of the transformation $w^q = s$ are

1. A circle of radius ω_{n1} in the s-plane maps into a circle of radius $(\omega_{n1})^{1/q}$ in the w -plane.
2. A constant zeta radial in the s-plane maps into a constant zeta radial in the w-plane. This is illustrated in Figure 5.2.2 where an s-plane radial at an angle $\theta = \theta_1$ maps into a w -plane radial at an angle $\phi = \frac{\theta_1}{q}$.

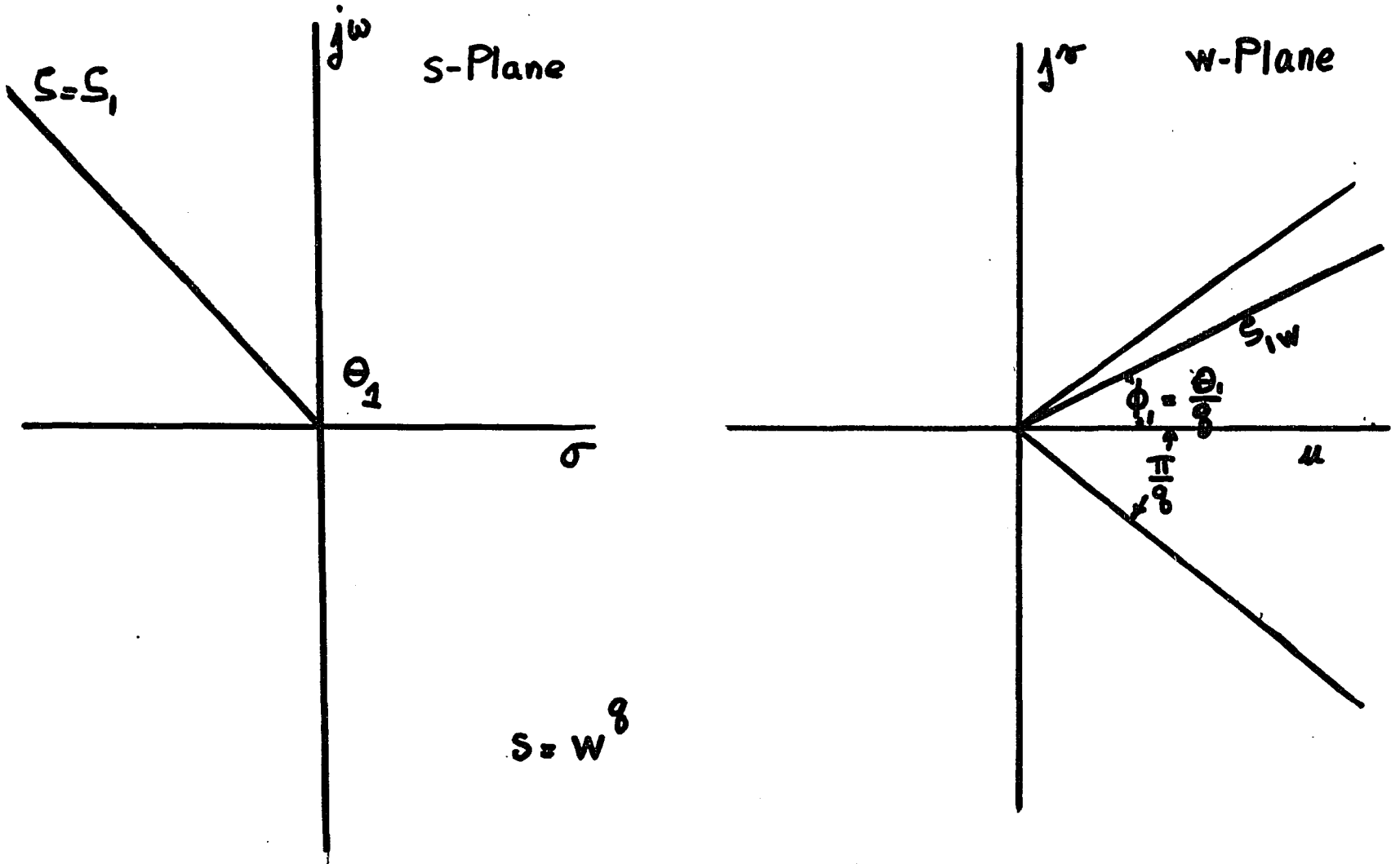

FIGURE 5.2.2 s-PLANE AND w- PLANE DIAGRAMS FOR $w^q=s$

5.3 Application of the Conformal - Parameter Plane Mapping Technique to Systems Containing Distributed Parameter Elements with Transfer Functions of the Form $\exp(-(sT)^{p/q})$

Consider the linear unity feedback control system with a hypothetical distributed parameter element in the forward path shown in Figure 5.3.1. The ratio of C(s) to R(s) is

$$\frac{C}{R}(s) = \frac{KN(s)e^{-(sT)^{p/q}}}{D(s) + KN(s)e^{-(sT)^{p/q}}} = \frac{KN(s)}{D(s)e^{(sT)^{p/q}} + KN(s)} \qquad (5.3.1)$$

where N(s) and D(s) are rational polynominals in s, T is a constant of the distributed parameter element, p and q are integers with $p < q$ and s is the complex variable.

$$s = \sigma + j\omega = -\zeta\omega_n + j\omega_n(1-\zeta^2)^{1/2} \qquad (5.3.2)$$

Since the ratio of p to q is less than unity the characteristic equation will be multivalued as well as transcendental. The characteristic equation F(s) is given by

$$F(s) = D(s)\exp(sT)^{p/q} + KN(s) = 0 \qquad (5.3.3)$$

is a "q" valued function of "s". If F(s) is mapped onto a complex plane "w" where w is defined as $w^q = s$, the characteristic equation can be represented as a single valued function of w. Therefore

$$F(w) = D(w^q)\exp(w^p T^{p/q}) + KN(w^q) = 0 \qquad (5.3.4)$$

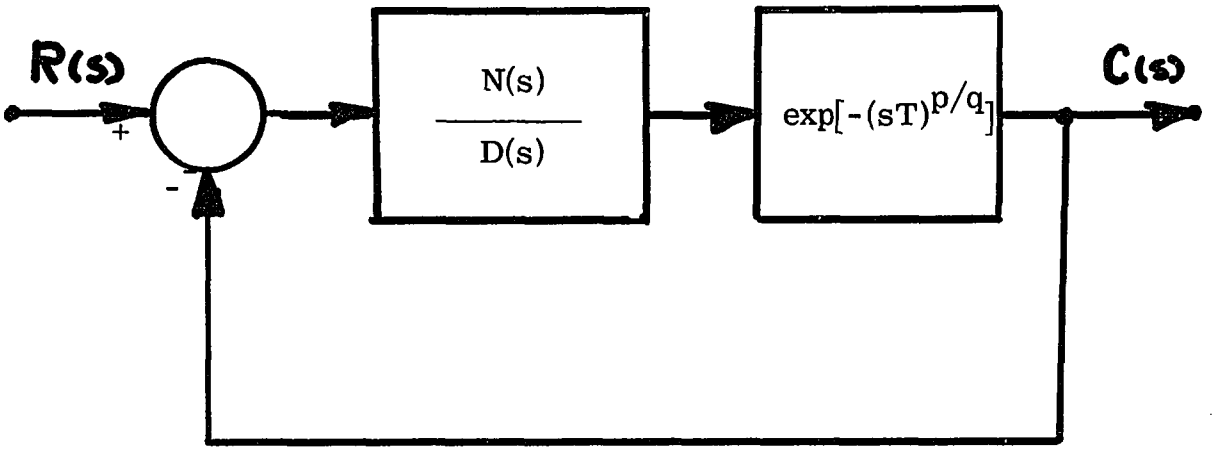

FIGURE 5.3.1 DIAGRAM OF SYSTEM CONTAINING HYPOTHETICAL WITH TRANSFER FUNCTION $\exp[-(sT)^{p/q}]$

The above transformation has mapped a "q" sheeted Riemann surface in s onto a single sheet in w . The principal sheet of the Riemann surface in s has been reduced to a sector with angle $\phi = \pm \pi/q$. The equivalent of the left half and right half planes of the principal sheet "s" are also shown in Figure 5.2.2 .

5.3.1 Systems in which p is equal to unity. Consider equation (5.3.4) when p = 1. Under this restriction

$$F(w) = D(w^q)\exp(w\,T^{1/q}) + KN(w^q) = 0 \qquad (5.3.5)$$

and the characteristic equation appears similar in form to one which would result if the distributed parameter element were transport lag. Therefore application of Eisenberg's technique[29] is possible for this case. The procedure for this class of systems is to first

determine roots of $F(w) = 0$ by parameter plane techniques. Applying the technique in Chapter 3 Section 6, of separating real and imaginary terms and noting that in the w-plane

$$\zeta_w = -\cos(\theta/q), \quad \omega_w = (\omega_n)^{1/q}, \quad \zeta = -\cos\theta \ , \qquad (5.3.6)$$

$$-\psi_w = -\zeta_w \omega_w T^{1/q}, \quad \delta_w = \omega_w (1-\zeta_w^2)^{1/2} T^{1/q} \qquad (5.3.7)$$

the characteristic equation (5.3.5) can be written as

$$F(\omega_w, \zeta_w) = \alpha_w B_{1w} + \beta_w C_{1w} + D_{1w} + j[\alpha_w B_{2w} + \beta_w C_{2w} + D_{2w}] \qquad (5.3.8)$$

where upon referring to (4.2.12) and taking note of (5.3.6) and (5.3.7)

$$
\begin{aligned}
B_{1w} &= B_1(\zeta_w, \omega_w, \psi_w, \delta_w) \\
C_{1w} &= C_1(\zeta_w, \omega_w, \psi_w, \delta_w) \\
D_{1w} &= D_1(\zeta_w, \omega_w, \psi_w, \delta_w) \\
B_{2w} &= B_2(\zeta_w, \omega_w, \psi_w, \delta_w) \\
C_{2w} &= C_2(\zeta_w, \omega_w, \psi_w, \delta_w) \\
D_{2w} &= D_2(\zeta_w, \omega_w, \psi_w, \delta_w)
\end{aligned}
\tag{5.3.9}
$$

Setting F(w) = 0 by setting both the real and imaginary parts of (5.3.8) equal to zero gives

$$
\begin{aligned}
\alpha_w B_{1w} + \beta_w C_{1w} &= -D_{1w} \\
\alpha_w B_{2w} + \beta_w C_{2w} &= -D_{2w}
\end{aligned}
\tag{5.3.10}
$$

Solving (5.3.10) for α_w and β_w gives

$$
\alpha_w = \frac{C_{1w}D_{2w} - D_{1w}C_{2w}}{\Delta_w} \qquad \beta_w = \frac{D_{1w}B_{2w} - D_{2w}B_{1w}}{\Delta_w}
\tag{5.3.11}
$$

$$
\Delta_w = B_{1w}C_{2w} - C_{1w}B_{2w}
$$

The above procedure provides the $\alpha_w - \beta_w$ equations via a double mapping operation. The first mapping operation $s = w^q$ is conformal (i.e. angles relationships are preserved). The second mapping which

involves mapping from the complex w plane onto the algebraic $\alpha_w - \beta_w$ plane is not conformal. It should be noted that constant zeta radials in the s-plane map into constant zeta radials in the w-plane in accordance with the relationship

$$\zeta_w = -\cos(\theta/q) \text{ where } \zeta = -\cos\theta$$

for the $\zeta = 0$ radial $\theta = \pi/2$, and $\zeta_w = -\cos(\pi/2q)$. Furthermore constant ω_n contours on the s-plane map onto constant ω_w contours on the w-plane according to the relationship $\omega_w = (\omega_n)^{1/q}$. Therefore a circle of radius ω_{n1} in "s" maps into a circle of radius $r = (\omega_{n1})^{1/q}$ in w (see Figure 5.2.2). Also, while the degree of the characteristic equation is increased by a factor of "q" in the transformation from s to w, the number of terms remain constant. That is the transformed characteristic equation will contain only terms in w^{qn}, $w^{q(n-1)}$, $w^{q(n-2)}$. . . . w^0. Thus the number of terms of F(w) involved in the derivation of the $\alpha_w - \beta_w$ equations is the same as the number of terms in F(s), used in the derivation of $\alpha - \beta$ equations.

The results presented above are now illustrated by means of the following example. Consider the example of the control system of Figure 4.6.1 in Chapter 4. From Figure 4.6.1

$$G(s) = \frac{N(s+W)}{D(s)} = \frac{K(s+W)}{s^2} \qquad (5.3.12)$$

and

$$\frac{C}{R}(s) = \frac{K(s+W)}{s^2 \exp[(sT)^{1/2}] + Ks + KW} \qquad (5.3.13)$$

For stability investigation of this sytem, form the characteristic equation

$$F(s) = s^2 \exp[(sT)^{1/2}] + Ks + KW = 0 \qquad (5.3.14)$$

Introducing the transformation $w^2 = s$ into (5.5.14) yields

$$F(w) = w^4 \exp(wT^{1/2}) + Kw^2 + KW = 0 \qquad (5.3.15)$$

Defining $\alpha_w = K$, $\beta_w = KW$, F(w) becomes

$$F(w) = w^4 \exp(wT^{1/2}) + \alpha_w w^2 + \beta_w = 0 \qquad (5.5.16)$$

The contours corresponding to $\zeta = 0$ and $\zeta = 0.35$ in the s-plane are $\zeta_w = -0.707$ and $\zeta_w = -0.570$ respectively in the w plane. These contours are shown in Figure 5.3.2 for T=1.

5.3.2 Systems in which p is greater than unity. When the value of p in equation (5.1.1) is greater than unity, the transformed characteristic equation, $F(w) = 0$, of (5.3.1) becomes

$$F(w) = D(w^q) \exp(w^p T^{p/q}) + KN(w^q) = 0 \qquad (5.3.17)$$

where p is an integer. Now consider the exponential term of (5.3.17)

$$F_D(w) = \exp(w^p T^{p/q}) \qquad 5.3.18)$$

where $T^{p/q}$ is a constant and w is a complex variable defined as

$$w = -\zeta_w \omega_w + j\,\omega_w (1-\zeta_w^2)^{1/2}$$

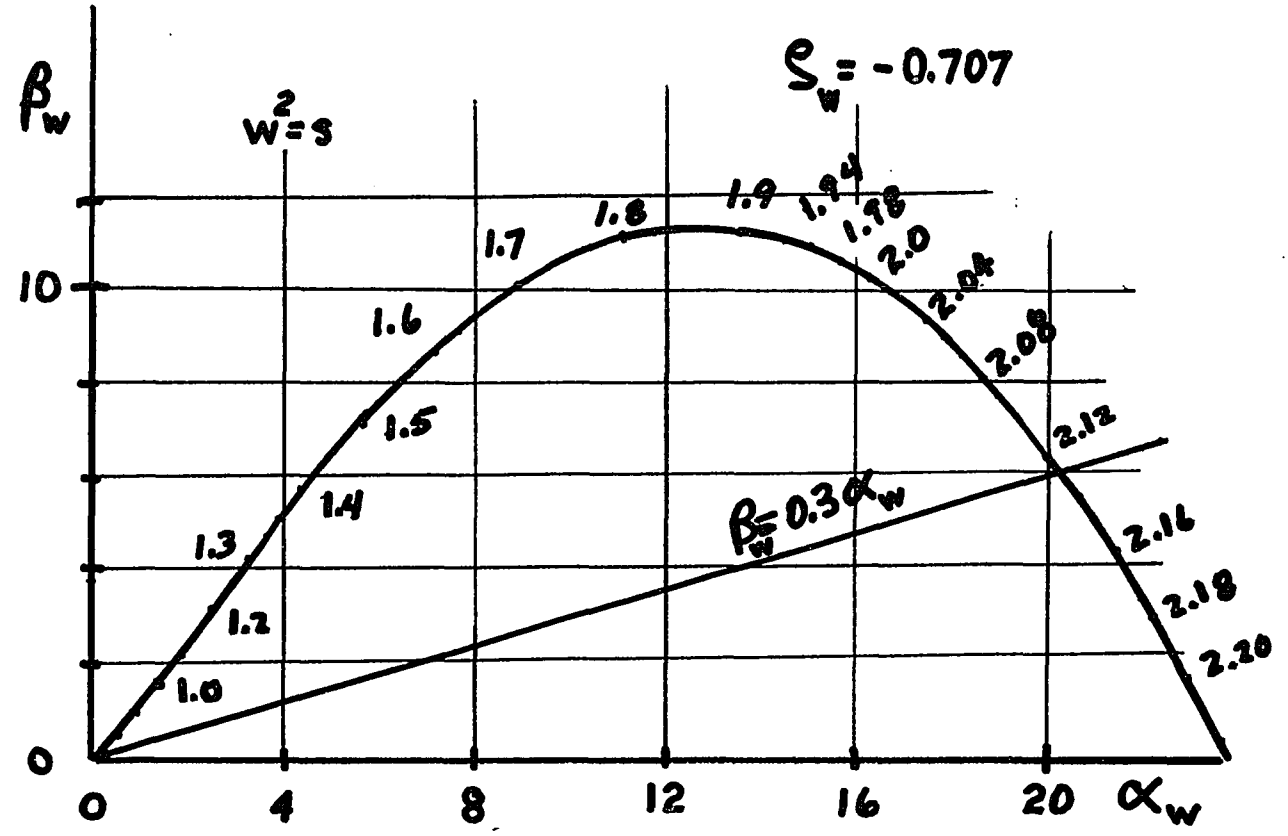

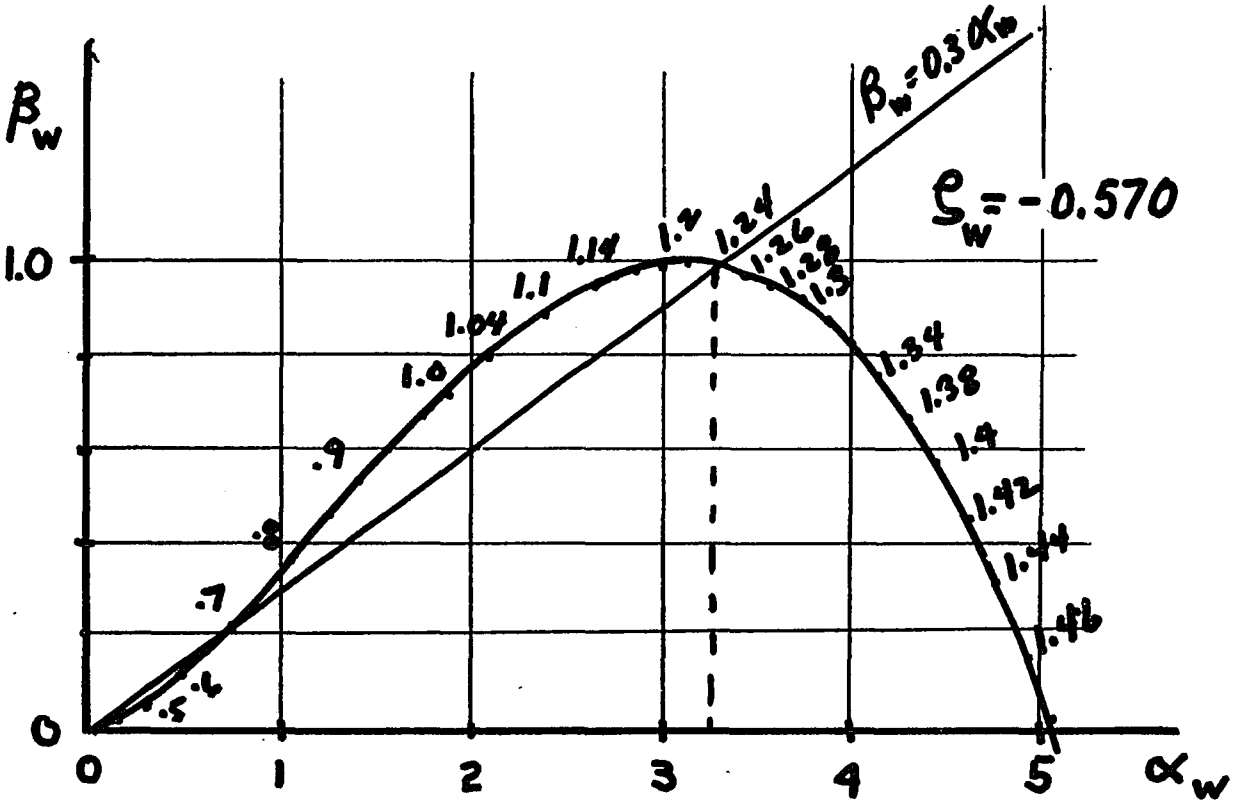

FIGURE 5.3.2 α_w - β_w CONTOURS CORRESPONDING TO $\zeta = 0$ AND $\zeta = 0.35$ IN s-PLANE ($w^2 = s$)

From equations (4.2.7) and (4.2.8) in chapter 4,

$$w^p = \omega_w^p [(-1)^p T_p (\zeta_w) + j (-1)^{p+1} (1- \zeta_w^2)^{1/2} U_p (\zeta_w)] \quad (5.3.19)$$

where $T_p(\zeta_w)$ and $U_p(\zeta_w)$ are respectively Chebychev functions of the first and second kind. Expressing (5.3.18) in polar vector notation by making use of (5.3.19) produces

$$\exp(w^p T^{p/q}) = \exp(- \psi_w + j \delta_w)$$
$$= \exp \left\{ T^{p/q} \omega_w^p [(-1)^p T_p (\zeta_w) + j(-1)^{p+1} (1- \zeta_w^2)^{1/2} U_p (\zeta_w)] \right\} \quad (5.3.20)$$

Thus

$$- \psi_w = (-1)^p T^{p/q} (\omega_w)^p T_p (\zeta_w) \quad (5.3.21)$$
$$\delta_w = (-1)^{p+1} T^{p/q} (\omega_w)^p (1 - \zeta^2)^{1/2} U_p (\zeta_w)$$

These equations for $- \psi_w$ and δ_w coupled with (5.3.6), the equations for α_w and β_w allow application of the technique of Chapter 4 in order to map from the complex w-plane to the algebraic $\alpha_w - \beta_w$ plane. Specifically, (5.3.21) and (5.3.6) are used to obtain the parameter plane coefficients (5.3.9) which are in turn used in (5.3.11) to obtain α_w, β_w and Δ_w. Thus the parameter plane technique can now be applied to feedback systems containing transfer functions of the form exp ($s^p T$) where p is an integer greater than unity. Polynominals for $- \psi_w$ and δ_w corresponding to various values of the integer p are summarized in Table 5.3.1.

p	$-\psi_w$	δ_w
1	$-\omega_w T^{1/q} \zeta_w$	$T^{1/q} \omega_w [1-\zeta_w^2]^{1/2}$
2	$\omega_w^2 T^{2/q} (2\zeta_w^2 - 1)$	$-T^{2/q} \omega_w^2 [1-\zeta_w^2]^{1/2} 2\zeta_w$
3	$-\omega_w^3 T^{3/q} (4\zeta_w^3 - 3\zeta_w)$	$T^{3/q} \omega_w^3 [1-\zeta_w^2]^{1/2} (4\zeta_w^2 - 1)$
4	$\omega_w^4 T^{4/q} (8\zeta_w^4 - 8\zeta_w^2 + 1)$	$-T^{4/q} \omega_w^4 [1-\zeta_w^2]^{1/2} (8\zeta_w^3 - 4\zeta_w)$
5	$-\omega_w^5 T^{5/q} (16\zeta_w^5 - 20\zeta_w^3 + 5\zeta_w)$	$T^{5/q} \omega_w^5 [1-\zeta_w^2]^{1/2} (16\zeta_w^4 - 12\zeta_w^2 + 1)$
6	$\omega_w^6 T^{6/q} (32\zeta_w^6 - 48\zeta_w^4 + 18\zeta_w^2 - 1)$	$-T^{6/q} \omega_w^6 [1-\zeta_w^2]^{1/2} (32\zeta_w^5 - 32\zeta_w^3 + 6\zeta_w)$
7	$-\omega_w^7 T^{7/q} (64\zeta_w^7 - 112\zeta_w^5 + 56\zeta_w^3 - 7\zeta_w)$	$T^{7/q} \omega_w^7 [1-\zeta_w^2]^{1/2} (64\zeta_w^6 - 80\zeta_w^4 + 24\zeta_w^2 - 1)$

TABLE 5.3.1 Expressions for $-\psi_w$ and δ_w for Various Integer Values in the Transfer Function $\exp(w^p T^{p/q})$

These results are now illustrated by means of the following example. Consider again the control system of Figure 4.6.1 and represent the distributed lag transfer function as

$$F_D(s) = \exp\ (-(Ts)^{2/4}) \qquad (5.3.22)$$

Introducing the transformation $w^4 = s$ gives

$$F(w) = w^8 \exp(w^2 T^{2/4}) + K w^4 + KW = 0 \qquad (5.3.23)$$

Defining $\alpha_w = K$, $\beta_w = KW$, and setting $T = 1$ gives

$$F(s) = w^8 \exp(w^2) + \alpha_w w^4 + \beta_w = 0 \qquad (5.3.24)$$

The contours corresponding to $\zeta = 0$ and $\zeta = 0.35$ the s-plane are $\zeta_w = -0.9239$ and $\zeta_w = -0.8860$ respectively in the w-plane. The first traversal of these contours are shown in Figure 5.3.3. A more complete plot of the $\zeta_w = -0.9239$ contour contained in Figure 5.3.4.

5.4 w-plane Equivalent of Constant Sigma Lines in the s-plane

The parameter plane contours for constant sigma lines in the s-plane can be found by utilizing the parameter plane equations developed in Chapter 4, section 10. However, when the characteristic equation $F(s) = 0$ is transformed by a transformation of the type

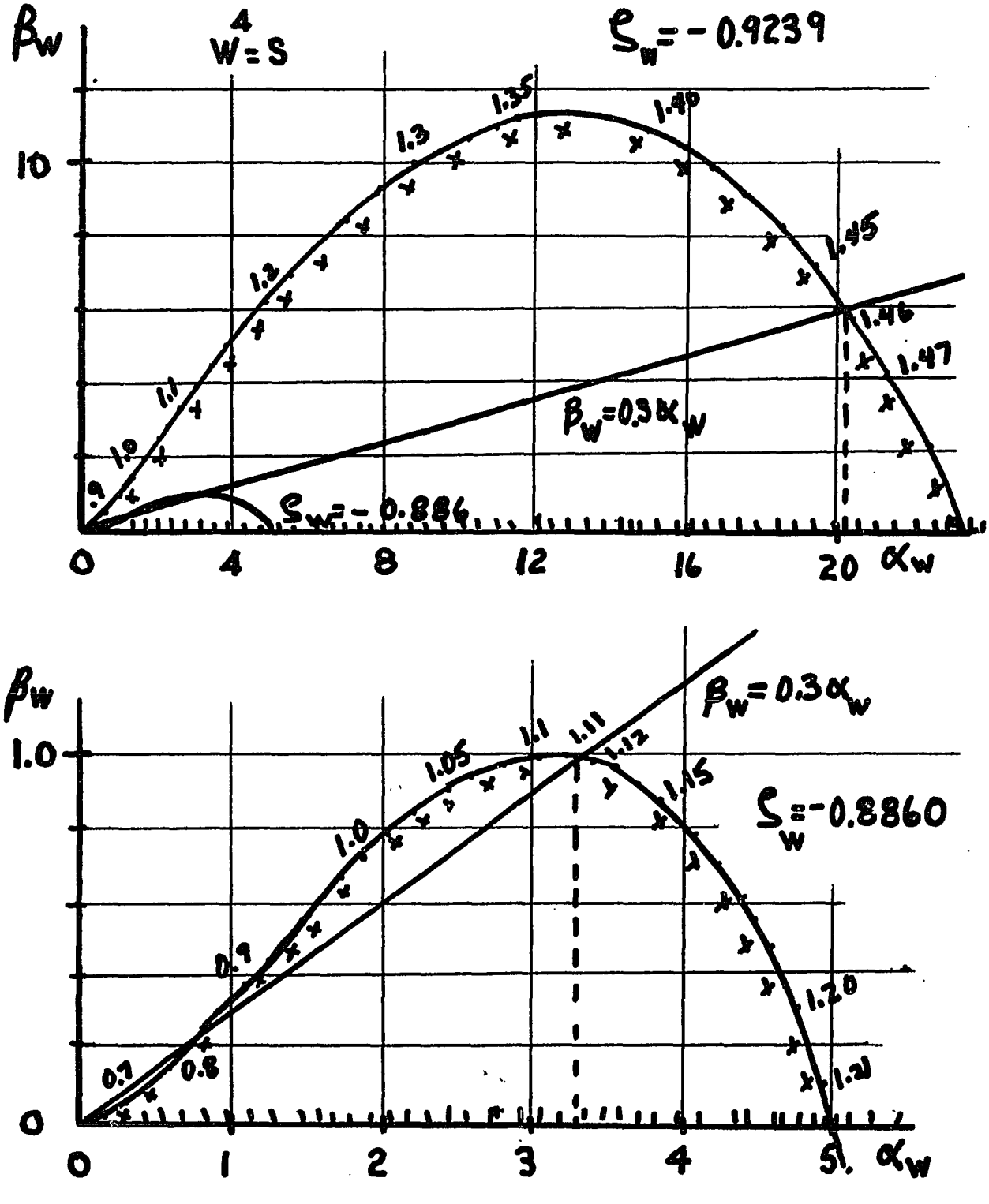

FIGURE 5.3.3 $\alpha_w - \beta_w$ CONTOURS CORRESPONDING TO $\zeta = 0$ AND $\zeta = 0.35$ IN s- PLANE ($w^4 = s$)

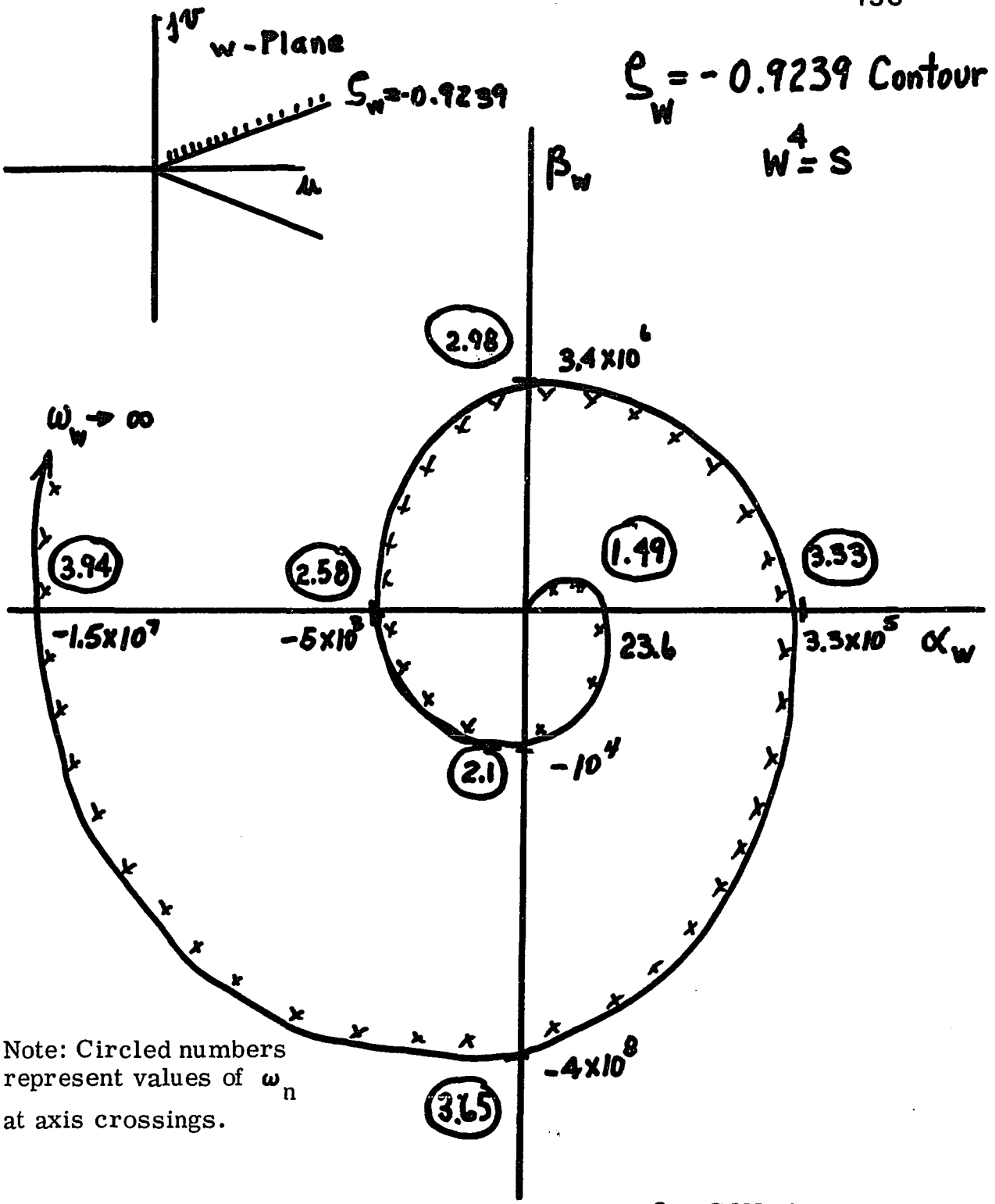

Note: Circled numbers represent values of ω_n at axis crossings.

FIGURE 5.3.4 MORE COMPETE PLOT OF $\alpha_w - \beta_w$ CONTOUR SHOWING SEVERAL TRAVERSALS (w^4=s)

$w^q = s$, (q being an integer), it is of interest to determine first the equivalent contour in the w -plane and then how this w -plane contour may be mapped directly into the $\alpha_w - \beta_w$ plane.

The parameter plane equation corresponding to a w -plane contour equivalent of a constant sigma line in the s-plane can be found by utilizing (5.3.11) and (5.3.9) in which ζ_w and ω_w are appropriately defined. In order to define these variables consider the s-plane and w-plane diagrams of Figure 5.2 .2. Referring to this figure, and assuming $w^q = s$ the following relationships hold

$$\omega_{n1} = (\sigma_1^2 + \omega^2)^{1/2} \qquad (5.4.1)$$

$$\theta_1 = \text{Tan}^{-1} (\frac{\omega}{\sigma_1}) \qquad (5.4.2)$$

$$\omega_w = \omega_n^{1/q} = (\sigma_1^2 + \omega^2)^{1/2q} \qquad (5.4.3)$$

$$\phi_1 = \frac{\theta_1}{q} = \frac{1}{q} \text{Tan}^{-1}(\frac{\omega}{\sigma_1}) \qquad (5.4.4)$$

$$\zeta_w = -\cos \phi_1 \qquad (5.4.5)$$

Equations (5.4.3) and (5.4.5) are the transitional relationships which enable the $\alpha_w - \beta_w$ contours to be obtained. For a given value of $\sigma = \sigma_1$, and a given value of q each value of ω provides a pair of values ω_w and ζ_w through use of (5.4.3) and (5.4.5) respectively. These values of ω_w and ζ_w coupled with values of $-\psi_w$ and δ_w (defined either

by (5.3.7) or (5.3.21) are used to produce values for the functions of (5.3.9) which in turn are used to give values of α_w and β_w through (5.3.11).

The application of this method can be demonstrated by considering the problem of Section 5.3 in which the characteristic equation is

$$F(s) = s^2 \exp(\sqrt{s}) + \alpha s + \beta = 0 \qquad (5.4.6)$$

When the transformation $w^2 = s$ is applied

$$F(w) = w^4 \exp(w) + \alpha w^2 + \beta = 0 \qquad (5.4.7)$$

where

$$\omega_w = (\sigma_1^2 + \omega^2)^{1/4} \qquad (5.4.8)$$

$$\zeta_w = -\cos\left(\frac{1}{2}\tan^{-1}\left(\frac{\omega}{\sigma_1}\right)\right)$$

by equation (5.3.7)

$$\psi_w = -\zeta_w \omega_w \qquad (5.4.9)$$

$$\delta_w = \omega_w (1-\zeta_w^2)^{1/2}$$

If the imaginary axis ($\sigma_1 = 0$) is to be mapped $\omega_n = \omega$ and

$$\omega_w = \omega_n^{1/2}, \qquad \zeta_w = -0.707 \qquad (5.4.10)$$

$$-\psi_w = \sqrt{\frac{\omega}{2}}, \quad \delta_w = \sqrt{\frac{\omega}{2}}$$

and (5.3.9) become

$$B_{1w} = 0, \quad C_{1w} = 1,$$

$$D_{1w} = -\omega^2 \cos\left(\sqrt{\frac{\omega}{2}}\right) \exp\left(\sqrt{\frac{\omega}{2}}\right) \tag{5.4.11}$$

$$B_{2w} = \omega, \quad C_{2w} = 0$$

$$D_{2w} = -\omega^2 \sin\left(\sqrt{\frac{\omega}{2}}\right) \exp\left(\sqrt{\frac{\omega}{2}}\right)$$

Substitution into (5.3.11) gives

$$\alpha_w = \omega \exp\left(\sqrt{\frac{\omega}{2}}\right) \sin\left(\sqrt{\frac{\omega}{2}}\right) \tag{5.4.12}$$

$$\beta_w = \omega^2 \exp\left(\sqrt{\frac{\omega}{2}}\right) \cos\left(\sqrt{\frac{\omega}{2}}\right)$$

$$\Delta_w = -\omega$$

Equations (5.4.12) are identical in form to equations (4.6.4) of Chapter 4. This is to be expected since they both represent mapping of the same contour in the same system.

In general, the value of sigma is not zero and the value of ζ_w in (5.4.5) is a function of ω. The mapping of the equivalent contour in the w-plane is then easily performed with the aid of a digital computer.

CHAPTER 6

ANALYSIS OF SMITH LINEAR PREDICTOR CONTROL SYSTEMS WITH PLANTS CONTAINING DISTRIBUTED LAG

6.1 Introduction

The technique of linear predictor control for feedback systems containing transport lag was first suggested by Smith[105]. This technique utilizes a system controller, see Figure 6.1.1, that contains a model of the system plant and transport lag. The manner in which this controller compensates for the transport lag contained in the system plant can be explained as follows. When a step function $u(t)$ is introduced at the input there is no output $c(t)$ for T seconds due to the transport lag e^{-sT} in the plant. However this step change appears as an input to the minor feedback loop at point A and arrives immediately at point B. Since the plant dynamics are simulated in the minor feedback loop, the controller is energized for the first T seconds. When T seconds has elapsed the minor feedback loop opens and the input signal is transferred through the outer loop which includes the system transport lag. Thus the minor loop predicts what the system output will eventually be and introduces this in feedback until the actual output appears. The philosophy of this type of control is to separate out the transport lag, which is a part of the system for which it is impossible to compensate. After the design for the control of the remainder of the system is

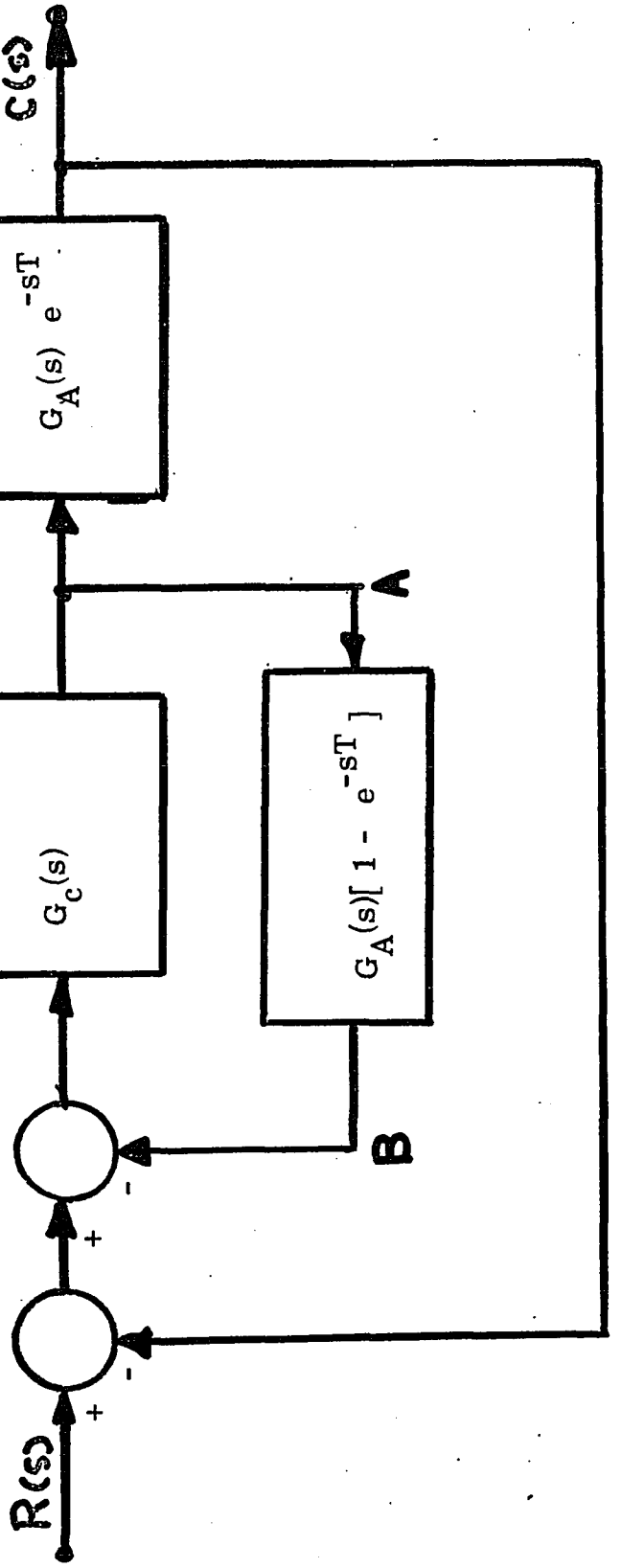

FIGURE 6.1.1 SMITH PREDICTOR MODEL

completed, the transport lag is reintroduced. If similar reasoning is applied to a control system in which the plant contains a distributed lag (instead of a transport lag), then a minor feedback loop can also be designed which predicts the system output. The block diagram of the predictor configuration applied to plants containing distributed lag is shown in Figure 6. 1. 2. From the configuration of Figure 6. 1. 2 if N_p/D_p is set equal to $\exp(-\sqrt{sT})$, the system transfer function is given by

$$\frac{C(s)}{R(s)} = \frac{G_A(s)G_c(s)\ \exp\left[-(sT)^{1/2}\right]}{1 + G_A(s)G_c(s)} \qquad (6.1.1)$$

The numerator of equation (6. 1. 1) contains a transcendental term $\exp\left[-(sT)^{1/2}\right]$. The denominator of equation (6. 1. 1), however, does not contain a transcendental term, so that reasonably large values of controller gain can be selected as in the case of systems without distributed lag.

This technique requires, however, that an exact model of the system plant and distributed lag be incorporated in the controller. Theoretically, this is possible but practical implementation contains many difficulties. These difficulties arise because it is difficult to perfectly synthesize the distributed lag term, $\exp\left[-(sT)^{1/2}\right]$, in the controller. One method of synthesis is to use a polynomial approximation to the transcendental function. However, there are many classes of polynomial functions both rational and irrational. One class of approximations to the

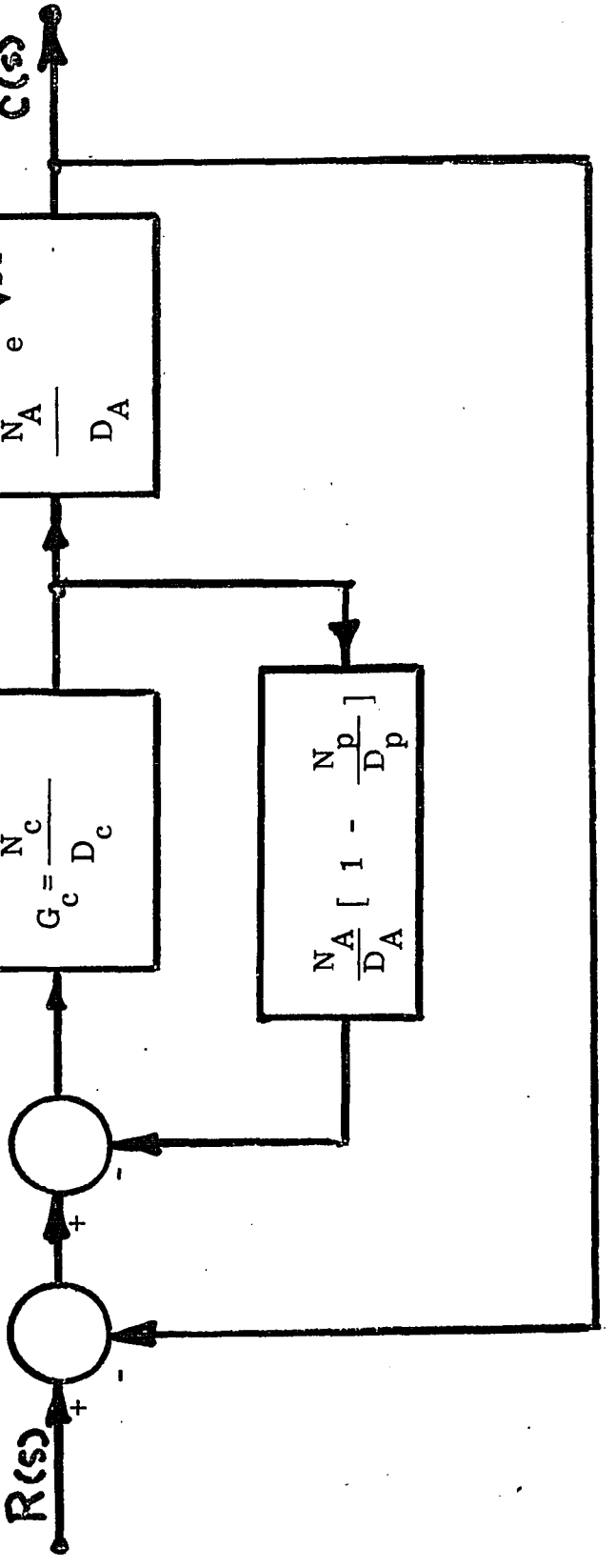

FIGURE 6.1.2 PREDICTOR MODEL APPLIED TO PLANT WITH DISTRIBUTED LAG

transcendental function, $\exp\left[-(sT)^{1/2}\right]$ was given by Pierre[80]. This class of approximants for a distributed lag are ratios of rational polynomials which have negative real roots. There are various orders of approximants with the higher order approximant being closer approximations to the transcendental function than the lower order approximants. However, the best choice of the approximation to the distributed lag in any given system should take into consideration the order of the system plant as well as plant time constants. Thus, choice of a lower order approximant may be, in addition to being easier to synthesize, a better choice from the viewpoint of performance than one of the higher order approximants. It is proposed to present a method by which various approximations to the distributed lag appearing in the controller can be examined. This treatment will employ parameter plane techniques and proceed in a manner similar to the one used by Eisenberg[30] in treating systems containing transport lag. However, the general s-plane variable $s = \sigma + j\omega$ (instead of $s = j\omega$) will be used in the derivation so that both absolute and relative stability can be investigated.

It was also observed, (in applying rational polynomial approximants to systems with distributed lag), that certain types of systems (1) were rendered stable for all positive values of controller gain. However, this

---

(1) These types of systems are ones in which the denominator term of (6. 1. 1) is at most a second order polynomial in the complex variable s.

unconditional stability with gain variation could be accompanied by extremely sluggish transient response unless the parameters associated with the polynomial approximant were optimized. Thus it is also proposed to investigate a method in which a rational polynomial approximant is used to achieve absolute stability for a system along with a minimum of deterioration in its transient response characteristics. This method also involves the use of parameter plane techniques and polynomial approximants[80]in a control system arranged in the predictor configuration.

6.2 Derivation of Parameter Plane Equations for the Predictor Configuration Applied to Systems with Distributed Parameter Elements.

The derivation will be presented of the α -β equations for a control system with a distributed lag element and a PI controller arranged in the predictor configuration. Application of either these equations or the more general equations of Chapter 4 Section 2 enables a designer to determine the "best"[(2)] choice of polynomial approximant to use in the predictor loop.

Consider the linear predictor control system shown in Figure 6.2.1 where R(s) is the Laplace transform of the input, C(s) is the Laplace transform of the output response and where

---

(2) Best choice is based on some criterion such as permits the largest system gain variation without becoming unstable.

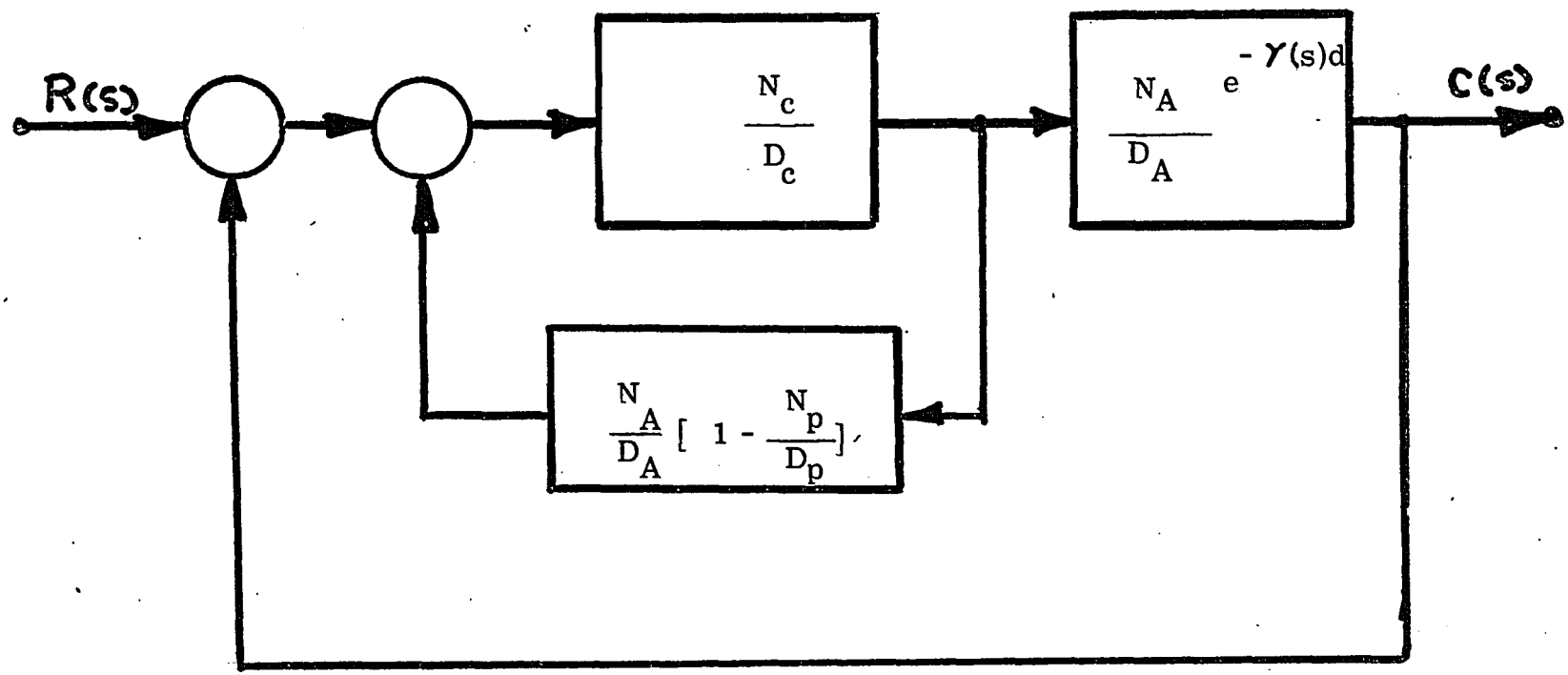

FIGURE 6.2.1 GENERALIZED PREDICTOR MODEL WITH DISTRIBUTED PARAMETER ELEMENT

$s = \sigma + j\omega$

$G_c(s) = \frac{N_c(s)}{D_c(s)}$ the system controller

$G_A(s) = \frac{N_A(s)}{D_A(s)}$ the system plant

$\exp(-\gamma(s)d)$ = the transfer function of the distributed parameter element

$\gamma(s) = \sqrt{(Ls+R)(Cs+G)}$

$\frac{Np(s)}{Dp(s)}$ = the polynomial approximation to $\exp(-\gamma(s)d)$ appearing in the Smith predictor controller

The system transfer function $\frac{C(s)}{R(s)}$ is given by

$$\frac{C(s)}{R(s)} = \frac{N_A(s)N_c(s)D_p(s)\exp(-\gamma(s)d)}{D_A(s)D_c(s)D_p(s)+N_A(s)N_c(s)[D_p(s)-N_p(s)+D_p(s)\exp(-\gamma(s)d)]} \qquad (6.2.1)$$

If $G_c(s)$ is a controller of the proportional-integral (PI) type then

$$G_c(s) = \frac{N_c(s)}{D_c(s)} = K(1+\frac{1}{sT_R}) = K(\frac{s+W}{s}) \qquad (6.2.2)$$

where K is the controller gain and W is the reciprocal of the reset time.

Substituting (6.2.2) into (6.2.1) and defining

$$\alpha = K, \qquad \beta = KW = W\alpha \qquad (6.2.3)$$

gives

$$\frac{C(s)}{R(s)} = \frac{N_A(s)D_p(s)(\alpha s+\beta)\ \exp(-\gamma(s)d)}{F(s)} \qquad (6.2.4)$$

where $F(s) = 0$, the system characteristic equation, is

$$F(s) = s\left[D_A(s)D_p(s) + \alpha N_A(s)\left\{D_p(s) - N_p(s) + D_p \exp(-\gamma(s)d)\right\}\right]$$
$$+ \beta N_A(s)\left[D_p(s) - N_p(s) + D_p \exp(-\gamma(s)d)\right] = 0 \qquad (6.2.5)$$

In order to investigate the stability of the system define

$$s = -\zeta\ \omega_n + \omega_n(1-\zeta^2)^{1/2} \qquad (6.2.6)$$

and also define

$$N_A(s) = N_{AR} + jN_{AI}, \quad D_A(s) = D_{AR} + jD_{AI}$$

$$N_p(s) = N_{pR} + jN_{pI}, \quad D_p(s) = D_{pR} + jD_{pI}$$

$$\exp(-\gamma(s)d) = \exp(\psi - j\delta) = e^{\psi}\cos\delta - je^{\psi}\sin\delta \qquad (6.2.7)$$

where $-\psi$ and δ are defined in Region A of the principal sheet of the s-plane by equations (4.3.17) for the general case of the electrical transmission line. Note that for the case of distributed lag (i.e., $L=G=0$) equations (4.3.17) become

$$\psi = -\sqrt{\frac{\omega_n T(1-\zeta)}{2}}, \quad \delta = \sqrt{\frac{\omega_n T(1+\zeta)}{2}} \qquad (6.2.8)$$

Substituting (6.2.7) and (6.2.6) into (6.2.5), separating real and imaginary parts, and equating each part to zero gives

$$\alpha B_1 + \beta C_1 = -D_1$$

$$\alpha B_2 + \beta C_2 = -D_2 \qquad (6.2.9)$$

where

$$B_1 = -\zeta\omega_n Re_3 - \omega_n(1-\zeta^2)^{1/2} Im_3$$

$$C_1 = Re_3$$

$$D_1 = -\zeta\omega_n Re_1 - \omega_n(1-\zeta^2)^{1/2} Im_1$$

$$B_2 = -\zeta\omega_n Im_3 + \omega_n(1-\zeta^2)^{1/2} Re_3$$

$$C_2 = Im_3$$

$$D_2 = -\zeta\omega_n Im_1 + \omega_n(1-\zeta^2)^{1/2} Re_1 \qquad (6.2.10)$$

and

$$Re_1 = D_{AR}D_{pR} - D_{AI}D_{pI}$$

$$Im_1 = D_{AR}D_{pI} - D_{AI}D_{pR}$$

$$Re_3 = N_{AR}(D_{pI}-N_{pR}+D_{pR}\exp(\psi)\cos\delta + D_{pI}\exp(\psi)\sin\delta)$$

$$- N_{AI}(D_{pI}-N_{pI}+D_{pI}\exp(\psi)\sin\delta - D_{pR}\exp(\psi)\cos\delta)$$

$$Im_3 = N_{AI}(D_{pR}-N_{pR}+D_{pR}\exp(\psi)\cos\delta + D_{pI}\exp(\psi)\sin\delta)$$

$$+N_{AR}(D_{pI}-N_{pI}+D_{pI}\exp(\psi)\sin\delta - D_{pR}\exp(\psi)\cos\delta) \qquad (6.2.11)$$

Equations (6.2.9) can be solved for the controller parameters $\alpha = K_c$ and $\beta = K_c W$ giving (4.2.13) repeated below

$$\alpha = \frac{C_1D_2 - D_1C_2}{\Delta}, \quad \beta = \frac{D_1B_2 - D_2B_1}{\Delta}$$

$$\Delta = B_1C_2 - B_2C_1 \qquad (6.2.12)$$

This method of representing the variable system parameter is a special case of the general parameter plane approach to systems with distributed parameter elements developed in section 4.2 of chapter 4. Through application of (6.2.12) in conjunction with (6.2.11), (6.2.10) and (4.3.17), the absolute as well as relative stability can be determined. This determination can be made as a function of $\frac{N_p(s)}{D_p(s)}$, the polynomial approximation chosen in addition to variation of the two free system parameters α and β.

Since the choice of the polynomial approximation is of importance, some of these polynomials should be examined. A family of rational polynomial approximants were developed by Pierre[80]and these will be considered here. The development of these polynomials for the case of a distributed lag as well as the more general case of a transmission line with non-zero values of R, L, G, and C is set forth in Appendix VI.

6.3 Example of the Predictor Configuration with a Distributed Lag Element in the Plant

The parameter plane technique and the results of Appendix VI will now be applied to a feedback control system containing a distributed lag. The system configuration is shown in Figure 6.1.2. The transfer function of the plant is

$$G_A(s) = \frac{N_A(s)}{D_A(s)} = \frac{1}{s} \qquad (6.3.1)$$

The controller is of the proportional integral type with transfer function given by (6.2.2) repeated below:

$$G_c(s) = \frac{N_c(s)}{D_c(s)} = \frac{K(s+W)}{s} \qquad (6.3.2)$$

The polynomial approximations to the controller distributed lag which will be used in the local feedback loop around the controller are given below:

1) No Prediction

$$\frac{N_p(s)}{D_p(s)} = 1, \quad D_1(s) - N_p(s) = 0 \qquad (6.3.3)$$

2) Exact Prediction

$$\frac{N_p(s)}{D_p(s)} = e^{-\sqrt{sT}}, \quad D_p(s) - N_p(s) = 1 - e^{-\sqrt{sT}} \qquad (6.3.4)$$

3) Polynomial Approximants

$$G_{1,1} = \frac{N_p(s)}{D_p(s)} = \frac{1}{1+shT}; \quad D_p(s) - N_p(s) = shT \qquad (6.3.5)$$

$$G_{1,2} = \frac{N_p(s)}{D_p(s)} = \frac{1 + shT}{1+s(2h+1)T+s^2hT^2};$$

$$D_p(s)-N_p(s) = s(h+1)T+s^2hT^2 \qquad (6.3.6)$$

$$G_{2,2} = \frac{N_p(s)}{D_p(s)} = \frac{1}{\frac{1+s(2h+1)T}{4}+\frac{s^2h^2T^2}{16}};$$

$$D_p(s)-N_p(s)=\frac{s(2h+1)T}{4}+\frac{sh^2T^2}{16} \qquad (6.3.7)$$

$$G_{1,3}=\frac{N_p(s)}{D_p(s)}=\frac{1+s(2h+1)T+s^2hT^2}{1+s(3h+3)T+s^2(4h+1)T^2+s^3hT^3};$$

$$D_p(s)-N_p(s)=s(h+2)T+s^2(3h+1)T^2+s^3hT^3 \qquad (6.3.8)$$

Where T is the distributed lag constant and h is the loading constant of Appendix VI. The parameter h is a positive real constant which relates the load admittance, Y_L, of the finite network approximation for the distributed lag to the network load admittance Y, that is, referring to Figure VI. 1 in Appendix VI

$$h=\frac{Y_L}{Y} \qquad (6.3.9)$$

For the system of Figure 6.1.2 , the transformation is

$$\frac{C}{R}(s)=\frac{K(s+W)D_p e^{-\sqrt{sT}}}{s^2D_p+K(s+W)(D_p-N_p)+K(s+W)D_p e^{-\sqrt{sT}}} \qquad (6.3.10)$$

and the characteristic equation is

$$F(s)=s^2D_p+K(s+W)(D_p-N_p)+K(s+W)D_p e^{-\sqrt{sT}}=0 \qquad (6.3.11)$$

Considering now, the α - β contours when $\zeta = 0$ for each of the approximations to $\exp(-(sT)^{1/2})$ given by (6.3.3) to (6.3.8) inclusive produces the following results.

6.3.1 No prediction. When $\frac{N_{p(s)}}{D_p(s)} = 1$, (6.3.11) becomes

$$F(s) = s^2 + K(s+W)\, e^{-\sqrt{sT}} = 0 \qquad (6.3.12)$$

When T = 1, the system reduces to the one discussed in chapter 4, section 6. The $\alpha - \beta$ contour when $\zeta = 0$ for this system is shown in Figure 4.6.2 where

$$\alpha = K, \qquad \beta = KW \qquad (6.3.13)$$

This curve is repeated in Figure 6.3.1 .

6.3.2 Exact prediction. If the ratio $N_p(s)/D(s)$ is defined by (6.3.4), the characteristic equation (6.3.11) becomes

$$F(s) = s^2 + Ks + KW = 0 \qquad (6.3.14)$$

When α and β are defined by (6.3.13)

$$F(s) = s^2 + \alpha s + \beta = 0$$

Applying parameter plane techniques (Chapter 3 section 5) gives

$$\alpha = \omega_n U_2(\zeta)$$

$$\beta = \omega_n^2 \qquad (6.3.15)$$

For $\zeta = 0$, (6.3.15) reduces to

$$\alpha = 0, \quad \beta = \omega_n^2 \qquad (6.3.16)$$

and for $\zeta = 1$

$$\alpha = 2\omega_n, \quad \beta = \omega_n^2 \qquad (6.3.17)$$

Both curves are plotted in Figure 6.3.1 along with the $\zeta = 0$ curve corresponding to the no prediction system of equation (6.3.12)

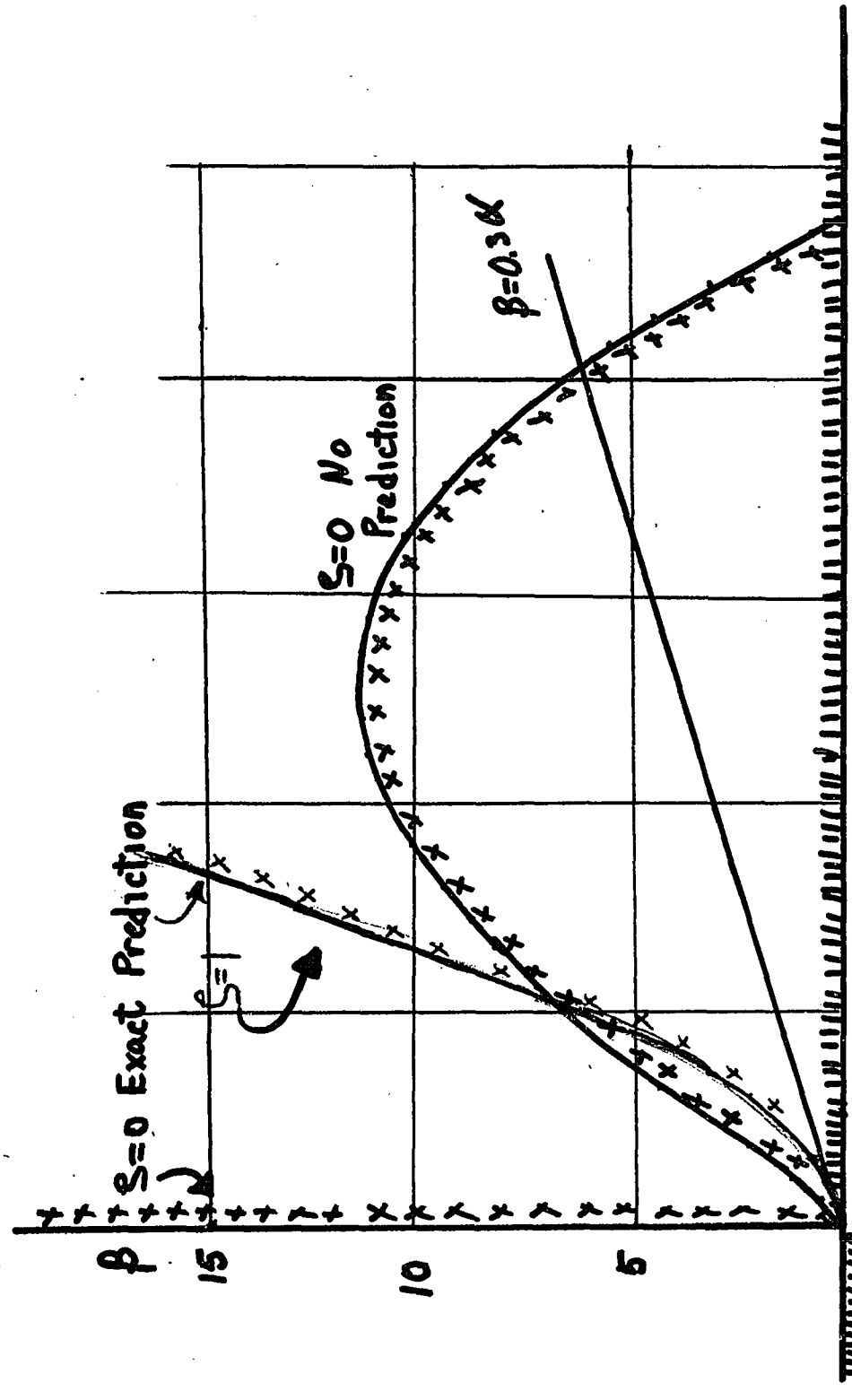

FIGURE 6.3.1 α - β CURVES NO PREDICTION AND EXACT PREDICTION

6.3.3 Polynomial approximants: If the ratio $N_p(s)/D_p(s)$ is defined by (6.3.5), the characteristic equation (6.3.11) becomes

$$F(s) = s^3hT+s^2(1+ \alpha hT+ \alpha hTe^{-\sqrt{sT}})+s(\beta hT+ \alpha e^{-\sqrt{sT}} + \beta hTe^{-\sqrt{sT}}) + \beta e^{-\sqrt{sT}} = 0 \qquad (6.3.18)$$

Notice that in addition to α and β the characteristic equation is also a function of parameters h and T. The absolute stability of the system with characteristic equation (6.3.18) will be examined with T set equal to unity when h takes on various values. The α - β equations for this system are obtained through use of either the method of Section 6.2 or the method of Chapter 4. The α - β equations for the ζ = 0 radial corresponding to various values of h are shown in Figure 6.3.2. From this figure, it can be seen that the contour for h = 0 corresponds to the case of no prediction where when h $\geq$ 1, the ζ = 0 contours approach the positive portion of the β axis. Figure 6.3.2 also shows the when h is less than 0.03 the α - β contour crosses the α axis first on its initial traversal whereas when h is equal to or greater than 0.03 the contour crosses the positive portion of the β axis first and never crosses the positive portion of the α axis. Thus for values of h greater than 0.03 there is no intersection with $\beta = 0.3\alpha$ line in the first quadrant. This means that when W = 0.3 and h $\geq$ 0.03 no positive value of system gain can cause the system to become unstable. The α - β contours corresponding to values of h between 0.029 and 0.030 are plotted in

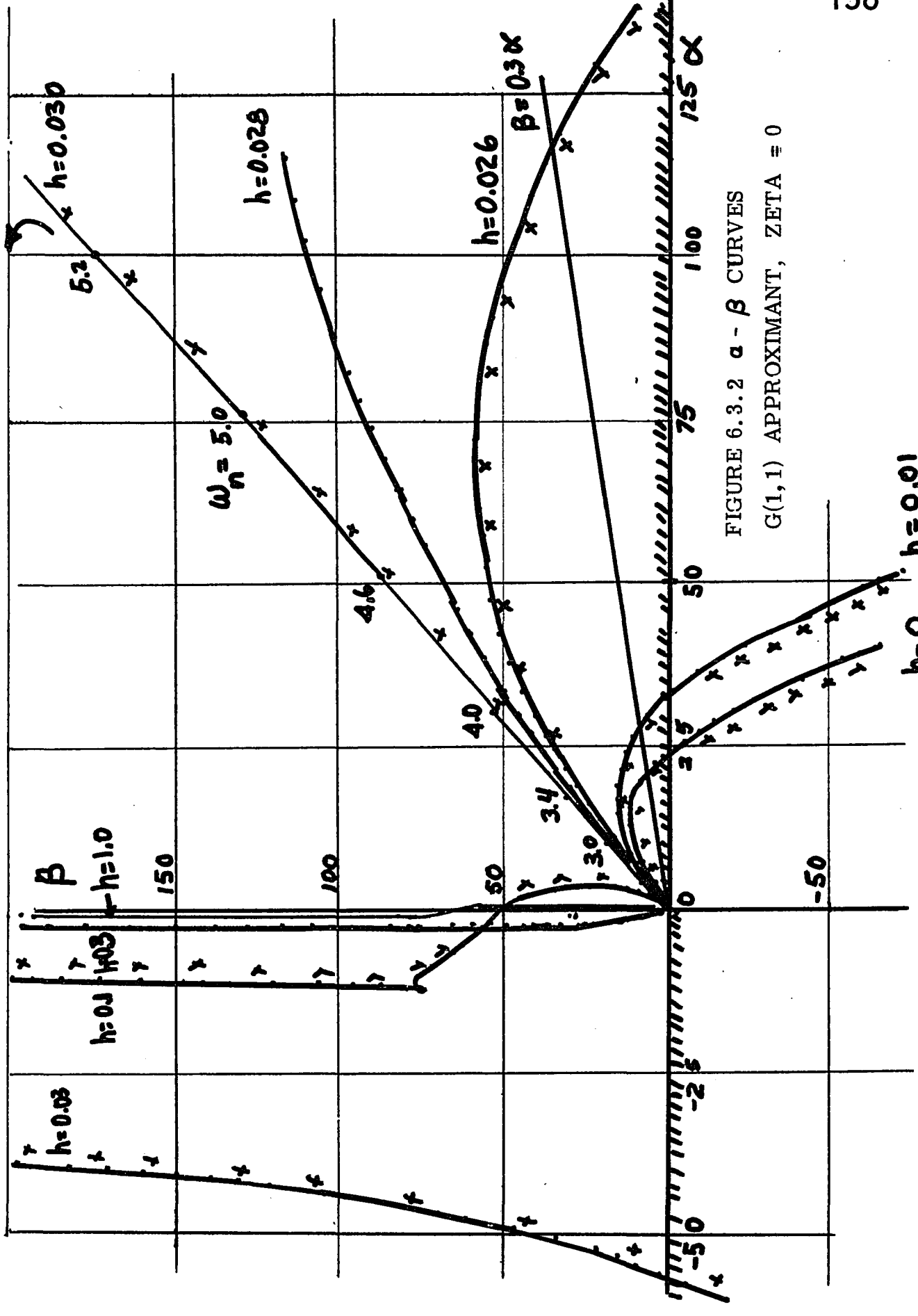

FIGURE 6.3.2 $\alpha - \beta$ CURVES
G(1,1) APPROXIMANT, ZETA = 0

Figure 6.3.3. This figure indicates that when h is greater than 0.0298 values of W ranging from 0 to 1.7 can be used and still produce an unconditionally stable system with respect to gain.

The mapping of α - β contours corresponding to higher order approximants are presented in Figures 6.3.4, 6.3.5, and 6.3.6. These contours are to be expected since by referring to Table VI.2 Appendix VI it can be seen that

$$\lim_{h \to 0} G(m,n) = \lim_{h \to 1} G(m,n-1)$$

Thus the polynominal G(1,2) at h = 0, T = 1 is equivalent to G(1,1) at h = 1, T = 1. These contours corresponding to the higher order approximations of the distributed lag all cross the positive portion of the β axis first. Use of these approximants also result in systems in which are stable for positive values of gain.

Since, in this case, the use of almost any approximant results in an unconditionally stable system the question to be considered is which approximant will also produce the fastest response for a given working point M (α_1, β_1) in the α - β plane. Thus the α - β contour for ζ = 0.35 will be determined for various values of h when approximant G(1,1) is used. These contours are shown in Figure 6.3.7. This figure shows that point M on the h = 0 contour corresponds to operation at K = 3.30, W = 0.3 in the system with no prediction (see section 4.6). The h = 0.03

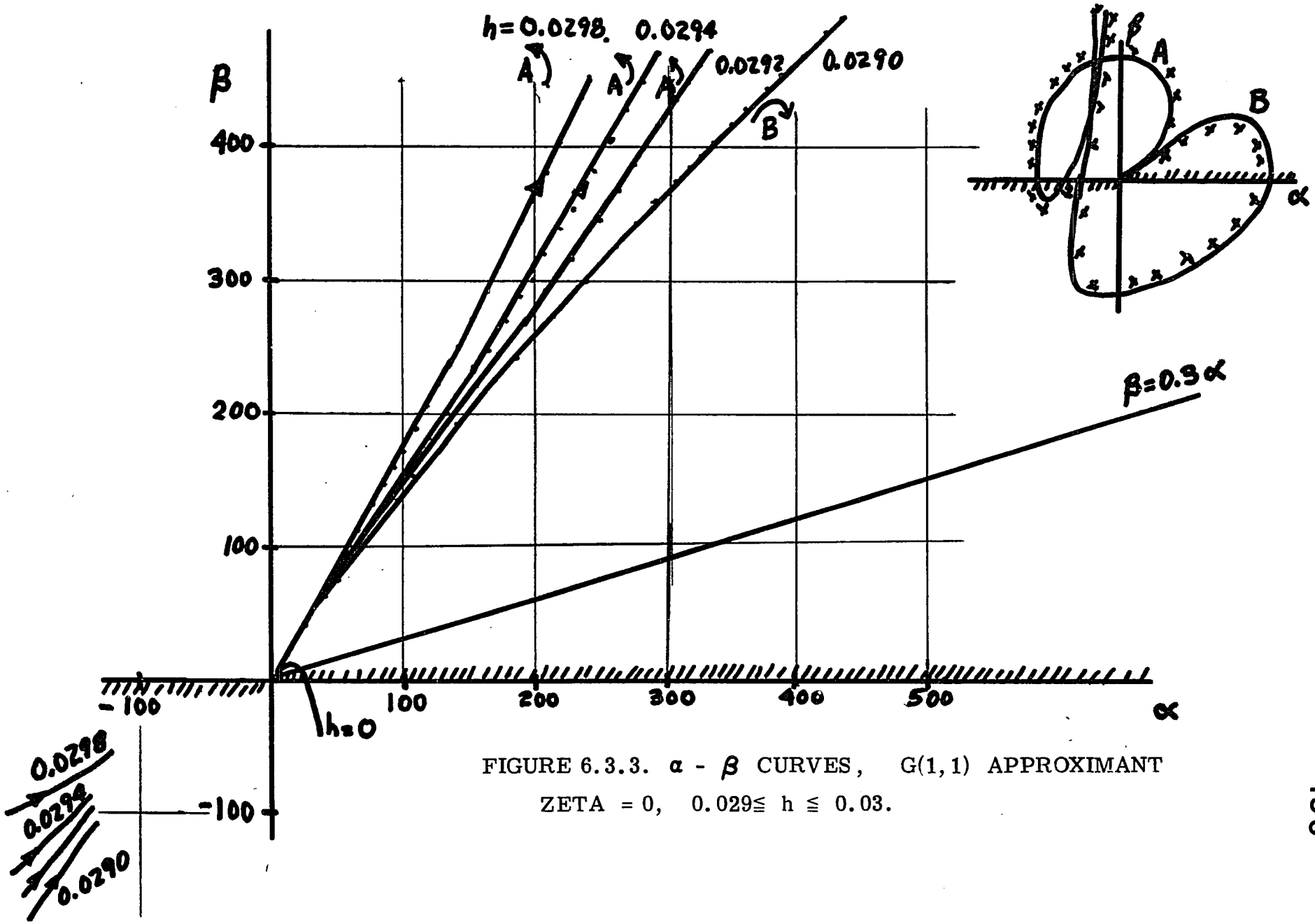

FIGURE 6.3.3. α - β CURVES, G(1,1) APPROXIMANT

ZETA = 0, $0.029 \leqq h \leqq 0.03$.

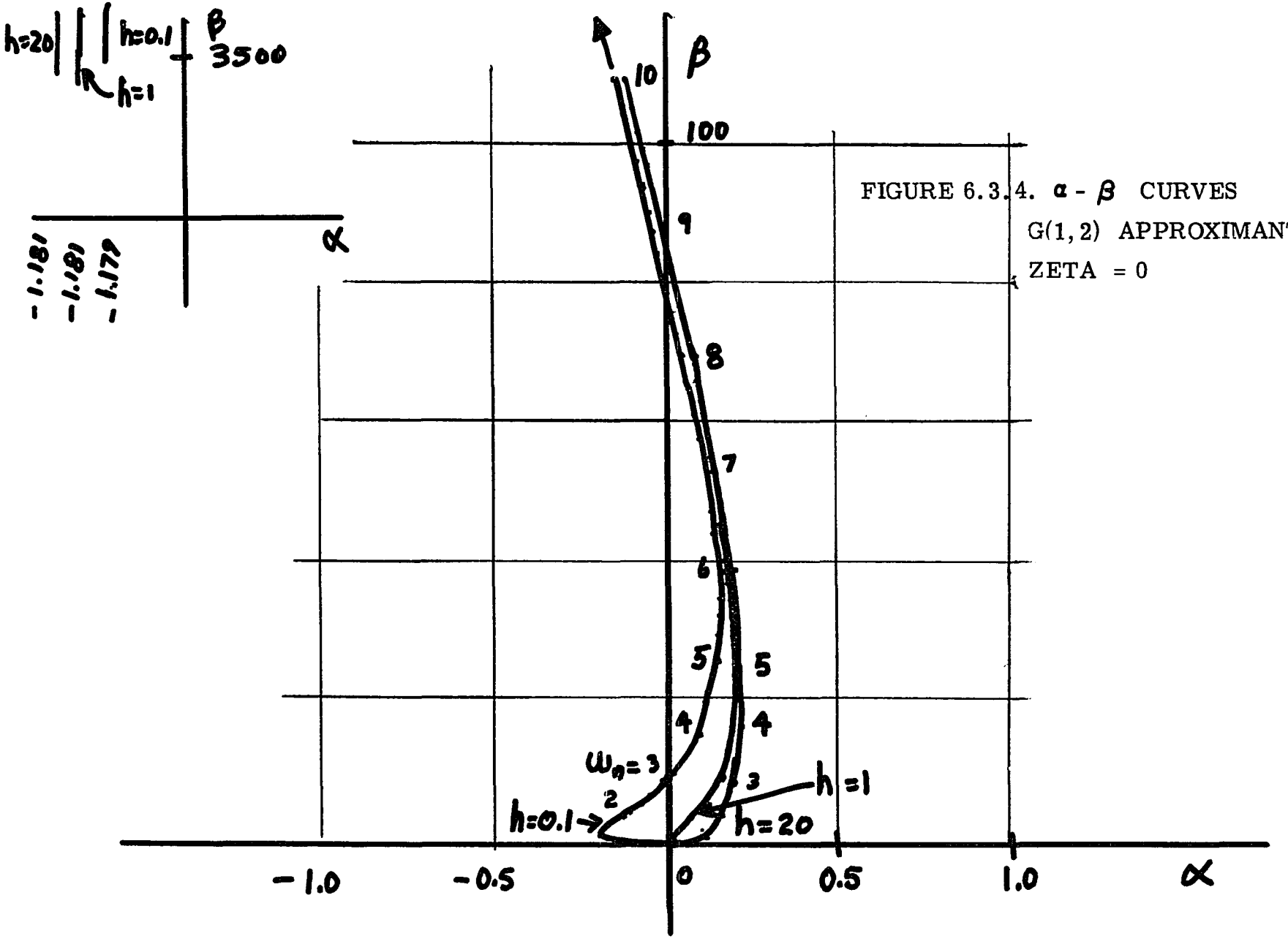

FIGURE 6.3.4. $\alpha - \beta$ CURVES
G(1, 2) APPROXIMANT
ZETA = 0

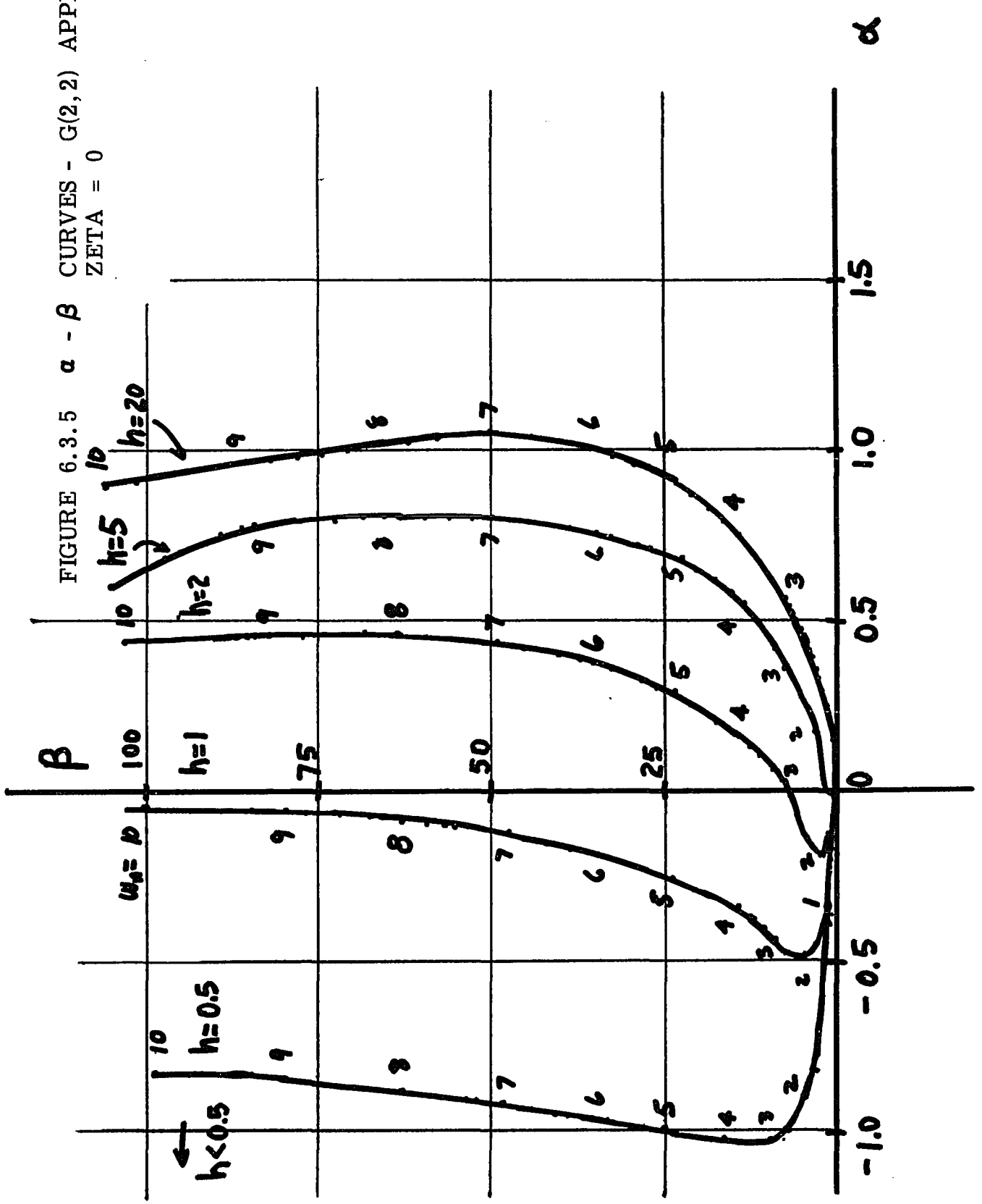

FIGURE 6.3.5 α - β CURVES - G(2,2) APPROXIMANT
ZETA = 0

FIGURE 6.3.6 α - β CURVES

G(1,3) APPROXIMANT, ZETA= 0

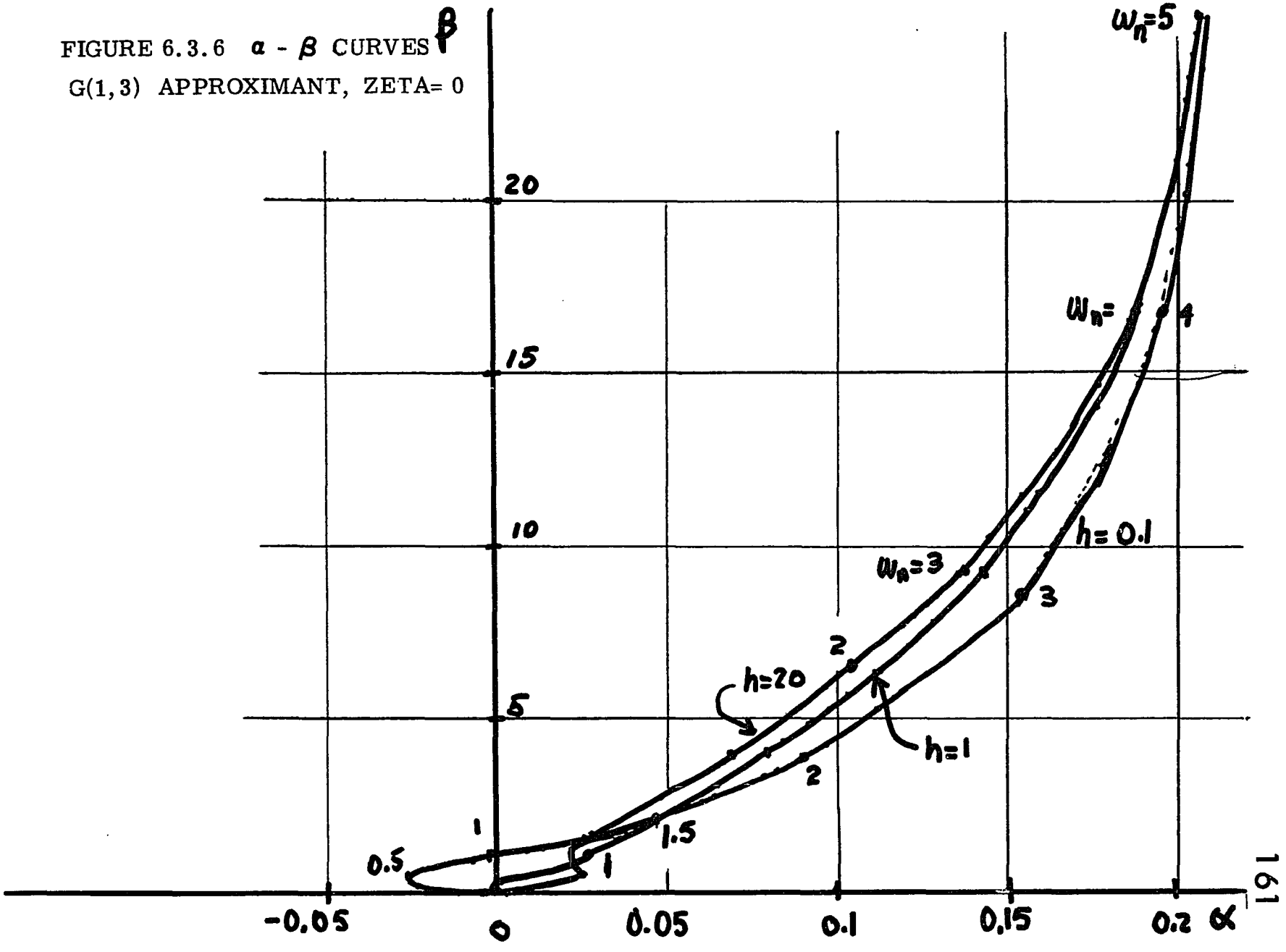

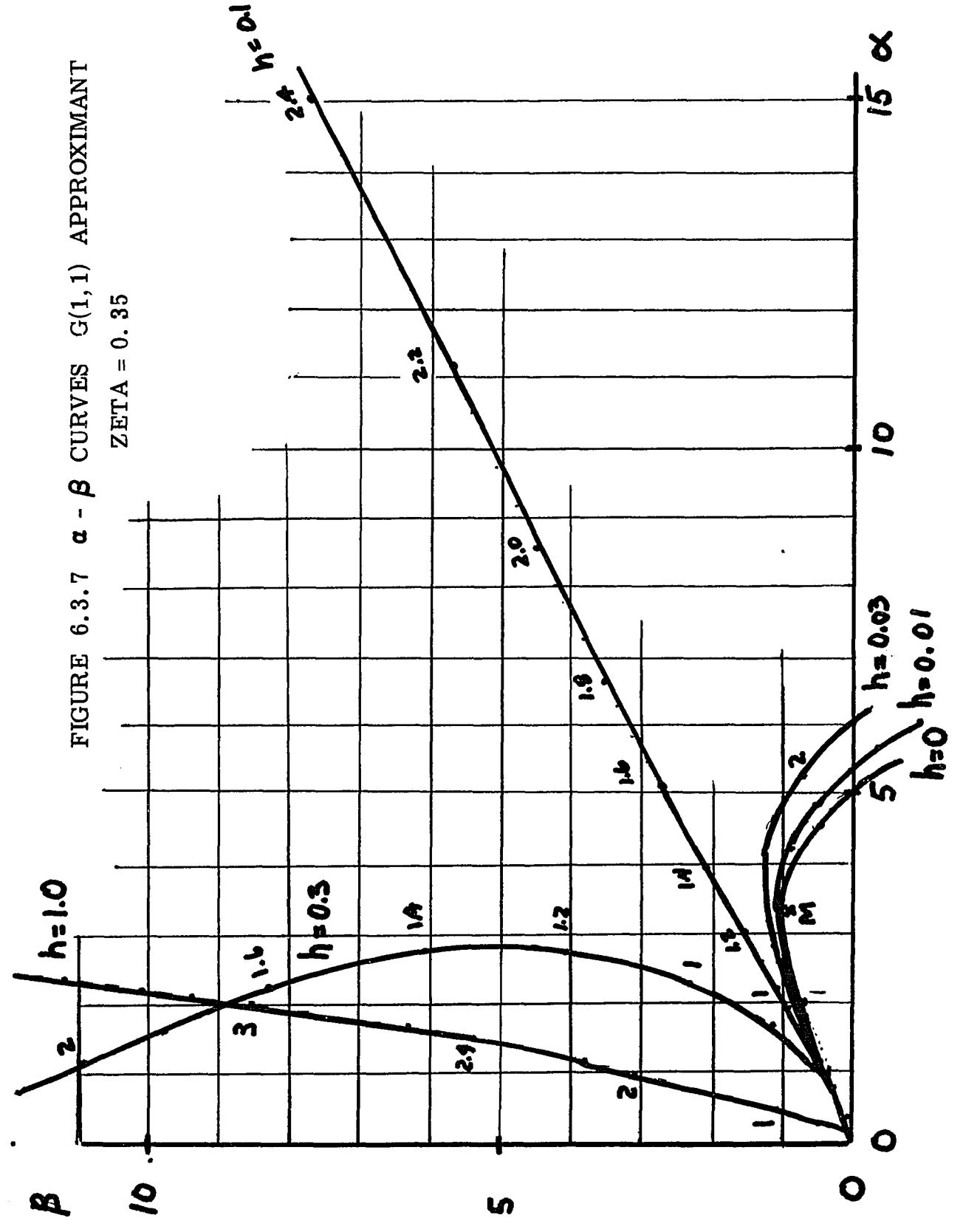

FIGURE 6.3.7 α - β CURVES G(1,1) APPROXIMANT

ZETA = 0.35

curve in Figure 6.3.7 is slightly displaced from the h= 0 curve. This curve thus provides a system which is unconditionally stable with respect to system gain and also indicates that there is only a slight damping of the transient response compared with the uncompensated system at a given operating point. Thus the system of (6.3.10) can be made unconditionally stable with gain variations (when T= 1) through use of a network with transfer function

$$\frac{N_p(s)}{D_p(s)} = \frac{1}{1 + 0.03\ s}$$

as an approximation for the distributed lag. This polynomial approximation will produce the least amount of damping of the uncompensated response at the specified value of gain and reset time consistent with this unconditional stability.

CHAPTER 7

TRANSIENT RESPONSE OF LINEAR FEEDBACK SYSTEMS WITH DISTRIBUTED LAG USING DOMINANT ROOT AND GEOMETRIC TECHNIQUES

7-1. Introduction

For a given feedback system containing lumped parameter elements Mulligan [71] showed that properties of its transient response such as time to peak, first peak overshoot and settling time can be easily determined from the s-plane location of a pair of complex conjugate roots of the characteristic equation. This pair of roots, however, must be dominant in nature. The effect of the non-dominant roots as well as zeros of the closed loop transfer function upon time to peak, first peak overshoot and settling time were considered by Chu [24] . He presented a geometric interpretation of time to peak as a function of angles between other roots and the dominant root of the characteristic equation as well as angles between system zeros and the dominant root. Similarly, he showed that the peak overshoot can be determined by considering the ratio of the length of lines in the s-plane between all other roots and one of the dominant roots to the length of lines between all other roots and the origin. Eisenberg [30] extended the technique to feedback systems with transport lag. He showed that the dominant

root and geometric approaches remained valid if one referenced the time measurements from the value of the transport lag instead of from time zero.

The purpose of this chapter is to extend the dominant root and geometric methods to feedback systems with distributed lag. This extension is complicated by the fact that the characteristic equation for the system with distributed lag is multi-valued as well as transcendental. These properties give rise to irrational integrals when determining the transient response by the inverse Laplace transform technique.

7.2 Derivation of the Transient Response Equations

Consider the linear feedback system of Figure 7.2.1. The system shown consists of a combination of lumped parameter elements with transfer function, G(s), and a distributed parameter network with transfer function $F_D(s)$ in cascade. The transfer function of the distributed parameter network is defined as

$$F_D(s) = \exp(-\gamma(s)d) \qquad (7.2.1)$$

where

$$\gamma(s) = \sqrt{(Ls+R)(Cs+G)} \qquad (7.2.2)$$

and where d is the length of the network, L, C, R, and G are respectively the inductance, capacitance, resistance and conductance per unit length. Also, s is the complex variable

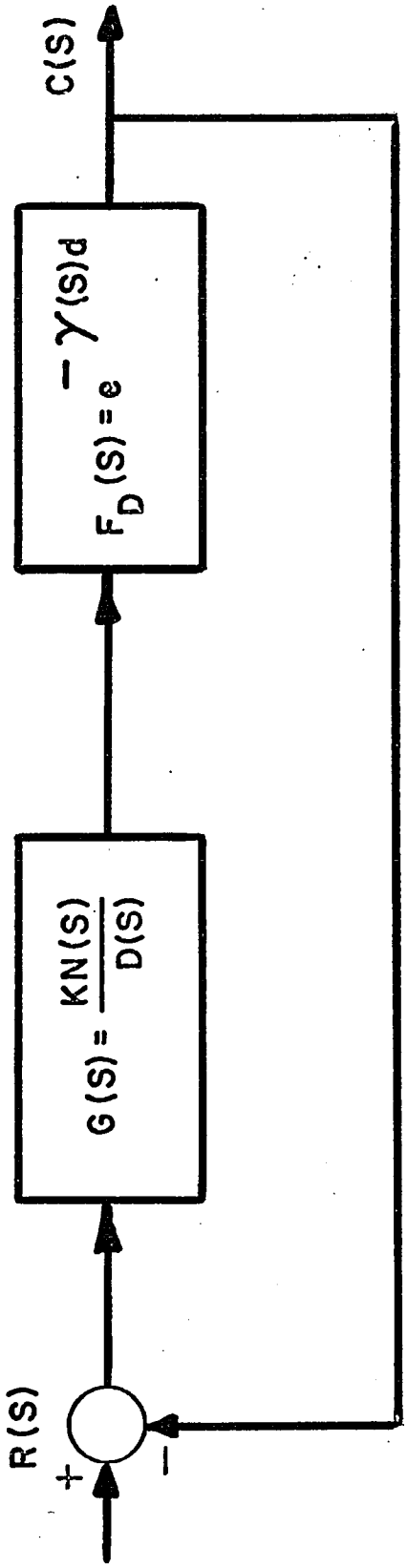

FIGURE 7.2.1 SYSTEM DIAGRAM

$$s = \sigma + j\omega = -\zeta\omega_n + j\omega_n\sqrt{1-\zeta^2} \qquad (7.2.3)$$

where ζ is the dimensionless ratio and ω_n is the undamped natural frequency. The system transfer function is given by

$$\frac{C}{R}(s) = \frac{G(s)\exp(-\gamma(s)d)}{1+G(s)\exp(-\gamma(s)d)} = \frac{KN(s)\exp(-\gamma(s)d)}{D(s)+KN(s)\exp(-\gamma(s)d)} \qquad (7.2.4)$$

where K is the gain and G(s) is defined in Figure 7.2.1 as $\frac{KN(s)}{D(s)}$.

The characteristic equation is therefore

$$F(s) = D(s) + KN(s)\exp(-\gamma(s)d) = 0 \qquad (7.2.5)$$

It is assumed in equation (7.2.4) that the order of N(s) is equal to or smaller than the order of D(s) and that no multiple roots of F(s) exist. The first assumption is true in most applications. Also, the second assumption can be realized since the designer utilizing either parameter plane [122] or root locus techniques [40] can control s-plane root locations and therefore prevent the existence of multiple roots.

In this discussion, a unit step function is selected as the standard test input signal. This type of test signal has been chosen because many other types of input signals can be approximated by combinations of step functions. Assuming a unit step input signal applied to the system of (7.2.4), the Laplace transform of the output signal c(t) is

$$C(s) = \frac{KN(s)\exp(-\gamma(s)d)}{sF(s)} \qquad (7.2.6)$$

The output response function c(t) is found by taking the inverse Laplace transform of (7.2.6) utilizing the Bromwich-Wagner integral. That is

$$c(t) = \lim_{\beta \to \infty} \frac{1}{2\pi j} \int_{\alpha - j\beta}^{\alpha + j\beta} C(s)\exp(st)ds \qquad (7.2.7)$$

The transient response is evaluated by performing a contour integration around the path shown in Figure 7.2.2. Note that if the general form of equation (7.2.2) is assumed (i.e., L,R,C and G not equal to zero), two branch points exist in the s-plane. These points are located on the negative real axis at $s_1 = -R/L$ and $s_2 = -G/C$ with the variable -a representing the larger (less negative) and variable -b representing the smaller (more negative) of these two branch points. In addition, singularities exist which are produced by the roots of the characteristic equation as well as the singularity at the origin due to the unit step function. A typical s-plane configuration depicting branch points, singularities of F(s), and a singularity at the origin due to a-unit step input is shown in Figure 7.2.2. Since the path of integration chosen is closed and simply connected, the contour integral is equal to the sum of the residues at the enclosed singularities. Furthermore the integral of (7.2.7) represents the integral along path A'A of Figure 7.2.2.

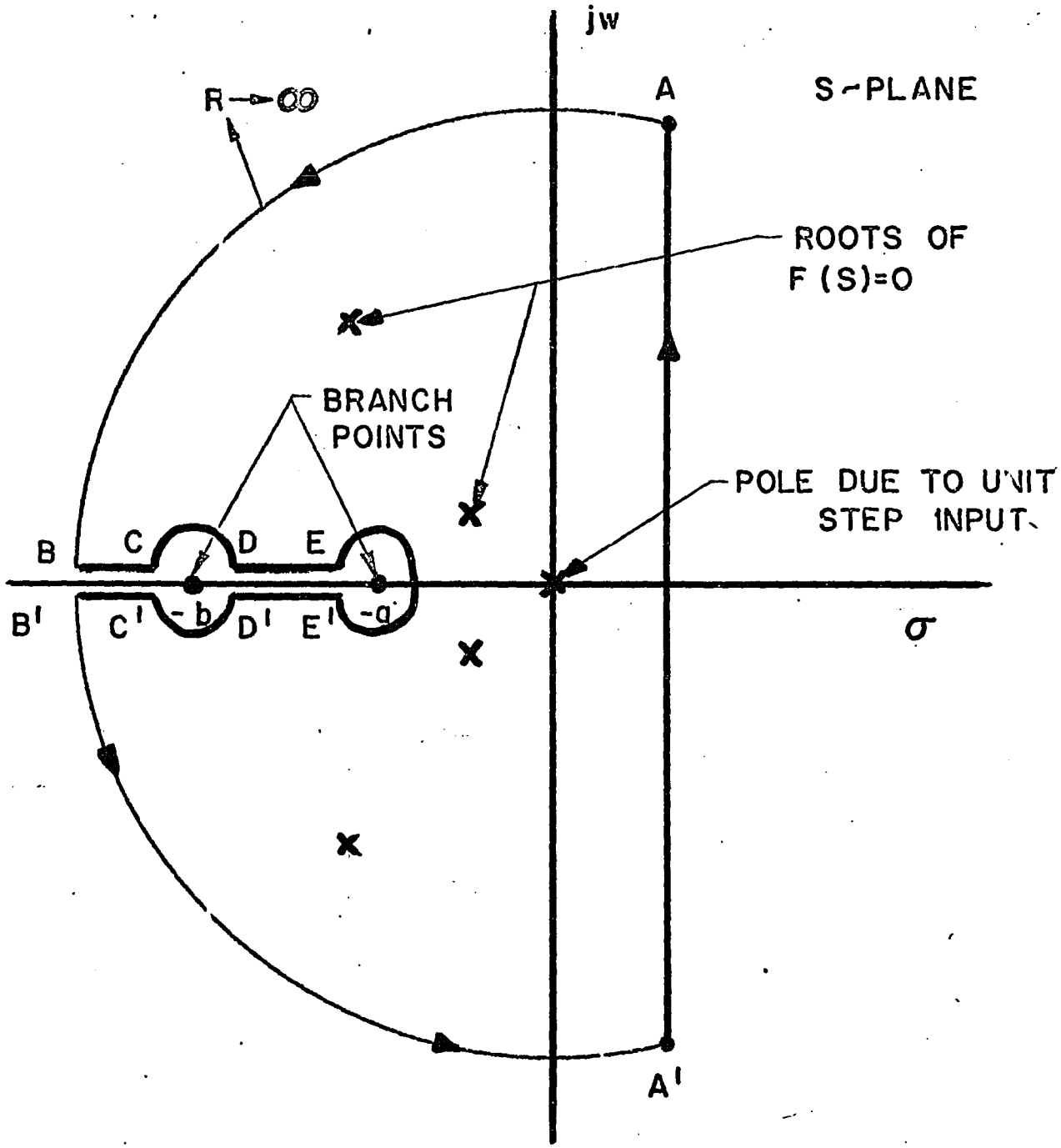

FIGURE 7.2.2 s-PLANE CONFIGURATION SHOWING PATH OF INTEGRATION FOR SYSTEM WITH DISTRIBUTED PARAMETER ELEMENT

Therefore

$$c(t) = \frac{-1}{2\pi j}\left[I_{AB} + I_{BC} + I_{CD} + I_{EE'} + I_{E'D'} + I_{D'C'} + I_{C'B'} + I_{B'A'} \right]$$

$$+ \begin{array}{l}\text{Residue of } C(s)e^{st} \\ \text{at } s = 0\end{array} + \sum_{i=1}^{n} \begin{array}{l}\text{Residues of } C(s)e^{st} \\ \text{of roots of } F(s) = 0 \\ \text{falling within contour} \\ \text{evaluated at } s = s_i\end{array} \qquad (7.2.8)$$

where

$$I_{XY} = \int_{X}^{Y} C(s)e^{st}ds$$

and the residue of $C(s)e^{st}$ at a root $s=s_i$ is given by,

$$\text{Residue} = \frac{KN(s_i)\exp(-\gamma(s_i)d)\exp(s_i t)}{s_i F'(s_i)} \qquad (7.2.9)$$

It should also be noted that "n", the upper limit of summation of residues evaluated at roots of F(s)=0 in (7.2.8) will be finite in many cases although the characteristic equation is transcendental. This is because the remaining infinite number of roots will be in the secondary sheet of the s-plane which need not be considered because the contour of integration avoids the s-plane branch cut [27].

Focusing attention upon the integral portion of (8), all integrals except I_{DE} and $I_{E'D'}$ can be shown to be equal to zero.[1]

Defining $s = r\exp(j\pi)$ in I_{DE} and $s = r\exp(-j\pi)$ in $I_{E'D'}$, and combining the sum of these two integrals into one expression I_{BR} produces

$$I_{BR} = j2K\int_a^b \frac{N(-r)D(-r)\exp(-rt)\mathrm{Sin}(Yd)dr}{[D^2(-r) + K^2N^2(-r) + 2KD(-r)\mathrm{Cos}(Yd)]\ r} \tag{7.2.10}$$

where $Y = \sqrt{|(-Lr + R)\ (-Cr + G)|}$

Evaluating the residue of $C(s)\exp(st)$ at $s = 0$ yields

$$\underset{s=0}{\mathrm{Res.}} = \frac{KN(0)\exp(-d\,(RG)^{1/2})}{F(0)} = c(\infty) \tag{7.2.11}$$

Substituting (7.2.11) and (7.2.10) into (7.2.8) gives

$$c(t) = c(\infty) + \sum_{i=1}^{n} \begin{array}{l}\text{Residues of } C(s)\exp(st) \\ \text{at roots of } F(s) = 0 \\ \text{within contour of} \\ \text{integration (i.e., at} \\ s = s_i)\end{array} - \frac{I_{BR}}{2\pi j} \tag{7.2.12}$$

---

[1] When $a = 0$ the singularity due to the input step function exists at the branch point. In this case $I_{E'E'}$ has a non zero value equal to $\frac{KN(0)\exp(-\sqrt{RG}d)}{F(0)}$ and the residue of $C(s)e^{st}$ at $s = 0$ is no longer required.

This form of the solution obtained from the complex inversion integral provides some insight into the behavior of c(t). The first two terms appear to be similar to those obtained when systems with either lumped parameter elements, transport lag or combinations of both are considered. The integral term, which results from integration along the branch cut, arises when treating systems with characteristic equations that are multivalued functions of s. For example, in systems with transport lag the integral term is equal to zero. This integral is of the Laplace type with finite limits (if one considers the variable t to represent s and r to represent t) and its value tends to zero as t approaches infinity, representing a component of the transient response which diminishes with time. Although this integral term will be ignored initially, methods of evaluating its contribution at specific values of time will be outlined in a subsequent section. The first two terms are the more important terms in (7.2.12). In particular the first term represents the final value of c(t) while the second term represents the results of evaluation of the residues of C(s)exp(st) at the roots of F(s) = 0 within the contour of integration.

The time to peak, T_p, is found by differentiating (7.2.12) with respect to time, setting the derivative equal to zero, and solving the resulting equation for the smallest value of t.

Thus

$$\frac{dc(t)}{dt} = 0 = \sum_{i=1}^{n} \frac{KN(s_i)\exp(s_i t)\exp(-\gamma(s_i)d)}{F'(s)} - \frac{1}{2\pi j}\frac{dI_{BR}}{dt} \tag{7.2.13}$$

represents the equation from which T_p can be determined. A good approximation to this equation of computing T_p is obtained by neglecting the derivative term $\frac{dI_{BR}}{dt}$. Once T_p has been determined the fractional amount of the first overshoot, M, is found by evaluating

$$M = \frac{c(T_p) - c(\infty)}{c(\infty)} \tag{7.2.14}$$

or upon substituting (7.2.12) into (7.2.14) and noting the residue evaluation formula (7.2.9) gives

(7.2.15)

$$M = \frac{N(s_i)\exp(-\gamma(s_i)\exp(s_i T_p)F(0)}{N(0)\exp(-d(RG)^{1/2})s_i F'(s_i)} - \frac{F(0)I_{BR}}{K 2\pi j N(0)\exp(-d(RG)^{1/2})}$$

There are different criteria for settling time. Using the definition of the time at which the response falls to within two percent of its final value, the settling time is found to be

$$T_s = \frac{4}{|\sigma_d|} \quad \text{seconds} \tag{7.2.16}$$

where σ_d is the real part of either the dominant pole or dominant complex conjugate pole pair. Note that while (7.2.13) and (7.2.14) were developed without regard to dominance of roots (7.2.16) assumes the existence of a dominant root or root pair.

7.3 Transient Response Assuming Dominant Roots

In the design of lumped parameter feedback systems, the determination of controller parameters is often guided by the concept of placing the poles and zeros of the transfer function in s-plane locations so as to achieve the desired transient response. Furthermore, it is desirable to place the remaining roots and zeros of the transfer function in s-plane locations which will maintain this dominance. This dominant root philosophy is maintained in this work on feedback systems with distributed parameter elements because of the following reasons:

1. System parameters which permit root placement in the desired locations can be easily determined.
2. Although the characteristic equation for this type of system is, in general, both multi-valued and transcendental, there is a subclass of distributed parameter networks in which only a finite number of roots of $F(s)=0$ exist within the contour of integration. Therefore residues need only be evalued at a

finite number of points in the s-plane in determining the transient response. Furthermore, for systems in which an infinite number of roots exist within the contour of integration, the dominant root philosophy can still be used in determining transient response.

3. The integral term of equation (7.2.12) can in most cases be neglected when considering the response at values of time equal to or greater than the time to peak T_p. Thus in a design procedure its contribution can be neglected initially and its actual contribution evaluated later.

Therefore assuming

1) The placement of dominant roots at $s_1 = \sigma_1 + j\ \omega_1$ and $s_1 = \sigma_1 - j\ \omega_1$

2) The integral I_{BR} of (7.2.12) can be neglected initially.

3) $$F_D(s) = \exp(-\gamma(s)d) = \exp(\psi - j\delta) \qquad (7.3.1)$$

where ψ and δ are defined on the upper half of the principal sheet

$$\psi = -d\ \sqrt{\frac{H^{1/2} + J}{2}} \qquad (7.3.2)$$

$$\delta = d\ \sqrt{\frac{H^{1/2} - J}{2}} \qquad (7.3.3)$$

and where

$$H = (\omega_n^2 L^2 - 2RL\zeta\omega_n + R^2)(\omega_n^2 C^2 - 2GC\zeta\omega_n + G^2) \qquad (7.3.4)$$

$$J = \omega_n^2 LC(2\zeta^2 - 1) + RG - \zeta\omega_n(RC + LG) \qquad (7.3.5)$$

Equation (7.2.12) is approximated by

$$c(t) \approx \frac{KN(0)\exp(d\sqrt{RG})}{F(0)} +$$

$$\left| \frac{2KN(s_1)\, e^{\psi(s_1)}}{s_1 F'(s_1)} \right| e^{\sigma_1 t} \cos(\omega_1 t + \angle N(s_1) - \angle s_1 - \angle F'(s_1) - \delta(s_1)) \qquad (7.3.6)$$

Also the time to peak, T_p, and the fractional amount of first overshoot, M, are given by

$$T_p = \frac{1}{\omega_1}\left[\frac{\pi}{2} - \angle N(s_1) + \angle F'(s_1) + \delta(s_1)\right] \qquad (7.3.7)$$

and

$$M = \frac{2\omega_1}{\omega_n^2} \frac{N(s_1)F(0)\exp(\psi(s_1))}{N(0)F'(s_1)\exp(-d(RG)^{1/2})} \exp(\sigma_1 T_p) \qquad (7.3.8)$$

Equations (7.3.7) and (7.3.8) can be interpreted geometrically when the distributed parameter element is a distributed lag network. Before showing this, it is noted that for lumped parameter systems,

Chu [24] presented an s-plane interpretation for T_p and M. The basis for this interpretation is that one pair of s-plane roots ($s = \sigma_1 + j\ \omega_1$) of $F(s) = 0$ are dominant. Thus he expressed T_p and M as

$$T_p = \frac{1}{\omega_1}\left[\frac{\pi}{2} - \left\{\begin{array}{l}\text{Sum of angles from}\\ \text{the zeros to the dominant}\\ \text{root } s_1 = \sigma_1 + j\ \omega_1\end{array}\right\} + \left\{\begin{array}{l}\text{Sum of angles from the}\\ \text{other roots of } F(s) = 0\\ \text{to the dominant root}\\ s_1 = \sigma_1 + j\ \omega_1\end{array}\right\}\right] \qquad (7.3.9)$$

$$M = \frac{2\omega_1}{\omega_{n_1}^2} \times \left[\frac{\text{Product of distances from zeros to the dominant root } s_1 = \sigma_1 + j\omega_1}{\text{Product of distances from zeros to the origin}}\right] \times \left[\frac{\text{Product of distances from the roots of } F(s) = 0 \text{ to the origin}}{\text{Product of distances from the other roots of } F(s) = 0 \text{ to the dominant root } s_1 = \sigma_1 + j\omega_1}\right] e^{\sigma_1 T_p} \qquad (7.3.10)$$

Eisenberg [30] extended Chu's interpretation to systems with transport lag, showing that T_p and M can still be interpreted from s-plane root locations if T_p is measured relative to $t = T$ (the amount of transport lag).

For systems with distributed lag, equations (7.3.7) and (7.3.8) can be interpreted geometrically in the following manner. This double-valued function can be represented as a single valued function on a two sheeted Riemann surface with the principal sheet defined the angular range $-\pi \leqq \theta \leqq +\pi$ and the secondary sheet defined by $\pi \leqq \theta \leqq 3\pi$. However, the root locations representing solutions of the characteristic equation can exist on either sheet of this Riemann surface. Thus a problem exists when attempting to measure a distance and angle between a root or the second sheet and the dominant root on the first sheet of the s-plane. This difficulty can be resolved by performing measurements of distances and angles in a plane which renders the characteristic equation single valued. This plane is defined as the complex w-plane (see Figure 7.3.1) where for distributed lag the complex variable w is related to the complex variable s by the transformation

$$w^2 = s \tag{7.3.11}$$

Under this transformation, a dominant roots of $F(s) = 0$ located at

$$s_1 = \omega_{n_1} \exp(j\,\theta_1) = \sigma_1 + j\,\omega_1 \tag{7.3.12}$$

is transformed to a w-plane location

$$w_1 = \sqrt{\omega_{n_1}}\, \exp(j\,\theta_1/2) = u_1 + jv_1 \tag{7.3.13}$$

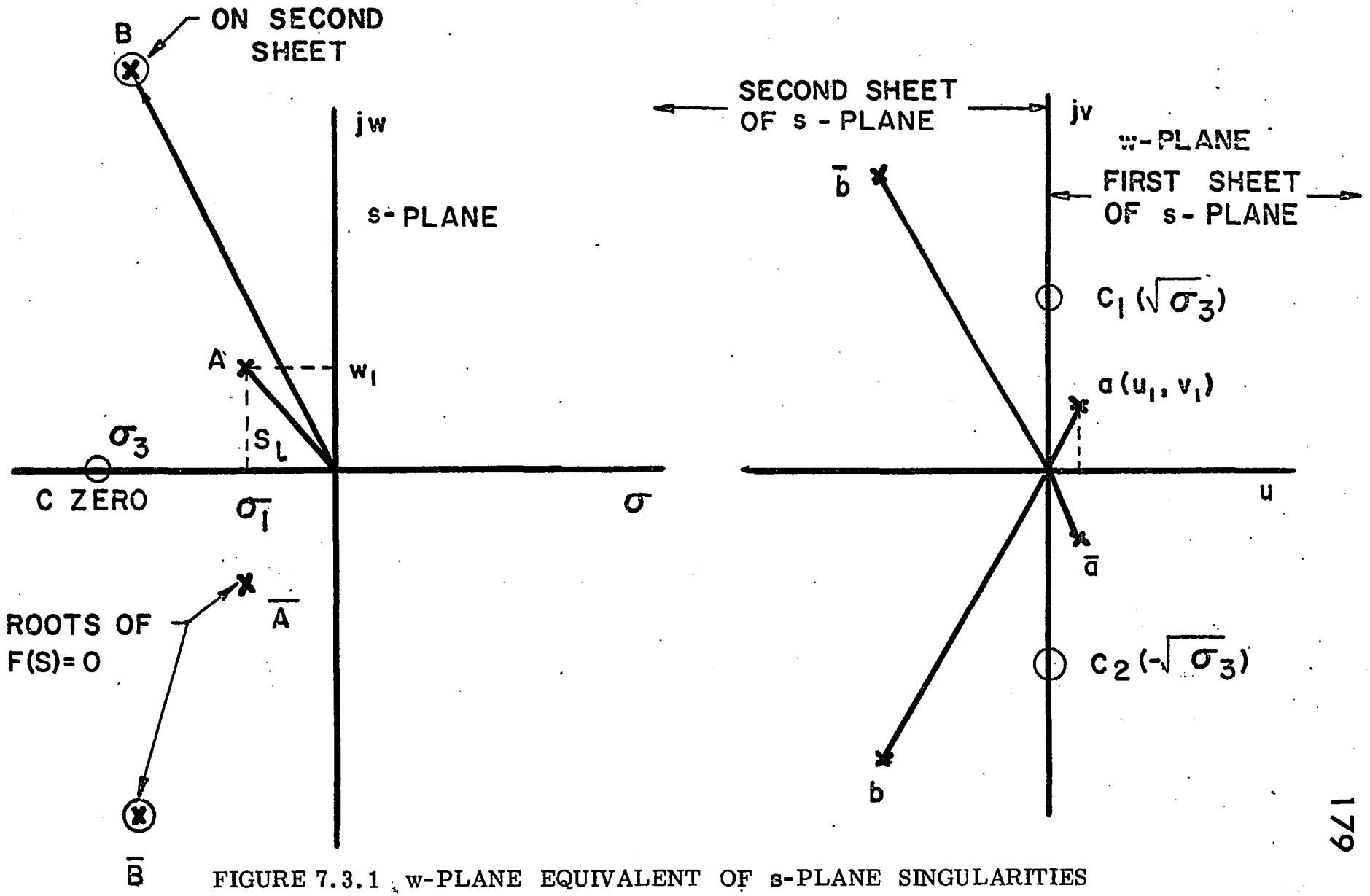

FIGURE 7.3.1 w-PLANE EQUIVALENT OF s-PLANE SINGULARITIES

Furthermore as illustrated in Figure 7.3.1, roots located on the second sheet of the s-plane transform into roots located in the left hand portion of the w-plane. Also, a simple zero located at $s = -\sigma_3$ transforms into a complex conjugate pair of roots located at $w = \pm j\sqrt{\sigma_3}$.

Returning to the question of interpreting (7.3.7) and (7.3.8) for systems with distributed lag, the w-plane equivalent to the various terms comprising these equations will now be examined. Consider the transformed characteristic equation F(w) =0 given by

$$F(w) = \prod_{m=1}^{\infty} (w-w_m)(w - \bar{w}_m) \qquad (7.3.14)$$

The function F(s)=0 is represented in the w-plane as F(w)=0 the magnitude of which is equal to the product of the distances from all w-plane roots to the origin. The derivative of F(s) with respect to s is given by

$$F'(s) = F'(w) \frac{dw}{ds} \qquad (7.3.15)$$

and F'(s) evaluated at $s=s_1$ is found by evaluating F'(w) and dw/ds at $w=w_1$, the image of s_1 in the w-plane.

Taking the derivative of (7.3.14) at $w=w_1$ and noting that $\frac{dw}{ds}$ for distributed lag is $\frac{1}{2w}$, (7.3.15) becomes

$$F'(s) = \frac{(w_1 - \bar{w}_1)}{2w_1} \prod_{m=2}^{\infty} (w_1 - \bar{w}_m)(w_1 - w_m) \qquad (7.3.16)$$

The magnitude of (7.3.16) is equal to the product of the distances from all other w-plane roots to the dominant root $w_1 = u_1 + jv_1$ divided by twice the distance from the origin to the dominant root. The phase of (7.3.16) is equal to the sum of the w-plane angles from the other roots of $F(w)=0$ to the dominant root minus the angle of the dominant root.

The numerator function, N(s), of G(s) in Figure 7.2.1 is a single valued function of s and it can be shown that the sum of the s-plane angles from zeros (i.e., roots of $N(s) = 0$) to the dominant root $s_1 = \sigma_1 + j\ \omega_1$ is equal to the sum of the w-plane angles from the images of the zeros to the image of the dominant root. Also, the ratio of the product of s-plane distances between zeros and the origin remains unchanged upon transformation from the s-plane to the w-plane.

The functions - $\delta(s_1)$ and $\exp(\psi(s_1))$ are respectively the phase and magnitude of the distributed parameter transfer function. For distributed lag, $L = G = O$ and $T = RCd^2$. Thus $F_D(s) = \exp(-\sqrt{sT})$ and for roots on the upper half of the principal sheet

$$\delta(s_1) = \sqrt{\omega_{n_1} T}\,\mathrm{Sin}\,(\theta_1/2) = \sqrt{Tw_1}\,\mathrm{Sin}\,\phi_1 \qquad (7.3.17)$$

$$\exp(\psi(s_1)) = \exp\left[-\sqrt{\omega_{n_1} T}\,\mathrm{Cos}\left(\frac{\theta_1}{2}\right)\right] = e^{\sqrt{Tw_1}\cos\phi_1}$$

where

$$\phi_1 = \theta_1/2 \text{ and } w_1 = \sqrt{\omega_{n_1}}$$

Substituting the above transformation for F(s), F'(s), N(s) and $F_D(s)$ where appropriate into (7.3.7) and (7.3.8) and noting that for distributed lag

$$\omega_1 = 2u_1v_1,\ \exp(-d(RG)^{1/2}) = 1,\ \sigma_1 = u_1^2 - v_1^2, \qquad (7.3.18)$$

$$\omega_{n_1} = (u_1^2 + v_1^2)$$

equation (7.3.7) becomes

$$T_p = \frac{1}{2u_1v_1}\left[\frac{\pi}{2} - \left\{\begin{array}{l}\text{Sum of angles}\\ \text{from zeros to}\\ \text{the dominant}\\ \text{root } w_1 = u_1 + jv_1\\ \text{in the w-plane}\end{array}\right\} + \left\{\begin{array}{l}\text{Sum of angles}\\ \text{from all other}\\ \text{roots to the}\\ \text{dominant root}\\ w_1 = u_1 + jv_1 \text{ in}\\ \text{the w-plane}\end{array}\right\}\right.$$

$$\left. + (T)^{1/2} w_1\,\mathrm{Sin}\,\phi_1 - \phi_1\right] \qquad (7.3.19)$$

where $w_1 = \sqrt{\omega_{n_1}}$ and $\phi_1 = \theta_1/2$ are the magnitude and phase of the w-plane vector from the origin to the dominant root $w_1 = u_1 + jv_1$.

Considering equation (7.3.16) for the fractional overshoot M and noting

1) The distance from each of the two dominant roots to the origin in the w-plane is $(\omega_{n_1})^{1/2}$

2) The distance between dominant roots in the w-plane is $2(\omega_{n_1})^{1/2} \text{Sin}\ (\theta_1/2)$

3) The interpretation for $F(s)=0$ and $F'(s_1)$ in the w-plane is obtained from (7.3.14) and (7.3.16) respectively.

4) The identities $\text{Sin}\ (\theta_1/2) = \dfrac{\text{Sin}\ \theta_1}{2\ \text{Cos}\ (\theta_1/2)}$ and $\omega_1 = \omega_{n_1} \text{Sin}\ \theta_1$

The expression for fraction overshoot (7.3.16) can be rewritten as

$$M = \left[\frac{\text{Product of the distances from the zeros to the dominant root } w_1 = u + jv_1}{\text{Product of the distances from the zeros to the origin of the w-plane.}}\right] \times \left[\frac{\text{Product of the distances from all roots except the dominant pair to the origin of the w-plane}}{\text{Product of distances from all roots except the other dominant root to the dominant root } w_1 = u_1 + jv_1}\right]$$

$$\times \exp\left(-\sqrt{\omega_{n_1}}\, T \cos(\theta_1/2)\right) \exp\left((u_1^2 - v_1^2)\, T_p\right) \times 4 \cos(\theta_1/2) \qquad (7.3.20)$$

where $\sqrt{\omega_{n_1}}$ and $\theta_1/2$ are the magnitude and phase of the vector from the origin to the dominant root $u_1 + jv_1$.

7.4 Approximation for T_p and M in Systems with Distributed Lag Considering Only Dominant Roots

Approximate values for T_p and M can be obtained for feedback systems with distributed lag from a set of universal curves under the following conditions:

1) A dominant pair of roots of F(s) = 0 exists.
2) Either roots of F(w) = 0 or system zeros (i.e., roots of N(w) = 0) lie sufficiently far to the left of the dominant pair in the w-plane so that their contributions to the output transient response are negligible.
3) The location of system zeros either close to the origin or near the dominant root in the w-plane, and their resultant effect on system transient response, are cancelled by roots of the system characteristic equation located nearby.

If a system is assumed which meets the above mentioned conditions, the approximate equation for T_p becomes

$$T_p = \frac{1}{\omega_1} \left[\pi + \sqrt{\omega_n T} \operatorname{Sin} (\theta/2) - \theta/2 \right] \qquad (7.4.1)$$

defining $\omega_1 = \omega_n \sin \theta$, $x^2 = \omega_n T$ and $y = \frac{T_p}{T}$ yields upon substitution into (7.4.1) and solving for x gives

$$x = \frac{\operatorname{Sin} (\theta/2)}{2 y \operatorname{Sin} \theta} \pm 1/2 \sqrt{\frac{\operatorname{Sin}^2(\theta/2)}{y^2 \operatorname{Sin}^2 \theta} + \frac{4(\pi - \theta/2)}{y \operatorname{Sin} \theta}} \qquad (7.4.2)$$

Since only the second quadrant of the s-plane is of interest and y is positive, one of the solutions of (7.4.2) is positive and one is negative. Considering only the positive solution yields upon squaring (7.4.2).

$$x^2 = \omega_n T = \frac{\sin^2(\theta/2)}{4y^2 \sin^2\theta} \left[1 + \sqrt{1 + \frac{4(\pi - \theta/2)\, y \sin\theta}{\sin^2(\theta/2)}}\right]^2 \qquad (7.4.3)$$

Equation (7.4.3) represents the magnitude of a vector in the sT-plane as a function of the sT-plane angle θ and a dimensionless constant y. A family of curves can be obtained in which x^2 is plotted as a function of θ with y as a parameter. These curves are shown in Figure 7.4.1. Given a point in the sT-plane and the value of the distributed lag constant T, the root location $\sigma_1 + j\,\omega_1$ and the time to peak T_p can be determined by means of Figure 7.4.1. Thus this figure relates dominant root locations in the s-plane to time to peak for feedback systems with distributed lag.

The approximation for settling time (2% criterion) assuming the presence of a dominant root pair if $T_s = \frac{4}{|\sigma|} = \frac{4T}{|\sigma T|}$ or

$$\frac{T_s}{T} = \frac{4}{|\sigma T|} \qquad (7.4.4)$$

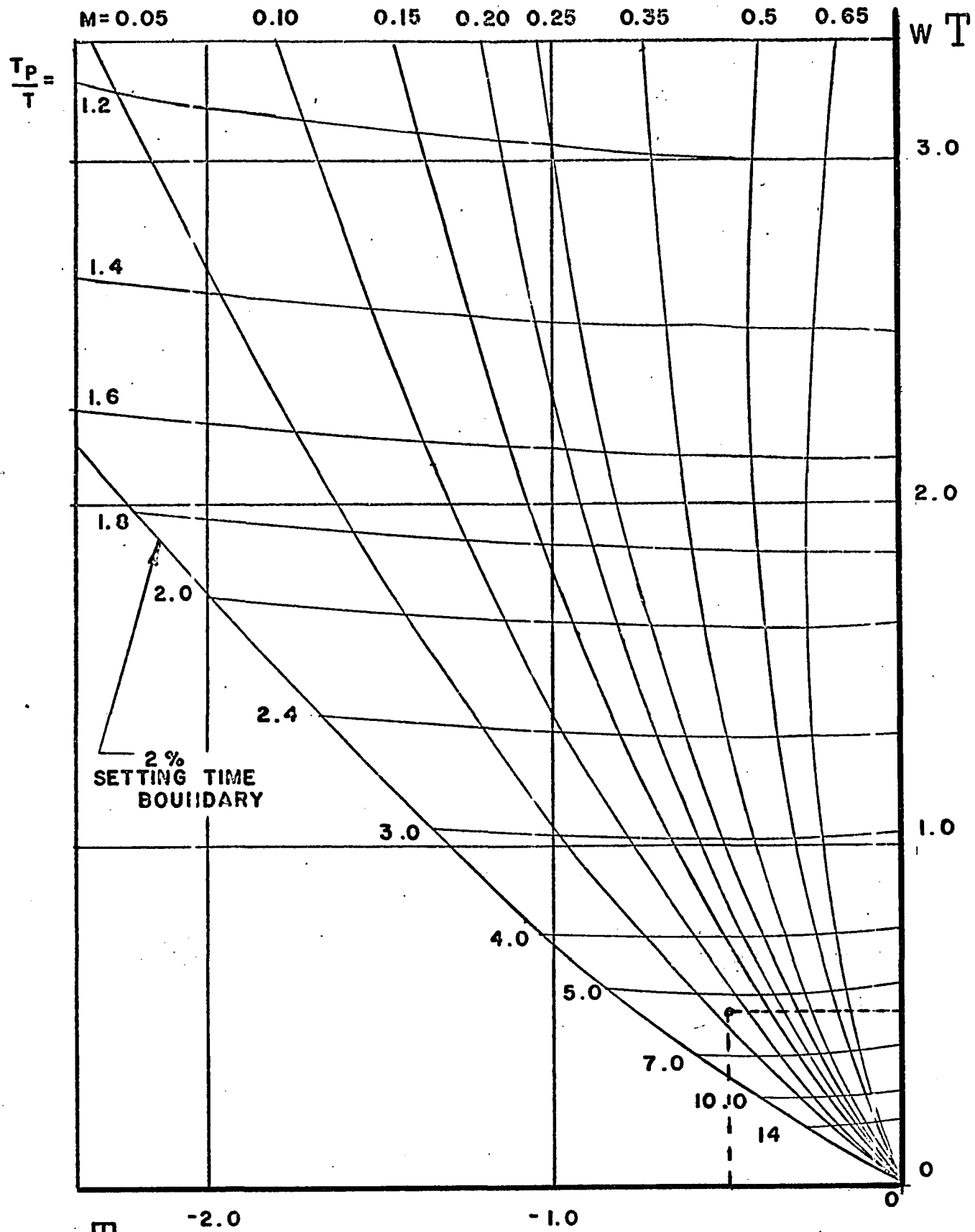

FIGURE 7.4.1 sT-PLANE CURVES OF CONSTANT Tp/T AND M FOR DISTRIBUTED LAG

Thus given a value of σT, $\frac{T_s}{T}$ is determined and since $\frac{T_s}{T} \geq \frac{T_p}{T}$ this value determines a boundary limit for the $\frac{T_p}{T}$ curves as a function of σT. This boundary is also shown in Figure 7.4.1. For roots located below this boundary, the settling time constant dominates and there is practically no peaking of the transient response.

The fractional overshoot M for a dominant root system with distributed lag is given by (7.3.20) as

$$M = 4 \operatorname{Cos}(\theta_1/2) \exp\left[-\sqrt{\omega_{n_1} T} \operatorname{Cos}(\theta_1/2)\right] \exp(\sigma_1 T_p) \tag{7.4.5}$$

Substituting the value of T_p from (7.4.1) into (7.4.5) and noting that $\operatorname{Tan}\theta_1 = \omega_1/\sigma_1$ yields

$$\frac{M}{4 \operatorname{Cos}(\theta_1/2)} = \exp\left[-\sqrt{\omega_{n_1} T} \operatorname{Cos}(\theta_1/2) + \frac{\pi + \sqrt{\omega_{n_1} T} \operatorname{Sin}(\theta_1/2) - \theta_1/2}{\operatorname{Tan}\theta_1}\right]$$

Taking the natural logarithm of (7.4.6) and re-arranging terms gives

$$\ln\left(\frac{M}{4 \operatorname{Cos}(\theta_1/2)}\right) - \frac{(\pi - \theta_1/2)}{\operatorname{Tan}\theta_1} = \sqrt{\omega_{n_1} T}\left[\frac{\operatorname{Sin}(\theta_1/2)}{\operatorname{Tan}\theta_1} - \operatorname{Cos}(\theta_1/2)\right] \tag{7.4.7}$$

Setting $x^2 = \omega_{n_1} T$ and noting that

$$\left(\frac{\operatorname{Sin}\theta/2}{\operatorname{Tan}\theta} - \operatorname{Cos}\theta/2\right) = -\frac{1}{2 \operatorname{Cos}(\theta/2)} \tag{7.4.8}$$

upon solving for x^2 gives

$$x^2 = \omega_{n_1} T = 4 \operatorname{Cos}^2 (\theta_1/2) \left[\frac{(\pi - \theta_1/2)}{\operatorname{Tan} \theta_1} + \ln \left(\frac{4 \operatorname{Cos} (\theta_1/2)}{M} \right) \right]^2 \tag{7.4.9}$$

Equation (7.4.9) represents the magnitude of a vector in the sT-plane as a function of the sT-plane angle θ, and the fractional peak overshoot M. A family of curves can be obtained from (7.4.9) in which x^2 is plotted as a function of θ_1 with M as a parameter. Some curves from this family are also shown in Figure 7.4.1. These are curves of constant fractional overshoot as θ_1 is varied from $\pi/2$ to π .

7.5 Illustrative Example

The use of equations (7.3.19) and (7.3.20) as well as Figure 7.4.1 will be demonstrated by an example. Consider the feedback system with distributed lag shown in Figure 7.5.1. This system has been treated previously by a number of authors [32] and [81]. When the gain is unity Elgerd [32] showed that the characteristic equation

$$F(s) = s + e^{-\sqrt{s}} = 0 \tag{7.5.1}$$

is satisfied by an infinite number of pairs of roots and that the two root pairs are

$$\begin{aligned} s_{1,\bar{1}} &= -0.5108 \pm j\, 0.5105 = 0.72 \angle \pm 135^\circ \\ s_{2,\bar{2}} &= -11.91 \pm j\, 36.72 = 38.4 \angle \pm 469^\circ \end{aligned} \tag{7.5.2}$$

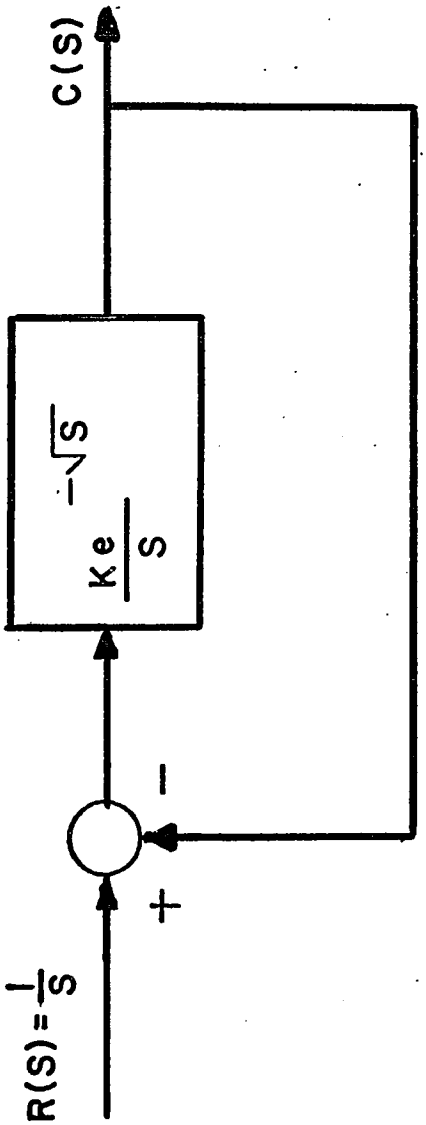

FIGURE 7.5.1 SYSTEM DIAGRAM - ILLUSTRATIVE EXAMPLE

Notice that the first pair of roots appear on the principal sheet of the Riemann surface while the second pair of roots are on the second sheet. The w-plane locations of these roots under the transformation $w^2 = s$ are

$$w_{1,\overline{1}} = 0.325 \pm j\,0.785 = .849 \quad \underline{/\pm 67.5^{o}} \qquad (7.5.3)$$

$$w_{2,\overline{2}} = 3.595 \pm j\,5.04 + 6.2 \quad \underline{/\pm 234.5^{o}}$$

These roots are shown in the w-plane representation of Figure 7.5.2 Apply (7.3.19) to Figure 7.5.2 yields.

$$T_p = \frac{1}{0.5105}\left[\frac{\pi}{2} + \frac{\pi}{2} - \text{Tan}^{-1}\left(\frac{4.255}{3.925}\right) + \text{Tan}^{-1}\left(\frac{5.825}{3.925}\right) + .849\,\text{Sin}\,(67.5^{o}) - \frac{67.5 \times \pi}{180}\right] = \frac{2.895}{0.5105} = 5.65 \text{ seconds}$$

Similarly, applying the data from Figure 7.5.2 to (7.3.20) gives

$$M = 4\,\text{Cos}\,(67.5^{o}) \times \frac{(6.2)(6.2)}{(5.77)(7.01)} \times e^{-.849\cos(67.5^{o}) - 0.51\,(5.65)}$$

$$M = 0.0632$$

The transient response for this network was calculated by Pierre [81] and is shown in Figure 7.5.3. Referring to Figure 7.5.3, the time to peak T_p is 5.1 seconds and the fractional overshoot is 0.11. Thus application of equations (7.3.19) and (7.3.20) produces approximate errors of 11% in T_p and an absolute error of 0.05 in M.

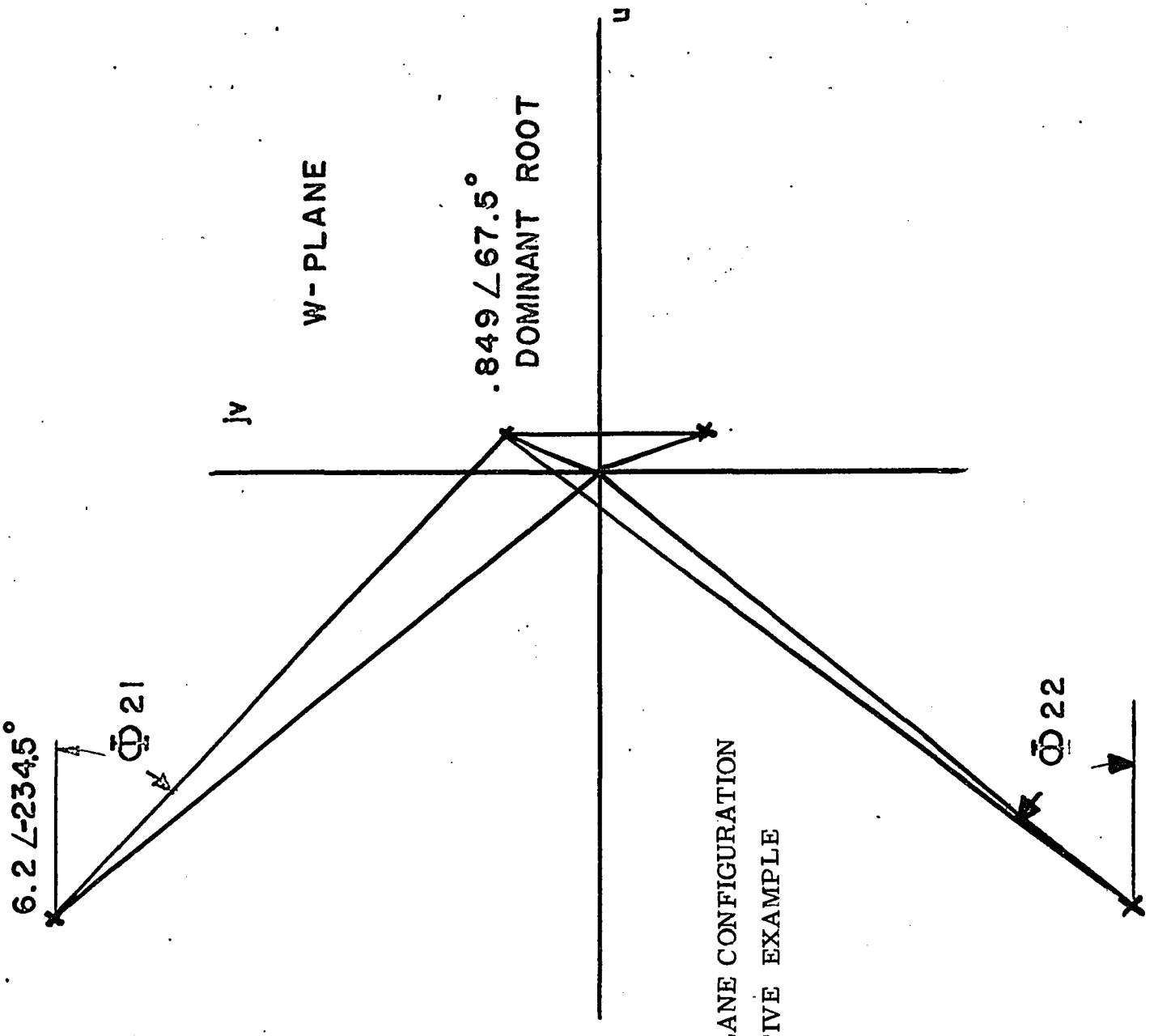

FIGURE 7.5.2 w-PLANE CONFIGURATION
ILLUSTRATIVE EXAMPLE

The results obtained from (7.3.19) and (7.3.20) will be compared to those obtained through application of (7.3.6) which also neglects the integral term. For the system of Figure 7.5.1

$$N(s) = 1,\ F(s) = s + Ke^{-\sqrt{s}} \quad = 0, L = G = 0$$

and the roots in the principal sheet corresponding to K = 1 are located at

$$s_{1,\bar{1}} = -0.5108 \pm j\,0.5105 = 0.72 \quad \underline{/\pm 135^{o}} \qquad (7.5.4)$$

Substituting the preceding information into (7.3.6) and noting that F'(s) can be written as

$$F'(s) = 1 - \frac{Ke^{-\sqrt{s}}}{2\sqrt{s}} \quad = 1 + \frac{\sqrt{s}}{2} = 0 \qquad (7.5.5)$$

yields

$$c(t) = 1 + 1.775\, e^{-0.51t} \cos (0.51t - 113.1^{o}) \qquad (7.5.6)$$

This equation is also plotted as a function of time in Figure 7.5.3. Notice that the difference between these two curves is a maximum at t = 0 and decreases with time. The amplitude error in the vicinity of T_p (i.e., $t \approx 5$ seconds) is approximately 0.04. Equation (7.3.6) takes into account the amplitude and phase contributions of all roots of F(s) = 0 through the evaluation of F(s) at each of the roots of F(s) = 0 on the principal sheet. A third method of estimating T_p and M is through use of Figure 7.4.1.

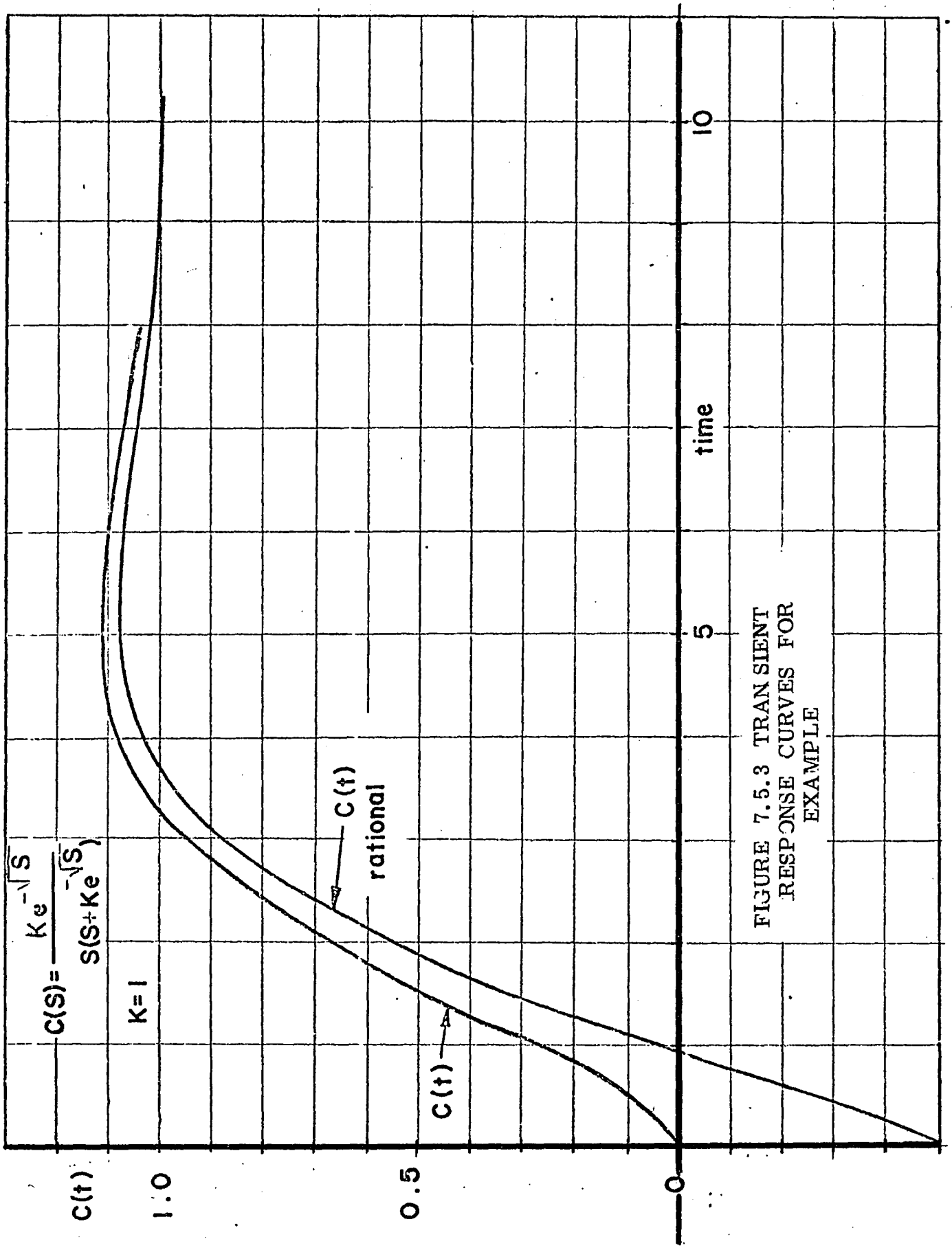

FIGURE 7.5.3 TRANSIENT RESPONSE CURVES FOR EXAMPLE

For the dominant root s = -0.511 + j 0.511, Figure 7.4.1 indicates T_p = 5.4 seconds and M = 0.07. The results of the four methods of obtaining T_p and M are summarized in the table below.

K=1 $F(s)=s+e^{-\sqrt{s}}=0$	Exact Method	Geometric Interpretation 2 prs. of roots	Approx. Method Equation (7.3.6)	Dominant Root Method Figure 7.4.1
T_p in seconds	5.10	5.65	5.20	5.40
M	0.110	0.063	0.08	0.07

Calculations for the system of Figure 7.5.1 are repeated for system gains of 2 and 4 respectively. The values of T_p and M by the exact method, the geometric interpretation method using two pairs of roots, the approximate method of equation (7.3.6) and the dominant root method of Figure 7.4.1 are presented below.

K=2 $F(s)=s+2e^{-\sqrt{s}}=0$	Exact Method	Geometric Interpretation 2 prs. of roots	Approx. Method Equation (7.3.6)	Dominant Root Method Figure 7.4.1
T_p in seconds	2.9	3.23	3.1	3.05
M	0.21	0.12	0.17	0.15
K=4 $F(s)=s+4e^{-\sqrt{s}}=0$				
T_p in sec.	1.80	2.01	1.85	1.90
M	0.34	0.21	0.31	0.25

7.6 Methods of Evaluating the Irrational Integral Term

The transient response equation (7.2.12) consists of the sum of the rational component and the irrational integral component given by

$$c(t) = -\frac{I_{BR}}{2\pi j} \qquad (7.6.1)$$

where I_{BR} is defined by (7.2.10). The integral defined by this equation is with respect to the function r (the distance along the negative real axis of the s-plane is a parameter) and t (the time variable). The value of this integral decreases at t increases because of the exponential term exp (-rt). The contribution of (7.6.1) to the transient response was neglected in developing the various approximations because of the assumption that $c(t)_{Irr}$ can be neglected for values of t equal to or greater than the time to peak T_p. This assumption should be verified.

The irrational integral term of equation (7.6.1) can be evaluated in any one of the following ways:

1. Direct numerical integration of equation (7.2.10) - that is set $t=T_i$, select a value for dr and integrate.
2. Numerical Integration using Gauss Quadrature Techniques - this involves substituting a finite summation for the integration operation. This technique is described in detail by Bellman [11]. However, care should be taken in applying these techniques since they are designed for rational polynomials.

3. Asymptotic Expansion - this method consists of:

   a) Substituting the series expansions of sin (Yd) and cos (Yd) in equation (7.2.10).

   b) Performing the division operation.

   c) Integrating term by term.

   If the limits of integrations of (7.2.10) are zero and infinity, the integration is equivalent to a transform operation.

The asymptotic expansion method will be illustrated for the sample problem. For the system of Figure 7.5.1,

$$N(-r)=1,\ D(-r)=-r,\ Y=(RCr)^{1/2}$$

and upon evaluating I_{BR} utilizing (7.2.10), (7.6.1) becomes

$$c(t)_{Irr} = \frac{K}{\pi}\int_0^{\infty} \frac{\exp(-rt)\ \sin(\sqrt{r})\ dr}{[\,K^2 - 2K\,r\cos(\sqrt{r}) + r^2\,]\,r} = \frac{-I_{BR}}{2\pi j} \qquad (7.6.2)$$

Expanding sin ($\sqrt{r}$) and cos ($\sqrt{r}$) and dividing the resultant polynomial fraction yields

$$c(t)_{Irr} = \frac{K}{\pi}\int_0^{\infty} \left[\frac{r^{1/2}}{K^2} + \frac{(12-K)\,r^{3/2}}{6K^3} + \frac{(K^2-160K+360)r^{5/2}}{120K^4} + \cdots\right] e^{-rt}dr \qquad (7.6.3)$$

Taking the Laplace transform of each term yields

$$c(t;K)_{Irr} = \frac{K}{\pi}\left[\frac{\Gamma(3/2)}{K^2\,t^{3/2}} + \frac{\Gamma(5/2)\,(12-K)}{6K^3\ t^{5/2}} + \frac{\Gamma(7/2)\,(K^2-160K+360)}{K^4\ 120\ t^{7/2}} + \cdots\right] \qquad (7.6.4)$$

where $\Gamma(n) = (n-1)\ \Gamma(n-1)$ and $\Gamma(1/2) = 1.722$

thus for K=1, and $t=T_p = 5.2$, (7.6.4) becomes

$$c(5.2;1)_{Irr} = \frac{1}{\pi}\ (0.073 + 0.040 + 0.017) = +0.041 \qquad (7.6.5)$$

The value of $c(t)_{Irr}$ in (7.6.5) accounts for most of the error in evaluating M in Section 7.5. Thus correcting the values of M computed in table for K=1 yields values of M of 0.104, 0.121 and 0.111 for the three different approximate methods compared to the exact value of 0.110 thereby reducing the error in M substantially.

7.7 Conclusions and Discussion

The transient response for a feedback system with a distributed parameter element can be thought of consisting of the sum of two types of terms; a rational function and an irrational integral function. This response can be approximated for values of time equal to or greater than the time to peak, T_p, by neglecting the irrational integral term. The transient response for these types of systems can therefore consist of evaluation of residues in much the same manner as lumped constant systems.

The geometric method developed by Chu [24] for lumped constant systems has been extended to systems with distributed lag through the use of a transformation in which the complex s-plane

is mapped into a complex w-plane. The extension of the geometric method can be used to determine transient response parameters T_p and M although results obtained are not as accurate as those obtained through the additional evaluation of the rational portion of the transient response equation.

The curves of Figure 7.4.1 in which the location of the dominant root in the s-plane is related to transient response parameters T_p, M, and T_s, can be used to yield an accurate approximation of T_p. However, larger errors result in determining the overshoot parameter, M. There is however a large systematic component in this error because the approximation for M is based upon the use of the approximate value of T_p. Since approximate values T_p tend to be higher than the actual values, approximate values of M in Figure 7.4.1 tend to be lower than actual values. More accurate values of M can be obtained through evaluation of the irrational integral term at $t=T_p$.

CHAPTER 8

CONCLUSIONS

A method has been presented for the determination of absolute and relative stability as well as s-plane root locations of linear time invariant feedback systems containing distributed parameter elements. This method represents an extension of par ameter plane techniques as developed by Vishnegradski [120], Neimark [72], Mitrovic [69], Siljak [99], and Eisenberg [29]. Results are presented in terms of two variable system parameters as opposed to conventional techniques (such as root locus, Nyquist , and Bode diagrams) which can treat stability with respect to at most only one variable system parameter. Although development of the method is accomplished utilizing the uniform transmission line model, the method is general and can be applied to other types of distributed parameter elements. The investigation of stability is not any more complex for multi-loop feedback systems than for single loop systems because the closed loop system transfer function is utilized in parameter plane. Furthermore, the technique is well suited for solution utilizing a digital computer and higher order systems can be treated with practically the same ease as low -order systems. The method includes treatment of multi-valued functions of the complex variable s , branch points , and branch cuts as well as Riemann surfaces. In addition, a theorem is derived

by which the number of real roots (and their values) can be determined for a system with specified parameters (α_1, β_1) in the parameter plane.

The parameter plane is applied to a hypothetical class of transfer functions of the form

$$F_D(s) = \exp(-(sT)^{p/q})$$

where p and q are integers and p is less than q. This method uses a complex transformation which maps a function from the s-plane to a w-plane in which the function is single valued. Parameter plane techniques are then introduced in order to determine absolute and relative stability.

The parameter plane is then applied to control systems in which an auxiliary predictor loop is added around the conventional controller. This predictor loop is designed to cancel the effects of the distributed parameter element in the plant. The problem of a system with distributed lag is considered and since a distributed lag element is difficult to synthesize, the predictor loop utilizes a rational polynomial approximation for this element. The application of the parameter plane here presents the designer with a method

of determining the optimum polynomial approximant to use in order to achieve a system which will remain stable with variations of two system parameters (such as system gain and reset time) and retain practically the same transient response as the uncompensated system.

The parameter plane is also applied in order to place roots of the system characteristic equation in s-plane locations so that a desired transient response can be achieved. Transient response characteristics such as time to first peak, T_p, first peak overshoot, M, and settling time, T_s, are related to s-plane locations of "dominant roots" for systems with distributed lag. Several different techniques are developed and compared. A set of curves is presented which relate T_p, M, and T_s to s-plane locations of the dominant root in systems with distributed lag. These curves can then serve as a tool in the design of systems with distributed lag when transient response is specified.

CHAPTER 9

SUGGESTIONS FOR FUTURE INVESTIGATION

The theory and techniques developed in this dissertation can be applied in a number of areas. Specifically, application of the parameter plane theory to systems in which the distributed parameter element has a transfer function other than the uniform transmission line would provide insight into their behavior. These types of systems are often formulated as models of biological elements and processes and the response of these systems when two or more parameters are varied simultaneously would be of value. The approach here would be to first develop the expressions for $-\psi$ and δ, then determine the manner in which branch points of the function effect the partitioning of the s- plane, and finally map s- plane contours into the $\alpha - \beta$ plane.

There are many instances in the design of systems where the sensitivity of the system to parameter variations is of concern. The generalized Mitrovic method was applied to the sensitivity problem by Kokotovic [52] and real and complex root sensitivities were defined. These definitions can be applied to systems with distributed parameters. If for example:

$$F(s) = \sum_{k=0}^{n} a_k s^k = 0$$

and

$$a_k = \alpha (b_k + c_k e^{\gamma d}) + \beta (d_k + e_k e^{\gamma d}) + f_k + g_k e^{\gamma d}$$

where

$$\gamma = \sqrt{(Ls + R)(Cs + G)} \qquad ; d \text{ is a unit of length}$$

The coefficients a_k are therefore a function of line parameters L , C, R, G, and d and the various sensitivities of roots of $F(s) = 0$ with respect to variations in these parameters can be found.

Other extensions of the parameter plane technique to systems with distributed parameter elements include :

- Systems in which parameters α and β occur non-linearly as products in the expression for the coefficient a_k. That is, the coefficients are expressed by :

$$a_k = \alpha b_k + \alpha c_k e^{\gamma(s)d} + \beta d_k + \beta e_k e^{\gamma(s)d} + f_k + g_k e^{\gamma(s)d} + \alpha \beta h_k e^{\gamma(s)d} + \alpha \beta i_k e^{\gamma(s)d}$$

- To systems in which the distributed parameter element is terminated in an arbitrary load impedance.
- To systems which contain more than one type of distributed parameter element . An example of such a system is one which contains both transport and distributed lag.

Another area of interest is the determination of the transient response of feedback systems containing an element belonging to the hypothetical class of functions discussed in Chapter 5. The author has begun further work in this area. For example, curves

of constant T_p/T and M in the sT-plane have been derived for various ratios of p/q assuming the effect of a dominant root pair only. (see Chapter 7, Section 4 for a description of the method). Some of these curves are shown in Figures 9.1 and 9.2 . However, the resultant error in determining transient response characteristics compared with the exact method has to be determined.

The concept of approximating the closed loop response of an unknown system by choosing a model in which the open loop response of the system is approximated by a specific of the class of functions discussed in Chapter 5 is one worthy of investigation. The equations for the open loop response of this class of functions can be developed and specific responses obtained by numerical integration using a computer. The question of how errors between the measured open loop response and the open loop response of the model chosen effect the closed loop response of the system is of interest here.

Finally, in the determination of the transient response of systems containing a transmission line type of distributed parameter element further work should be done in :

- attempting to identify and isolate systematic errors.
- developing iterative techniques for obtaining the transient response parameters from the location of the dominant roots
- developing techniques for determining the bounds of the irrational integral term in the transient response equation.

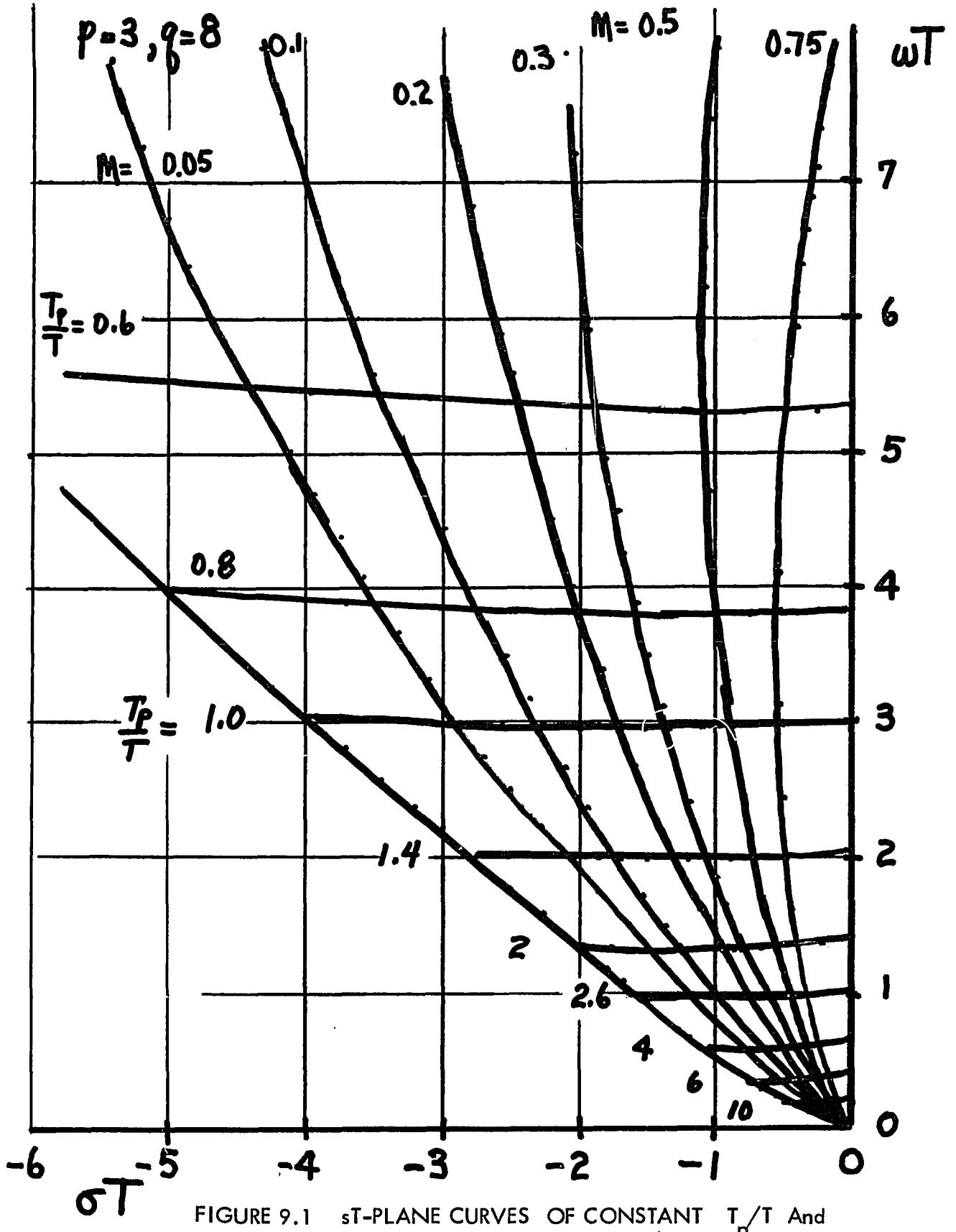

FIGURE 9.1 sT-PLANE CURVES OF CONSTANT T_p/T And M For SYSTEM With ELEMENT $\exp(-(sT)^{3/8})$

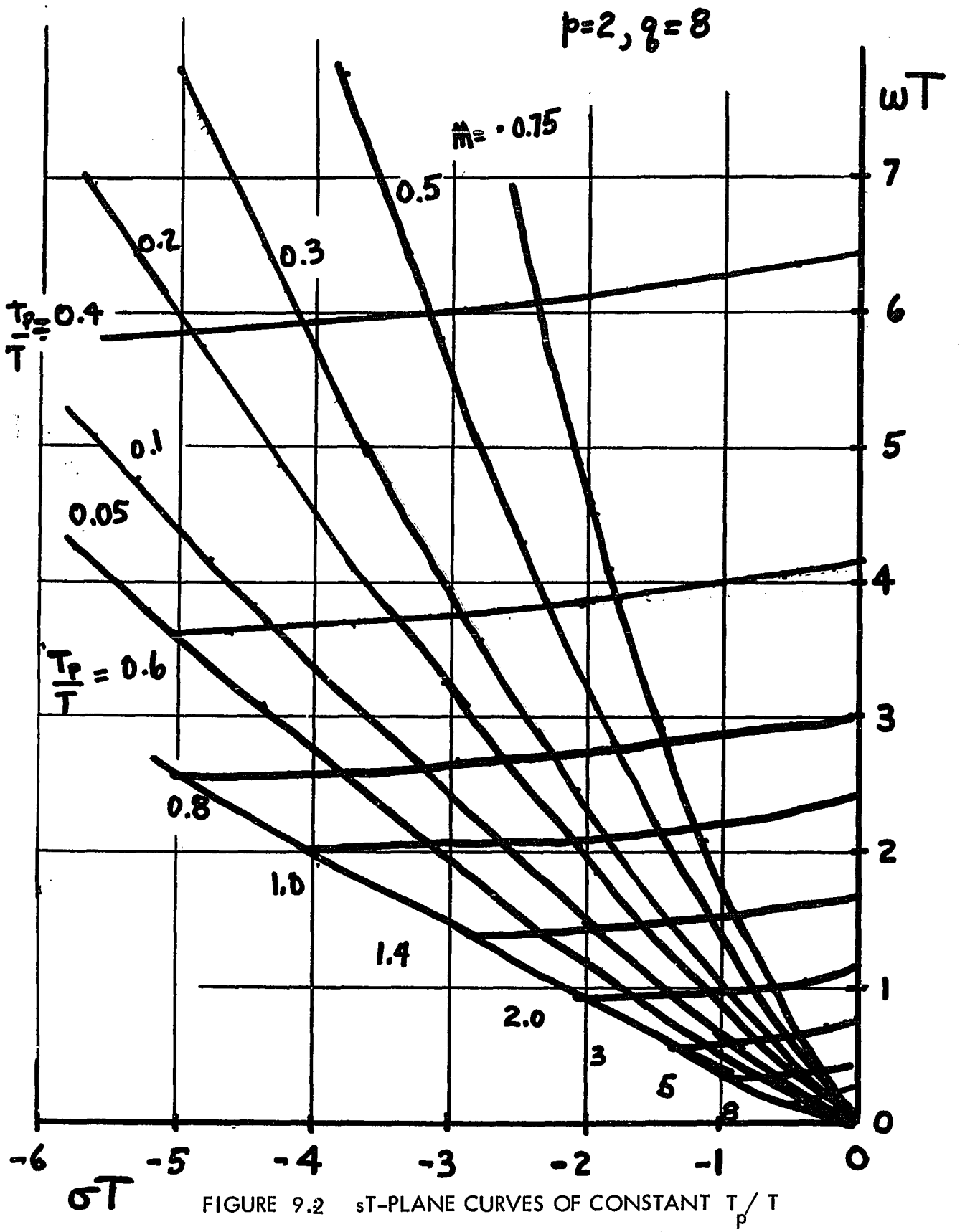

FIGURE 9.2 sT-PLANE CURVES OF CONSTANT T_p/T And M For SYSTEM With ELEMENT $\exp(-(sT)^{2/8})$

APPENDIX I

CONSIDERATION OF INITIAL CONDITIONS IN DISTRIBUTED PARAMETER SYSTEMS

Given a uniform RLGC tramsmission line, the voltage along the line, $v(x,t)$, is expressible in a partial differential equation of the form

$$\frac{\partial^2 v(x,t)}{\partial x^2} = LC \frac{\partial^2 v(x,t)}{\partial t^2} + (RC + LG)\frac{\partial v(x,t)}{\partial t} + RG\, v(x,t) \qquad (I.1)$$

If the initial conditions on the line are defined as $v(x, 0+)$ and $\dot{v}(x, 0+)$ respectively, the Laplace transform of the time variable of (I. 1) isgiven by the ordinary differential equation

$$\frac{d^2V(x,s)}{dx^2} = s^2 LCV(x,s) - sLC\, v(x,0+) - \frac{LC\, dv(x,0+)}{dt}$$

$$+s(RC+LG)\, V(x,\, s) - (RG+LG)v\,(x,0+) + RG\, V(x,s) \qquad (I.2)$$

Upon combining terms (I. 2) can be expressed as

$$\frac{d^2V(x,s)}{dx^2} - W(s)\, V(x,s) = -U(s)\, v(x,0+) - \frac{LC\, dv(x,0+)}{dt} \qquad (I.3)$$

where

$$W(s) = s^2 LC + s(RC + LG) + RG$$

and

$$U(s) = s\, LC + (RC + LG)$$

Since (I. 3) is a second order linear differential equation in x, its solution can be written as the sum of the complementary and particular

solutions. That is

$$V(x,s) = V(x,s)_c + V(x,s)_p \tag{I.4}$$

where the complementary solution is obtained by considering (I.3) with the right half portion set equal to zero. Thus

$$V(x,s)_c = A \exp(-\sqrt{W(s)}\,x) + B \exp(+\sqrt{W(s)}\,x) \tag{I.5}$$

and the particular solution is

$$V(x,s)_p = F_p(x,s) \tag{I.6}$$

that is, some function of x and s defined by the initial conditions on the line at t=0 and consideration of the right hand portion of equation (I.3). If the line is assumed to be terminated in its characteristic impedance, B=0 and (I.4) becomes

$$V(x,s) = A \exp(-\sqrt{W(s)}\,x) + F_p(x,s) \tag{I.7}$$

If the source voltage is defined, the boundary condition V(0, s) is specified and evaluation of (I.7) at x=0 yields

$$V(0,s) = A + F_p(0,s) \tag{I.8}$$

Thus

$$A = V(0,s) - F_p(0,s) \tag{I.9}$$

and (I.7) can be rewritten as

$$V(x,s) = [\,V(0,s) - F_p(0,s)\,] \exp(-\sqrt{W}\,x) + F_p(x,s) \tag{I.10}$$

where the functional dependence of W on s is understood and has been omitted. The output voltage at the termination (i.e. x=d) is

$$V(d,s) = [\,V(0,s) - F_p(0,s)\,] \exp(-\sqrt{W}\,d) + F_p(d,s) \tag{I.11}$$

Equation (I. 11) can be represented at t=0 by the transfer function diagram of Figure I.1 . Once initial conditions $v(x, 0+)$ and $\frac{dv(x, 0+)}{dt}$ are specified, $F_p(x, s)$ can be evaluated by one of a number of methods (i.e. undetermined coefficients, variation of parameters).

Consider the system diagram of Figure I.2 in which the distributed parameter is combined with lumped constant elements. Assuming the initial conditions of the lumped elements are zero, the transform of the closed -loop response at t=0 is

$$C(s) = \frac{F_p(d, s) - F_p(0, s) \exp(-\psi d) + R(s)H(s) \exp(-\psi d)}{(1 + H(s) \exp(-\gamma d))} \qquad (I.12)$$

Equation (I. 12) consists of three terms; the first two terms are due to initial conditions associated with the distributed parameter element and the third term is due to the system when all initial conditions are zero. Equation (I. 12) is not necessarily stable if the transform

$$C(s)_o = \frac{R(s) H(s) \exp(-\gamma d)}{1 + H(s) \exp(-\gamma d)} \qquad (I.13)$$

does not contain any singularities in the right portion of the principal branch of the s-plane because the functions due to initial conditions appear to be arbitrary. However, if the following is assumed;

1. The impulse response of (I. 13) is bounded

   (i.e. $\lim_{t \to \infty} c(t) = 0$)

2. The only means of producing functions $F_p(d, s)$ and

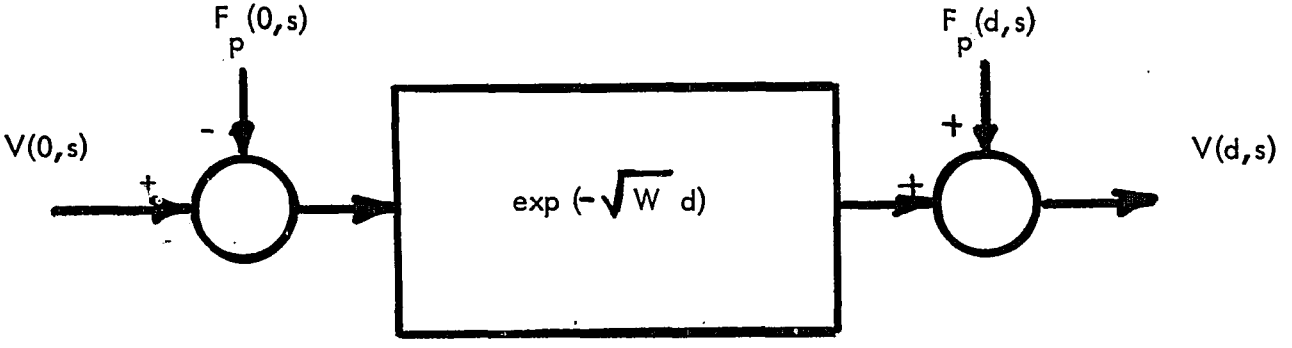

FIGURE 1.1 TRANSFER FUNCTION DIAGRAM AT t=0 SHOWING DISTRIBUTED PARAMETER AND INITIAL CONDITIONS

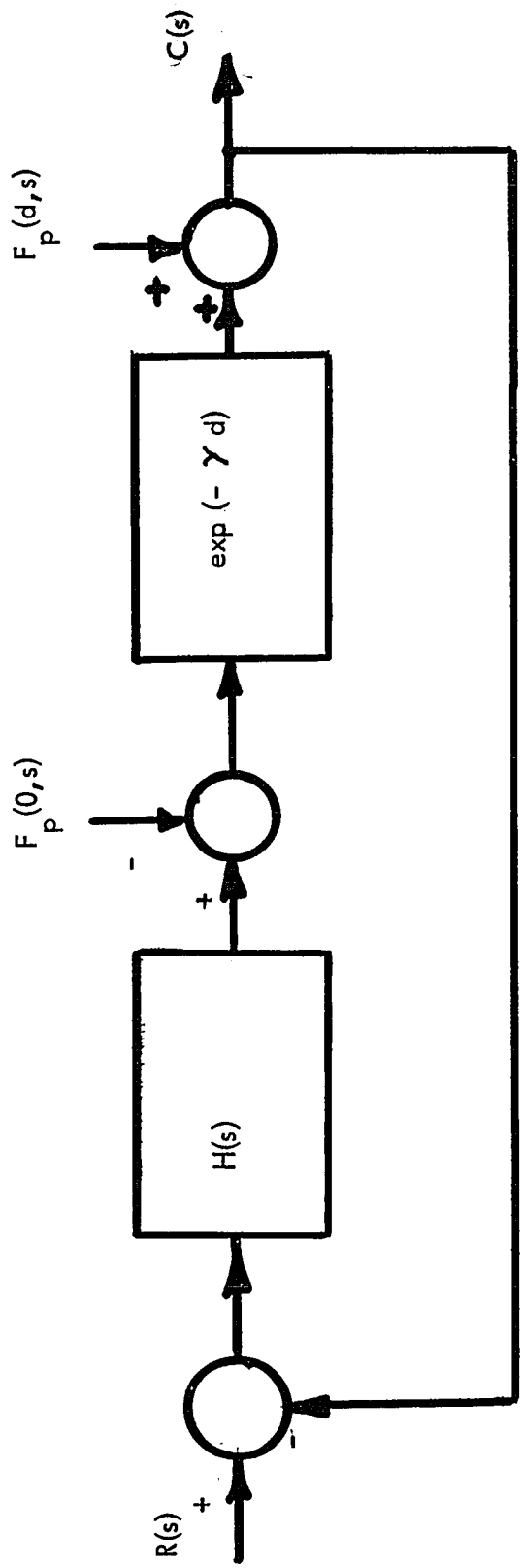

FIGURE I. 2 SYSTEM DIAGRAM AT t=0 SHOWING LUMPED ELEMENTS AND A DISTRIBUTED ELEMENT WITH ITS INITIAL CONDITIONS

$F_p(0, s)$ is through excitation applied to the input terminals of the distributed parameter element at some time previous to t=0.

3. This excitation function $v(0, t)$ is bounded (i. e. $v(0, t) = 0$ as t approaches zero with $-\infty \leqq t \leqq 0$).

then the initial condition functions $F_p(d, s)$ and $F_p(0, s)$ are constrained such that a stable system results. This is because an observer at time $t=t_1 \geq 0$ cannot distinguish whether the state of the system is due to a system with initial conditions $v(x, 0+)$ and $\frac{dv(x, 0+)}{dt}$ coupled with an input $c_1(t)$ or a system with zero initial conditions and an input $c(t) = c_0(t) + c_1(t)$ where $c_0(t)$ alone would produce the aforementioned initial conditions at t=0.

APPENDIX II

CONSTRUCTION OF $\alpha - \beta$ CONTOURS FOR $\omega_n < 0$

The objective is to prove that it is only necessary to compute values of α, β for $\omega_n > 0$ when considering an s-plane contour which is symmetrical with respect to the real axis.

This can be proven by referring to equations (4.2.12) and noting that the equations for B_1, C_1, and D_1 remain unchanged and equations B_2, C_2, and D_2 change sign when the signs of variables ω_n, ζ and δ are reversed.

Now Figure 4.3.2a illustrates the s-plane as consisting of three pairs of symmetrical regions separated by the real axis. These pairs are B and C, A_L and D_L, A_R and D_R. The signs of variables ψ_n, ζ, δ and $-\psi$ associated with each of these regions are summarized below. The signs of ω_n and ζ are obtained from Figure 4.2.2 and the signs of δ and $-\psi$ are obtained from Table 4.3.1.

Variable	Symmetrical Pair B	C	Symmetrical Pair A_L	D_L	Symmetrical Pair A_R	D_R
ω_n	+	-	+	-	+	-
ζ	+	-	+	-	-	+
δ	+	-	+	-	+	-
ψ	-	-	+	+	+	+

Since the signs of ω_n, ζ and δ change and the sign of $-\psi$ remains unchanged for symmetrical points in the lower half plane

$$B_1(-\omega_n) = B_1(\omega_n)$$
$$C_1(-\omega_n) = C_1(\omega_n)$$
$$D_1(-\omega_n) = D_1(\omega_n)$$
$$B_2(-\omega_n) = -B_2(\omega_n)$$
$$C_2(-\omega_n) = -C_2(\omega_n)$$
$$D_2(-\omega_n) = -D_2(\omega_n)$$

Therefore for $\omega_n < 0$ substitution into (4.2.13) gives

$$\alpha(-\omega_n) = \alpha(\omega_n),\ \beta(-\omega_n) = \beta(\omega_n),\ \Delta(-\omega_n) = -\Delta(\omega_n)$$

Thus, when traversing contours in the s-plane for values of $\omega_n < 0$, the sign of Δ changes but the values of α and β are the same. It follows that the $\alpha - \beta$ curve for $\omega_n < 0$, $\zeta < 0$ falls directly over the curve obtained for $\omega_n > 0$, $\zeta > 0$ and is shaded on the same side. The result is a doubly shaded curve.

APPENDIX III

DERIVATION OF THE LIMIT FUNCTION $F_1 (\zeta = 1)$

It is required that the limit be found for the function

$$F_1 (\zeta = 1) = F_1 (1) = \lim_{\zeta \to 1} \frac{\sin \delta}{(1 - \zeta^2)^{1/2}} \qquad \text{(III. 1)}$$

where δ is defined by (4. 3. 17).

Since $\delta = 0$ and $\zeta = 1$ along segment 1 of Figure 4. 7. 1, equation (III. 1) is indeterminate when taken to the limit. Applying L'Hospital's rule to (III. 1) gives

$$F_1 (1) = - \lim_{\zeta \to 1} \frac{d\delta}{d\zeta} (1 - \zeta^2)^{1/2} \qquad \text{(III. 2)}$$

The derivative function of (III. 2) can be found by differentiating the function δ in (4. 3. 17) with respect to the variable ζ. This gives

$$\frac{d\delta}{d\zeta} = \frac{A(\zeta)}{\delta} \qquad \text{(III. 3)}$$

where for segment 1

$$A_1(1) = - \frac{d^2 \omega_n^2 [\, 2 \omega_n L C - (RC + LG)\,]^2}{4 (\omega_n L - R)(\omega_n C - G)} \qquad \text{(III. 4)}$$

Thus (III. 2) can be rewritten as

$$F_1(1) = - A_1(1) \lim_{\zeta \to 1} \frac{(1 - \zeta^2)^{1/2}}{\delta} = - A_1(1)\ N_1(1) \qquad \text{(III. 5)}$$

Equation (III. 5) is also indeterminate when taken to the limit. Thus applying L'Hospitals rule again gives

$$F_1(1) = A_1(1) \lim_{\zeta \to 1} \frac{1}{(1 - \zeta^2)^{1/2} \frac{d\delta}{d\zeta}} \tag{III. 6}$$

which by virtue of (III. 3) is

$$F_1(1) = \lim_{\zeta \to 1} \frac{\delta}{(1 - \zeta^2)^{1/2}} = \frac{1}{N_1(1)} \tag{III. 7}$$

Substituting (III. 7) into (III. 5) and noting that (RC + LG) is greater than $2\omega_n LC$ on segment 1 gives

$$F_1(1) = (-A_1)^{1/2} = \frac{d\omega_n (RC + LG - 2\omega_n LC)}{2[(\omega_n L - R)(\omega_n C - G)]^{1/2}} \tag{III. 8}$$

Equation (III. 8) is valid for segment 1 of the negative real axis. Along segment 2, the limit function can be shown to be

$$F_2(1) = \frac{d\omega_n (2\omega_n LC - (RC + LG))}{2[(\omega_n L - R)(\omega_n C - G)]^{1/2}} \tag{III. 9}$$

since $2\omega_n LC$ is greater than (RC + LG) along this segment. However, along segment 3, δ is not, in general, equal to zero and thus the limit of (III. 1) does not apply.

When $\zeta = -1$ (i.e., along the positive real axis) a similar development to the one used above will show

$$F_4(\zeta = -1) = F_4(-1) = \frac{d\,\omega_n\,(2\,\omega_n\,LC + RC + LG)}{2\,[\,(\omega_n L + R)(\omega_n C + G)\,]^{1/2}} \qquad \text{(III.10)}$$

APPENDIX IV

PROOF OF THEOREM FOR DETERMINING REAL ROOTS

A theorem will be proven which states that the number of negative real roots of the characteristic equation $F(s) = 0$ for a system with a distributed parameter element with transfer function

$$F_D(s) = \exp (- \gamma (s) d)$$

is equal to the number of straight lines drawn through a working point $M(\alpha_1, \beta_1)$ that are tangent to certain portions of the $\zeta = 1$ curve. Also, the values of these roots are equal to the negative of the frequencies $\omega_{n1}, \omega_{n2}, \ldots\ldots \omega_{nk}$ noted on this curve.

The validity of this theorem will be examined for values of the negative real roots on each of the three line segments of Figure 4.7.1. Along segment 1, the real root equation is

$$F(\sigma) = \sum_{k=0}^{n} a_k(\sigma)\, \sigma^k = 0 \qquad \text{(IV.1)}$$

where σ takes on negative values in the range $-a < \sigma \leq 0$. Substituting equation (4.2.6), Chapter 4 into (IV.1) above gives (4.7.2) repeated below

$$\alpha \sum_{k=0}^{n} \sigma^k (b_k + c_k e^{\gamma d}) + \beta \sum_{k=0}^{n} \sigma^k (d_k + e_k e^{\gamma d}) + \sum_{k=0}^{n} \sigma^k (f_k + g_k e^{\gamma d}) = 0 \qquad \text{(IV.2)}$$

where

$$\gamma(\sigma) = [(L\sigma + R) (C\sigma + G)]^{1/2} \qquad \text{(IV.3)}$$

The value of $\gamma(\sigma)$ will be real and positive along segment 1 and thus equation (IV.2) will only contain real terms . Thus for a given value of σ on segment 1 (IV.2) represents a straight line in the α - β plane. For a given working point $M(\alpha_1, \beta_1)$ in the α -β plane, every value of σ that satisfies (IV.2) is a real root of the characteristic equation. Therefore, if the slope of the ζ=1 curve is the same as the slope of (IV.2) , the value of the slope of the ζ=1 curve where it is tangent to (IV.2) is also a real root of $F(s) = 0$ at the operating point $M(\alpha_1, \beta_1)$.

To prove this consider the slope of (IV.2) at the point $\alpha = \alpha_1, \beta = \beta_1$

$$\frac{d\beta}{d\alpha} = - \frac{\sum_{k=0}^{n} \sigma^k (b_k + c_k \exp (\gamma(\sigma)d)}{\sum_{k=0}^{n} \sigma^k (d_k + e_k \exp(\gamma(\sigma)d)} \qquad \text{(IV.4)}$$

Now consider equation (4.5.11) Chapter 4 and determine $\frac{d\beta}{d\alpha}$ when ζ =+1. Note that when ζ =+1

$$s = - \omega_n = \sigma \qquad \text{(IV.5)}$$

or the real root value of σ equals the negative of the frequency. Therefore, the theorem will be proven for segment 1 if the tangent at any point on the α - β curve for ζ=+1 between $0 \leqq \omega_n \leqq$ a is identical to the straight line obtained when mapping this segment of the negative real axis. The expression for this tangent to the α - β curve for ζ=+1 is found by determining the derivative $\frac{d\beta}{d\alpha}$ of equations (4.2.13).

Performing this operation gives

$$\frac{d\beta}{d\alpha} = \frac{d\beta / d\omega_n}{d\alpha / d\omega_n} = \frac{N'_2 J - N_2 J'}{N'_1 J - N_1 J'} \qquad \text{(IV. 6)}$$

where

$$N_2 = D_1 B_2 - D_2 B_1$$

$$N_1 = C_1 D_2 - C_2 D_1$$

$$J = B_1 C_2 - B_2 C_1$$

The prime denotes differentiation with respect to ω_n and the functions B_1, C_1, D_1, B_2, C_2, and D_2 are defined by equations (4. 2. 12).

Performing the indicated operations of (IV. 6) produces a sixteen term expression with each term consisting of the product of four functions in both the numerator and denominator.

However, considering (IV. 6) when $\zeta = 1$ and assuming initially that values of ω_n will be restricted to segment 1 produces

$$\frac{d\beta_1}{d\alpha_1} = \frac{N'_{2,1} J_1 - N_{2,1} J'_1}{N'_{1,1} J_1 - N_{1,1} J'_1} \qquad \text{(IV. 7)}$$

where

$$N_{2,1} = D_{1,1}\,\overline{B_{2,1}} - \overline{D_{2,1}}\,B_{1,1}$$

$$N_{1,1} = C_{1,1}\,\overline{D_{2,1}} - \overline{C_{2,1}}\,D_{1,1}$$

$$J_1 = B_{1,1}\,\overline{C_{2,1}} - \overline{B_{2,1}}\,C_{1,1}$$

the prime denotes differentiation with respect to ω_n and the functions $B_{1,1}$, $C_{1,1}$, $D_{1,1}$, $\overline{B_{2,1}}$, $\overline{C_{2,1}}$, and $\overline{D_{2,1}}$ are defined by equations (4.5.5) and (4.5.10).

Consider the function $B_{1,1}$ of (4.5.5). Differentiating with respect to ω_n gives

$$B'_{1,1} = \sum_{k=0}^{n} -k(-\omega_n)^{k-1}\,[b_k + c_k \exp(-\psi_1)] - (-\omega_n)^k c_k \exp(-\psi_1)\,\psi'_1 \qquad \text{(IV. 8)}$$

where ψ'_1 for a uniform transmission line is obtained by differentiating (4.5.2) and is given by

$$\psi'_1 = \frac{d\psi_1}{d\omega_n} = \frac{d[LG+RC-2\,\omega_n LC]}{2\,[(R-\omega_n L)(G-\omega_n C)]^{1/2}} \qquad \text{(IV. 9)}$$

Also considering $\overline{B_{2,1}}$ from (4.5.10)

$$\overline{B_{2,1}} = \sum_{k=0}^{n} -k(-\omega_n)^k [b_k + c_k \exp(-\psi_1)] + (-\omega_n)^k c_k \exp(-\psi_1)\,F_1(1)$$

(IV. 10)

whereby (4.5.9)

$$F_1(1) = \frac{\omega_n \, d[LG+RC-2\,\omega_n LC\,]}{2\,[(R-\omega_n L)(G-\omega_n C)\,]^{1/2}} = \omega_n \, d\,\psi_1 / d\,\omega_n \qquad \text{(IV.11)}$$

Thus if the relationship of (IV.11) holds, upon comparing (IV. 8) and (IV.10) it can be shown that

$$-\omega_n \, B'_{1,1} = \overline{B_{2,1}} \qquad \text{(IV.12)}$$

Similarly for segment 1 it can also be shown that

$$\begin{aligned} -\omega_n \, C'_{1,1} &= \overline{C_{2,1}} \\ -\omega_n \, D'_{1,1} &= \overline{D_{2,1}} \end{aligned} \qquad \text{(IV.13)}$$

Returning to (IV.7), performing the indicated operations and substituting the identities (IV.12) and (IV.13) yields after considerable manipulation

$$\frac{d\beta_1}{d\alpha_1} \, (\xi=1) = \frac{-B_{1,1}}{C_{1,1}} \qquad \text{(IV.14)}$$

A similar argument can be used to show that (IV.14) also holds for segment 2 as well as for the positive real axis ($\xi = -1$). That is

$$\frac{d\beta_2}{d\alpha_2} \, (\xi=1) = \frac{-B_{1,2}}{C_{1,2}} \text{ , and } \frac{d\beta}{d\alpha} (\xi=-1) = \frac{-B_1}{C_1} \, (\xi=-1) \qquad \text{(IV.15)}$$

Substituting equations (4.5.5) into (IV.14) yields

$$\frac{d\beta}{d\alpha}(\omega_n, \zeta=1) = -\frac{\sum_{k=0}^{n}(-\omega_n)^k(b_k + c_k \exp(-\psi_1))}{\sum_{k=0}^{n}(-\omega_n)^k(d_k + e_k \exp(-\psi_1))} \qquad \text{(IV.16)}$$

where $-\psi_1$ by (4.5.2) is

$$-\psi_1 = d[(R - \omega_n L)(G - \omega_n C)]^{1/2} \qquad \text{(IV.17)}$$

By virtue of(IV.5) substituting into (IV.16) and into (IV.17) gives

$$\frac{d\beta}{d\alpha}(\omega_n = -\sigma, \zeta=1) = \frac{d\beta_1}{d\alpha_1} \qquad \text{(IV.18)}$$

and

$$-\psi_1(\omega_n = -\sigma) = \gamma(\sigma) \qquad \text{(IV.19)}$$

Thus the slope at any point ω_{n1} (where $0 \leqq \omega_{n1} \leqq a$) on the $\alpha-\beta$ plane curve for $\zeta=+1$ is equal to the slope obtained when mapping segment 1 of the negative real axis at the point $\sigma_1 = -\omega_{n1}$. A similar argument can be used to show that the theorem also holds along segment 2 of the negative real axis.

Values of sigma along segment 3 produce imaginary values of the distributed parameter variable gamma. Thus equation (IV.2) is no longer purely real and is expressed by

$$\alpha\sum_{k=0}^{n}\sigma^k(b_k + c_k\cos\gamma) + \beta\sum_{k=0}^{n}\sigma^k(d_k + e_k\cos\gamma) + \sum_{k=0}^{n}\sigma^k(f_k + g_k\cos\gamma) + j[\alpha\sum_{k=0}^{n}\sigma^k c_k + \beta\sum_{k=0}^{n}\sigma^k e_k + \sum_{k=0}^{n}\sigma^k g_k]\sin\gamma \qquad \text{(IV.20)}$$

where

$$Y(\sigma) = d\left[\ \left|(L\sigma+R)(C\sigma+G)\right|\ \right]^{1/2} \qquad \text{(IV.21)}$$

and $-b \leqq \sigma \leqq -a$. The equations for $\zeta = +1$ along segment 3 are found by by substituting equation(4.5.12) into (4.2.11). Equation (4.2.11) is given by

$$\begin{aligned} F(\omega_n, +1) = \alpha \sum_{k=0}^{n} (-\omega_n)^k [b_k + c_k \cos\delta] + \beta \sum_{k=0}^{n} (-\omega_n)^k [d_k + e_k \cos\delta] \\ + \sum_{k=0}^{n} (-\omega_n)^k [f_k + g_k \cos\delta] \quad + \quad j[\sin\delta \left(\alpha \sum_{k=0}^{n} (-\omega_n)^k c_k\right. \\ \left. + \beta \sum_{k=0}^{n} (-\omega_n)^k e_k + \sum_{k=0}^{n} (-\omega_n)^k g_k\right)] = 0 \end{aligned} \qquad \text{(IV.22)}$$

where δ is defined by (4.5.4). Since $\sigma = -\omega_n$ along the negative real axis

$$\delta(-\omega_n) \quad = \quad Y(\sigma) \qquad \text{(IV.23)}$$

and thus comparing (IV.20) with (IV.22) yields

$$\begin{aligned} F(\sigma)_{real} &= F(\omega_n, \zeta = 1)_{real} \\ F(\sigma)_{imag} &= F(\omega_n, \zeta = 1)_{imag} \end{aligned} \qquad \text{(IV.24)}$$

Thus for segment 3, the $\alpha - \beta$ equations for the $\zeta = 1$ and the $F(\sigma)$ curve are identical and the theorem does not apply . Reasoning similar to that employed in proving the theorem for segments 1 and 2 can be used to show that the number of positive real, roots of the characteristic equation at working point $M(\alpha_1, \beta_1)$ can be established by determining the number of tangents that can be drawn from $M(\alpha_1, \beta_1)$ to the $\zeta = -1$ curve. Furthermore, the values of these roots are equal to the value of ω_n on the $\zeta = -1$ curve at the point of tangency . If

the characteristic equation has any positive real roots on the principal sheet of the s-plane , this would indicate instability.

In summary, the number of real roots of the characteristic equation when the system parameters are specified by working point M(α_1, β_1) can be found by first determining the number of tangents that can be drawn to segments 1 and 2 of the ζ =+1 curve in the α -β plane. If the working point M(α_1, β_1) is located on segment 3 of the ζ =+1 curve then an additional negative root exists and is equal to the negative of the value of ω_n on the ζ =+1 curve. If the working point is not located on segment 3 of the ζ =+1 curve, the characteristic equation does not have any negative real roots between $-b \leqq \omega_n \leqq -a$. Positive real roots, if any, can be found by determining the number of tangent lines that can be drawn from the working point to the ζ =-1 curve,

APPENDIX V

TRANSIENT RESPONSE OF CHU'S SYSTEM WITH DISTRIBUTED LAG

Given the closed loop transfer function $\frac{C}{R}(s)$, the transient response can be obtained by first multiplying $\frac{C}{R}(s)$ by $R(s)$, by the Laplace transform of the input signal $r(t)$, and then obtaining the inverse Laplace transform of the resulting function. Therefore, for a unit step input, the transform of the output functions for Chu's problem of section 4.6, Chapter 4 is given by

$$C(s) = \frac{K(s+W)}{s(s^2 e^{\sqrt{s}} + Ks + KW)} \qquad (V.1)$$

Finding the inverse Laplace transform of (V . 1) in tables is not likely since the denominator equation is transcendental. Therefore, transformation of this function must be accomplished formally by means of the Bromwich-Wagner Integral. Thus .

$$c(t) = \frac{1}{2\pi j}\int_{\alpha-j\beta}^{\alpha+j\beta} \frac{K(s+W)e^{st}ds}{s(s^2 e^{\sqrt{s}} + Ks + KW)} \qquad (V.2)$$

This integral can be evaluated by considering the contour shown in Figure V . 1. From the figure and the fact that the closed contour does not contain any singularities.

$$c(t) = I_{AA} = \frac{1}{2\pi j}\left[I_{AB} + I_{BC} + I_{CC'} + I_{C'B'} + I_{B'A'} \right] \qquad (V.3)$$

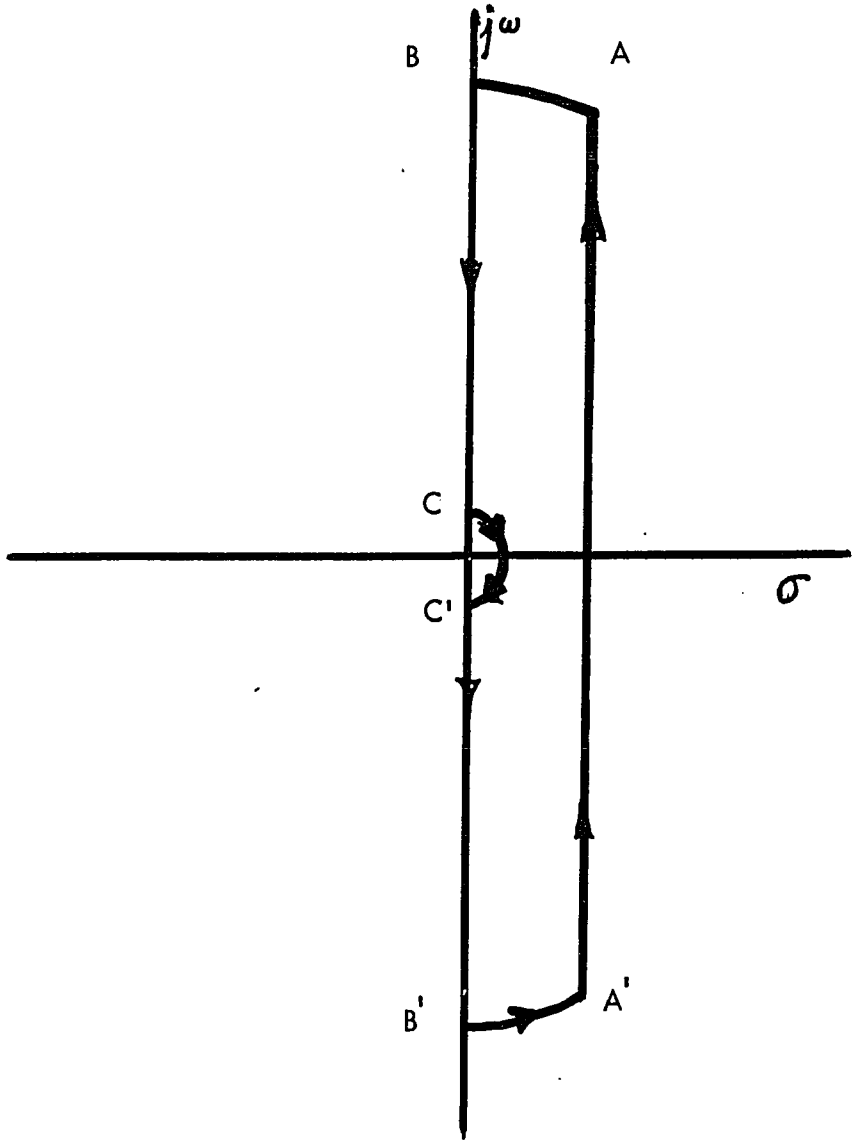

FIGURE V.1 CONTOUR OF INTEGRATION

where $I_{XY} = \int_X^Y C(s) \exp(st)\, ds$ (V.4)

Integrals I_{AB} and $I_{B'A'}$ are zero by Jordans lemma and integration around the branch point at the origin gives

$$I_{CC'} = -j\pi \tag{V.5}$$

Setting $s = r \exp(j\pi/2)$ for path BC and $s = r \exp(-j\pi/2)$ for path C'B', integrating C(s) exp(st) along each of these paths, and combining expressions yields after some manipulation

$$I_{BR} = I_{BC} + I_{C'B'}$$

$$I_{BR} = 2jK \int_0^{\infty} \frac{[r^3 e^x \cos(rt-x) + Wr^2 e^x \sin(rt-x) - K(W^2+r^2)\sin(rt)]\ dr}{[r^4 e^{2x} - 2Kr^2 e^x (r\sin x + W\cos x) + K^2(W^2+r^2)]\ r} \tag{V.6}$$

where

$$x = [r/2]^{1/2}, \qquad r = 2x^2 \tag{V.7}$$

Combining the results of (V.6) and (V.5) into (V.3) gives

$$c(t) = 1/2 - I_{BR}/2\pi j \tag{V.8}$$

Equation (V.8) was evaluated for W =0.3 and K =3.30 using an IBM 1650 computer. The response is shown in Figure V.2.

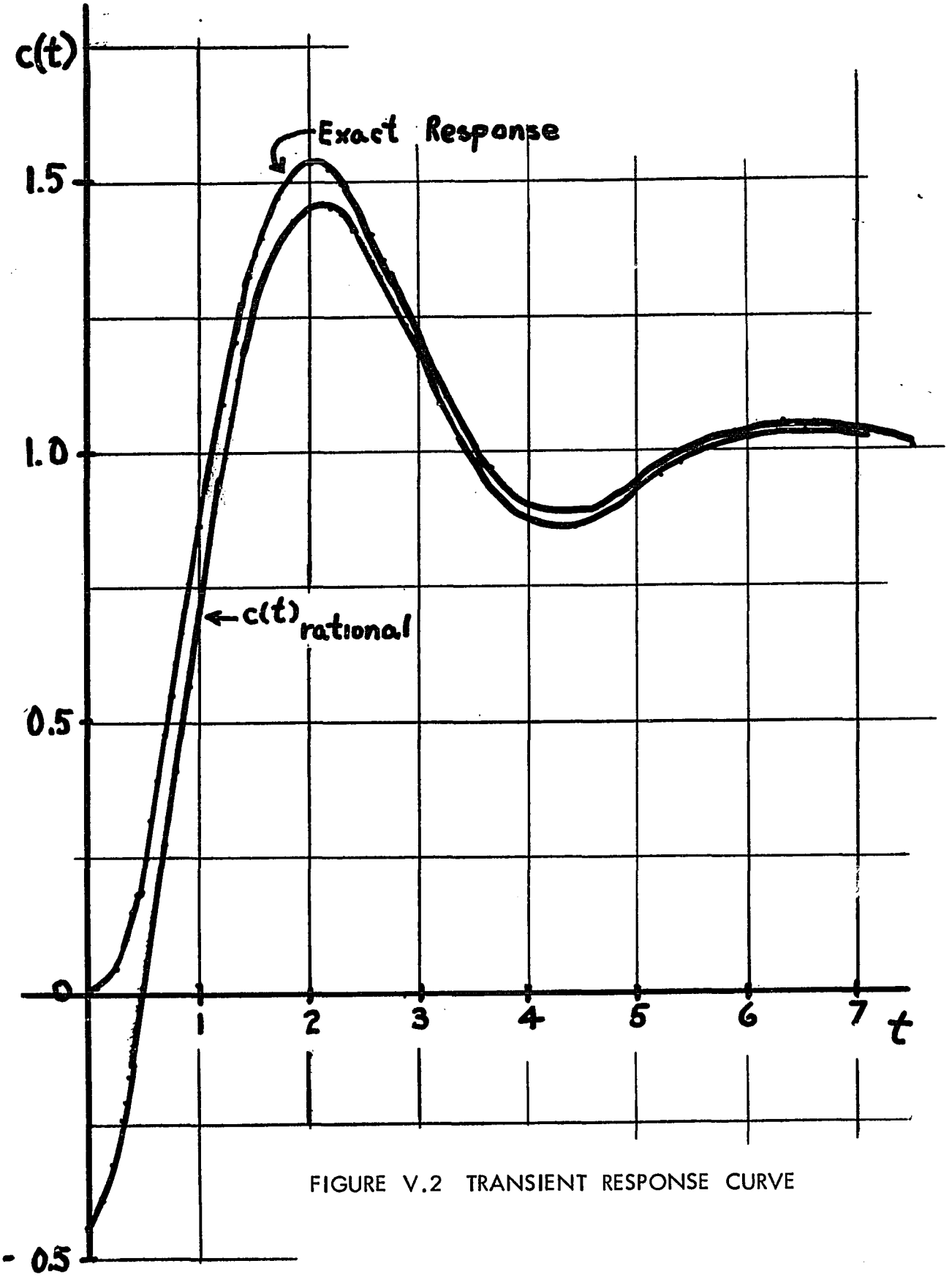

FIGURE V.2 TRANSIENT RESPONSE CURVE

APPENDIX VI

RATIONAL FRACTIONAL APPROXIMATIONS FOR DISTRIBUTED PARAMETER ELEMENTS

A method of approximating an exponential transfer function of the form

$$F_D(s) = \exp(-W(s)^{1/2}) \tag{VI.1}$$

was developed by Pierre [80] . This development was accomplished by first considering rational fractional approximations for a distributed lag

$$F_D(s) = \exp(-(sT)^{1/2}) \tag{VI.2}$$

and then extending the method to obtain approximations to (VI.1).

Consider the problem of trying to approximate the principal sheet of $\exp(-(sT)^{1/2})$ by a single valued rational function g(s). For one or more values on the principal sheet the magnitude of g(s) (since it is not a constant) differs from that of (VI.2) by an infinite amount. Furthermore, suppose that values of the complex variable s which produce an infinite difference are located on the negative real axis.

With this constraint in mind, consider the circuit of Figure VI.1 and let Z(s) and Y(s) represent the series impedance and shunt admittance per stage respectively. Also let $q = Z(s) \cdot Y(s)$ and $q_e = Z(s) \cdot Y_e(s)$.

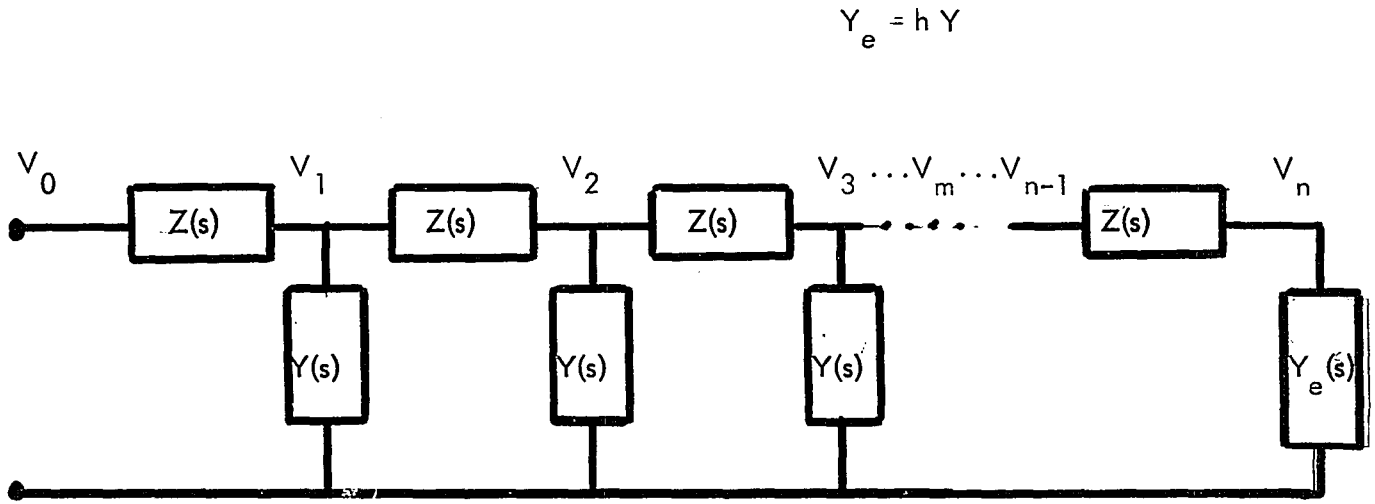

FIGURE VI.1 GENERALIZED NETWORK DIAGRAM FOR POLYNOMIAL APPROXIMANT

For a single section line (n=1) the ratio G(1, 0; 1) of $V_1(s)$ to $V_0(s)$ is

$$G(1,\ 0;\ 1) = \left.\frac{V_1(s)}{V_0(s)}\right|_{n=1} = 1 - \frac{1}{1 + (\frac{1}{q_e})} \qquad \text{(VI. 3)}$$

For n=2 the ratio of $V_1(s)$ to $V_0(s)$ is

$$\left.\frac{V_1(s)}{V_0(s)}\right|_{n=2} = G(1, 0;2) = 1 - \frac{1}{1+ \dfrac{1}{q + \dfrac{1}{1 + \dfrac{1}{q_e}}}} \qquad \text{(VI. 4)}$$

$$G\ (\ 1, 0;n\ ) = \frac{1}{q\ + 2\ - G(1, 0;1\ )}$$

For n stages the ratio $V_1(s)$ to $V_2(s)$ can be shown to be

$$\frac{V_1(s)}{V_0(s)} = G(1, 0;n\ ) = \frac{1}{q + 2\ - G\ (1, 0;n-1\ )} = \frac{B_n(q)}{P_n(\ q)}$$

or

$$G(1, 0;n\ ) = \frac{P_{n-1}(q)}{(q+2)\ P_{n-1}(q) - B_{n-1}(q)} = \frac{P_{n-1}(q)}{(q+2)\ P_{n-1}(q) - P_{n-2}(q)} = \frac{P_{n-1}(q)}{P_n(q)} \qquad \text{(VI. 5)}$$

where $P_n(q)$ is a polynomial in q.

The ratio of $V_m(s)$ to $V_0(s)$ [i. e. $G(m, 0; n)$] is also of interest In order to obtain this ratio consider two identically structured transmission lines, one having n sections and the other having n-j sections.

Also consider a point on each of these lines such that the number of sections to the right of section k-j of the n-j section line is equal to the number of sections to the right of section k of the n section line. Thus

$$\left| \frac{V_k(s)}{V_{k-1}(s)} \right|_n = \left| \frac{V_{k-j}(s)}{V_{k-j-1}(s)} \right|_{n-j} \qquad \text{(VI. 6)}$$

or

$$G(k,\ k-1\ ;\ n\ ) = G\ (\ k-j,\ k-j-1;\ \ n-j\ ) \qquad \text{(VI. 7)}$$

where $0 \leqq j < k \leqq n$

The ratio $\left| \frac{V_m(s)}{V_0(s)} \right|_{n \text{ stages}}$ can be determined. It is

$$G(\ m, 0;\ n\ ) = \frac{V_m(s)}{V_0(s)} = \left| \left(\frac{V_1}{V_0}\right)\ \left(\frac{V_2}{V_1}\right)\left(\frac{V_3}{V_2}\right)\ \left(\frac{V_4}{V_3}\right) \ldots\ldots \left(\frac{V_m}{V_{m-1}}\right) \right|_{n\text{-stages}}$$

or

$$G(m,\ 0;\ n\ ) = G(1,\ 0;\ n\ )\ G(2,\ 1;n)\ \ G(3,\ 2;n)\ \ldots\ldots G(m,\ m-1;n) \qquad \text{(VI. 8)}$$

Substituting (VI. 7) for each term of (VI. 8) gives

$$G(m, 0;n) = G(1, 0;n-)\cdot G(1, 0;\ n-1)\cdot G(1, 0;n-2)\ldots\ldots G(1, 0;n-m+1)$$

$$G(m, 0;n) = \prod_{k=0}^{m-1} G(1, 0;n-k\ ) \qquad \text{(VI. 9)}$$

Substituting (VI. 5) into (VI . 9) produces

$$G(m, 0;\ n) = P_{n-m}(q)\ /\ P_n(q) \qquad \text{(VI. 10)}$$

where the polynomial $P_n(q)$ is related to $P_{n-1}(q)$ and $P_{n-2}\ (q)$

by the recursion relationship of (VI. 5)

$$P_n(q) = (2+q)\, P_{n-1}(q) - P_{n-2}(q) \qquad \text{(VI. 11)}$$

Polynomial $P_1(q)$ to $P_7(q)$ are listed in Table VI. 1 . Evaluation of the roots of these polynomials shows that they are real and negative when $q_e = h\, q$ where h is any positive real number.

Consider now the problem of approximating the distributed lag element $\exp(- (sT)^{1/2})$ on the principal sheet by a rational function. For distributed lag $Z(s) = R$ and $Y(s) = sC$ in Figure VI. 1. If there are m stages between input and output mR and mC are respectively the interposed resistance and capacitance. For a fixed line length d as m increases R and C decrease such that the product $m^2RC=T$ remains constant. Thus

$$q = Z(s)\ Y(s) = s\, R\, C = sT/\, m^2 \qquad \text{(VI. 12)}$$

and

$$G(m, 0;n) = \frac{P_{n-m}\,(sT/\, m^2)}{P_n\ (sT/m^2)} \qquad \text{(VI. 13)}$$

As m increases toward infinity, n increases proportional to m^2 and the poles and zeros of (VI. 13) cluster on the negative real axis of the s- plane. The function $G(m, 0; m^2)$ thus approaches $\exp(-(sT)^{1/2})$ on the principal sheet of the s-plane except for points lying on the branch cut. Various rational fractional approximations for distributed lag are summarized in Table VI. 2. These approximations are the ones to be used in the predictor problem in Chapter 6.

n	P_n
1	$1 + q_e$
2	$(1+ q) + q_e(2 +q)$
3	$(1 + 3q + q^2) + q_e (3 + 4q + q^2)$
4	$(1 + 6q + 5q^2 + q^3) + q_e (4 + 10q + 6q^2 + q^3)$
5	$(1 + 10q + 15q^2 + 7q^3 + q^4) + q_e (5 + 20q + 21q^2 + 8q^3 + q^4)$
6	$(1 + 15q + 35q^2 + 28q^3 + 9q^4 + q^5) + q_e (6 + 35q + 56q^2 + 36q^3 + 10q^4 + q^5)$
7	$(1+ 21q+ 20q^2+ 84q^3+ 45q^4 + 11q^5+ q^6) + q_e (7 +56q +126q^2 +120q^3 +55q^4+12q^5+q^6)$

TABLE VI .1 POLYNOMIALS USED IN THE APPROXIMATION FOR $\exp (- W(s)^{1/2})$

TABLE VI.2 POLYNOMIAL APPROXIMATION FOR $\exp(-(sT)^{1/2})$

$$G(1,1) = \frac{1}{1 + sTh}$$

$$G(1,2) = \frac{1 + sTh}{1 + sT(2h+1) + s^2hT^2}$$

$$G(2,2) = \frac{1}{1 + sT(2h+1)/4 + s^2hT^2/16}$$

$$G(1,3) = \frac{1 + sT(2h+1) + s^2hT^2}{1 + sT(3h+3) + s^2T^2(4h+1) + s^3hT^3}$$

$$G(2,3) = \frac{1 + shT/4}{1 + sT(3h+3)/4 + s^2T^2(4h+1)/16 + s^3hT^3/64}$$

$$G(3,3) = \frac{1}{1 + sT(3h+3)/9 + s^2T^2(4h+1)/81 + s^3hT^3/729}$$

$$G(1,4) = \frac{1 + sT(3h+3) + s^2T^2(4h+1) + s^3hT^3}{1 + sT(4h+6) + s^2T^2(10h+5) + s^3T^3(6h+1) + s^4hT^4}$$

$$G(2,4) = \frac{1 + sT(2h+1)/4 + s^2hT^2/16}{1 + sT(4h+6)/4 + s^2T^2(10h+5)/16 + s^3T^3(6h+1)/64 + s^4hT^4/256}$$

$$G(3,4) = \frac{1 + sTh/9}{1 + sT(4h+6)/9 + s^2T^2(10h+5)/81 + s^3T^3(6h+1)/729 + s^4T^4h/6561}$$

$$G(4,4) = \frac{1}{1 + \frac{sT(4h+6)}{16} + \frac{s^2T^2(10h+5)}{256} + \frac{s^3T^3(6h+1)}{4096} + \frac{s^4T^4h}{65,536}}$$

Cosider the general function W(s) of (VI. 1) . If (VI. 1) is a rational function, $\exp(-W(s)^{1/2})$ can be rationally approximated by a function derived by substituting W(s) for sT in equation (VI. 13). Thus

$$G_W(m, 0;n) = \frac{P_{n-m}(W(s)/m^2)}{P_n(W(s)/m^2)} \qquad \text{(VI. 14)}$$

The region over which this approximation is valid is determined by the zeros of the approximation. To illustrate the use of (VI. 14), consider the rational approximation for $\exp(-[(s+a)(s+b)]^{1/2})$ over the half plane $s = -\frac{(a+b)}{2}$ on the principal sheet of the s-plane. Since $W = (s+a)(s+b)$, equation (VI. 14) becomes

$$G_W(m, 0;n) = \frac{P_{n-m}[(s+a)(s+b)/m^2]}{P_n[(s+a)(s+b)/m^2]} \qquad \text{(VI. 15)}$$

The zeros of the polynomials in equation (VI. 15) are on the negative real axis between $s= -a$ and $s = -b$ and on the line parallel to the imaginary axis which passes through the point $s = -(a+b)/2$.

REFERENCES

1 Adams, J.L., "An Investigation of The Effects of Time Lag Due to Long Transmission Distances upon Remote Control. Phase 1, Tracking Experiments," Technical Note D-1211, National Aeronautics and Space Administration, Dec. 1961, 16 pp.

2 Andrews, G.M., "Automatic Control With Artificial Inertia," Journal of the Aeronautical Sciences, Vol. 24, 1957, p. 306.

3 Aris, R., "The Optimal Design of Chemical Reactors" (book), Academic Press, New York, N.Y., 1961, 191 pp.

4 Atkins, W.T.J., "Theory of Time-Delay Networks," Proceedings, Institution of Electrical Engineers, Vol. 108, part B, 1961, p. 500.

5 Baker, A.N. and May, G.W., "Charge Analysis of Transistor Operation Including Delay Effects," Transactions, Professional Group on Electron Devices, Institute of Radio Engineers, Vol. ED-8, 1961, pp. 152-154.

6 Ball, B.J., "Distributed Lag in Feedback Control Systems," PhD Thesis, 1962, Texas A & M College.

7 Ball, B.J. and Rekoff, M.G., Jr., "An Analysis of the Distributed Lag" ISA Transactions, Vol. 5, No. 2, April 1966, pp. 146-155.

8 Bekey, G.A., "Mathematical Models of the Human Operator," Instruments and Control Systems, Vol. 33, 1960, pp. 1121-1123.

9 Bellman, R. and Danskin, J.M., Jr., "The Stability Theory of Differential-Difference Equations," Report P-381, The Rand Corporation, Santa Monica, Calif., 1953, 27 pp.

10 Bellman, R., "Stability Theory and Adjoint Operators for Linear Differential-Difference Equations," Transactions, American Mathematical Society, Vol. 92, 1959, pp. 470-500.

11 Bellman, R.E., Kalaba, R.E. and Lockett, J.A., "Numerical Inversion of the Laplace Transform," (Book) American Elsevier Publishing Co., Inc., New York, 1966.

12 Bittel, R.H., "A Tangential Approximation for the Analysis of Quasi-Optimal Control Systems" (M Sc. Thesis) University of Santa Clara, 1967.

13 Boxer, R. and Thaler, S., "A Simplified Method of Solving Linear and Non-Linear Systems," Proceedings, Institute of Radio Engineers, Vol. 45, 1956, pp. 89-101.

14 Brinn, I.A., "On the Stability of Certain Systems With Distributed and Lumped Parameters," Autom. Remote Control 23(7), 798-807, July, 1962.

15 Buckley, P.S., "Automatic Control of Processes With Dead Time," Automatic and Remote Control (Proceedings of the First International Congress of the IFAC, Moscow, USSR, 1960), Vol. 1, Butterworths Scientific Publications, London, England, 1961, pp. 33-40.

16 Callender, A., Hartree, D., and Porter, A., "Time Lag in a Control System," Philosophical Transactions. Royal Society of London, Vol. A235, 1936, pp. 415-444.

17 Callender, A., Hartree, D., Porter, A., and Stevenson, A.B., "Time Lag in a Control System-II," Proceedings, Royal Society of London, Vol. A161, 1937, pp. 460-476.

18 Carlson, G.E., and Halijak, C.A., "Simulation of the Fractional Derivative Operator s 1/2 And the Fractional Integral Operator 1/s 1/2," Kansas State University Bulletin, Kansas State University, Manhattan, Kansas, Vol. 45, no. 7, 1961, pp. 1-22.

19 Carson, J.R., "Electrical Circuit Theory and the Operational Calculus" (book), Chelsea, New York, N.Y., second edition 1953, 193 pp.

20 Castro, P.S., "Microsystem Circuit Analysis," Electrical Engineering, Vol. 80, 1961, pp. 535-542.

21 Choksy, N.H., "Analystic Determination of the Stability of Servomechanisms and Other Automatic Control Systems Having Transcendental Characteristic Equations," Ph.D. Thesis, University of Wisconsin, Madison, Wisc., 1955, 75 pp.

22 Choksy, N.H., "Time-Lag Systems-A Bibliography," Professional Group on Automatic Control, Institute of Radio Engineers, Vol. AC-5, 1960, pp. 66-70.

23 Chu, Yaohan, "Feedback Control Systems with Dead-Time Lag or Distributed Lag by Root-Locus Method," AIEE Transactions, Applications and Industry, Part II, Vol. 71, November, 1952, pp. 291-296.

24 Chu, Yaohan, "Synthesis of Feedback Control Systems by Phase-Angle Loci," AIEE Transactions, Applications and Industry, Part II, Vol. 71, November, 1952, pp. 330-333.

25 Churchill, R.V., "Complex Variables and Applications," second edition, McGraw-Hill Book Co., Inc., New York, 1960.

26 Crocco, L., Gray, J., and Harrje, D.T., "On the Importance of the Sensitive Time Lag in Longitudinal High-Frequency Combustion Instability," Jet Propulsion, Vol. 28, 1958, pp. 841-843.

27 Doetsch, G., Book "Guide to the Application of Laplace Transforms" Van Nostrand, Princeton, N.J., 1961.

28 Duffin, R.J., "The Difference-Differential Equation of Electron Energy Distribution in a Gas," Journal of Mathematical Analysis and Applications, Vol. 1, 1960, pp. 342-354.

29 Eisenberg, L., "Stability of Linear Systems with Transport Lag," IEEE Transactions on Automatic Control, Vol, AG-11, No. 2, pp. 247-254.

30 Eisenberg, L., "Design of Linear Feedback Control Systems with Transport Lag by Parameter Plane Techniques" Dr. Sc. Thesis, Newark College of Engineering, 1966.

31 Eisenberg, L., "Analysis of Smith Linear Predictor Control Systems," ISA Transactions, Vol. 6, Issue 4, 1968, pp. 329-334.

32 Elgerd, O.I., "Analysis of Linear Control Systems Containing Distributed and Lumped Parameters - A Comparative Study," International Convention Record, Institute of Radio Engineers, part 4, 1961, pp. 61-68.

33 Elkind, J.I., and Forgise, C.D., "Characteristics of the Human Operator in Simple Control Systems," Transactions, Professional Group on Automatic Control, Institute of Radio Engineers, Vol. AC-4, 1959, pp. 44-55.

34 Evans, W.R., "Analysis of Control Systems," AIEE Transactions, Part II, Vol. 67, 1948, pp. 547-551.

35 Forsyth, G.E. and Rosenbloom, P.C., "Numerical Analysis and Partial Differential Equations," (book), Wiley, New York,N.Y., 1958, 204 pp.

36 Forsyth, A.R., "Theory of Differential Equations, Vol. 5 & Vol. 6 (bound as one), - Part IV, Partial Differential Equations," Dover, New York, N.Y., 1959, 596 pp.

37 Frank, W.L., "Finding Zeros of Arbitrary Functions," Journal, Association for Computing Machinery, Vol. 5, 1958, pp. 154-160.

38 Fuller, W.D. and Happ, W.W., "Design Procedures for Film-Type Distributed Parameter Circuits," Proceedings, National Electronics Conference, Chicago, Ill., Vol. 17, 1961, pp. 601.

39 Gantmacher, F.R., "The Theory of Matrices" Vol. 2, New York, 1960.

40 Ghausi, M.S., and Kelly, J.J., "Introduction to Distributed Parameter Networks," (Book) Holt, Rinehart and Winston, Inc., New York, 1968, Chapter 5.

41 Gladwin, A.S., "Stability Criteria for an Electrical or Mechanical System with Distributed Parameters," British Journal of Applied Physics, Vol. 6, 1955, pp. 400-402.

42 Gyftopoulos, E.P. and Smets, H.B., "Transfer Functions of Distributed Parameter Nuclear Reactor Systems," Nuclear Science and Engineering, Vol. 5, 1959, pp. 405-414.

43 Happ, W.W. and Castro, P.S., "Distributed Parameter Circuits and Microsystems Electronics," Proceedings, National Electronics Conference, Vol. 16, 1960, pp. 448-460.

44 Happ, W.W. and Castro, P.S., "Distributed Parameter Circuit Design Techniques," Proceedings, National Electronics Conference, Chicago, Ill., Vol. 17, 1961, pp. 44-70.

45 Heins, A.E., "On the Solution of Linear Differential-Difference Equations," Journal of Mathematics and Physics, Vol. 19, 1940, pp. 163-157.

46 Higgins, T.J. and Holland, D.B., "The Human Being as a Link in an Automatic Control System," Transactions, Professional Group on Medical Electronics, Institute of Radio Engineers, Vol. ME-6, 1959, pp. 125-133.

47 Hollister, F.H., "Network Analysis and Design by Parameter Plane Techniques" (Dictoral Dissertation) U.S. Naval Postgraduate School, Monterey, California, 1965.

48 Holm, C., Distributed-Parameter Networks for Microminiaturization," Electrical Manufacturing, Vol. 65, April 1960, pp. 92-96.

49 Kadymov, Y.B., "Methods of Studying the Stability of Automatic Control Systems with Distributed Parameters with Allowance for Losses," Automation and Remote Control, Vol. 20, 1959, pp. 500-503.

50 Kalman, E.E. and Bertram, J.E., "Central Synthesis Procedure for Computer Control of Single and Multi-Loop Linear Systems," AIEE Transactions, Part 2, Vol. 77, 1958, pp. 602-609.

51 Kiseda, J.R. and Ford, D.J., "Ripple-Type Time-Delay Networks Using Elliptic Functions," AIEE Transactions, part 1, Vol. 79, 1960, pp. 996-1002.

52 Kokotovic, P. and Siljak, D.D., "The Sensitivity Problem in Continuous and Sampled-Data Linear Control Systems by Generalized Mitrovic's Method," IEEE Transactions on Applications and Industry, Vol. 83, no. 74, September, 1964, pp. 321-324.

53 Kramer, J.D.R., "On Control of Linear Systems with Time Lags," Information and Control, Vol. 3, 1961, pp. 299-326.

54 Kuh, E.S., "Synthesis of Lumped Parameter Precision Delay Line," Convention Record, Institute of Radio Engineers, Vol. 5, part 2, 1957, pp. 160-174.

55 Kinz, K.S., "Numerical Analysis," (book), McGraw-Hill, New York, N.Y., 1957, 575 pp.

56 Landy, J.J. and Fiedler, G.J., "Multi-Loop Automatic Temperature Control System Design for Fluid Dynamics Facility Having Several Long Transport Delays," Transaction, Institute of Radio Engineers, Professional Group on Automatic Control, Vol. AC-4, 1959, pp. 81-96.

57 Lansky, Z.J., "Comparison of Hydraulic and Pneumatic Systems," Machine Design, Vol. 34, no. 3, 1962, pp. 17-22.

58 Leggett, D.A., "Analysis and Synthesis of Distributed Servomechanisms," Master of Science Thesis, University of California, Los Angeles, Calif., June 1954.

59 Lindholm, F.A. and Happ, W.W., "Transient in Microsystems," Technical Report LMSD 703107, Microsystems Electronics Department, Lockheed Missle and Space Co., Palo Alto, Calif., 1960.

60 Lie, Y.C. and Chin, Y.S.," On the Equivalence Problem of Differential Equations and Difference-Differential Equations in the Theory of Stability," Science Record, new series, Vol. 2, 1958, pp. 129-133.

61 Luke, Y.L., "How to Analyze Control Systems with Time Lag," Electronic Industries, Vol. 19, no. 7, 1960, pp. 75-78.

62 Luke, Y.L., "Rational Approximations to the Exponential Function," Journal, Association for Computing Machinery, Vol. 4, pp. 24-29.

63 Luke, Y.L., "On Economic Representation of Transcendental Functions," Journal of Mathematics and Physics, Vol. 38, 1960, pp. 279-294.

64 Lupfer, D.E. and Oglesby, M.W., "Applying Dead Time Compensation for Linear Predictor Process Control," Journal, Instrument Society of America, Vol. 8, no. 11, 1961, pp. 53-57.

65 Lupfer, D.E. and Oglesby, M.W., "The Application of Dead Time Compensation to a Chemical Reactor for Automatic Control of Production Rate," Transactions, Instrument Society of America, Vol. 1, 1962, pp. 72-80.

66 Malcolm, R.B., "The Application of Laplace Transforms to Distributed Parameter Problems," Proceedings, National Electronics Conference, 20, pp. 784-789, 1964.

67 Maybury, S. and Smith, B., "High-Frequency Base-Transport Factor and Transit Time of Graded-Base Transistors," Transactions, Professional Group on Electron Devices, Institute of Radio Engineers, Vol. ED-9, 1962, pp. 161-163.

68 Meerov, M.V., "Introduction to the Dynamics of Automatic Regulating of Electrical Machines," Translated by J.S. Shapiro, London: Butterworths, 1961.

69 Mitrovic, Dusan, "Graphical Analysis and Synthesis of Feedback Control Systems I--Theory and Analysis," AIEE Transactions, Applications and Industry, Part II, Vol. 77, 1958, pp. 476-487.

70 Moore, J.B. and Dorf, R.C., "The Design of an Attitude Control System for a Space Vehicle," Proceedings, National Electronics Conference, Vol. xxii, 1966, pp. 715-717.

71 Mulligan, J.H., Jr., "The Effect of Pole and Zero Locations on the Transcient Response of Linear Dynamic Systems," Proceedings of the I.R.E., Vol. 37, May 1949, pp. 516-529

72 Neimark, J.I., "About Determination of Parameter Values Which Insure Stability of Automatic Control Systems," Automatika i Telemechanika, no. 3, 1948.

73 Neufeld, J., "On the Operational Solution of Linear Mixed Difference-Differential Equations," Proceedings, Cambridge Philosophical Society, Vol. 30, 1934, pp. 389-391.

74 Nichols, N.B., "The Linear Properties of Pneumatic Transmission Lines," Transactions, Instrument Society of America, Vol. 1, no. 1, pp. 5-14.

75 Oldenbourg, R.C. and Sartorius, H., "The Dynamics of Automatic Controls (book)," (Translated and Published by the American Society of Mechanical Engineers, New York, N.Y., 1948, 276 pp.

76 Oldenbourg, R.C., "Deviation Dependent Step-By-Step Control as a Means to Achieve Optimum Control for Plants with Large Distance Velocity Lags," Automatic and Manual Control (book), Butterworths Scientific Publications, London, England, 1952, pp. 235-244.

77 Papoulis, A., "Feedback Systems with Nonrational Transfer Functions," Proceedings, Symposium on Active Networks and Feedback Systems, Brooklyn Polytechnic Institute, New York, N.Y., 1961, pp. 111-123.

78 Phillips, R.A., "Analysis of Tandem Cold Reduction Mill with Automatic Guage Control," AIEE Transactions, part 2, Vol. 75, 1956, pp. 355-363.

79 Pierre, D.A. and Higgins, T.J., "Pole Location and Stability of Distributed Parameter Feedback Systems," Proceedings, National Electronics Conference, 20, pp. 801-803, 1964.

80 Pierre, D.A., "Rational Fraction Approximation Formula for Exp (- sD) with Applications," Journal, SIAM, 12(1), 93-104, March, 1964.

81 Pierre, D.A., "Transient Analysis and Synthesis of Linear Control Systems Containing Distributed-Parameter Elements," (PhD Thesis), University of Wisconsin, 1962.

82 Pinney, E., "Ordinary Difference-Differential Equations (book)," University of California Press, Berkeley, California, 1958, 262 pp.

83 Pipes, L.A., "The Analysis of Retarded Control Systems," Journal of Applied Physics, Vol. 19, 1948, pp. 617-623.

84 Pipes, L.A., "Applied Mathematics for Engineers and Physicists," (Book), McGraw-Hill Book Company, Inc., New York, N.Y., 1958.

85 Pontryagin, L., "On Zeros of Some Transcendental Functions (in Russian," Izvestiya, Akad. Nauk SSSR, Ser. Math., Vol. 6, 1942, pp. 115-134; American Mathematical Society Translations, Vol. 1, 1955, pp.95-110.

86 Radant, M.E., "Distributed Elements in a Servomechanism, Master of Science Thesis, University of California, Los Angeles, Calif., August, 1956.

87 Raxumihin, B.S., "The Application of Lyapunov's Method of Problems in the Stability of Systems with Delay," Automation and Remote Control, Vol. 21, 1960, pp. 515-520; Automitika i Telemekhanika, Vol. 21, 1960, pp. 740-748.

88 Reckoff, M.G., Jr., "Finding Phase Angle Loci of a Distributed Lag," Control Engineering, Vol. 9, no. 1, 1962, pp. 71-72.

89 Reswick, J.B., "A Dead-Time Controller," Automatic and Remote Control (Proceedings of the First International Congress of the IFAC, Moscow, USSR, 1960), Vol. 3, Butterworths Scientific Publications, London, England, 1961, pp. 329-335.

90 Rothbart, A., "Bibliography on Magnetostrictive Delay Lines," Transactions, Professional Group on Electronic Computers, Institute of Radio Engineers, col. EC-10, 1961, p. 285.

91 Sandell, R.P. and Ceaglske, N.H., "Frequency Response of Pneumatic Transmission Lines," Journal, Instrument Society of America, Vol. 3, 1956, pp. 482-485.

92 Satche, M., "Discussion of Ansoff's Paper, Reference no. 206," Journal of Applied Mechanics, Vol. 16, 1949, pp. 419-420.

93 Schliessmann, H., "A Method for the Optimum Control of Systems with Dead Time, (in German) Regelungstechnik, Vol. 7, 1959, pp. 272-280, 418-421.

94 Schroeder, W., "Analysis and Synthesis of Sampled-Data and Continuous Control Systems with Pure Time Delays," Electronics Research Laboratory Report, series no. 60, issue no. 156, University of California, Berkeley, Calif., June, 1956.

95 Schultz, M.A., "Control of Nuclear Reactors and Power Plants (book," McGraw-Hill, New York, N.Y., 1955, 313 pp; second edition, 1961, 462 pp.

96 Shimanov, S.N., "On the Instability of the Motion of Systems with Retardation," Journal of Applied Mathematics and Mechanics, Vol. 24, 1960, pp. 70-81.

97 Shimanov, S.N., "On the Stability in the Critical Case of a Zero Root for Systems with Time-Lag," Journal of Applied Mathematics and Mechanics, Vol. 24, 1960, pp. 653-668.

98 Siljak, D.D., "Generalization of Mitrovic's Method," IEEE Transactions on Applications and Industry, Vol. 83, no. 74, September, 1964, pp. 314-320.

99 Siljak, D.D., "Analysis and Synthesis of Feedback Control Systems in the in the Parameter Plane," IEEE Transactions on Applications and Industry, Vol. 83, no. 75, November, 1964, pp. 449-466.

100 Siljak, D.D., "Sampled-Data Control Systems with Transport Lag by Mitrovic's Algebraic Method," AIEE Transactions, part 2, Vol. 80, 1961, pp. 247-252.

101 Smith, J.M. Otto, "Feedback Control Systems, New York, McGraw-Hill Book Company, Inc., 1958.

102 Smith, J.M. Otto, "Closer Control of Loops with Dead Time," Chemical Engineering Progress, Vol. 53, 1957.

103 Smith, J.M. Otto, "Mixed Distributed and Lumped Parameter Systems," WESCON Convention Record, Institute of Radio Engineers, part 2, 1957, pp. 122-132.

104 Smith, J.M. Otto, "Posicast Control of Damped Oscillatory Systems," Proceedings, Institute of Radio Engineers, Vol. 45, 1957, pp. 1249-1255.

105 Smith, J.M. Otto, "A Controller to Overcome Dead Time," Journal, Instrument Society of America, Vol. 6, no. 2, 1959, pp. 28-33.

106 Sneddon, L.N., "Fourier Transforms," (book), McGraw-Hill, New York, N.Y., 1951, 542 pp.

107 So, H.C. and Thaler, G.J., "Modified Posicast Method of Control," AIEE Transactions, part 2, Vol. 79, 1960, pp. 320-326.

108 Soble, A.B., "Rational Fraction Approximation to Exponentials," Transactions, Professional Group on Circuit Theory, Institute of Radio Engineers, Vol. CT-9, 1961, pp. 366-367.

109 Solodovnikov, V.V., Topcheev, Y.I. and Krutikova, G.V., "Transient Response from Frequency Response," (book), Infosearch, Ltd., London, England, 1958, 193 pp.

110 Stark, L. and Herman, H.T., "The Transfer Function of a Photo-Receptor Organ," Kybernetile, Vol. 1, 1961, pp. 124-129.

111 Stewart, J.L., "Generalized Pade Approximation," Proceedings, Institute of Radio Engineers, Vol. 48, 1960, pp. 2003-2008.

112 Storch L., "Synthesis of Constant Time-Delay Ladder Networks Using Bessel Polynomials," Proceedings, Institute of Radio Engineers, Vol. 42, 1954, pp. 1666-1675.

113 Takahashi, Y., "Transfer Function Analysis of Heat Exchange Processes," Automatic and Manual Control (book), Butterworths Scientific Publications, London, England, 1952, pp. 235-244.

114 Thaler, J. George, and Brown, R.G., "Analysis and Design of Feedback Control Systems," New York: McGraw-Hill Book Company, Inc., 1960.

115 Thaler, G.J. and Han, K.W. "Control System Analysis and Design Using Parameter Space Method " IEEE Trans. on Automatic Control , v AC 11, #3, July 1966, pp 560-563.

116 Tranter, C.J., "Integral Transforms in Mathematical Physics," (book), Wiley, New York, N.Y., 1959 (reprinting of enlarged second edition), 133 pp.

117 Trick, T.N. and Bourguin, J.J., "Stability of Distributed R-C Networks," Tenth Midwestern Symposium on Circuit Theory, Purdue University, May 18-19, 1967.

118 Truxal, J.G., "Automatic Feedback Control System Synthesis," (book), McGraw-Hill, New York, N.Y., 675 pp. See especially Chapter 9.

119 Van. L., "Stability of Solutions of Equations with Lagging Argument," Science Record, new series, Vol. 3, 1959, pp. 280-288.

120 Vishnegradski, I.A., "On Direct Action Regulators," News of the St. Petersburg Technological Institute, 1877, pp. 21-62.

121 Wangersky, P.J., and Cunningham, W.J., "Time Lag in Prey-Predator Population Models," Ecology, Vol. 38, 1957, pp. 136-139.

122 Weinberg M. and Eisenberg L., "Stability of Linear Feedback Control Systems with Distributed Parameter Elements Via the Parameter Plane," Proceedings of the 23rd Annual ISA Conference, October 1968.

123 Williams, T.J. and Harnett, R.T., "Automatic Control in Continuous Distillation," Chemical Engineering Progress, Vol. 53, 1957, pp. 220-225.

124 Wrangham, D.A., "The Elements of Heat Flow," (book), Chatto and Windus, London, England, 1961, 486 pp.

125 Jackson, D.L., "Variable Time Delay by Pade Approximations," Transactions, Professional Group on Electronic Computers, Institute of Radio Engineers, Vol. EC-10, 1961, p. 783.

VITA

Name: Murray Weinberg

Elementary and Secondary School Education:

Public School No. 16, Brooklyn, New York

Brooklyn Technical High School, Brooklyn, New York

Colleges and Universities: Years attended and Degrees

College of the City of New York, 1945-1950, B. E. E.

Newark College of Engineering, 1956-1961, M. Sc. E. E.

Newark College of Engineering, 1962-Present

Professional Experience:

1950-1955 - Electronic Engineer, National Bureau of Standards, Washington, D. C.

1956-1957 - Senior Engineer, Monroe Calculating Machine Co., Orange, New Jersey

1957-1958 - Project Engineer, Philco Corp., Philadelphia, Pa.

1958-Present - Section Head, ITT Defense Communications, Nutley, New Jersey

Time Devoted to Research:

This dissertation is the result of more than two years of research. One year of full-time research was performed at Newark College of Engineering under an educational leave of absence plan sponsored by ITT Defense Communications of Nutley, N. J.